Towards the development of standardized potency assays in regenerative medicine bioprocessing for the treatment of ischemic cardiac injury

Thesis submitted for the degree of
Doctor of Philosophy in Biochemical Engineering

by

Fatumina Said Abukar

December 2017

Regenerative Medicine Bioprocessing Unit
Department of Biochemical Engineering
University College London

Thesis declaration

I, Fatumina Said Abukar, confirm that the work presented in this thesis is my own. Where information has been derived from other sources, I confirm that this has been indicated in the thesis.

Abstract

The mechanisms by which mesenchymal cells can repair the infarcted myocardium are still unclear and are made more challenging by the fact that hMSCs engraft in the myocardium for only a short amount of time. This thesis first examined the ability of commercial bone marrow (BM) MSCs expanded in low serum (<5% FBS medium), umbilical cord (UC) MSCs and individual donor BM-MSCs to perform biologically relevant functions. The characterization studies showed that the differently-sourced hMSCs successfully underwent tri-lineage differentiation and displayed similar expression levels of positive MSC markers. Additionally to this, there was a tendency for cells at increased *in vitro* age to display reduced expression of CD105.

Biologic priming of cells using sJag1 typically enhanced MSC attachment to fibronectin, although to varying degrees in the different MSC types. In addition, vascular support assays revealed that MSCs displayed pericyte-like behaviour lining the outside of the vessels and bridging in between endothelial cells during network formation.

Assessment of how bioprocess parameters affect vascular tubule formation revealed that economic benefits can be derived by using lower volumes of alternative matrix substrates. In addition, automated counting tools achieved an unbiased measurement compared to manual counting processes. Finally, from a perspective of the vascular endothelial cells used in the assays, it was possible to extend their use an additional 50%, from passage 10 to passage 15 before losing functional capacity.

With further work, these assays could be optimized for high-throughput screening and be used in industry as surrogate tests for quality control (QC) hence enabling the advancement of well-characterized cell therapy products.

Impact statement

Currently, there are no potency assays in the clinical setting that give a reliable measurement of MSC mode of action other than simple surface marker expression, which does not predict function. This thesis aimed to take a methodological approach to measure key functions of hMSCs and endothelial tubule formation and to study the interactions between key bioprocess parameters affecting assay costs, robustness and reproducibility. Furthermore, from an engineering perspective, it was vital to control and mimic variables found in the *in vivo* environment such as oxygen tension and biological substrates to make measurements closer to the values obtained when injecting the cells in physiological areas. Additionally, another focus of this project was to biologically prime the MSCs to enhance their predicted mode of action and therefore to enhance the ease with which it can be measured.

Not much work has been done on potency assays in cell therapy. Therefore, the results from this study will also fill a void in the literature and can form the basis of future assay development work in both industry and academia. The comparative studies between differently-sourced MSCs and the data obtained from priming the mesenchymal cells with biological ligands will be useful to companies looking to develop products catering to research and industrial application. The results from this project will also validate or reject both the proposed mechanisms of action of MSCs and the differences between differently-sourced MSCs by revealing key critical quality attributes of mesenchymal cells.

Heart transplantation is scarce due to the high costs associated with it, the lack of donors and the need for patient-donor matched organ. For this reason, gaining an understanding of the MOA of MSCs will also accelerate their application in the treatment of ischemic injury and enable their use as a viable alternative to heart transplantation.

Acknowledgments

First, praises and thanks to Allah S.W.T for giving me the strength to persevere and have a positive attitude during the most difficult times of my PhD. I would like to express my gratitude to my supervisor Professor Ivan Wall for allowing me to take on this exciting project in an area that I enjoy, for his guidance and for the valuable feedback on my thesis writing. I would like to extend my gratitude to Professor Mike Hoare for his support, valuable feedback and for always keeping me on track, all of which have also contributed to improving the quality of my writing. Also, Professor Nicolas Szita for his insight and advice in personal and professional matters, Professor Gary Lye, and Kim Morgan for believing in me and being supportive of my science communication adventures.

My sincerest thanks go to my colleagues within the Advanced Centre for Biochemical Engineering to name a few: Nehal, Elisabetta, Tania, Luba, Mike, Hadiza, Shaleem, Dave, Damiano, Carlotta, Gregorio, Chika and Daniel for your friendship and for always having words of encouragement when things were not always working, as it happens in science! Special thanks to Giulia Detela, Billy, Ya, Reema, and Zhuming for always being happy to help, for the laughs and for making the lab a positive space to work in. Also, many thanks to the Engineering and Physical Sciences Research Council (EPSRC) for funding this doctorate. A special thank you to Asma, for being my Ride or Die throughout this PhD. Working days (and nights) in the lab would not have been as much fun without our chats, tea breaks and every memorable experience we have shared together.

Finally, special recognition goes out to my siblings Sabrina, Mohamed, and Sheima for their love and encouragement. In particular, Sheima for believing in me, listening to all of my dilemmas and giving me tough love when needed. To my family and friends especially Safa and Hafsa for constantly motivating me and having no doubts in my abilities to succeed. To my parents Dr Said Abukar Abati and Khadija Omar Mohamed for being my inspirations and for teaching me the importance of hard work and perseverance and to my aunty Fatma and uncle Amir for their selfless love and constant support during the past fifteen years. No words can describe how lucky I feel to have you in my life.

Table of contents

List of figures

List of tables

List of abbreviations

AM - Acute myocardial infarction

AMI - Acute myocardial infacrtion

AM-MSC - Amniotic membrane mesenchymal stromal cell

ANOVA - Analysis of variance

AT - Adipose tissue

bFGF - Basic fibroblast growth factor

BM - Bone marrow

BM-MNC - Bone marrow mononuclear cell

BM-MSC - Bone marrow mesenchymal stromal cell

BSA - Bovine serum albumin

CAM - Chick chorioallantoic membrane

cDNA - Complementary DNA

CHD - Coronary heart disease

CM - Cardiomyocyte

CO_2 - Carbon dioxide

CPP - Critical process parameter

CQA - Critical quality attribute

CSC - Canadian Cardiovascular Society

CSC - Cardiac stem cell

CXCR4 - C-X-C chemokine receptor type 4

DAPI - 4, 6-diamidino-2-phenylindole

dH_2O - Distilled water

Dll - Delta-like ligand

DMEM - Dulbecco's Modified Eagle's Medium

DMSO - Dimethyl sulfoxide

DNA - Deoxyribonucleic acid

DOE - Design of experiments

EBM-2 - Endothelial Growth Basal Medium-2

EC - Endothelial cell

ECM - Extracellular matrix

EDTA - Ethylenediaminetetraacetic acid

EDV - End-diastolic volume

EF - Ejection fraction

EGFP - Enhanced green fluorescent protein

EGM-2 - Endothelial Growth Medium-2

ELISA - Enzyme-linked immunosorbent assay

EMA - European Medicines Agency

EPC - Endothelial progenitor cell

ESC - Embryonic stem cell

ESV - End-systolic volume

FBS - Foetal bovine serum

FDA - Food and Drug Administration

FGF - Fibroblast growth factor

FN - Fibronectin

G-CSF - Granulocyte – colony stimulating factor

gDNA - Genomic DNA

GFR - Growth factor reduced

GvHD - Graft versus host disease

HCL - Hydrochloric acid

hEGF - Human epidermal growth factor

hESC - Human embryonic stem cell

HGF - hepatocyte growth factor

HIF- Hypoxia-inducible factor

HLA-ABC - Human leukocyte antigens-ABC

HMEC - Human microvascular endothelial cell

hMSC - human mesenchymal stromal cell

HSC - Hematopoietic stem cell

hUC-MSC - Human umbilical cord mesenchymal stromal cell

HUVEC - Human umbilical vein endothelial cell

ICH - International Conference on Harmonization

IL-1ra - Interleukin-1 receptor antagonist

iPSC - Induced pluripotent stem cell

ISCT - International Society for Cellular Therapy

Jagged - Jag

KIPV - Key process input variable

KPOV - Key process output variable

l - Litre

LVEF - Left ventricular ejection

LVGFP - Lentiviral green fluorescent protein

M- CSF - Macrophage colony-stimulating factor

MCP-1 - Monocyte chemoattractant protein 1

mg - Milligram

MI - Myocardial infarction

ml - Millilitre

mm - Millimetre

MOA - Mechanism of action

MSC - Mesenchymal stromal cell

N_2 - Nitrogen

NC - Negative control

ng - Nanogram

NRT - No reverse transcriptase control

NTC - No template control

O_2 - Oxygen

P - Passage

PAT - Process analytical technology

PBS - Phosphate buffered saline

PDGF - Platelet-derived growth factor

PDL - Population doubling level

PFA - Paraformaldehyde

pO_2 - Partial pressure of oxygen

QbD - Quality by design

QC - Quality control

qPCR - Quantified polymerase chain reaction

QTPP - quality target product profile

R3-IGF-1 - Recombinant 3-insulin-like growth factor-1

RNA - Ribonucleic acid

SV - Stroke volume

T/E - Trypsin/EDTA

TNF - Tumour necrosis factor

UC - Umbilical cord

UCB - Umbilical cord blood

UT - Untreated

VEGF - Vascular endothelial growth factor

VEGFR - Vascular endothelial growth factor receptor

vWF - Von Willebrand factor

µm - Micrometre

Chapter 1: Literature review

1.1: Overview of the vascular system

The vascular network is organized in a hierarchical fashion and it branches in a complex network of vessels which enables the circulation of nutrients as well as blood, immune cells and other molecules to the body tissues via diffusion and convection (Jain, 2003). The heart pumps oxygenated blood through the circulatory system via the arteries. The arteries successively branch into smaller branches until they divide into arterioles. These vessels supply blood to the cells of the body's tissues and organs. The arterioles then divide into capillaries, which are the smallest blood vessels in the body, and they are the sites through which exchange of substances between blood and the cells of tissues and organs takes place. As blood flows through the capillaries, oxygen and nutrients move out into the cells and waste matter from the cells moves into the capillaries. These then merge to form venules and veins which transport the de-oxygenated blood to the heart and the lungs (Jain, 2003).

Blood cells are composed of two main cell types: endothelial cells (ECs) and perivascular cells- also known as pericytes, vascular smooth muscle cells or mural cells. ECs line the inner wall of vessels in contact with the blood, whilst perivascular cells form a thick wall around the endothelial layer (Wanjare et al., 2013). Pericytes are perivascular cells that wrap around the endothelial cells of capillaries (diameter <10 μm) and micro-vessels (10 μm - 100 μm) throughout the body (Crisan et al., 2012). These are usually found at the junction points of small vessels and capillaries where they stretch themselves along the length of the vessels across several capillaries in the vasculature (Armulik et al., 2011). Differently from ECs, pericytes have a prominent round nucleus and protruding finger-like extensions that they use to attach to the wall of endothelial cells. In addition, they can be easily distinguished from other perivascular cells such as smooth muscle cells which can be found wrapping around larger blood vessels (Crisan et al., 2012). Previous work showed that the EC-pericyte ratio around blood vessels is tissue-specific and that it ranges from 1:1 in retina tissues to 10:1 in lungs (Herrmann et al., 2016).

Pericytes provide a fundamental structural support role for blood vessels. For example, one of their main functions is to prevent blood vessels from becoming haemorrhagic and hyperdilated, which can lead to serious conditions such as diabetic retinopathy. These particular groups are known as microvascular pericytes and they are usually found around the walls of capillaries. Here they communicate with endothelial cells via gap junctions which in turn control the proliferative abilities of endothelial cells (Berger et al., 2005).

1.1.1: The process of vessel formation

The key processes involved in vessel formation are vasculogenesis and angiogenesis. Vasculogenesis is the *de novo* synthesis of blood vessels from endothelial cell precursors (angioblasts) and stem cells, whereas angiogenesis is the formation of new blood vessels from existing blood vessels e.g. sprouting and branching (Jain, 2003). During embryonic development, one of the first organs that forms is the vasculature (Jain, 2003; Velazquez, 2009). Firstly, the angioblasts (i.e. endothelial cell precursors) differentiate into endothelial cells which ultimately assemble into the immature vascular network through vasculogenesis (Carmeliet and Jain, 2011). The vascular network then expands through sprouting of vessels via angiogenesis. The immature vascular network is stabilized through the recruitment of mural cells (vascular smooth muscle cells and pericytes), and the generation of the extracellular matrix (ECM). Branching, remodelling, and pruning of the vascular network is achieved using signalling pathways involved in branch formation as well as cues coming from various basement membranes and ECM components (Jain, 2003).

Signalling molecules and mechanical factors triggered by cell-cell contact promote the migration of ECs. During angiogenesis, the breakdown of proteins of the basal lamina leads to a localized thinning of the basement membrane which reduces the stiffness of the ECM (Ingber, 2002). Subsequently, the cells adhering to the thinned local sections of the ECM experience increased tension on their adhesion receptors. The mechanical signals triggered by this change in stiffness are converted into

biochemical cues which trigger movement and result in the formation of branching patterns characteristic of growing vascular networks (Shin et al., 2001). Both angiogenesis and vasculogenesis are also key processes during wound healing, which consists of the activation and migration of pre-existing mature endothelial cells, degradation of the ECM and remodelling of the vasculature (Jain, 2003, Velazquez, 2009).

1.1.2: Regulation of angiogenesis by hypoxia

One of the key variables that decide on the extent of angiogenesis and vessel growth is the oxygen level in a given tissue. Moreover, it has been reported that a hypoxic environment up-regulates many angiogenic factors including vascular endothelial growth factor (VEGF), in both normal and pathological conditions (Semenza, 1999). Such growth factors induce endothelial cells to break out of their stable positions in the vessel and sprout, branch and pattern in a stable network until reaching quiescence (Fraisl et al., 2009; Stamati et al., 2014). The up-regulation of angiogenic factors is achieved through the hypoxia-inducible factor-1α (HIF-1α). HIFs are a group of transcription factors that are expressed by endothelial cells based on the amount of oxygen within the cellular environment, especially hypoxia (Krock et al., 2011). Most of the tissues in the body have a partial pressure of oxygen (pO_2) of 1% to 7%; for example bone marrow stem cells can be found in oxygen environments of less than 1% whilst blood vessels have a pO_2 of 5% to 7% (Krock et al., 2011; Kusuma et al., 2014). Several studies have demonstrated that hypoxia is a key component of some cellular niches (Kusuma et al., 2014). Furthermore, HIF-1 promotes angiogenesis and vascular remodelling in wound healing, through the mobilization of angiogenic cells from distant sites (including bone marrow, pericytes and endothelial cells from other tissues; (Rezvani et al., 2011). Earlier studies demonstrated that when constant amounts of the active form of HIF-1α were expressed in a mouse skin, this was enough to mobilize circulating angiogenic cells and improve wound healing in diabetic mice (Liu et al., 2008). Several research groups have also reported that subjecting stem cells to hypoxia improved their migration abilities in both *in vitro* and *in vivo* studies (De Becker and Riet, 2016). In support to these findings, It has also been shown that decrease in HIF-1α expression causes poor wound

vascularization and healing (Zhang et al., 2010). Furthermore, these studies suggest that the hypoxia/HIF signalling pathway has a key role in the formation of a “normal vasculature” and it could be a key therapeutic target for vascular diseases. In addition, since the majority of the tissues in the body have a pO_2 of ~5% (Krock et al., 2011), it may be beneficial for *in vitro* experiments to be carried out in environments that closely mimic these conditions.

1.2: Dual pumping function of the heart

The heart is a highly vascularized muscular organ found between the sternum (breastbone) and the vertebrae (backbone). Its function is to pump blood through the blood vessels for oxygen and nutrient distribution to all cells in the body. The heart is divided into four chambers: left and right ventricles (lower chambers) and left and right atria (upper chambers). Both atria and ventricles act as functional syncytium respectively, meaning that they work electrically and mechanically as a single unit. During the cardiac cycle, deoxygenated blood coming from the systemic circulation enters the right side of the heart which pumps the blood through the pulmonary artery, into the pulmonary circulation (closed loop vessels carrying blood between the heart and the lungs). Then oxygenated blood coming from the pulmonary circulation is returned to the left side of the heart, which pumps the blood into the systemic circulation via the aorta (Katz, 2011).

1.2.1: Cell types found in the heart

The four chambers of the heart are made of different cell types which allow for its normal structural, biochemical, mechanical and electrical functioning (Xin et al., 2013). The cardiac muscle is made of cardiomyocytes (CMs) whilst cardiac fibroblasts which make more than 50% of the cells in the heart can be found in the cardiac skeleton and within the myocardial interstitium (Xin et al., 2013; Furtado et al., 2016;). Fibroblasts are also highly connected to other cell types including ECs and cardiomyocytes (Katz et al., 2012; Furtado et al., 2016). The coronary arteries, which carry blood between the heart and the lungs, are made of smooth muscle cells that allow for the circulation of blood within the heart vessels.

The electric impulses coming from the sinoatrial node, which is made of a group of specialised cardiomyocytes (pacemaker cells) initiate heart contraction. This activates the atrioventricular node (found between the atria and the ventricles). The ventricles are then made of Purkinje fibres which is another group of specialised cardiomyocytes that receive the conductive signal from the atrioventricular node to stimulate ventricular contraction (Xin et al., 2013).

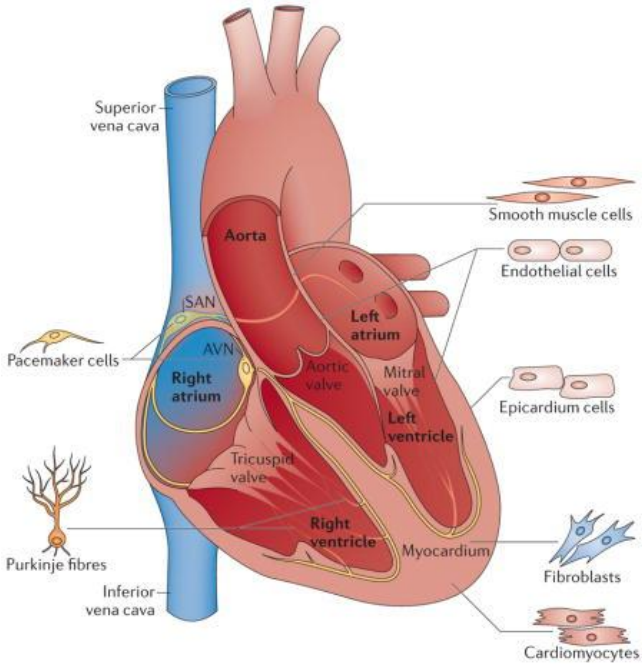

Figure 1-1: Different cell types in the heart (Xin et al., 2013).

1.3: Myocardial infarction and remodelling process

Heart failure initiated by myocardial infarction (MI) accounts for 29% of deaths worldwide, and it is caused by the interruption of the blood supply to a part of the heart caused by a blocked coronary artery (Li et al., 2014; Richardson et al., 2015). The inefficient supply of oxygen to the heart leads to a high loss of mature contracting cardiomyocytes in the infarcted zone which is then subject to a pathological remodelling process, consisting of an inflammatory response and the formation of a dense collagenous scar (Richardson et al., 2015). This scar tissue does not have the contractile, mechanical and electrical properties of the normal myocardium and it hinders the ability of the heart ventricles to pump blood efficiently (Jawad et al., 2007; Richardson et al., 2015). The process of wound healing is divided into three stages: inflammation/necrosis,

fibrosis/proliferation and long-term remodelling/maturation (Richardson et al., 2015; Dobaczewski et al., 2010).

During necrosis which lasts for the first week or more of infarct healing in large animals and humans, the dying CMs undergo a wound healing process involving the secretion of intracellular proteins into the circulation and they trigger an inflammatory response (Burchfield et al., 2013). Following this, several inflammatory cells such as neutrophils, macrophages, and lymphocytes infiltrate in the necrotic tissue within hours of injury and remove the dead myocytes (Richardson et al., 2015). Fibroblasts then proliferate to the zone of injury and differentiate into myofibroblasts to release extracellular matrix proteins such as collagen I and fibronectin (FN) to replace the infarcted tissue with a fibrotic scar, this proliferative phase can last from one to several weeks (Burchfield et al., 2013; Richardson et al., 2015). The proliferation and activation of the fibroblasts are triggered by several cell sources including adult epicardial cells undergoing endothelial to mesenchymal transition and collagen-secreting bone marrow-derived cells (Haudek et al., 2006; Burchfield et al., 2013).

The final phase which is also known as long-term remodelling/maturation lasts a couple of months in large animals and humans (Richardson et al., 2015). This stage involves the increase in collagen crosslinking as well as the expression of cross-linking enzymes and proteoglycans which bind to collagen to support scar maturation. The myocyte hypertrophy which involves the increase in size of the skeletal muscle and the tightly cross-linked collagen fibres reduces the contractile ability and cardiac output of the heart (Richardson et al., 2015). Since the heart has limited regenerative abilities after injury, there is a need to develop therapies that can target the scar tissue and promote heart regeneration (Bartunek et al., 2013).

1.3.1: Therapeutic treatments for MI

Currently, there are no treatments that can reverse the loss of myocardial tissue and whilst treatments for heart failure are available, they do not lead to sufficient heart recovery (Bartunek et al., 2013). Examples of medical heart failure treatments include the use of angiotensin-converting enzyme inhibitors which

work by relaxing and opening the blood vessels to reduce the amount of force needed by the heart to pump blood (Donnelly and Manning, 2007). Other treatments involve the use of beta-adrenoceptor antagonists which reduce the myocardial oxygen requirement below the level that would cause angina (O'Rourke, 2007). This is a term used to describe the sensation of chest pain experienced by several patients and it is caused by the imbalance between oxygen supply and oxygen demand in the heart; antianginal therapies can also be taken together hence taking advantage of their different modes of action (O'Rourke, 2007).

In the case of patients suffering from severe forms of heart failure, their only viable alternative is to undergo heart transplantation which is scarce because of the high costs associated with it, the lack of donors and the need for patient-donor matched organs (Zammaretti and Jaconi, 2004; Menasché, 2008). Usually, patients are treated with a left ventricular assist device, a mechanical pump connected to the myocardium through surgery which enables the heart to pump blood (Kirklin et al., 2013; Wilson et al., 2009). The left ventricular assist device is sometimes given to patients on the waiting list however, this method can prolong the patient's life for only several weeks or months (Kirklin et al., 2013; Wilson et al., 2009). As a result, stem cell therapy is increasingly being considered as a potential means to trigger innate mechanisms of heart regeneration (Bartunek et al., 2013).

1.4: What is regenerative medicine?

Regenerative medicine is a multidisciplinary approach to heal, replace or regenerate organs damaged by age, disease, or trauma (Mao and Mooney, 2015). The current methods for organ transplantation suffer from severe immune complications and lack of donor supply (Mao and Mooney, 2015). For this reason, during the past 20 years the cell therapy industry has focused on a combination of technologies including the use of soluble molecules such as growth factors, gene therapy, stem cell transplantation, tissue engineering and cell reprogramming for the treatment of several diseases including diabetes, cardiovascular conditions and cancer (Mason and Dunnill, 2008; Ratcliffe et al., 2011). However, the success of this industry depends on the manufacture of sufficient and consistent

cell numbers without significant batch variation (Ratcliffe et al., 2011). For this reason, it is fundamental for the critical quality attributes of identity, potency, purity, and safety of the cell-based products to be identified (Carmen et al., 2012).

1.4.1: Potency assays for assessing biological function of cell-products

Critical characteristics to be specified as part of good manufacturing practices are Identity, potency, purity, and safety (Carmen et al., 2012). Potency characterization is one of the earliest studies to be carried and it can be defined as the measurement of biologic function based on the cell product attributes (Bravery et al., 2013). Potency assays generally focus on a key aspect of product function and they require short time scales. According to the European Medicines Agency, potency assays must be established by phase 3 (European Medicines Agency, 2016). In the context of regenerative therapy for ischemic injuries, it makes sense to predict that functional requirements of the cell therapy product include the ability to support vasculature around the affected region. Therefore, there is a need to develop rapid and easy-to-use assays that can provide process conditions that closely reflect the physiologic environment. These assays would then become ideal precursors to second-generation surrogate tests that make rapid measurements of protein, transcript or metabolite components.

1.4.1.1: Culture medium considerations

The large-scale expansion of stem cell *in vitro* involves the use of various cell culture media. However, the majority media used are supplemented with serum to achieve effective cell proliferation (Tekkatte et al., 2011). FBS is the most commonly used serum source for cell expansion because it enhances cell proliferation capacity (Tekkatte et al., 2011). Due to its properties, most hMSC expansion systems make use of 5-15% FBS (Chen et al., 2013). In the past couple of years, the scientific community has been pressurized by regulatory agencies to reduce/eliminate the dependence or to find alternatives to serum medium, such as human blood-derived supplements and chemically defined serum-free medium (A. K.-L. Chen et al., 2013; Tekkatte et al., 2011). Table 1-1 highlights some of the disadvantages of the use of serum in culture systems.

Disadvantages	**References**
High risk of contamination: virus, bacteria and mycoplasma.	(Erickson et al., 1991; Escobedo-Lucea et al., 2013)
Undefined media: batch-to-batch variation even within the same type of serum, making standardization of cell-based assays difficult.	(A. K.-L. Chen et al., 2013)
Enhanced attachment of non-MSCs to culture dishes by FBS, leading to heterogeneous population.	(Knepper et al., 1998; Chen et al., 2013)
FBS xenogeneic proteins internalized into stem cells with the risk of transmitting unknown infection agents after transplantation of cells into patients.	(Mackensen et al., 2000; Escobedo-Lucea et al., 2013)
Ethical issues: pain inflicted to foetal calves using inhumane methods to extract the blood and limited availability of serum.	(A. K.-L. Chen et al., 2013; Jochems et al., 2002)

Table 1-1: Summary of the drawbacks of using serum in cell culture systems.

1.5: Cell types used for myocardial tissue regeneration

Current regenerative medicine approaches involve the transplantation of endogenous or exogenous stem cell populations to the ischemic injured heart where they have displayed the ability to differentiate into cardiomyocytes or ECs, inhibit cell death, promote neovascularization, and activate endogenous progenitors and in some cases to also positively modulate the ECM (Sanganalmath and Bolli, 2013). The following section will describe the best cell types that showed positive outcomes *in vitro* and *in vivo* for cardiac regeneration.

1.5.1: Embryonic stem cells (ESCs)

ESCs are sourced from the inner mass of blastocysts and their ability to give rise to several cell types makes them a potential therapy for the regeneration of organs such as the heart (Elnakish et al., 2012). For example, Wu and colleagues showed that when ESCs were cultured as single cells for 13 days, they differentiated into cardiomyocytes and smooth muscle cells (Wu et al., 2006). Moreover *in vivo* studies showed that when ESCs were transplanted into the ischemic injured myocardium in rats these were able to differentiate into myocardial cells with structural and functional properties similar to those of the endogenous myocardial cells, hence leading to improved cardiac function (Min et al., 2002; Menasché et al., 2014). Even though ESCs may be an optimal cell source for cardiac regeneration, there are still challenges that need to be overcome for their successful application in clinics; some of these are listed below:

- Their infinite proliferation properties mean that cells can divide non-stop *in vivo* and lead to teratoma formation (Menasché et al., 2014).
- Give rise to heterogeneous cell populations (Menasché et al., 2014; Osafune et al., 2008).
- ESC therapy will be allogeneic hence requiring immunosuppression of the patients before transplantation - giving drugs for long periods of time to the patient dulls the immune response and increases susceptibility to disease (Menasché et al., 2014).
- There are ethical issues associated with sourcing ESCs from the early embryo (Elnakish et al., 2012).

1.5.2: Adult stem cells for cardiac therapy

Adult stem cells are found in the adult tissue and they can either make more copies of themselves or differentiate into specific lineages, usually the one from the tissue they are sourced from. In addition, they do not pose the risk of being rejected by the body because of their immunological compatibility and they can be extracted from an individual's fat or bone marrow hence avoiding ethical concerns. These advantages make them desirable for application in ischemic cardiac regeneration.

1.5.2.1: Skeletal myoblasts

Skeletal myoblasts are committed progenitors of skeletal muscle cells with a high proliferative potential, commitment to a myogenic lineage, and resistance to ischemia which made them desirable for applications in cardiac regeneration (Dowell et al., 2003). These were the first cells to be used in clinical trials for the treatment of the injured myocardium (Menasché et al., 2003). Previous work showed that when the skeletal myoblasts were injected into the infarcted myocardium of rats, there was the formation of islands of cells of different sizes that maintained characteristics of both skeletal and cardiac cells which led to improved cardiac function (Taylor et al., 1998; Dowell et al., 2003). However, despite their potential for heart therapy, previous clinical work showed that the cardiomyocytes derived from the skeletal myoblasts fail to integrate and work in complete synchrony with the native tissue, which can lead to life-threatening ventricular arrhythmias (Menasché, 2008). Moreover, the reported positive effect of skeletal myoblasts on the function of the left ventricle was only short-term (Menasché, 2008). Therefore there is still the need to carry out extensive *in vitro* and *in vivo* studies to confirm their safety and feasibility for clinical studies.

1.5.2.2: Haematopoietic stem cells (HSCs)

Hematopoietic stem cells (HSCs) are obtained from the bone marrow and they are multipotent stem cells that can undergo lymphoid and myeloid lineages meaning that they can give rise to all of the blood cell types (Bryder et al., 2006). The first study that proved the existence of HSCs involved the injection of a cell

suspension sourced from the bone marrow into irradiated mice. Following this, colonies constituting various differentiated cells of multiple blood lineages were observed in their spleens. Because the bone marrow suspension included several cell types, these cells were initially referred to as colony-forming units (Till and McCulloch, 1961).

HSCs can be recognised by the expression of CD90 and CD34, and by the lack of expression of lineage markers such as CD14 (monocyte/macrophage) and CD38 in humans (Bryder et al., 2006; Ishikawa et al., 2006). CD34-/CD38+ expression has been reported in mice. Hence, there is a need to carefully assess the results from animal studies and these differences should be taken into account in clinical work (Balsam et al., 2004; Bryder et al., 2006). Early studies using HSCs have shown that they have a positive impact on neovascularization and cardiac regeneration (Jackson et al., 2001). Contrastingly, Balsam and colleagues reported that when HSCs were injected into the infarcted heart of mice, they failed to express cardiac-specific tissue markers and instead they differentiated into blood cells and failed to induce myocardial regeneration (Balsam et al., 2004).

More recently, a study by Lemcke and colleagues showed that HSC-MSC co-transplantation could be more beneficial for promoting heart regeneration (Lemcke et al., 2017). Similarly, to Balsam and colleagues, this study showed that HSCs are associated with blood vessel formation. Additionally, it also demonstrated that MSCs communicate via gap junctions with the surrounding cardiac cells, which favour their differentiation into cardiac cells. Gap junctions are specialized cell-cell contacts that enable the transfer of molecules between adjacent cells. Overall this study confirmed that both HSCs and MSCs act through different mechanisms to promote heart regeneration even though there was not a clear benefit on MI-treated hearts upon co-transplantation (Lemcke et al., 2017). For this reason, it may be beneficial to study the MSC-HSC possible synergistic actions by performing *in vitro* studies that could look at separate aspects of angiogenesis (Staton et al., 2007).

Pre-stimulation strategies could also be adopted on to enhance the recruitment of bone marrow cells in disease and to promote cardiac regeneration.

For example, it has been reported that the mobilization of HSCs towards the ischemic injured heart can be enhanced in response to granulocyte-colony stimulating factor which inhibits the CXCR4/SDF-1α signalling (pathway involved in stem/progenitor cell trafficking) and is involved in the retention of HSCs in the bone marrow (Pitchford et al., 2009).

1.5.2.3: Endothelial progenitor cells (EPCs)

Endothelial progenitor cells (EPCs) are CD34+ mononuclear cells residing in the bone marrow (Kamei et al., 2017). Evidence suggests that tissue ischemia mobilizes EPCs to the ischemic site where they differentiate into endothelial cells and form blood vessels (Kawamoto et al., 2003; Rosenstrauch et al., 2005). Moreover, several studies showed that when ECs were transplanted into the ischemic areas *in vivo* they were able to reduce ischemia and enhance neovascularization in the infarcted zone (Kawamoto et al., 2003; Liao et al., 2017). It was shown that the mobilization of EPCs can be enhanced through VEGF pre-treatment in response to inhibition of CXCR4 signalling which is involved in stem/progenitor cell trafficking (Pitchford et al., 2009). Moreover, several studies agreed on the importance of ECs in the formation of new blood vessels through integration to the ischemic area and the release of proangiogenic factors including VEGF, angiopoietin-1, hepatocyte growth factor and platelet-derived growth factor (PDGF). All of this mechanisms provide nutritional support and attenuate apoptosis for the resident EPCs and cardiac cells (Kamei et al., 2017; Liao et al., 2017). EPCs may also increase ischemia-induced inflammatory factors such as interleukin-8 and worsen the ischemic injury (van der Strate et al., 2007; Liao et al., 2017).

1.5.2.4: Cardiac stem cells (CSCs)

The mammalian heart houses one or several clusters of an endogenous population of cardiac stem cells (CSCs) (Basciano et al., 2011). CSCs have been shown to differentiate into cardiomyocytes and to improve cardiac function through paracrine signalling after they have been transplanted into the ischemic heart (Chimenti et al., 2010; Nguyen et al., 2016). Similarly, it has been reported

that cardiosphere-derived cells, which are cells migrating out of cardiac tissue fragments to form spheres, can differentiate into CMs this was observed in both *in vivo* and *in vitro* studies. However, the drawback of both cardiac stem cells and cardiosphere-derived cells is that their isolation involves the harvesting of cardiac tissue through percutaneous endomyocardial biopsies or surgical extraction, followed by digestion, expansion, and purification of the wanted cell types this process is time-consuming as it takes over a month to acquire a clinically relevant number (Makkar et al., 2012). In addition, it has been previously shown that the ability of CSCs to promote cardiac regeneration may be hindered by the low oxygen environment and inflammatory response around the ischemic tissue (Kubo et al., 2008).

1.6: Overview of MSCs

Mesenchymal stromal cells (also termed mesenchymal stem cells or multipotent stromal cells) are multipotent non-hematopoietic stem cells that have the ability to differentiate into a variety of tissues including osteoblasts and chondrocytes (Williams and Hare, 2011).

Recent work has put forward various hypotheses to uncover the ontogeny of MSCs, and the most accepted is that MSCs originate from pericytes (Huang et al., 2011; Herrmann et al., 2016). For every blood vessel in the body mesenchymal cells are observed in perivascular locations (Caplan and Correa, 2011). Several studies reported that both pericytes and smooth muscle cells tend to transdifferentiate into a variety of cell lines including osteocytes, chondrocytes, and neural lineages. In addition, pericytes were shown to express MSC markers such as CD146 and NG2 (Crisan et al., 2008, 2012). CD146+ pericytes (negative for CD34, CD45, and CD56) have been shown to possess the same multipotential capacity of MSCs (Crisan et al., 2012, 2008; Huang et al., 2011). Similarly to MSCs, pericytes also act through paracrine/juxtacrine signalling to recruit host stem cells to the site of injury.

MSCs are a promising therapy for many diseases because of their immunosuppressive and immune privilege roles. For this reasons, they have been widely studied for the treatment of damaged tissue such as bone,

muscle, and ligaments. Their immunosuppressive role indicates that they have the ability to suppress the functions of cells of the immune system such as T cells and B cells. Whilst, immune privilege indicates that they do not trigger the immunological defence mechanisms observed with allogeneic cells. The immunosuppressive and immune privilege properties of MSCs make them ideal for the treatment of graft-versus-host disease which is a lethal complication in allogeneic HSC transplantation recipients (Amorin et al., 2014; Hass et al., 2011).

Not all MSCs possess immune privilege features and this can result in contradictory results between research groups. In fact, conflicting results showed that MSCs are not immune privileged and that their immunosuppressive role *in vivo* causes graft rejection (Le Blanc et al., 2004, Nauta et al., 2006). For example, in a study carried out by Nauta et al., (2006), allogeneic bone marrow with or without the presence of host or donor MSCs was introduced into sub-lethally conditioned mice recipients. This study showed that the addition of host MSCs led to a longer engraftment that resulted in less rejection of donor BM cells. On the other hand, the co-transplantation with allogeneic donor MSCs was followed by the rejection of the allogeneic donor BM cells (Nauta et al., 2006). Some more recent findings have shown that the immune privilege state of MSCs is not stable (Hass et al., 2011). In support of this theory, some *in vitro* and *in vivo* studies observed that when MSCs differentiate they adopt an immunogenic phenotype that leads to immune rejection (Hass et al., 2011). These findings suggest that there is a need to develop potency assays, which can better characterize MSCs. These data inconsistencies could be due to several factors, including heterogeneity between primary cells from different sources (e.g. bone marrow and umbilical cord), poor characterization methods (i.e. use of surface markers) and population diversity within cell cultures (Hass et al., 2011).

MSCs can be sourced from adult tissue such as bone marrow and adipose tissue or foetal tissue such as Wharton's jelly, placenta, and umbilical cord blood. MSCs from different origins have some similarities but they may also present different proliferation profiles, differentiation potential and gene expression profiles (Eckert et al., 2013). Typically, mesenchymal cells are

sourced from the bone marrow where they support hematopoietic differentiation *in vitro*. Here they only represent a small population of less than 0.01% (Fortier and Travis, 2011; Le Blanc et al., 2003).

1.6.1: Biological differences between BM-MSCs and umbilical cord MSCs (UC-MSCs)

Currently the bone marrow and the adipose tissue are the main sources for clinical work; however, their collection involves invasive methods of cell extraction (Jin et al., 2013). In addition, comparative studies between younger (<35 years) and older (<60 years) donors showed that adult stem cells derived from elderly donors may not be effective in clinical work (Alves et al., 2012; Scruggs et al., 2013; Bruna et al., 2016). Hence, there is a need to use other alternative sources such as neonatal tissues including the placenta and the umbilical cord (Jin et al., 2013). Several studies have shown that the umbilical cord (UC) is abundant in MSCs compared to other sources such as the bone marrow (Acosta et al., 2013). Moreover, the mesenchymal cells from the UC do not pose any ethical or practical objections and they can be easily isolated using non-invasive methods. However, Kern and colleagues showed that the success rate of isolating MSCs for the bone marrow and adipose tissue was 100% compared to only 63% for UCB (Kern et al., 2006).

Evidence suggests that UC-MSCs possess greater proliferation capacity and faster population doubling *in vitro* than BM-MSCs (Jin et al., 2013; Chen et al., 2014). Furthermore, in one study it was observed that the faster population doubling of UC-MSCs against BM-MSCs remained constant after 30 passages. On the other hand, the bone marrow MSCs in this study not only showed a slower population doubling than umbilical cord-derived MSCs but their doubling time became longer after passage 6 (Lu et al., 2006; Kern et al., 2006; Maglieri et al., 2010). Similarly, Mennan and colleagues, who compared MSCs from various compartments of the umbilical cord against BM-MSCs, reported that all UC-derived MSCs displayed a faster proliferation capacity than BM-MSCs, with mean doubling times of 2-3 from P0 to P3 (Mennan et al., 2013). On the other hand, the mean doubling time for the BM-MSCs in this study was of ~5 days (P1-P2) and ~11-12 days (P2-P3) (Mennan et al., 2013).

Umbilical cord blood cells can be harvested in different ways, for example by puncturing the umbilical vein with a syringe for blood extraction following cryopreservation and storage in a blood bank for future use (Acosta et al., 2013). Cryopreservation was shown to not impact on the proliferation potential of these cells which means that they remain viable even after long periods of time (Acosta et al., 2013). For example, an early study assessed the expansion potential and engraftment of UCB derived cells previously stored frozen for 15 years compared to freshly sourced cord blood cells. The study indicated the cells that were previously cryopreserved maintained their extensive proliferative, self-renewal and *ex vivo* expansion capabilities. This study also showed that UC derived cells display higher engraftment capabilities compared to the bone-derived cells (Broxmeyer et al., 2003; Acosta et al., 2013).

UC-MSCs have been reported to possess “immature immunogenicity” which suggests that they are less likely to cause graft-versus-host disease during allogeneic transplantations (Acosta et al., 2013). In support of this hypothesis, a recent study carried out by Jin and colleagues showed that UC-MSCs present higher anti-inflammatory effects compared to MSCs from other sources. The study was carried out by measuring the number of secreted factors during inflammation and it demonstrated that UC-MSCs secrete the highest amount of angiopoietin-1, an inflammatory factor that modulates anti-inflammatory responses (Jin et al., 2013).

Earlier studies reported that hUC-MSCs display low levels of human leukocyte antigens-ABC (HLA-ABC) which have been shown to be an obstacle for allogeneic transplantation. Therefore, the lower expression of these markers makes UC-MSCs favourable for allogeneic cell transplantations (Maglieri et al., 2010). In addition, Wegmeyer and colleagues showed that compared to BM-MSCs, UC-MSCs secrete a higher level of hepatocyte growth factor (HGF), monocyte chemoattractant protein 1 (MCP-1), and macrophage colony-stimulating factor (M-CSF) cytokines (Wegmeyer et al., 2013). In particular, these proteins have been shown to have a role in MSC differentiation and inhibition of T-cell proliferation. However, BM-MSCs were shown to secrete

higher levels of interleukin-1 receptor antagonist (IL-1ra) which is mainly linked to anti-inflammatory and anti-fibrotic responses (Wegmeyer et al., 2013).

UC-MSCs share a range of neural markers, differentiating markers and extracellular adhesion molecules with BM-MSCS including CD13, CD29, CD44, CD73, CD90, CD105 and CD146. This means that they have similar differentiation capacity, cell cycle status, haematopoietic supportive function and cytokines to BM-MSCs (Maglieri et al., 2010; Lu et al., 2006). However, some studies have also reported contradictory data in regards to the expression of CD105 which is one of the markers required for MSC verification as outlined by the ISCT (Dominici et al., 2006). Although, most studies showed that CD105 is expressed by UC-MSCs even at later passages (> passage 16; Shi et al., 2015), some studies have also reported that UC-MSCs either do not express CD105 (Kadam et al., 2009) or they only express it until passage 5 (Bakhshi et al., 2008; Arutyunyan et al., 2016). Differently from the bone marrow cells, UC-MSCs have also been shown to express genes associated with embryonic stem cells (Kowsari et al., 2017). However, the expression of such markers was only observed under specific conditions. For example in early passage or post oxygen reduction from 21% to 5% O_2 (Arutyunyan et al., 2016).

In terms of differentiation potential, no differences were reported in the ability of UC-MSCs to undergo chondrogenic differentiation when compared to BM-MSCs (Nagamura-Inoue et al., 2014). On the other hand, previous work showed that UC-MSCs undergo insufficient osteogenic differentiation (even though they have been shown to express osteocyte related genes) in comparison to BM-MSCs which were able to easily undergo osteogenic differentiation (Mennan et al., 2013). Furthermore, differences have also been observed between UC-MSCs derived from different regions of the umbilical cord, and it has been reported that Wharton's jelly MSCs and whole UC-derived MSCs possess better differentiation abilities than MSCs derived from other regions such as those derived from the UC lining (Mennan et al., 2013). As for adipogenic differentiation, UC-MSCs were shown to produce small lipid vacuoles and less mature adipocytes than BM-MSCs (Mennan et al., 2013). Therefore, UC-MSCs may maintain their multipotency for an extended period of time compared to BM-MSCs.

UC-MSCs have also been shown to have less inter-donor variability compared to other MSCs (Wegmeyer et al., 2013). For example, in a study by Wegmeyer and colleagues, BM-MSCs, UC-MSCs and amniotic membrane (AM) MSCs were compared in terms of their biological functions. The study showed that whilst there were no differences in terms of the genetic background between AM-MSCs and UC-MSCs, contrasting results were observed in terms of their inter-donor variability. In fact, AM-MSCs displayed high inter-donor variability since only two of the five AM-MSC preparations met the minimal ISCT criteria for MSCs, whilst these differences were not observed between different populations of UC-MSCs. Therefore, the superior robustness and evident identity of UC-MSC stocks from different donors indicated that cells from the umbilical cord can be a reliable alternative for cell therapy applications (Wegmeyer et al., 2013).

Hypoxic pre-conditioning was also shown to unveil further differences between UC-MSCs and those from other sources. For example, one study compared MSCs from the BM, AT and UC that were subject to 1.5% O_2. The study showed that the levels of lactate production were significantly lower in UC-MSCs compared to those from other sources and the same was observed under normoxic conditions (Lavrentieva et al., 2010).

UC-MSCs have also been shown to have higher angiogenesis abilities than BM-MSCs. For example, one study showed that in Matrigel and co-culture assays, both BM-MSCS and UC-MSCs were able to undergo endothelial cell differentiation and form capillary-like networks. However, the UC-MSCs used in this study demonstrated a significantly higher number of total tubule length, diameter, and area than differentiated BM-MSCs. In support of these results, the RT-qPCR data from this study and immunocytochemical analyses showed that there was a higher expression of endothelial specific markers in UC-MSCs (Chen et al., 2009). Recent studies have also reported that the use of UC conditioned medium increased the lengths of the tubes formed in UC-MSC and HUVEC angiogenesis assays *in vitro* which are more representative of the capillaries formed *in vivo* (Shen et al., 2015).

In terms of migration, some studies have shown that BM-MSCs have higher migration abilities than UC-MSCs as observed in migration and scratch assays *in vitro* (Huang et al., 2015).

Overall, umbilical cord and bone marrow-derived MSCs share many similarities. However, UC-MSCs have been shown to possess several advantages over BM-MSCs including higher immunomodulatory abilities, proliferation and easier isolation, which makes them an excellent replacement to BM-MSCs for the treatment of several diseases.

1.6.2: Characterization of MSCs

In order to be able to compare results from different research groups using hMSCs from different sources, different methods of expansion and isolation and different characterization protocols, the Mesenchymal and Tissue Stem Cell Committee of the International Society for Cell Therapy (ISCT) proposed a standard minimum criteria to define hMSCs for *in vitro* and pre-clinical studies (Dominici et al., 2006). Three specifications were proposed:

1. hMSCs must display adherence to plastic when maintained in standard culture conditions (Dominici et al., 2006).

2. hMSCs must express high levels (≥ 95% positive) of CD73, CD90 and CD105, and lack expression (≤ 2% positive) of CD11b or CD14, CD19 or CD79α, CD34, CD45 and HLA-DR (unless stimulated by interferon-γ (IFN-γ) surface molecules (Dominici et al., 2006)).

3. hMSCs must be able to undergo tri-lineage differentiation which is the ability of the cells to differentiate into osteoblasts, adipocytes, and chondroblasts when using the standard *in vitro* tissue culture-differentiating conditions (Caplan, 2007).

1.6.3: Effect of cell age on the potency of MSCs

Several studies have looked into the effects of sequential passaging on the functional characteristics and morphology of MSCs (Dominici et al., 2006; Ullah et al., 2015; Choi et al., 2015). The long-term passaging of MSCs (>5 passages)

leads to less spatially organized, bigger in size and more heterogeneous cell cultures (Lo Surdo and Bauer, 2012; Whitfield et al., 2013, Jin et al., 2013).

Earlier studies compared BM-MSCs from three different passage numbers (P3, P5, and P6) and showed that younger and older cells meet the ISCT guidelines highlighted in section 1.6.2 (Dominici et al., 2006). In support of these results, a more recent study showed that following long-term expansion (up to passage 12), BM-MSCs and UC-MSCs display a decrease in proliferation capacity over time whilst still expressing MSC markers. In addition, cell age contributes to a decrease in immunosuppressive properties, this has been reported for both UC-MSCs and BM-MSCs (de Witte et al., 2017).

However, some studies showed that the effect of cell age on bone marrow MSCs is more significant. For example, Beane and colleagues demonstrated that old BM-MSCs display impaired proliferation, senescence, and chondrogenic response, whilst this was not observed in muscle-derived and adipose-derived MSCs (Beane et al., 2014).

Overall cell age affects cell proliferation but there is still need to confirm whether serial passaging has a significant impact on cell functionality or not. These contrasting results suggest that there is a need to standardize techniques between research groups to obtain comparative results.

1.7: Potential of MSCs for MI in clinical trials

Currently, there are over 493 clinical trials that are looking at the therapeutic use of MSCs with a focus on safety and efficacy of the cell product (Squillaro et al., 2016). Moreover, much of this work shows that the infusion of bone marrow stem cells has a positive impact on cardiac function (Wollert et al., 2004; Lunde et al., 2006; Wen et al., 2011; Acosta et al., 2013; Cashman et al., 2013). The positive results from animal studies have led to the initiation of phase I and phase II trials using BM-MSCs in humans. An indicator of prognosis in AMI patients is the left ventricular ejection fraction (LVEF) and the lower the LVEF the poorer is the patient's survival (Nair et al., 2015).

LVEF can be calculated using the following formula:

$$E_f = \frac{SV}{EDV} = \frac{EDV - ESV}{EDV}$$

Where:

EF = Ejection fraction
SV = Stroke volume (volume pumped from left ventricle per beat)
EDV = End-diastolic volume (volume of blood in a ventricle immediately before a cardiac contraction begins)
ESV = End-systolic volume (volume of blood in a ventricle at the end of contraction/systole)

The majority of clinical trials have used autologous bone marrow cells since it avoids the potential of rejection hence graft versus host disease (GvHD) which would require the patients being immunosuppressed (Wolf et al., 2009). However, using allogeneic therapies is a more attractive option as it can lead to the treatment of a larger number of patients.

1.7.1: Clinical outcomes of stem cells looking at LVEF

Several phase I and phase II trials have investigated the use of stem cells as a regenerative strategy to treat acute myocardial infarction (AMI) with LVEF being the most common endpoint, even though the results have been modest.

One of the first randomised trials looking at the use of progenitor cells for the treatment of AMI was the TOPCARE-AMI trial in which either bone marrow-derived progenitor cells (n = 29) or circulating progenitor cells (n = 30) were administered to the patients 5 days after percutaneous coronary intervention. The trial indicated an increase in LVEF (50 ± 10% to 58 ± 10%; $p < 0.001$) and no significant differences between the two cell types however, no appropriate control was available for comparison (Schachinger et al., 2004). Similarly, Yousef and colleagues studied the long-term benefits of bone marrow cells into the infarct zone of patients who suffered an AMI.

The study was performed on 62 patients who were administered BMCs 7 ± 2 days after AMI and with a control group of 62 patients who had similar LVEF and diagnosis. The benefits of BMCs were investigated after 3, 12 and 60 months. The results from this study, showed an improved EF with an 8% reduction in infarct size and with a significant reduction in mortality after 5 years in comparison to the control groups (Yousef et al., 2009).

The BOOST trial also looked at the effect of bone marrow stem cells (BMSCs) in patients following injection 5-7 days after AMI. The study showed a 6.7% increase in LVEF after 6 months when compared to the control groups. However, the benefits of the BMSCs were not observed after 18 months (Wollert et al., 2004). Similarly, the REPAIR-AMI trial which had 204 participants, showed that the administration of BMCs to the infarct zone led to improvement in LVEF compared to placebo (+5.5% versus +3.0%) at 4 month follow-up (Marenzi and Bartorelli, 2007; Nait et al., 2017). The largest phase II trial of autologous bone marrow mononuclear cells is the BAMI study which showed a 2.5% increase in EF against the control group. The ongoing BAMI trial is a phase III trial with a 20 year follow-up which would give further insights into the benefits of cell therapy in patients suffering from AMI (Mathur et al., 2017). Furthermore, because these trials used heterogeneous populations it is difficult to attribute the positive effects on LVEF to a specific set of cells. Overall most studies using bone marrow stem cells have shown an improvement in LVEF ranging from 3% in the REGENT trial (n = 200) to 13.1% observed in the CARDIAC study (n = 38) (Pinepoli et al., 2010; Maglieri et al., 2010, Hare et al., 2012).

The Cochrane review examined 33 randomised clinical trials (1765 patients) which showed a consistent improvement in left ventricular function in patients who were administered stem cells in comparison to those who underwent existing medical treatments. The conclusion from this review was that there is a lot of heterogeneity between studies (Martin-Rendon et al., 2008). However, various studies have also failed to show the presence of bone marrow cells in the myocardium after 1 to 3 months of infusion with some not detecting MSCs post 2 weeks of injection (Chin et al., 2003; Kurtz, 2008) which

indicates that there is a need to find an agreement in terms of delivery method, administration and cell preparation.

Some of the studies that showed a positive outcome following BM-MSC administration include the POSEIDON trial which looked at the effect of autologous and allogeneic BM-MSCs in patients suffering ischemic cardiomyopathy. This study was only performed on 5 patients per experimental group with no placebo controls. However, the results were encouraging and this was evidenced by a 1.96% increase in EF in both groups although not statistically significant (Hare et al., 2012). Similarly, Yang and colleagues transplanted autologous BM-MSCs in 16 patients with anterior MI and reported approximately a 9% increase in left ventricular ejection (after six months) from baseline (Yang et al., 2010). Whilst, in another study cardiac improvement following BM-MSC injection was observed after 3 months (Chen et al., 2004). Contrarily from the data in these clinical trials, other studies showed no improvement in LVEF upon infusion of BM-MSCs (Janssens et al., 2006).

A recent randomised clinical trial reported that UC-MSCs can be used as a replacement to BM-MSCs for the treatment of patients with heart failure and reduced ejection fractions (Bartolucci et al., 2017). 15 patients were used for each experimental and placebo groups. The study indicated a significant increase in LVEF after 12 months between the experimental and placebo groups ($7.07 \pm 6.2\%$ versus $1.85 \pm 5.6\%$; $p = 0.028$).

In another study, 116 patients with acute MI were randomly chosen to receive infusion of Wharton's jelly derived MSCs or placebo into the zone of injury. The patients were monitored over time in which there was a significant increase in perfusion at the infarct site with a 7.8% increase in LVEF in the MSC group at 18 months over the baseline compared to a 2.8% increase in the placebo group (Gao et al., 2015).

The majority of these clinical studies have small sample size as well as a high degree of heterogeneity in terms of cell product, the methodology used and cell dosing (Hare et al., 2012; Nair et al., 2015). Other treatments for heart

disease include using adipose tissue (AT) regenerative cells which have many similarities with MSCs. However, a clinical study performed on 14 patients administered with AT cells showed that there were no improvements in LVEF compared to the control group (Houtgraaf et al., 2012). Granulocyte-colony stimulating factors (G-CSF) were also shown to improve MI. G-CSFs are glycoproteins that stimulate the bone marrow to release granulocytes and stem cells into the blood-stream. In the MAGIC trial it was observed that when G-CSFs were infused together with BMSCs, LVEF increased from 46.4% ± 8.1% at baseline to 54.3% ± 11% after 6 months (Steinwender et al., 2006).

ACE inhibitors have been long shown to improve survival in AMI patients. For example, the SOLVD trial compared the administration of the ACE inhibitor enalapril (2.5-20 mg/day) to placebo for a year. The results showed a significant increase in LVEF from 0.25% to 0.29% ($p < 0.01$) in the enalapril group (Konstam, 1992). Currently, there are not many studies comparing the effect of pharmaceutical drugs used for the treatment of AMI and stem cells. However, pharmaceutical drugs are only used to subsidise symptoms and they do not aim to regenerate the heart tissue.

A recent phase III randomised multicentric trial compared the improvements in LVEF of patients with AMI who were infused with bone marrow stem cells in comparison to standard medical therapy. This study compared 125 patients who received 5-10 x 10^8 autologous bone marrow stem cells in addition to standard medical therapy and 125 patients that only received the standard medical therapy but no stem cells. The follow-up results after 6 months showed that in both groups there was an increase in mean change in LVEF of 7.05% in the stem cell groups and 4.1% in the non-stem cell groups which indicated a benefit in using stem cells for AMI (Nair et al., 2015). It is notable that the type of standard medical therapy used in this trial was not specified (Nair et al., 2015).

1.8: Clinical and pre-clinical outcomes of therapeutic angiogenesis and engraftment

Therapeutic angiogenesis and engraftment are strategies used to promote reperfusion to tissue and organs through the formation of new vessels and/or repair of existing vessels to affected ischemic tissue. MSCs have been shown to have pro-angiogenesis features and contribute to the formation of vasculature *in vivo* in a variety of vascular diseases (Tao et al., 2016).

The engraftment of MSCs is mediated by the interaction between cell surface receptors and glycoproteins found in the extracellular matrix (ECM) of the cells. The lack of cell engraftment is known to lead to anoikis (Ezquer et al., 2017). This is apoptosis induced by the loss of anchorage-dependent attachment to the ECM which results in cell death (Ezquer et al., 2017).

MSCs are known to improve cardiac function in patients with MI through their direct engraftment and integration at the site of injury. For example, in a pre-clinical study in swine, it was observed that the robust engraftment of BM-MSCs at the zone of injury attenuated the degree of contractile dysfunction at 4 weeks (5.4% ± 2.2% versus − 3.37% ± 2.7% in control) and reduced the extent of wall thinning which might have resulted from increased angiogenesis and perfusion at the zone of injury (Shake et al., 2001). Next, a phase I clinical study looked at the effect of infusing 1 x 10^6 cells/kg of allogeneic MSCs for the first infusion and 5 x 10^6 cells/kg for the second infusion into 5-6 children with osteogenesis imperfecta (Horwitz et al., 2002). This is a condition where the bones break easily due to a detective type I collagen. The data from this study indicated that the engraftment of mesenchymal cells at the site of injury resulted in clinically measurable benefits. In fact, cell engraftment was observed in different sites including bone and marrow stroma. Furthermore, striking benefits were observed in two of the patients where there was a significant improvement in bone growth ranging from 67% to 94% of the predicted median values over the first 6 months after MSC therapy. The data from this study, also indicated that the fraction of donor-derived osteoblasts in the biopsies was less than 1% and this suggests that low levels of MSC engraftment can result in clinical benefits (Horwitz et al., 2002).

Even though cell adhesion appears to have clinical outcomes and improve cardiac function, the engraftment of the MSCs is too low to account for the benefits observed in clinical trials (Becker et al., 2016). In fact, in most studies, MSCs only show limited engraftment or no engraftment at all which indicates that these cells may also be acting through other mechanisms for therapeutic effect (Becker et al., 2016).

MSCs are known to secrete several paracrine factors including fibroblast growth factor (FGF) and vascular endothelial growth factor (VEGF) which have been reported to promote local angiogenesis in pre-clinical and clinical studies (Schumacher et al., 1998, Prasajak et al., 2013; Lu et al., 2016). For example, in one study it was observed that when bone marrow mononuclear cells (BM-MNCs) were administered to the ischemic myocardium of swine, the cells expressed bFGF, VEGF and angiopoietin-1 as well as levels of TNF-alpha which was previously shown to increase cell engraftment (Prasajak et al., 2013). The results from this study showed that after 3 weeks following the injection of the BM-MNCs into the ischemic tissue, there was an increase in capillary density and blood flow at the zone of injury. Therefore, the data from this study suggested that the release of these factors might have promoted angiogenesis at the infarct site (Kamihata et al., 2001). In another study, which used a mouse aortic ring assay, BMC conditioned medium was shown to promote the formation of a significant number of tubes ($p < 0.01$; almost two-fold increase) which stimulated cell sprouting. Therefore, the increase in capillary density observed in this study, was associated with a reduction in necrotic and apoptotic cell death confirmed through staining assays (Korf-Klingebiel et al., 2008).

The importance of angiogenesis/branching *in vivo* is also evidenced by the clinical results from phase I trials. Clinical trials using pro-angiogenic factors have been limited to phase I studies and involved small sample sizes.

In an early pre-clinical study it was observed that the intracoronary injection of FGF-2 in 21 dogs with ischemia led to significant improvements in left ventricular function and 40% increase in transmural collateral flow (i.e. alternate circulation around a blocked artery or vein via nearby minor vessels). These improvements were observed as a result of vessel sprouting and capillary network formation

from the original coronary vessels with 6.7 ± 1.4 vessels/mm^2 capillary density for the experimental group versus 3.5 ± 0.7 vessels/mm^2 for the control group ($p < 0.05$; Unger et al., 1994).

Using genes encoding angiogenic cytokines such as VEGF is also another strategy used on patients who suffer from MI to promote the formation of collateral blood vessels which would allow for re-perfusion around the ischemic area (Losordo et al., 1998). For example, in an early phase I trial, naked plasmid DNA encoding VEGF (phVEGF165) was administered to 5 patients (aged 63.8 ± 3.4 years) who were unsuccessful with conventional therapy and who suffered angina (no placebo group). When phVEGF165 was injected at the site of injury, 2/5 patients showed an LVEF improvement of 5% and reduced ischemia in 5/5 patients. Myocardial perfusion was improved by the positive change in the mean number of normally perfused segments per patient which increased from 6.0 ± 1.1 before gene transfer to 8.0 ± 0.7 ($p < 0.05$) at day 60 after gene transfer, and a reduction of irreversibly ischemic segments from 2.4 ± 0.2 to 1.2 ± 0.4 ($p < 0.05$) at day 60 follow-up examination (Losordo et al., 1998). Similarly, in a phase II clinical trial (with placebo controls, 27 patients), phVEGF-2 was administered to three treatment groups at 200 µg, 800 µg, or 2000 µg. The results from this study, indicated that there was an improvement in Canadian Cardiovascular Society (CCS) angina class in phVEGF2-treated versus placebo-treated patients (-1.3 versus -0.1, $p = 0.04$). The improvements observed in the angina class and in the other endpoints of the study, were associated with a significant increase in vessel formation (5.9 ± 1.0% to 13.2 ± 1.3% in phVEGF-2 patients; $p = 0.004$) which followed a reduction in ischemic site from 6.4 ± 2.2 cm^2 before gene transfer to 2.6 ± 1.4 cm^2 after gene transfer (Losordo et al., 2002).

Overall the results from these studies indicate that increasing the number of blood vessels in ischemic areas via pro-angiogenic factors is desirable for optimal therapeutic effect in AMI. Therefore, it can be concluded that future biological assays should also be aiming to improve angiogenesis and cell engraftment as endpoints.

1.9: Mode of action of MSCs for cardiac repair

Evidence suggests that there are various mechanisms (listed below) by which MSCs can repair the infarcted myocardium.

Mode of action	**References**
MSCs induce the reprogramming of CMs into cardiac progenitor cells that can repair the heart.	Acquistapace et al., 2011
MSCs transdifferentiate into CMs and restore cardiac function.	Tomita et al., 1999; Yoon et al., 2005
MSCs trigger cardiac repair through paracrine signalling.	Koninckx et al., 2009; Wollert et al., 2004; Cashman et al., 2013
MSCs trigger tissue repair by reacquiring a pericyte phenotype.	Kean et al., 2013; Melero-Martin et al., 2008; Gnecchi et al., 2012; Au et al., 2008
Electrophysiological MSC-CM coupling may improve functionality of cardiac tissue.	Mayourian et al., 2016

Table 1-2: Mode of action of MSCs.

Several studies showed that the co-culture of MSCs with cardiomyocytes triggers their reprogramming into cardiac progenitor cells. A study from Acquistapace and colleagues supported this theory and demonstrated that the MSC-CM co-cultures led to the increase in cardiac progenitor markers and proliferation (Acquistapace et al., 2011). MSCs have also been reported to transdifferentiate into cardiomyocytes in the injured cardiac tissue of animal models *in vitro* and *in vivo* thus leading to cardiac repair (Tomita et al., 1999; Yoon et al., 2005).

However, it has been shown that only <2% of the transplanted MSCs transdifferentiate into cardiomyocytes (Arnous et al., 2012). Further evidence has suggested that perhaps MSCs do not transdifferentiate but instead fuse with the CMs (Kouris et al., 2012). In opposition to this finding, Tsuji et al. (2010), carried out an experiment which involved the staining of human amniotic membrane-derived mesenchymal cells (hAMCs) with MitoTracker Red (Invitrogen, M7512), a red fluorescence dye, followed by co-culture with enhanced green fluorescent protein (EGFP) murine CMs. The study showed that MitoTracker positive cardiomyocytes were EGFP negative so there was

no cell fusion between the CMs and the hAMCs (Tsuji et al., 2010). Hence, this work disproved the MSC-CM cell fusion mechanism of action.

Of particular interest is the conclusion by Koninckx and colleagues, who stated that although transdifferentiation of MSCs may take place, paracrine effects do play a much bigger role in cardiac repair. The basis for Koninckx's conclusion was that the immature cardiomyocytes would most likely induce a minor effect in cardiac repair (Koninckx et al., 2009). On the other hand, paracrine factors secreted by the stem cells could improve the functionality of mature cardiomyocytes.

Various clinical trial studies showed that the beneficial effects of transplanted MSCs are transient. For example, in a study carried out by Wollert and colleagues which involved the transplantation of autologous derived BM stem cells it was observed that the effects only lasted for six months. Follow-up work showed that after 18 months the beneficial effects of MSCs were severely reduced (Wollert et al., 2004; Cashman et al., 2013). Although these data suggest that MSCs do repair the injured heart by releasing paracrine factors, the results also suggest that, as the stem cells differentiate or disappear by apoptosis, the concentration of the paracrine factors decreases hence affecting their beneficial effects (Wollert et al., 2004; Cashman et al., 2013).

MSCs have been shown to trigger angiogenesis by also assuming a "perivascular-like" phenotype in the basement membranes of newly forming capillaries where they favoured and contributed to their stabilization (Kean et al., 2013). Melero-Martin and colleagues performed a study which involved the co-implantation of endothelial progenitor cells and hMSCs into immunodeficient mice, and vascular network formation was observed within a week (Melero-Martin et al., 2008; Gnecchi et al., 2012). Similarly, Au et al. (2008) showed that when MSCs were co-transplanted with HUVECs they enhanced blood vessel assembly and adopted a perivascular phenotype (Au et al., 2008). However, it has also been previously reported that although pericytes are a subpopulation of bone marrow MSCs with vasculogenic potential, not all MSCs display a pericyte-like behaviour (Blocki et al., 2013). As multiple modes of action have been proposed for MSCs, there is a need to

develop assays that can precisely give information on their functional characteristics and speed the translation of MSC-based therapies into the clinical setting.

1.10: Preconditioning MSCs for clinical efficacy

A major challenge in the clinical efficacy of MSCs is the low viability of the engrafted cells in the zone of injury due to anoikis. Decreased cell survival can also be attributed to the hostile environment in the injured myocardium where a highly inflammatory and cytotoxic process takes place to remove anything unnecessary in the injured myocardium and leads to oxidative stress (Ezquerchen et al., 2017). Various research groups are now looking into strategies to improve cell survival for therapeutic efficacy.

1.10.1: Hypoxia pre-conditioning of MSCs *in vitro*

Several studies have shown that hypoxia (1-7% oxygen) positively impacts on migration, metabolism, angiogenesis, and cell stemness (Moriyama et al., 2014; De Becker and Riet, 2016) and that normoxia may hinder the therapeutic potential of hMSCs (Basciano et al., 2011). For example, Lan and colleagues showed that when BM-MSCs were subject to 1% O_2 for 24 hours, the cells were able to engraft in an animal model of idiopathic pulmonary fibrosis four times better than the untreated cells (Lan et al., 2015). The benefits of MSCs subject to hypoxic conditions were also observed in an acute myocardial infarction murine model. In this study, the authors reported a 2.5 fold increase in engraftment after one day of intravenous injection which led to a decrease in myocardial infarct site (Ezquer et al., 2017).

The results from different research groups have been difficult to compare due to differences in oxygen tension ranging from 0.1 to 5%, and different culture times ranging from a few minutes to 2 months (Bain et al., 2014; Basciano et al., 2011). For example, it was shown that when BM-MSCs were subject to 2% oxygen tension for 20 min there was an increase in their migration and a decrease in adhesion abilities (Bain et al., 2014). In another study it was observed that cells subject to 5% O_2 display increased level of adhesion and extracellular matrix molecules in MSCs (Basciano et al., 2011).

Many studies assessed whether levels of oxygen below 5% O_2 have an effect on the MSC function such as their differentiation abilities and angiogenesis potential. Holzwarth and colleagues showed that levels of oxygen between 3% and 5% (after 3 weeks in culture) did not impact on the differentiation of MSCs whilst the cells that were cultured in <1% O_2 showed impaired differentiation abilities (Holzwarth et al., 2010). In another study it was demonstrated that culturing MSCs at 5% O_2 (after 21 days in culture) inhibits osteoblast differentiation (Raheja et al., 2010). Whilst in a study by Zhang and colleagues hUC-MSCs were cultivated in 1%, 3% and 5% oxygen tensions following their induction to cardiomyocyte-like cells. However, it was observed that only when hUC-MSCs were pre-conditioned in 3% O_2 there was an enhanced proliferation and differentiation to cardiomyocyte-like cells, and no significant differences were observed at 1% O_2 and 5% O_2 (Zhang et al., 2015). Hypoxia was also shown to increase the secretion of HIF-1 in MSCs leading to a two-fold up-regulation of VEGF and a higher angiogenetic ability than normoxic MSCs (Zhang et al., 2012).

The effect of hypoxia is also source-specific. For example, in a study by Lavrentieva and colleagues, it was observed that hypoxic hUC-MSCs displayed much lower lactate levels than hBM-MSCs and adipose-derived MSCs (Lavrentieva et al., 2010). Moreover, low oxygen also appeared to impact differently on MSCs at different passages. For example, Basciano and colleagues observed that until passage 1, MSCs grew more slowly when subject to 5% O_2 than in normoxic conditions, whilst as they were expanded further they displayed a growth rate advantage compared to the cells cultured in ambient oxygen (Basciano et al., 2011). Overall, these studies indicate that hypoxia may be an optimal pre-conditioning strategy to increase the beneficial effects of MSCs and to investigate their mechanism of action in an environment that closely mimics the physiologic injury sites. However, there is a need to carry out further studies looking at the impact of different ‘low-oxygen’ conditions on the potency of cells and to compare the effects that it has on differently-sourced cells.

1.10.2: Engraftment strategies to increase angiogenesis, adhesion and migration

Two major contributors to the successful engraftment of MSCs at the site of tissue injury are cell adhesion and migration. In fact short adhesion times are required to avoid post-surgical complications (Chang et al., 2015). A recent study showed that it takes a minimum of 30 minutes for multi-layered MSC sheets to adhere to the heart tissue (Chang et al., 2015). As a result, various studies have investigated the effect of regulating key molecules involved in cell attachment such as integrin receptors (Lee et al., 2015; Veevers-Lowe et al., 2011).

A study carried out on the infarcted myocardium of a rat, showed that when MSCs were induced to overexpress tissue transglutaminase a co-receptor for fibronectin in cell adhesion associated with integrins, there was an increase in the ability of MSCs to attach, spread and migrate, leading to improved heart function. In this study, it was also reported that MSCs overexpressing tissue transglutaminase, showed a 20% increase in adhesion on FN and a 4.75% and 2.52% increase in spreading and migration (Song et al., 2007). FN is an ECM protein which contains the site for integrin α5β1 that MSCs express and during an MI it accumulates in the injured sites of the heart to stop the bleeding (Van Dijk et al., 2008; Veevers-Lowe, 2011). FN has been shown to increase the adhesion properties of BM stem cells *in vitro* (Van Dijk et al., 2008).

Recent studies showed that microRNAs may also have a role in enhancing MSC survival and adhesion (Lee et al., 2015). For example, Yu and colleagues showed that the expression of one microRNA, miR-125b, achieved through the knockdown of beta5 integrin protects MSCs from anoikis (Yu et al., 2012). The modulation of MSC pro-angiogenic factors gives insights on the activation of other signalling pathways involved in cell migration, proliferation, and network formation. For example, in one study it was observed that the knockdown of Neuropilin-1, a pro-angiogenic receptor, decreases cell proliferation and hinders platelet-derived growth factor receptor signalling which is involved in the mobilization of MSCs in neovascularization and tissue remodelling (Ball et al., 2010).

1.10.2.1: Engraftment of MSCs and Notch pathway

The Notch signalling pathway is highly conserved and plays an important role in regulating EC function during sprouting and angiogenesis by aiding communication between adjacent cells (Benedito et al., 2009; Lu et al., 2016). The Notch pathway can be triggered via the Notch ligands binding to their receptors. In mammals, these ligands are encoded by the Jagged (Jag1 and Jag2) and Delta-like (Dll1, Dll3, and Dll4) gene families (Gridley, 2010). The primary targets of the this signalling pathway are the Hes and Hey genes, the latter plays a key role in the development of the cardiovascular system (Rizzo et al., 2014).

Several studies showed that targeting the Notch signalling pathway may enhance responses relevant to cardiovascular regeneration using MSCs (Xie et al., 2013). For example, Semon and colleagues showed that when MSCs were pre-stimulated with tumour necrosis factor alpha, a key cytokine known to up-regulate Jagged1-mediated Notch signalling in EC tip cells, there was an increased cell adhesion to the endothelium (Johnston et al., 2009; Semon et al., 2010). The overexpression of Jag1 enhances angiogenesis whereas the opposite is observed in mutants that lack this gene (Benedito et al., 2009). Jagged1 was also shown to enhance the differentiation of MSCs into cardiomyocytes. For example, Li and colleagues showed that the addition of Jag1 in MSC-CM co-cultures enhanced the differentiation of the mesenchymal cells into cardiomyocytes (Li et al., 2006). Whilst in another study it was observed that the proliferation of cardiomyocytes is increased by direct co-culture with MSCs which act through paracrine mechanisms to up-regulate the Notch1-Jag1 pathway (Sassoli et al., 2011). Evidence also suggests that blocking Notch signalling in BM-MSCs promotes cell migration *in vitro* and up-regulates the cell receptor CXCR4 which is beneficial for cell survival and homing (Cao et al., 2013; Xie et al., 2013). Various studies have also looked into the effect of hypoxia on Notch signalling. For example, in one study it was observed that culturing human adipose progenitor cells in 5% O_2 increased their proliferative capacity and maintained their stemness. These benefits were linked to an increase in the levels of activated Notch1 by hypoxia and the expression of its downstream gene Hes1 (Moriyama et al., 2014). Similarly, Ciria and colleagues showed that cultivating MSCs in 1% O_2 for 4 hours leads to the overexpression of HIF-1 which induces

Notch-dependent migration and spreading of MSCs through the overexpression of the ligands Jagged 1-2 and Dll1, Dll3, and Dll4 (Ciria et al., 2017). Overall Notch signalling plays a key role in MSC cardiac differentiation, migration, proliferation and angiogenesis, all of which contribute to the recovery of the myocardium after cardiac injury (Li et al., 2010; Rizzo et al., 2014). Hence further work investigating the effect of MSC pre-stimulation by Notch ligands could be beneficial to speed their clinical application as a therapy to treat myocardial injury.

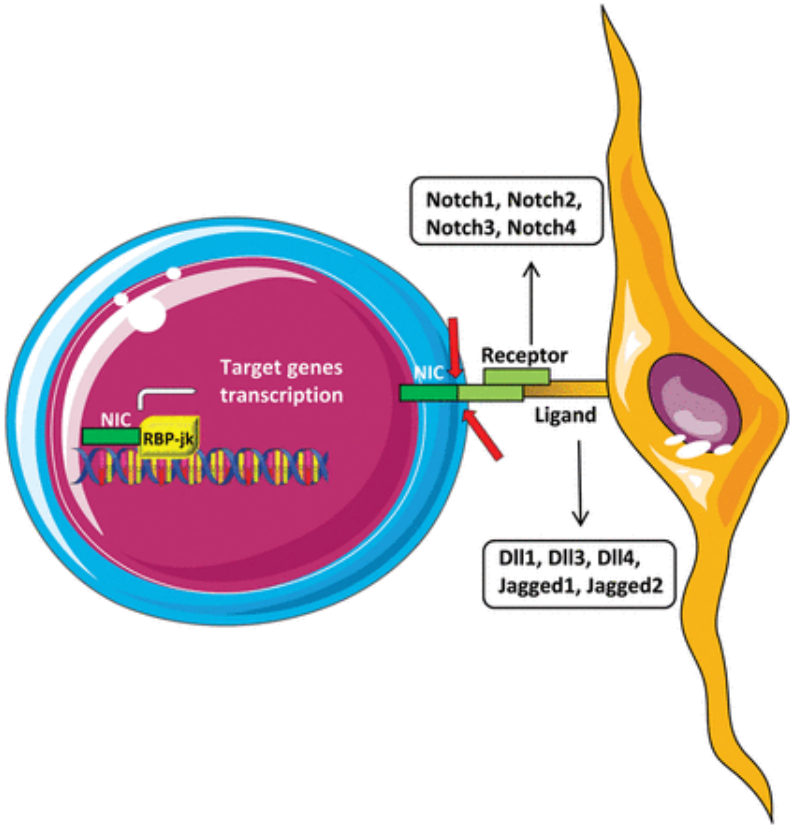

Figure 1-2: Notch signalling pathway- Notch receptors can be found on the cell surface. When Notch ligands bind to the Notch receptors (Notch1, Notch2, Notch3, and Notch4), two proteolytic cleavages take place leading to the release of the active form of Notch (NIC). NIC then migrates to the nucleus and binds to the transcription factor RBP-jk (recombination signal binding protein for the immunoglobulin kappa j region) and controls the transcription of specific genes (Rizzo et al., 2014).

1.11: In vitro angiogenesis assay methods

This section will give an overview of the methods used to carry out *in vitro* tubule formation assays. In addition, it will include a comparison of *in vivo* versus *in vitro* angiogenesis assays. Of interest to this work is endothelial cell-based assays seeded on Matrigel.

1.11.1: ECs for *in vitro* studies

In vitro assays are often used to study the regulatory role of angiogenic factors particularly on endothelial cells (Arnaoutova and Kleinman, 2010). Tubule assays use a range of ECs including human microvascular endothelial cells (HMECs), ECs sourced from mice and primary human umbilical vein endothelial cells (HUVECs). The last are the most widely used for *in vitro* assays because they are primary cells which can be easily isolated in the lab (Smith and Staton, 2007). However, the problem with primary cells is that they have limited function and replicative lifespan, with studies showing that ECs experience significant senescence after a sequence of ten serial passages (Smith and Staton, 2007; Suh et al., 2015). Moreover, Skinner and colleagues showed that ideally primary ECs should be used between P2 and P6, whilst it was observed that using the cells below P2 and above P10 is not beneficial for maximum tube formation, with a decrease in network formation observed after the sixth passage (DeCicco-Skinner et al., 2014).

Another problem encountered with primary cells is that they are sourced from various donors using different cell extraction techniques which hinders data comparison for *in vitro* assay work (Smith and Staton, 2007; Staton et al., 2009). This has increased the demand of well-characterized cell lines such as immortalised cells, which due to mutation can undergo indefinite division. However, immortalization involves changing cell characteristics and therefore it will affect the angiogenic potential of the cells and gene expression. Moreover, it may lead to subsequent cell phenotypic changes after several passages. For example, Nisato et al. (2004) showed that HMEC-1, a cell line established by Ades and colleagues, stopped forming tubules after 12 years (Nisato et al., 2004). Also, because of the higher cell maintenance costs and availability of

HMCE-1 cells, HUVECs will always be the preferred choice for regular *in vitro* studies (Ades et al., 1992; Nisato et al., 2004; Staton et al., 2009).

1.11.1.1: HUVECs

The majority of *in vitro* tubule assays have been performed using HUVECs because they are primary cells, they can be easily isolated in the lab and they are commercially available (Smith and Staton, 2007; Cao et al., 2017). HUVECs have also been shown to express more important endothelial markers than other endothelial cells e.g. vascular cell adhesion molecule 1 and signalling molecules which have a role in vascular physiology (Cao et al., 2017). Also, compared to other types of endothelial cells, HUVECs have been shown to respond to a variety of physiological stimuli such as shear stress, high glucose and hypoxic pre-conditioning (Zhang et al., 2012; Cao et al., 2017). For example, in one study it was observed that when HUVECs were subject to hypoxic pre-conditioning, there was a reduction in apoptosis. In addition, when the endothelial cells were co-cultured with MSCs in hypoxic conditions for 12, 24, 48 and 72 hours there was an increase in survival, migration, and angiogenesis (Zhang et al., 2012). Therefore, HUVECs can be used to test different factors on the endothelium through *in vitro* tube formation assays and to also give an insight on the function of other cell types in neovascularization (Zhang et al., 2012). Furthermore, when performing experiments it is important to recognise the differences between HUVECs and other types of endothelial cells. For example, palmitic acid can activate human microvascular endothelial cells *in vitro*, whilst no response is observed with HUVECs (Cao et al., 2017).

The growth of HUVECs *in vitro* is limited to a few passages even in optimal conditions which include the use of heparin, endothelial cell growth supplements and high serum concentrations (O' Donnell et al., 2000). The limited life-span of primary ECs is an issue for long term-studies (Smith and Staton, 2007). Therefore, recent studies have looked into the use of stem cells as a potential source of primary ECs (Cao et al., 2017). For example, it was shown that fibroblasts can be reprogrammed into iPSCs and then differentiated into functional endothelial cells (Margariti et al., 2012; Cao et al., 2017), hence

allowing for the production of large number of ECs and making iPSCs derived endothelial cells a potentially good model as primary ECs (White et al., 2013). In conclusion, whilst further work is needed to be carried out on stem cells to overcome the limited supplies of ECs, HUVECs will be the best option for *in vitro* vascular assays for the study angiogenesis (Smith and Staton 2007; Cao et al., 2017).

1.11.1.2: Heterogeneity of ECs

Endothelial cells have the ability to adapt to the needs of different tissues within the body. For this reason, they present a high degree of heterogeneity. ECs can differentiate based on their size, shape, thickness and the vascular bed they are derived from. The microenvironment is a deciding factor in endothelial cell phenotypic differences (Jackson and Nguyen, 1997). Jackson and Nguyen (1997) observed different secretion levels of angiogenic factors between HUVECs and human endothelial cells derived from neonatal foreskin (Jackson and Nguyen, 1997). Furthermore, a study by Gallery and colleagues showed that decidual microvascular endothelial cells need high concentrations of serum for growth (Gallery et al., 1991). Contrary to this conclusion, Jackson & Nguyen, 1997 showed that endothelial cells derived from the umbilical vein are not affected by the absence of serum (Jackson and Nguyen, 1997). These data suggest that different culture conditions may be required for cells derived from different tissues.

1.11.2: Endothelial cell tubule formation assays

In vitro tubule formation assays by endothelial cells can give valuable information on a particular step in vascular network formation such as proliferation, migration, or differentiation. Tubule formation can be achieved using a variety of substrates including but not limited to fibrin clots, collagen and Matrigel (Donovan et al., 2001; Gambino et al., 2017). The type of matrix used in these assays strongly affects the rate of tubule formation. For example, seeding cells on interstitial collagen (collagen I and collagen III) results in cell proliferation but very limited tubule formation. On the other hand, it was previously reported that when cells were plated on collagen from the basement membrane (collagen

IV and collagen V), there was not much proliferation occurring but the rate of tubule formation was high.

Both collagen and fibrin have been used to carry out 3-D *in vitro* assays since the 1980's and not so much for 2-D studies (Montesano et al., 1993; Calderon et al., 2017; Gambino et al., 2017). Tubule formation on collagen in 2-D tubule assays takes several days to be performed and they are difficult to quantify since not all of the cells form vessel-like networks (Arnaoutova and Kleinman, 2010). Instead, tubule formation on Matrigel only takes 4-12 hours, for this reason this has ultimately become the preferred matrix for this type of assay. Matrigel is a mixture of extracellular basement membrane proteins including collagen IV and laminin that is sourced from the mouse Engelbreth–Holm–Swarm sarcoma proteins (Faulkner et al., 2014).

Matrigel assays are easy to carry out and to quantify. For example tubule networks can be imaged through an inverted microscope and quantified based on their length, number of branch points and tubule area (Arnaoutova and Kleinman, 2010). Many companies including BD Biosciences have now developed a growth factor reduced (GFR) form of Matrigel. This GFR form contains very low levels of growth factors thus avoiding over-stimulation of endothelial cells observed with the standard Matrigel which interferes with efficacy studies of proangiogenic factors (Staton et al., 2004; Xie et al., 2016). One key disadvantage in using Matrigel is variability lot-to-lot which can majorly affect tubule formation activity as well as data robustness and reliability. For this reason, it is strongly recommended to purchase high quantities of the matrix and carry out experiments in triplicate wells (Arnaoutova and Kleinman, 2010).

1.11.2.1: Co-culture functional assays

Another type of tubule formation assays involves the co-culture of endothelial cells with stromal cells, such as fibroblasts, smooth muscle cells and blood vessel explants. These types of assays were developed to better mimic the *in vivo* capillary structures. In addition, they can be carried out with/without the aid of a matrix. Co-cultures performed without the aid of a basement membrane take 12-14 days compared to when the cells are co-cultured on Matrigel

(Donovan et al., 2001). This is because they require the fibroblasts to initially secrete extracellular matrix (ECM) components which act as a platform for tubule formation (Bishop et al., 1999).

The capillary-like structures in co-culture usually form in two-dimensional planes thus facilitating assay quantification and they also resemble more the capillary bed *in vivo* (Donovan et al., 2001; Smith and Staton, 2007). Co-culture assays where MSCs are co-cultured with ECs in conditions that mimic the physiological environment have been used to study the effect of MSCs in angiogenesis and to compare different cell types (Zhang et al., 2012; Ma et al., 2014). For example, Ma and colleagues co-cultured either adipose-derived MSCs or BM-MSCs with HUVECs concluding that they both had equal angiogenic potential (Ma et al., 2014).

1.12: In vivo angiogenesis assays

The table below summarizes the most widely used *in vivo* angiogenesis assays.

Assays	**Procedure**	**Quantification**	**References**
Chick chorioallantoic membrane (CAM) assay	The CAM embryo of the chick is used as a physiological environment for *in vivo* analysis of cells, pathogens and pharmacological reagents.	Microscopy, determining content and synthesis of DNA, protein and basement membranes	(Norrby, 2006; Staton et al., 2009)
Corneal micropocket assay	Given that the cornea is the only avascular transparent tissue in the body, it is optimal for assessing neovascularization. Usually, micropockets are made in the stroma of the cornea following implantation of slow release polymers.	Transmission and scanning electron microscopy	(Norrby, 2006; Staton et al., 2009)
Dorsal air sac model	Involves implantation of a chamber ring loaded with tumour cells on the mouse dorsal air sac to induce angiogenesis.	Microscopy- or photographs of the skin	(Oikawa et al., 1997; Staton et al., 2009)
Zebrafish assay	Involves implantation of cells in the zebrafish developing embryo followed by monitoring of vasculature development and angiogenesis after transplantation.	Microscopy	(Staton et al., 2004, 2009, Taylor et al., 2009)

Table 1-3: Summary table of *in vivo* angiogenesis assays.

1.13: In vitro versus in vivo angiogenesis assays

The table below summarizes the key comparison points between *in vitro* and *in vivo* angiogenesis assays.

	In vitro	**References**	***In vivo***	**References**
Advantages	-quick and easy to perform.	Staton et al., 2004; Smith and Staton, 2007; Tahergorabi and Khazaei, 2012	-Allows for the study of the complex physiological processes that occur *in vivo*.	Staton et al., 2009
Disadvantages	-Can behave differently depending on the culture conditions (i.e. still vs. flowing) and when seeded onto different matrices. -May not show comparable results to the *in vivo* work.	Staton et al., 2007	-Expensive, not easy to perform and time-consuming. -Difficult to quantify. -Involves using non-human tissue.	Guedez et al., 2003; Staton et al., 2007; Tahergorabi and Khazaei, 2012; Chen et al, 2013

Table 1-4: Summary of advantages and disadvantages of *in vitro* and *in vivo* angiogenesis assays.

Overall, all of these observations suggest that *in vitro* models of vasculogenesis and angiogenesis can give initial information on cell function. *In vivo* assays can then validate the results from the *in vitro* tests. Moreover, since *in vitro* assays are less time consuming, it is possible to carry our more tests whereas there are only a limited number of tests that can be carried out using *in vivo* assays (Auerbach et al., 2003; Tahergorabi and Khazaei, 2012).

1.14: Quantification of release assays

According to the guidelines set by the EMA, the measured biological function of a product from a potency assay should closely relate to the product's clinical response (European Medicines Agency, 2016). The type of assays performed,

can be either *in vitro* or *in vivo*. *In vitro* assays are usually used for short time scale experiments and examples include the enzyme-linked immunosorbent assay (ELISA) and microarray technology (Stroncek et al., 2007). Although *in vivo* animal models can directly measure the biological function of the product, there is an inherent variation between the results. Additionally, the testing of animal models is less cost-effective than experiments *in vitro*. This section will give a quick overview of three *in vitro* release tests: ELISA, transcriptome-based screening and metabolite screening.

1.14.1: ELISA for growth factor release

The enzyme-linked immunosorbent assay technique is commonly used for cell product characterization. This test quantifies the concentration of the protein of interest in a solution, by using antibodies specific to the particular protein. The reaction product is then detected through colour change of the solution and measured by using a spectrophotometer (Gan and Patel, 2013; Leng et al., 2008). ELISA has often been used as a surrogate for potency testing during the initial phase development of a biological product (Stroncek et al., 2007; Thej et al., 2017). This is because it is easy and quick to carry out and it allows for the processing of several samples in parallel. This test can be used to measure growth factor release and protein expression that are necessary for understanding cell function. However, it cannot confirm whether the product will display the desired potency (effect) *in vivo* or not and for this reason, there is a need to develop better assays that can address the complexity of cellular therapy products.

In the case of cytokine release by the inflammatory response, this simple test cannot give a full evaluation of the complexity and dynamic response of such process (Leng et al., 2008). Also, its performance is very much dependent on the user's skills, the manufacturer and the quality of the antibody (Aziz et al., 1999). This could lead to differences in cytokine levels when comparing the data of two different ELISA assays carried out in slightly different conditions. Moreover, ELISA-based assays have a dynamic range (range of linearity between cytokine concentration and absorbance reading in the standard curve) over which the samples will need to be diluted. This dilution lowers the

concentration of the cytokine to be quantified, and it may affect the concentration of other molecules contained in the solution such binding proteins. Additionally, it can lead to the amplification of differences in readings between samples that require dilution and samples that do not because they fit within the dynamic range (Leng et al., 2008). Overall, there is a need to look at technologies that can more directly determine the biological function of a cell product and overcome some of these drawbacks.

1.14.2: Gene expression microarrays and qPCR

The quantification of genes associated with a specific cell function could be used as a surrogate to *in vitro* potency testing. For example, quantitative real-time PCR has been used to quantify the expression of specific cytokines triggered by T-cell activation and to study other cell related processes including angiogenesis, cell-cycle, and apoptosis (Stroncek et al., 2007). qPCR can be used to screen single genes as well as groups of genes but it is not sufficient to screen a broader range of gene transcripts. Moreover, gene expression microarrays have been used to simultaneously measure the expression of more than a thousand genes (Stroncek et al., 2007). Microarray technology can screen all the gene expression profiles related to cell function and other cell characteristics such as stability and purity. Because this technology gives an indication of the signals that lead to cell death, it could be particularly useful for cell viability studies. The gene expression profiles can also detect the presence of other cell subpopulations thus giving an indication of cell purity (Stroncek et al., 2007).

Ultimately, because microarray screening gives a better insight in cell function compared to other techniques, it would be particularly beneficial to use it in the context of stem cell research. However, there are limitations associated with such technology for lot release testing. For example, there is a need to carry out several steps before gathering the data which means that until further technology advances are developed, it is very unlikely to carry out these steps in just a few hours (Stroncek et al., 2007).

1.14.3: Metabolomics screening

Metabolomics screening tests are generally used to quantify the presence of metabolites in biological specimens such as body tissues and body fluids (Dettmer et al., 2007). For this reason, it has found application in many disease-related studies including cardiovascular diseases (Dettmer et al., 2007). The advantage that metabolomics has over other analytical methods is that there are only a small number of human metabolites (≈7000) compared to the approximate 25 000 genes, 100 000 transcripts, and 1 000 000 proteins. The human metabolome is composed of a variety of compounds belonging to different compound classes, such as lipids, proteins, and nucleotides. These different compounds display not only a significant chemical diversity but are also found at different concentrations (Dettmer et al., 2007). Although there has been significant technological advancement during the past few years, the current analytical instruments available can measure only a limited number of analytes simultaneously in one single analysis. This suggests that there is a need to develop high throughput protocols that can profile a wider range of metabolites in a given biochemical pathway, in particular in the case of cell therapies. In this way, the data gathered would allow for a better understanding of metabolic perturbations, and could be integrated with other omics data (e.g. genomics and proteomics) to give a complete picture of biological function (Dettmer et al., 2007).

1.15: QbD for process standardization

In 2002, the Food and Drug Administration (FDA), decided to make improvements to the systematic and risk-based approach used in industry with the “cGMP for the 21st Century: A Risk-based Approach” initiative (FDA, 2004). This initiative involved the use of quality by design (QbD) and the publication of the process analytical technology (PAT) guidance (FDA, 2004). Furthermore, three guidance documents followed as part of the International Conference on Harmonization (ICH): Q8 Pharmaceutical Development and Q9 Quality Risk Management, in 2005, and ICH Q10 Pharmaceutical Quality System, in 2008. According to ICH Q8, QbD can be defined as a holistic approach to development that allows for predefined product specifications through the understanding of the products and processes, process control and quality risk management. Quality in itself is then

related to the suitability of a product to its intended use which includes attributes of identity, strength, and purity (FDA, ICH Q8 2009).

The aim of QbD is to make processes more cost-effective and improve the quality of the process or the product. This approach involves the interaction between product knowledge and process understanding for continuous improvement (Figure 1-3), which according to ICH Q8 can be gained through design of experiments (DOE), process analytical technology (PAT) and/or previous knowledge. Quality risk management can also be used to recognise the studies required to acquire such knowledge.

Figure 1-3: Quality by design (QbD) concept as presented by the FDA

QbD processes and product development should include the following elements (FDA, ICH Q8 2009):

- Defining the quality target product profile (QTPP) which is obtained from the desired product information such as safety and efficacy.
- Identifying potential critical quality attributes (CQAs) of the drug/cell product to study and control the product characteristics that affect product quality.
- Choosing appropriate manufacturing processes.
- Designing and implementing control strategy.

1.15.1: Development of cell-based potency assays

The cell-based therapy industry is faced with several bottlenecks, which include the intrinsic variability between cells, the lack of robust standard reference analytes and the difficulty in accurately measuring function. For this reason, there is a need to identify the sources of variation that affect the product and reduce/eliminate them. The difficulty in controlling the factors associated with cell quality has led to the failure of many cell-based bioprocesses (Ratcliffe et al., 2011). Along with other tests that are required for product quality and reproducibility, cell-based potency assays are integral to effective QbD as they ensure that only products that meet a specific requirement are given to patients (Porat et al., 2015). Potency can be defined as the mode of action of the cell product, as indicated by predefined laboratory tests or data from clinical studies, to achieve a given result (Porat et al., 2015). The optimization of cell-based potency assays is fundamentally important for cell-based therapy bioprocessing especially considering the biological complexity of cells, as well as variations between lots. As part of good manufacturing practice regulations, potency assays used for release testing are required to (Porat et al., 2015):

- Measure identity and strength (activity) of the product e.g. the indication of biological activities specific to the product with results that correlate to an effect in a relevant animal model and human trials.

- Provide quantitative data.
- Include appropriate reference materials, replicates and controls to make sure that the assays perform as expected. The controls selected for the assays will then be chosen based on the product being analysed and the assays used.
- Identify and establish the accuracy, sensitivity, specificity, and reproducibility of the assays used.
- Adhere to pre-defined acceptance and/or rejection criteria.
- Provide data to establish dating periods.
- Meet labelling requirements.

As part of QbD, a typical approach is to identify the key process input variables (KPIV) and key process output variables (KPOV) and have a range of acceptability in order to achieve good product standards. KPIVs can then be studied through a combination of design of experiments, mathematical models, or studies that lead to mechanistic understanding to gain a better understanding of the process.

Traditional pharmaceutical approaches involve a one-factor at a time approach where only one variable is tested per experiment. On the other hand, DOE involves the use of statistical designs to understand the product. Therefore, the output from the DOE can then be used to confirm CQAs and critical process parameters (CPPs) that need to be controlled (FDA, ICH Q8 2009). Typically DOE will divide the input variables into three categories: statistically controlled variables, variables that are not controlled but for which there is the possibility to control and those that cannot be controlled (Ratcliffe et al., 2011; Williams et al., 2012). In this way, it is possible to characterize and identify KIPVs, gather an understanding of how much variation there is in each process and determine the relationships between the different parameters.

1.16: Research aims

Currently, there are no potency assays in the clinical setting that give a reliable measurement of MSC mode of action other than simple surface marker expression that does not predict function. For this reason, there is a need to develop *in vitro* assays that can robustly predict the functional activity of the MSC product. In addition, the use of bone marrow MSCs can be potentially limiting as cells may lose functionality after a few passages and mesenchymal cells from other sources may differ in their engraftment abilities. The current work aims to:

- Carry out comparative studies between slightly-younger and slightly-older bone marrow (BM) and umbilical cord (UC) derived MSCs. This will be achieved by assessing the adhesion, migration and vascular support abilities of Notch ligand-primed bone marrow and umbilical cord MSCs on biologically relevant matrices.

- Use a methodological approach to determine key functions of HUVEC tubule formation.

- Explore strategies to improve the engraftment and angiogenic properties of differently-sourced MSCs. For example, by subjecting the cells to process conditions which mimic the physiologic environment.

Chapter 2: Materials and methods

The materials and methods described in this chapter apply generally to all the results sections reported later. Some detailed aspects of materials and methods will be described within the specific results chapter concerned.

Note: As the earlier data to convert the hUC-MSCs from passage number to PDL was not available, individual donor hBM-MSCs that were available in both PDL and passage number were compared with hUC-MSCs (only available in passage number) and commercial low-serum hBM-MSCs (only available in PDL). In this way, it was possible to use the same parameters to study the effect of cell source and different growth medium on MSC functionality.

2.1: Culture of human mesenchymal stromal cells (hMSCs)

2.1.1: Culture and expansion of human bone marrow MSCs (hBM-MSCs) and human umbilical cord MSCs (hUC-MSCs)

hMSCs from the bone marrow of individual donors (Dr Mike Watts, Department of Haematology, University College London Hospital, London UK) or from the umbilical cord (Dr John Girdlestone, NHS Blood and Transplant, London UK) were cultured in a humidified incubator under normal conditions (20% O_2, 5% CO_2 and 37 ^oC) at 4500 cells/cm^2 in a volume of either 7 ml (for T25 flasks) or 12 ml (for T75 flasks) of complete medium. The complete medium consisted of low glucose (1 g/l) Dulbecco's Modified Eagle Medium (DMEM, Gibco, Invitrogen, Paisley UK) supplemented with 10% v/v foetal bovine serum (FBS, Sera Laboratories International, West Sussex UK) and 1 ng/ml of recombinant basic fibroblast growth factor (bFGF, R&D Systems, Minneapolis USA). The complete hMSC growth medium was stored at 2 – 8 ^oC and used within two weeks of preparation. Cells were provided with fresh media after every 2 days and they were observed every day under an inverted light microscope (Evos FL Cell Imaging System, Thermo Scientific, Loughborough UK) to record morphology and check for contamination. hMSCs were passaged after reaching 80-90% confluency following washing with 1% Phosphate-Buffered Saline (PBS) and trypsinization with 1 ml and 2 ml of 0.25% Trypsin-EDTA (Invitrogen, Paisley UK)

for each T25 and T75 flask respectively. The flasks were placed back in the incubator for 3 minutes at normal conditions and the cell detachment was confirmed under the inverted light microscope. Following this, complete medium (double the amount of Trypsin/EDTA solution) was added into each flask to inactivate Trypsin. The cell suspension was then transferred to a 15 ml Falcon tube and centrifuged at 300 g for 3 minutes at room temperature. After discarding the supernatant, the cell pellet was resuspended in 5 ml of complete medium with a 5 ml Pasteur pipette. Cell density was then measured using the Trypan Blue exclusion method (explained in section 2.1.3:) and the hMSCs were seeded in either T25 or T75 flasks at 4500 cells/cm^2. Cell expansion for individual donor hBM-MSCs was carried out until passage 5 (P5) and cell expansion for hUC-MSCs was carried out until passage 12 (P12).

2.1.2: Culture and expansion of low serum commercial hBM-MSCs

Commercially available hBM-MSCs (RoosterBio Inc, Frederick Maryland US) were maintained in culture with their own High Performance Medium (low-serum <5%, SU003, and SU005, RoosterBio Inc) in T75 flasks for 5 days. The High Performance Medium was prepared according to the manufacturer's instructions. This involved bringing the hBM-MSC High Performance Medium Kit to room temperature and then adding 1 vial of hBM-MSC Medium Booster GTX (SU003) to 500 mL hBM-MSC Basal Medium (SU005). After reaching 80-90% confluency cells were detached from the flasks using 5 ml of TrypLE Express (Gibco, Life Technologies, 12604-021, Paisley UK) and incubated in a humidified incubator at normal conditions for 5 minutes. Cell detachment was assessed using an inverted light microscope and the cell suspension was then transferred to a 15 ml Falcon tube, followed by pelleting at 300 g for 3 minutes at room temperature. After discarding the supernatant, the cells were resuspended in the High Performance Medium and counted using the Trypan Blue exclusion method as described below. Cells were then seeded at 4500 cells/cm^2 in T75 flasks containing 12 ml of High Performance Medium. The RoosterBio Inc hBM-MSCs will be referred to as commercial hBM-MSCs throughout the thesis.

2.1.3: Cell counting

Cells were counted using the Trypan Blue exclusion method. Initially, cells were trypsinized, centrifuged and resuspended in complete medium. 100 µl aliquot of a single cell suspension was mixed in a 1:1 ratio with Trypan Blue by pipetting up and down, and 10 µl of the resulting cell suspension was pipetted inside the chamber between the haemocytometer glass slip and the haemocytometer. The cells present in the four corner primary squares of each grid (16 squares per corner) were counted under an inverted light microscope at X10 magnification (Evos FL Cell Imaging System, Thermo Scientific, Loughborough UK). Counts were carried out in duplicates and averaged. Only the cells that were not shown in blue under the light microscope and therefore did not stain with Trypan Blue were counted as viable cells. Cell viability was calculated by dividing the number of viable cells over the total number of dead and viable cells. The volume in of each of the counted squares of a haemocytometer is $0.1mm^3$ (or 10^{-4} ml). Therefore the number of viable cells/ml was calculated by taking the average number of cells per square and multiplying by the dilution factor and 10,000 to obtain the number of cells per ml of diluted sample.

2.1.4: Cell banking

Working cell banks were created for each differently-sourced MSC (P3 (PDL4) to P5 (PDL7) individual-donor hBM-MSCs, PDL10-PDL15 commercial hBM-MSCs and P9-P12 hUC-MSCs) to have enough material for the experiments outlined in this thesis. hMSCs were expanded in either T25 and then in T75 flasks until they reached 80-90% confluency. Following this, they were detached from the flasks and pelleted as described in section 2.1.1: and section 2.1.2:. hBM-MSCs and hUC-MSCs were resuspended respectively in a solution containing 10% Dimethyl sulfoxide (D5879, DMSO, Sigma Aldrich, Poole UK) and 90% FBS and gently mixed. Commercial hBM-MSCs were resuspended in CryoStor cryopreservation solution (C2999-100 ml, Sigma Aldrich, Poole UK). The cell concentration of each suspension was calculated as described in section 2.1.3 and adjusted to $1x10^6$ cells/ml using a 5 ml Pasteur pipette; 1 ml of cell solution was added into each cryovial (Nalgene, Invitrogen, Paisley UK). Cryovials were then placed into a freezing container within 2 min (Mr Frosty, Nalgene and Invitrogen, Paisley UK) with isopropan-2-ol and then moved to a -80 ^oC freezer overnight to gradually

reduce the temperature by 1 ^{o}C per minute so that the cells were not shocked. The following day, the freezing containers were moved into liquid nitrogen (-196 ^{o}C) for long term storage.

2.1.5: Cell thawing

1x10^{6} cells/ml of either individual donor hBM-MSCs, hUC-MSCs or commercial hBM-MSCs were thawed at 37 ^{o}C for 3 minutes. Following this, the cell suspension was added drop by drop (using a p1000 Gilson pipette) into a 15 ml Falcon tube containing 4 ml of pre-warmed growth medium. Cells were then pelleted at 300 g and 21 ^{o}C for 3 minutes and the supernatant discarded. Following this, the cell pellets were resuspended in 5 ml of their respective growth medium. Cells were counted, seeded in tissue culture flasks (T-flasks) at 4500 cells/cm^{2} and maintained in a humidified incubator at normal conditions until they were ready to be passaged.

2.2: Characterizing the growth kinetics of hMSCs

To determine the growth kinetics of MSCs, cells were cultured in T25 and T75 flasks until they reached 80-90% confluency. After 5 to 7 days, cells were harvested from the flasks and counted using the Trypan Blue exclusion method.

2.2.1: Fold increase

Fold increase is a measure describing how much the cells grow from one passage to another. Fold increase was calculated using the following formula:

Fold increase = C(n)/C(n-1)

Where: C(n) = cell number output at each given passage
C(n-1) = cell number output from previous passage

2.2.2: Population doubling level (PDL)

PDL represents the number of times of two-fold increase (doubling) in the total number of cells in culture. PDL number was calculated as follows:

$PDL = X + 3.32 \log_{10} (UCY/l)$

Where:

X = initial population doubling level
UCY = final cell yield or number of cells at the end of growth period
l = initial cell number seeded into the flask

2.3: Characterization of human MSCs (hMSCs)

2.3.1: Tri-lineage differentiation of hMSCs

hMSCs were tested for their ability to undergo trilineage differentiation to osteoblasts, adipocytes and chondroblasts using the StemPro differentiation kits from Invitrogen. Control wells containing hMSCs cultured in standard growth medium were run in parallel to the experimental wells and each condition was performed in triplicate.

2.3.1.1: Adipogenic differentiation

hMSCs were seeded on 12 well plates at 1 x 10^4 cells/cm^2 in growth medium and incubated at 37 ^oC for 3 days. After 3 days the growth medium was replaced with complete adipogenic differentiation medium (StemPro Adipogenesis Differentiation Kit, GIBCO and Invitrogen, Paisley UK) and cells were refed every 4 days. After 14 days in culture, cells were washed once with 1x PBS (without Ca and Mg), fixed with 4% paraformaldehyde (PFA) solution for 30 minutes and rinsed with 2 ml distilled water. Following fixation, 2 ml of 60% of Isopropanol was added to each well, left for 5 minutes and then removed. Cells were then stained with 2 ml of 3% w/v Oil-Red-O/isopropanol in distilled water and incubated at room temperature for 5 minutes. After removing the Oil-Red-O dye from the wells, cultures were rinsed with distilled water until the water rinsed off clear. Wells were visualized under a microscope (Nikon Eclipse Ti, Kingston UK).

2.3.1.2: Osteogenic differentiation

hMSCs were seeded on 12 well plates at 5 x 10^3 cells/cm^2 in growth medium at 37 ^oC for 3 days. The growth medium was then replaced with 1 ml of complete osteogenic differentiation medium (StemPro Osteogenesis Differentiation Kit, GIBCO and Invitrogen, Paisley UK) every 3 days. After 30 days cultures were rinsed with 1x PBS, fixed with 4% PFA solution for 30 minutes and washed with distilled water. Following fixation, cells were stained with 2% Alizarin Red solution (pH 4.2) for 5 minutes. Cells were then carefully washed with distilled water and visualized under the Nikon microscope.

2.3.1.3: Chondrogenic differentiation

hMSCs were trypsinized, centrifuged and resuspended in an appropriate volume of pre-warmed standard growth medium to generate a cell solution of 1.6 x 10^7 cells/ml. Micromass cultures were generated by seeding 5 µl droplets of the cell solution in the centre of a 6 well plate. Cultures were then incubated in normal conditions for 2 hours. After 2 hours, cultures were fed with 2 ml of pre-warmed chondrogenesis medium (StemPro Chondrogenesis Differentiation Kit, GIBCO and Invitrogen, Paisley UK). The chondrogenesis medium was replaced every 2 days and after 23 days in culture, the micromassess were washed once with 1x PBS and fixed with 4% PFA solution for 20 minutes at room temperature. Following fixation, cells were rinsed with distilled water and stained with 1% Alcian Blue (Sigma Aldrich, Poole UK) in 0.1 N Hydrochloric Acid (HCL) for 30 minutes. Cultures were then washed 3 times with 0.1 N HCL followed by x1 wash with distilled water to dilute the acidity. Stained cultures were imaged under the Nikon microscope.

2.4: Immunophenotype profile of hMSCs

Flow cytometry was carried out using the BD Stemflow™ Human MSC Analysis Kit (BD Bioscience, Oxford, UK). hMSCs were characterised for the expression of the positive markers CD105-PerCP, CD73-APC and CD90-FITC and the negative markers CD34-PE, CD45-FITC and CD11b-PE. Cells were cultured for 5-7 days followed by trypsinization and resuspension in 1 ml of 3% bovine serum albumin (BSA, Sigma Aldrich, Poole UK) in PBS for 30 minutes.

Each cell sample was then split between three 15 ml tubes (one untreated tube, one treated tube, two negative control tubes and one isotype control tube). Following this, cells were pelleted at 300 g for 4 minutes and resuspended in 200 µl of conjugated antibody solution for 20 minutes at 4 ^{o}C. hMSCs were then washed with 20 ml of 1x PBS and pelleted twice at 300 g for 4 minutes. Each pellet was resuspended in 1 ml PBS solution and processed with the BD Accuri™ C6 Flow Cytometer (BD Biosciences, Maryland USA).

Isotype	Fluorochrome	Vendor	Cat. number	Dilution ratio of antibody for staining
Mouse IgG1 , κ	PerCP-Cy5.5	BD Biosciences	550795	1:200
Mouse IgG1 , κ	FITC	BD Biosciences	555748	1:200
Mouse IgG1 , κ	PE	BD Biosciences	555749	1:200
Mouse IgG1 , κ	APC	BD Biosciences	555751	1:200

Table 2-1: list of isotype controls used for the staining of hMSCs.

Specificity	Fluorochrome	Vendor	Cat. number	Dilution ratio of antibody for staining
Mouse anti-human CD11b	PE	BD Biosciences	555388	1:100
Mouse anti-human CD34	PE	BD Biosciences	555822	1:100
Mouse anti-human CD45	FITC	BD Biosciences	555482	1:100
Mouse anti-human CD73	APC	BD Biosciences	560847	1:100
Mouse anti-human CD90	FITC	BD Biosciences	555595	1:100
Mouse anti-human CD105	PerCP-Cy™5.5	BD Biosciences	560819	1:80

Table 2-2: List of negative and positive antibodies used for the staining of hMSCs.

2.5: Priming of hMSCs by soluble Notch ligands

hMSCs were grown until they reached 80-90% confluency. Cells were then trypsinized and resuspended in 1% FBS/DMEM or High Performance Medium at 1.8 x 10^5 cells/ml. hMSCs were pre-stimulated for 45 minutes in the presence of 3.6 nM of either soluble recombinant human Jagged 1 (sJag1, 277-JG, R&D Systems, Minneapolis USA) or soluble recombinant human Delta-Like 4 (sDll4, 1506-D4, R&D Systems, Minneapolis USA). Hence, either 500 ng of sJag1 or 200 ng of sDll4 were added for each ml of hMSC suspension.

2.6: RNA extraction and quantitative polymerase chain reaction (qPCR) for gene expression analysis

2.6.1: RNA extraction

qPCR was performed to quantify the sJag1/sDll4 preconditioning effects on cells seeded on fibronectin coated wells. 1 x 10^6 hMSCs were seeded on fibronectin coated 6-well plates and incubated at 37 ^oC for 45 minutes. Following this, the non-adherent cells were washed away and the cells that remained attached were trypsinized, pelleted at 300 g for 4 minutes and left at -80 ^oC for qPCR analysis. RNA was extracted from the frozen cell pellets using the Qiagen RNeasy kit (Qiagen, Manchester UK). In brief, cells pellets were lysed using RTL buffer and homogenized by being centrifuged in Qiashredder columns (Qiagen, Manchester UK) at 10,000 RPM for 2 minutes. The RNA was extracted according to the manufacturer's instructions and collected in 40 µl RNase-free water, following quantification using a NanoDrop (ND1000; NanoDrop Products, Wilmington USA).

2.6.2: gDNA elimination

Before proceeding to cDNA synthesis, RNA samples must be free of contaminating genomic DNA (gDNA) which can be achieved through an elimination step. gDNA elimination was performed using the QuantiTect Reverse Transcription kit (Qiagen, Manchester UK) according to the manufacturer's instructions. Briefly, 2 µl gDNA wipeout buffer was added to 1 µg of template RNA and the volume was made to 14 µl using RNase-free water. The mix was then

centrifuged for a couple of seconds and placed in a thermocycler set at 42 ^{o}C heating for 2 min and then left to cool at 4^{o}C.

2.6.3: cDNA synthesis

A master mix was then prepared for cDNA synthesis. Briefly, a reaction containing 1 µl Quantiscript reverse transcriptase (RT), 4 µl RT buffer 5x, 1 µl RT primer mix and 14 µl of template RNA was prepared and placed in a thermocycler set at 42 ^{o}C for 15 min, followed by 95 ^{o}C heating for 3 min and then left to cool at 4^{o}C.

2.6.4: Two-step qPCR

qPCR was performed using 10X QuantiTect Primer Assay (Qiagen, Manchester UK) and a summary of the primers used can be found in table 2-6. Before the beginning of the experiment primers were reconstituted at room temperature in Tris-EDTA buffer to obtain a 1X working stock solution. A master mix was prepared for each gene to be analysed based on the number of reactions required. Each master mix included 12.5 µl 2X QuantiTect SYBR green (Qiagen), 1.5 µl 1X QuantiTect primers (Qiagen) and 6µl RNAse-free water for each gene. Afterwards, 20 µl of each master mix was aliquoted into each well of the 96-well plates. Following this, 5 µl of cDNA was ejected into each well according to the manufacturer's instructions. Gene expression was then detected using a CFX Connect Real time PCR Detection system (Bio-Rad, Hemel Hempstead UK). Each condition was run in duplicate and experiments were run independently three times using a CFX-Connect thermocycler (Bio-Rad Laboratories, Watford UK). No template controls (NTCs) were run in a single well for each gene to enable detection of contamination and no reverse transcriptase controls (NRT) were run in triplicate wells to detect DNA contamination. Refer to Table 2-3 for the RT-PCR cycling.

Step	Temperature	Duration
1 –PCR initial heat activation	95 ºC	15 min
2 –Denaturation	94 ºC	15 s
3 –Annealing	55 ºC	30 s
4 –Extension	72 ºC	72 s
5 –Go to Step 2 45X		
6 –Data Acquisition	65 ºC	5 s

Table 2-3: Summary of cycling conditions for qPCR.

2.6.4.1: Calculation of expression fold change

Gene expression was calculated manually by extracting the Cq values from the Bio-Rad CFX Manager software (Bio-Rad Laboratories, Watford UK) after which Cq values for each gene were averaged.

The relative quantification (RQ) for each gene was obtained by using the following formula:

Relative quantification = $2^{-(\Delta CTE - \Delta CTC)}$

Where:

ΔCTE = average of experimental Cq values
ΔCTC = average of control Cq values

The normalised RQ value (NRQ) for each gene was obtained by normalizing the RQ value from each gene to the RQ value of the house keeping gene 18S.

Gene	Supplier	Supplier Product Code	Location
18S	Qiagen	QT00199367	Manchester UK
HES1	Qiagen	QT00039648	Manchester UK
HEY1	Qiagen	QT00035644	Manchester UK
JAG1	Qiagen	QT00031948	Manchester UK
DLL4	Qiagen	QT00081004	Manchester UK
HIF1	Merck Millipore	MAB5382	New Jersey USA
HIF3	Qiagen	QT00059157	Manchester UK

Table 2-4: List of qPCR primers used.

2.7: Macro design to quantify staining

The following script was created using ImageJ (ImageJ software, National Institutes of Health, Maryland USA) to quantify the area, the integrated density and the mean intensity of the integrin β-1 staining in Chapter 3. The ImageJ batch processing tool was used to automate the analysis of all of the staining images.

The ImageJ macro was generated by recording a series of commands using the command recorder. The units of pixels were converted to micrometres by measuring the length of the scale bar on the image and using the "set scale" command to input the measured length. Each image was first converted to 8-bit grayscale to allow the use of the "thresholding" tool which only works with grayscale images. Following this, the thresholding tool was run for each image to select the stained regions. In order to tell imageJ what to measure, the "set measurements" dialog was opened and the wanted outputs selected e.g. integrated density. The "analyze particles" command was run to select the particle size range and to show the regions of interest using the "overlay mask" option. Following this, the "roi manager show all" command was selected to display all of the stained regions and the number of stained cells per image simultaneously.

```
run("Set Scale...", "distance=439 known=200 pixel=1 unit=um global");
run("8-bit");
run("Median...", "radius=2");
setAutoThreshold("Default dark");
//run("Threshold...");
setThreshold(7, 255);
run("Set Measurements...", "area mean standard integrated display redirect=None
decimal=3");
run("Analyze Particles...", "size=200-Infinity show=[Overlay Masks] display exclude add");
roiManager("Show All with labels");
roiManager("Show All");
```

2.8: Hypoxic chamber oxygen measurements

A low oxygen environment was achieved by purging a mixture of oxygen, carbon dioxide and nitrogen (2% O_2/5% CO_2/93% N_2 balanced) into an air-tight chamber. To quantitatively confirm that a low oxygen environment for the cells was achieved, sensors were attached to the top of the chamber and the bottom of 96-well plates (containing cell growth medium) that were put inside the chamber. Three measurements were taken because the oxygen profile in the liquid phase of the 96-well plates can be different from the air phase in the chamber. Oxygen

profiles were monitored over a period of 24 hours. In this way, it was possible to confirm that a low oxygen environment was maintained for more than 18 hours.

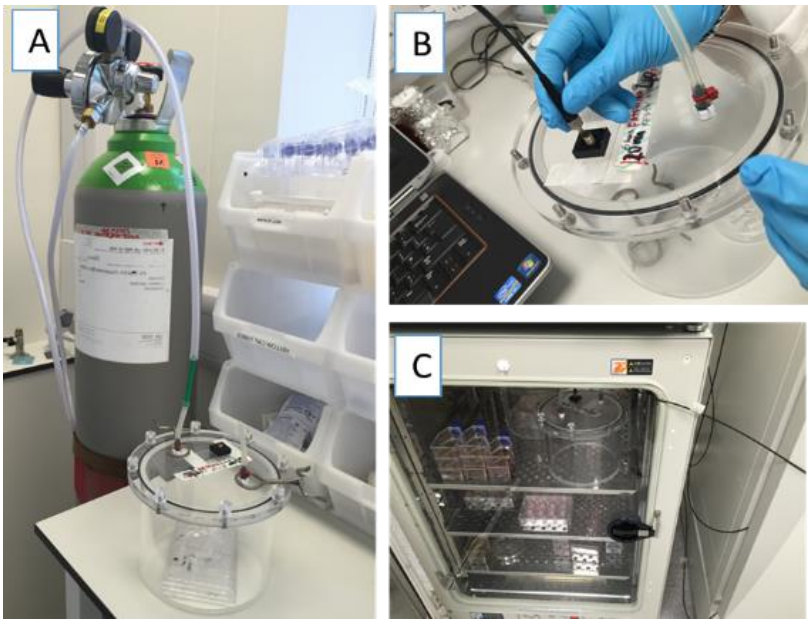

Figure 2-1:A) Set up for oxygen chamber measurement B) oxygen sensors were attached to the chambers C) the partial pressure of oxygen (PO_2) in the chambers was measured in a 5%CO_2/20% O_2 incubator to ensure optimum growth environment for the cells.

2.9: Cell culture techniques of primary human umbilical vein endothelial cells (HUVECs)

2.9.1: Thawing, culture and expansion of HUVECs

HUVECs were obtained from Dr Enca Martin-Rendon's lab at the University of Oxford. The cells were thawed at 37 ^oC for 3 minutes and resuspended in a 15 ml Falcon tube containing 4 ml of pre-warmed growth medium. The growth medium consisted of Endothelial Growth Medium-2 (EGM-2, Lonza, Slough UK) including Bullet-kit (Lonza; containing FBS, human epidermal growth factor, hydrocortisone, vascular endothelial growth factor, human bFGF, insulin like growth factor-1, ascorbic acid and heparin). The cell solution was then centrifuged at 300 g and 21 ^oC for 3 minutes. The supernatant was discarded and the cell pellet was resuspended in 3 ml of pre-warmed EGM-2 medium. HUVECs were expanded in T75 flasks and the medium was replaced every two days. Cells were then passaged after reaching 80-90% confluency following washing with 1x PBS and trypsinization with 0.25% Trypsin-EDTA (Invitrogen) for 3 minutes at 37^oC. EGM-2 (double the amount of Trypsin/EDTA solution) was added into each flask to

inactivate Trypsin. Cells were always seeded in a 1:3 ratio. Tubule assay experiments were carried out on early passage 7 HUVECs (P7), passage 10 HUVECs (P10), passage 13 HUVECs (P13) and passage 15 HUVECs (P15).

2.9.2: Characterization of HUVECs

HUVECs were tested for the expression of vWF and CD31. The endothelial cells were seeded on 12-well plates at 10000 cells/cm^2 and cultured in EGM-2 medium. After 2 days the medium was removed from each well and the cells were washed once with 1x PBS, fixed for 15 minutes in 4% PFA followed by 3 washes with PBS. Cells were then permeabilized using 0.25% Triton X-100 (BDH, Poole UK) in PBS solution for 10 minutes, washed 3 times with PBS and incubated for 1 hour at room temperature in 1% BSA/PBS. Cells were then incubated overnight at 4 ^oC with either Von Willebrand Factor (vWF, A0082, Dako, Ely UK) or CD31 (ab28364, Abcam, Cambridge UK) at 1:200 dilution in blocking solution. For the negative controls, the primary antibody was omitted. The following day each well was washed 3 times with PBS and incubated with the appropriate secondary antibodies at 1:200 dilution in PBS for 1 hour at room temperature. After x2 wash with 1x PBS, nuclei were counterstained with DAPI (1:2000 dilution in PBS) for 10 minutes, followed by x3 wash with PBS. The cells were left in PBS for imaging.

2.9.3: Cell banking of HUVECs

In order to have a sufficient number of HUVECs to carry out the experimental work, a working cell bank (P5-P12 HUVECs) was created. P3 HUVECs were expanded in T25 flasks and when they reached 80-90% confluency they were detached trypsinized, pelleted and resuspended in 5 ml EGM-2. Cells were then counted using the Trypan Blue exclusion method (section 2.1.3:), pelleted and resuspended in the appropriate volume of FBS to obtain $3x10^5$-$5x10^5$ cells/ml. 10% DMSO was added to the cell suspension drop by drop and gently mixed using a 5 ml pipette. Cells were then transferred to 1 ml cryovials and carefully placed in Mr Frosty freezing containers. The containers were then placed overnight in a -80 ^oC freezer and on the following day the cryovials were stored in liquid nitrogen.

2.10: In vitro vascular assays

2.10.1: Gel coating

The *in vitro* vascular assays were all performed in 96-well plates. Aliquots of Growth factor reduced Matrigel (GFR Matrigel, BD Biosciences, Maryland USA) and growth factor reduced Geltrex (GFR Geltrex, Life Technologies, Paisley UK) previously stored at -20 ^{o}C were thawed overnight on ice at 4 ^{o}C. The following day, 96-well plates were cooled on ice and each well was coated with either 35 µl or 55 µl of GFR Matrigel or GFR Geltrex using pre-cooled pipette tips. The plates were then incubated in an incubator set at 37 ^{o}C and 5% CO_2 for at least 30 minutes. Following this, cells were seeded on top of the gel coatings as described below.

2.10.2: Tubule assay formation on Matrigel and Geltrex

HUVECs were seeded into each of the wells at the desired concentrations (cells/ml) and a total volume of 150 µl suspension of cells in pre-warmed EGM-2 was gently mixed and seeded on either Matrigel-coated or Geltrex-coated wells of x2 96-well plates. Each condition was repeated in triplicate. One of the 96-well plates was first placed in a hypoxic chamber purged with 2% oxygen (2% O_2/5% CO_2/93% N_2 balanced) and then put together with the other plate in a humidified incubator set at 37 ^{o}C, 5% CO_2 and ambient oxygen (20% O_2). The networks formed were observed after 18-19 hours. Tubules were imaged using phase contrast imaging and branches were quantified manually and also by using the ImageJ angiogenesis analyser (ImageJ software, National Institutes of Health, Maryland USA).

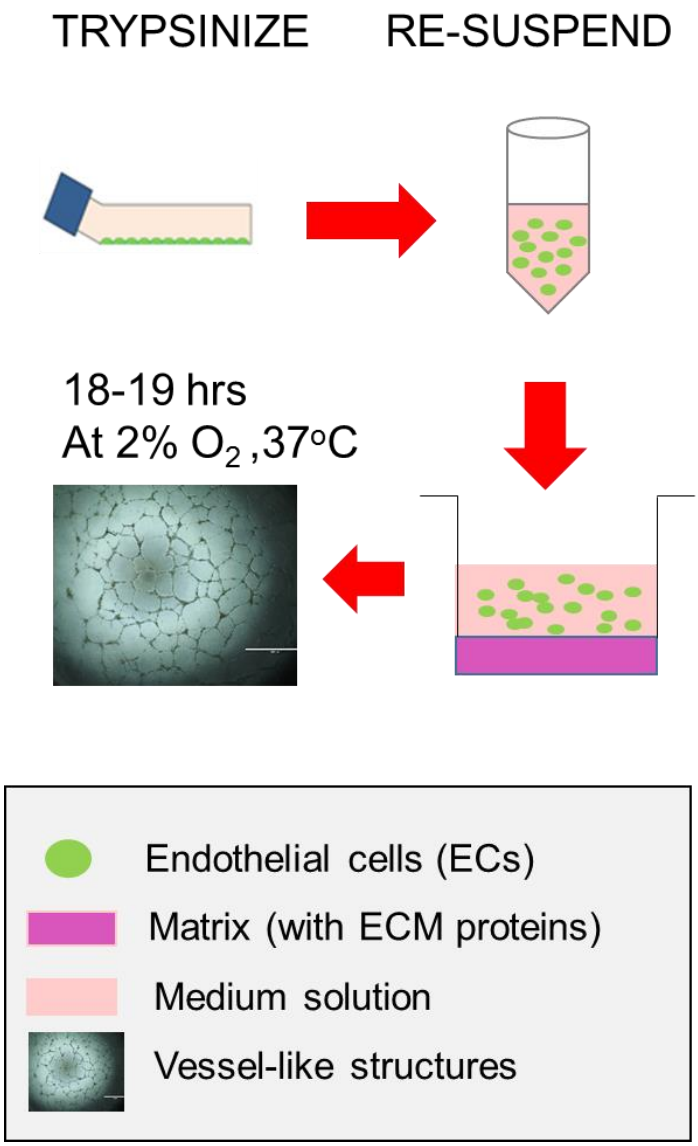

Figure 2-2: Diagram summarizing experimental setup for vascular tubule assays.

2.10.3: *In vitro* vascular assay quantification

Counts were performed on either whole well representative images taken at x2 magnification (2000 µm) or on whole well images taken at x4 magnification (1000 µm) and merged (PanoramaStudio2Pro software, Sulzfeld EU). The number of branch points was measured as the number of sprouts originating from a single tubule. Measurements were made based on 1 branch point = junction of 3 branches, 2 branch points = junction of 4 branches and 3 branch points = junction of 5 branches. Counts were performed either manually or using the automated counting technique using the ImageJ angiogenesis analyser. However, the ImageJ analyser was also used to quantify number of meshes (small areas enclosed by the tubules), average tubule length and cumulative tubule length of the branches (total length of all the branches in a given field) as these type of measurements would have been more time-consuming and more difficult to measure using the manual method (Staton et al., 2007). It is notable that in Chapter 4 the comparison between manual and automated counting technique was based on the number of branch points. In fact, whilst in the co-culture assays there were evident differences in branch length between the co-culture assays and the endothelial tubule assays, this was not the case for the data in Chapter 4 where only one type of assay was performed and therefore the average length of the branches was similar.

2.11: Statistical analysis

All experimental conditions were tested in triplicate. Experiments were performed independently at least two times. Results were presented as standard error of the mean (SEM) when comparing across three independent experiments or more, or standard deviation (SD) of the mean when comparing data within an experiment. Statistical significance was determined by Analysis of Variance (ANOVA) with Bonferroni post-hoc correction to obtain the adjusted p values for multiple comparisons. Data with p values less than 0.05 were considered statistically significant. GraphPad Prism v7 (GraphPad Software, La Jolla USA) was used to perform statistical analysis.

Chapter 3: A comparative analysis of cell retention responses of differently-sourced hMSCs

3.1: Introduction

The following section will summarize the relevant literature which was previously discussed in Chapter 1.

To understand how MSCs might behave when they are in the injury site, it is beneficial to consider the environment that they will experience and how this might affect them. Fibronectin (FN) is expressed after a myocardial infarction (MI). This protein is known to play a fundamental role in cell adhesion and migration (Van Dijk et al., 2008). During an MI, fibronectin deposits in the infarcted zone of the heart and forms a blood clot to stop the bleeding (Van Dijk et al., 2008). FN fragments also contain the site for integrin α5β1 that MSCs express and therefore the FN fragments may increase the adhesion of α5β1-expressing cells which could potentially improve engraftment (Van Dijk et al., 2008; Veevers-Lowe, 2011). For example, it was shown that MSCs induced to overexpress transglutaminase which is a co-receptor for fibronectin, showed increased adhesion and migration properties in the infarcted myocardium of a rat hence leading to improved heart function (Lee et al., 2015; Song et al., 2007). Moreover studies could be carried out to compare the effect of different FN concentrations on the adhesion abilities of MSCs. Fibronectin has also been shown to perform better than other types of extracellular matrix (ECM) molecules in enhancing the adhesion properties of bone marrow-derived stem cells *in vitro* (Van Dijk et al., 2008).

One of the main limitations in determining the mode of action of MSCs *in vivo* is their poor engraftment at the site of injury (Amado et al., 2005; Cheng et al., 2008). Several studies reported that targeting the Notch signalling pathway may enhance responses relevant to cardiovascular regeneration of MSCs (Xie et al., 2013). The Notch pathway is highly conserved and it has a fundamental role in cardiac development (Li et al., 2010). There are many molecules involved in Notch signalling. For example, tumour necrosis factor alpha, a key cytokine involved in inflammation and a potent regulator of the migration of MSCs *in vivo*,

is known to modulate key ligands involved in the Notch pathway (Benedito et al., 2009). Recent studies demonstrated that when MSCs were pre-stimulated with tumour necrosis factor alpha, cells remained engrafted in the endothelium for longer (Lu et al., 2016). In another study it was reported that blocking Notch signalling in bone marrow MSCs (BM-MSCs) promoted cell migration *in vitro* and up-regulated the cell receptor CXCR4 (Xie et al., 2013); the up-regulation of CXCR4 was shown to be beneficial for cell survival and homing (Cao et al., 2013).

To date bone marrow has been the main source of MSCs for clinical use. However, they are limited because their harvesting involves invasive methods and the number and differentiation potential as well as the maximum life span of BM-MSCs significantly declines with the age of the donor (Bruna et al., 2016). On the other hand, human umbilical cord MSCs (UC-MSCs) can be easily isolated using non-invasive methods (Jin et al., 2013). Moreover, they have been shown to have greater proliferation capacity and faster growth *in vitro* than BM-MSCs (Chen et al., 2014). The media used for cell culture is another challenge in the clinical application of MSCs (Chen et al., 2013). Even though serum containing medium allows for robust cell expansion, traditional formulations carry the risk of viral, bacterial and mycoplasma contamination from the serum as well as variations between batches which affect the reliability of experimental data (Witzeneder et al., 2013). Generally high amounts of foetal bovine serum (FBS) are added as a supplement to the culture media in which the cells grow, typically 5-15% (Chen et al., 2013). Current research is focused on reducing/eliminating the dependence on serum (Chen et al., 2013).

With the understanding that there is a need to reduce dependence on serum in MSC cultures and that MSCs from different origins may behave differently, the current study compared bone marrow-derived MSCs (expanded in complete DMEM medium) with hUC-MSCs as well as hBM-MSCs that came with their own low-serum medium (<5%, Rooster Bio, Maryland US). These comparative studies were performed to investigate differences in cell attachment and migration responses via priming with Notch factors, phenotype, and expression levels of MSC positive and negative markers.

3.2: Aim and hypotheses

3.2.1: Aim

- To test the functional abilities of hMSCs primed with Notch ligands and to compare differences in surface marker expression, proliferative capacities and differentiation patterns of differently-sourced hMSCs.

3.2.2: Hypotheses

- Differently-sourced MSCs will exert differences in functional abilities.

- The adhesion and migration ability of hMSCs can be enhanced by Notch ligand preconditioning.

- Stimulation of commercial hBM-MSCs with PDGF-BB will increase their migration potential.

3.3: Materials and methods

Adhesion assays were carried out on individual donor hBM-MSCs, commercial low-serum hBM-MSCs and hUC-MSCs at different passage (P) numbers or population doubling level (PDL). Individual donor hBM-MSCs were also referred to as gx11 hBM-MSCs, gx11 being the name arbitrarily given to the batch of hMSCs isolated from one specific donor. Migration assays were carried out on commercial hBM-MSCs expanded in their own low-serum high performance medium. All the general materials and methods are described in Chapter 2.

3.3.1: Adhesion assay

hMSCs were cultured until they reached 80-90% confluency. Cells were starved in 1% FBS/DMEM (no growth factors added) for 24 hours before the experiment. Meanwhile, 48-well plates were coated overnight at 4 ^{o}C, or at room temperature (in the biological safety cabinet) for 2 hours, with 200 µl of 10 µg/ml of human plasma FN (1 mg; Tebu Bio, Peterborough; UK). The excess FN was then removed from the wells followed by one wash with 1x PBS. Cells were then blocked for 1 hour with sterile 3% BSA/PBS. Meanwhile, MSCs were trypsinized and resuspended in 1% FBS/DMEM (no growth factors added). Viable cells were then counted using a haemocytometer and diluted to a concentration of 1.8 x 10^5 cells/ml. The cell suspension was then split between three tubes. In two of the tubes the MSCs were pre-stimulated respectively with soluble Jagged 1 (sJag1) at a concentration of 500 ng/ml and soluble Delta-like 4 (sDll4) at a concentration of 200 ng/ml, cells were then gently mixed and pre-stimulated for 45 minutes in a humidified incubator set at 37 ^{o}C and 5% CO_2. The third tube was used as a control (UT) with non-pre-stimulated hMSCs and it was run in parallel at the same conditions as the other two tubes. 1 ml of 1 x 10^4 per well was seeded into each of the well plates, the assays were performed in triplicate for each condition. Cells were incubated for the desired time before being washed once with PBS to remove the non-adhered cells. The attached cells were then fixed with 500 µl of 4% paraformaldehyde (PFA) and left in the hood for 15-20 minutes. Following fixation, the adhered cells were washed twice with PBS and stained with 1:3000 dilution of 4',6-diamidino-2-phenylindole (DAPI) for 3 minutes. Wells were then washed once or twice with 1x PBS and left in PBS for imaging under the Nikon

Eclipse TE2000-U microscope (Nikon, UK) for assessment of adhesion at 4x magnification (four random fields of view per well). The number of attached cells was quantified with the ImageJ software Cell Counter plugin. Experiments were performed independently at least two times.

3.3.1.1: Adhesion ligand expression analysis

Fixed cells from the adhesion assays were washed once with 1x PBS and permeabilized with 0.25% TRITON X-100/PBS for 10 min. After a three times wash with PBS, cells were blocked for 1 hour with 3% BSA/PBS at room temperature (RT). Cells were then incubated overnight at 4 ^{o}C with the primary antibody at the desired concentration and on the following day they were washed three times with PBS. The attached cells were then incubated with the secondary antibody (previously diluted at the desired concentration in 1x PBS) for 1 hour following a three times wash with PBS. Fluorescence images were taken using the Nikon Eclipse TE2000-U fluorescence microscope (Nikon UK Limited, Kingston, UK).

Host	Antibody	Reactivity	Type	Catalogue no.	Dilution
Rabbit	IgG	Human	Primary	AB52971; Abcam (total integrin β-1)	1:50
Mouse	IgG	Human	Primary	556048; BD Bioscience (active integrin β-1)	1:250
Goat	IgG Alexa Flur 448	Rabbit IgG	Secondary	A-21428; Thermofisher	1:200
Goat	IgG Alexa Flur 595	Mouse IgG	Secondary	A-11001; Thermofisher	1:200

Table 3-1: List of antibodies used to assess the adhesion of MSCs on FN surfaces.

3.3.2: Hypoxia

To mimic the environment within an ischemic heart, plates containing the cell solutions were placed in a modular in house manufactured chamber (Mondragon-Teran et al., 2009) purged with a gas mixture of 2% O_2/5% CO_2/ 93% N_2 balanced.

Cell age (passage number/PDL)	Cell type	Oxygen tension	Number of independent experiments (n) using same donor cells	Attachment time	Well plates used	Variables being investigated
P4 (PDL 5)	gx11 hBM-MSCs	20% O_2	n = 3	20 min & 45 min	48-well plates	Effect of attachment time and priming of MSCs with Notch ligands.
P6 (PDL 8)	gx11 hBM-MSCs	20% O_2	n = 3	20 min & 45 min	48-well plates	Effect of attachment time and priming of MSCs with Notch ligands.
P11	hUC-MSCs	20% O_2 and 2% O_2	n = 4	20 min & 45 min	48-well plates	Effect of attachment time and priming of MSCs with Notch ligands.
P13	hUC-MSCs	20% O_2 and 2% O_2	n = 4	20 min & 45 min	48-well plates	Effect of attachment time and priming of MSCs with Notch ligands.
PDL15	Commercial hBM-MSCs	20% O_2	n = 5	20 min & 45 min	48-well plates	Effect of attachment time and priming of MSCs with Notch ligands.
PDL 15	Commercial hBM-MSCs	20% O_2	n = 3 & n = 2	20 min & 45 min	96-well plates	Effect of different concentrations of FN and Notch ligands (sJag1 and sDll4) on cell adhesion.

Table 3-2: Summary of attachment assays.

Note: Experiments were carried out using different hMSC batches isolated from the same donor for each condition, and (n) represents the number of times (i.e. different days) the experiments were performed using same donor cells.

3.3.3: Transwell migration assay

Low-serum hBM-MSCs were cultured for five days in their own medium (Rooster Bio Inc, Maryland, US), following their adaptation in 1% FBS/DMEM for 24 hours prior to the migration experiment or left in their low-serum medium. Migration assays were performed in 24-well plates (BD; Oxford, UK) using 8-µm pore cell culture inserts (BD; Oxford, UK). Transwell inserts were coated overnight with 10 µg/ml of FN in 1x PBS. On the day of the experiment, inserts were washed with 1x PBS and transferred into new 24-transwell plates. 300 µl of serum free medium/low-serum medium containing 2 x 10^4 cells was loaded to the upper chamber of the inserts, whilst 800 µl of serum free medium/low-serum medium with or without 50 ng/ml Recombinant Human platelet-derived growth factor BB (PDGF-BB; R & D Systems, Abingdon, UK) was added to the lower chamber; the assays were performed in triplicate for each condition. After 3 hours of incubation at 37ºC, 5% CO_2, cells which adhered to the membrane were fixed with 4% PFA for 10 minutes, washed once with distilled water and then stained with 0.5% (w/v) crystal violet in 5% ethanol filtered solution for 30 minutes. Following this, the inserts were washed serially twice with PBS and any remaining cells were once more removed by gently scraping the upper surface of the membrane with cotton swabs. Transwell inserts were left to dry, mounted onto microscope slides and counted in four to five random fields of view at 10X magnification. The migrated cells were counted using the ImageJ software Cell Counter plugin.

Cell age (PDL)	Cell type	Supplier for cells and culture medium	Number of independent experiments using same donor cells	Migration time	Oxygen tension
PDL 15	hBM-MSCs	Rooster Bio Inc; Maryland, US	n = 3	4 hours	20%
PDL 15	hBM-MSCs	Rooster Bio Inc; Maryland, US	n = 3	4 hours	2%

Table 3-3: Summary of transwell migration assays.

3.4: Results

3.4.1: Characterization of hMSCs

3.4.1.1: Cell morphology

The morphological characteristics of hMSCs were observed using an inverted light microscope. hMSCs from different sources were seeded at 4500 cells/cm^2. All three differently-sourced hMSCs maintained their proliferative and plastic adherent abilities after being frozen down from liquid nitrogen and this was also observed for the older cells (Figure 3-1 A-F). No significant morphological differences were observed between the three differently-sourced hMSCs, in fact they all displayed a homogeneous monolayer with the cells adopting a small spindle-shaped morphology (Figure 3-1 A-F).

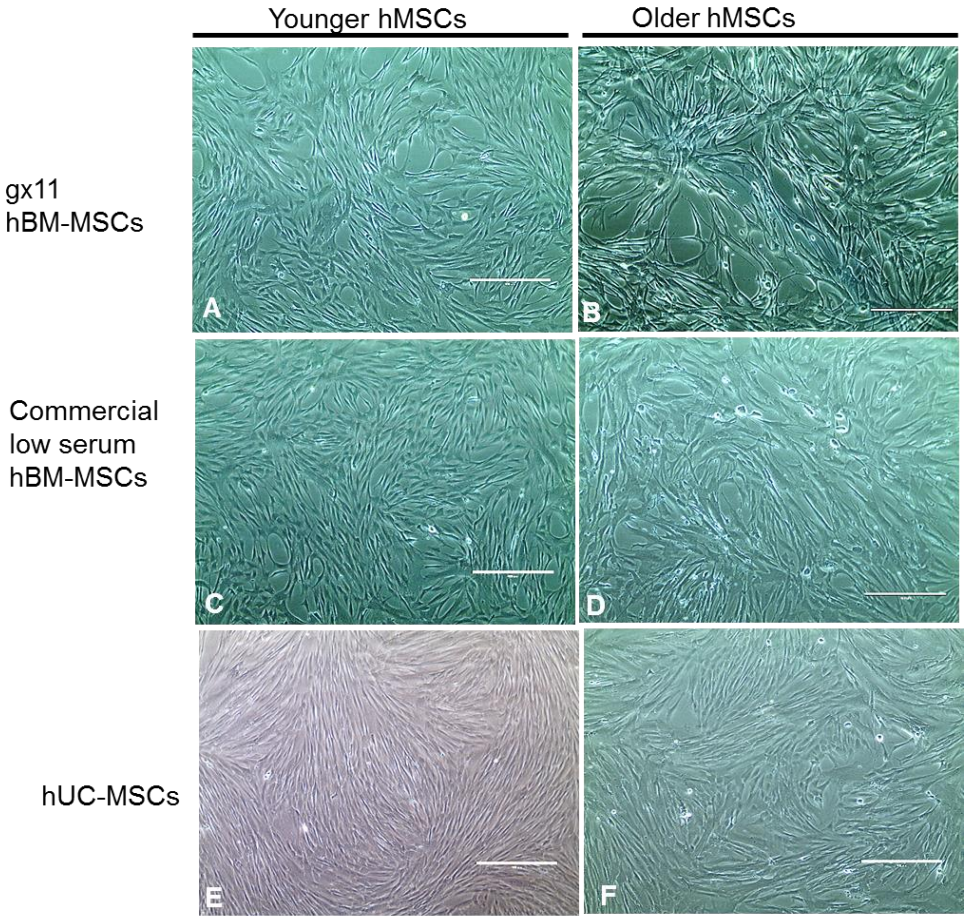

Figure 3-1: Cell morphology characterization of hMSCs after 5 days in culture. (A) Individual donor gx11 P4 (PDL 5) hBM-MSCs and (B) Individual donor P6 (PDL 8) gx11 hBM-MSCs were expanded in complete medium (C) PDL 14 commercial hBM-MSCs (D) and PDL 17 hBM-MSCs were expanded in their low-serum medium (E) P11 hUC-MSCs and (F) P13 hUC-MSCs were expanded in complete medium. Scale bars = 400 µm.

3.4.1.2: Tri-lineage differentiation

Osteogenic differentiation ability was determined by Alizarin Red staining of mineralization (Figure 3-2 4, 5 and 6) after culturing cells in osteogenic medium for 30 days. Adipogenic differentiation was determined using Oil-Red-O, which stains small lipid vacuoles in the cytoplasm of mature adipocytes, following 14 days culture in adipogenic medium (Figure 3-2 7, 8 and 9) and chondrogenic differentiation was evaluated using the pellet culture system (Figure 3-2 10, 11 and 12). Cells undergoing chondrogenic differentiation appeared blue when stained with Alcian Blue dye (Figure 3-2 10, 11 and 12). However, cells cultured in their standard medium displayed their usual morphologic characteristics (Figure 3-2 1, 2 and 3).

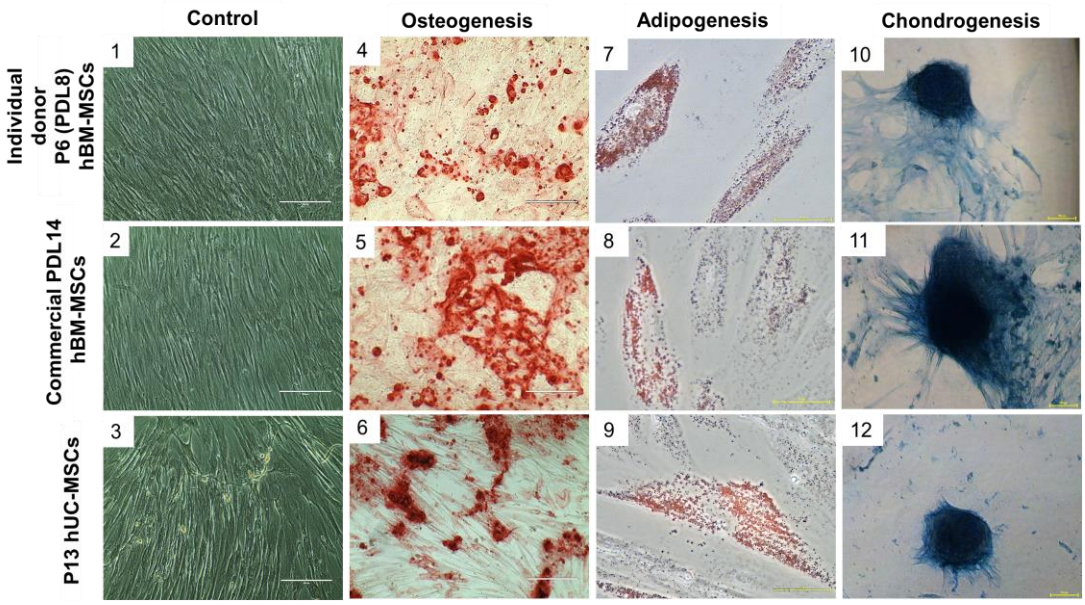

Figure 3-2: All different source hMSCs successfully underwent osteogenic, adipogenic and chondrogenic differentiation. hMSCs were stained with Alizarin Red for osteogenesis after 30 days in culture (4, 5 and 6), Oil-Red-O for adipogenesis after 14 days in culture (7, 8 and 9) and Alcian Blue for chondrogenesis after 23 days in culture (10, 11 and 12) respectively. Scale bars = 200 µm (1, 2, 3 and 4, 5 and 6), 50 µm (7, 8 and 9) and 100 µm (10, 11 and 12).

3.4.1.3: Immunophenotype

Flow cytometry was carried out on cell pellets of no less than 5 x 10^5 cells, to quantify the percentage of cells expressing positive MSC surface markers (>95% according to the ISCT guidelines, CD105, CD90 and CD73) and lacking the expression of the negative markers CD45 (pan-leukocyte marker), CD34 (labels primitive hematopoietic progenitor and endothelial cells), and CD11b (expressed on monocytes and macrophages) (<2% according to the ISCT guidelines)

(Domini et al., 2006). A cocktail of isotype controls was also used to detect background staining. The flow data was displayed using histogram plots which plotted a single parameter (FITC, PE or PercP intensity, x-axis) against the number of events (cells) detected (y-axis) by the machine. An event is a unit of data which represents a cell. The isotype controls for the differently-sourced hMSCs indicated low levels or the absence of non-specific interactions (0%-3.7%; see Figure 3-6 A, Figure 3-7 C, Figure 3-4 E, Figure 3-5 G and Figure 3-3 I). As seen in Figure 3-6 H and Figure 3-7 J, the slightly-younger and slightly-older hUC-MSCs highly expressed the positive markers (>95%) and showed no expression (<2%) of the negative markers; similarly individual donor hBM-MSCs also displayed a near pure population (Figure 3-3 A and B). Furthermore, old and young commercial low-serum hBM-MSCs (Figure 3-4 D and Figure 3-5 F) highly expressed the positive markers (>95%) and lacked the expression of MSC negative markers (<2%). However, the PDL17 commercial hBM-MSCs displayed a decrease in expression of CD105 (82.2%; Figure 3-5 F, 2). CD105 was observed to be consistently lower in expression than the other positive markers CD73 and CD90 which consistently showed expression levels of above 99%.

	P6 (PDL 8) hBM-MSCs	**Low-serum PDL 14 hBM-MSCs**	**Low-serum PDL 17 hBM-MSC**	**P11 hUC-MSCs**	**P13 hUC-MSCs**
CD90	99.8%	99.8%	99.8%	99.6%	99.5%
CD73	99.5%	99.6%	99.6%	99.5%	99.1%
CD105	95.2%	94.4%	**82.2**%	96.9%	96.4%
CD45	0.1%	0.6%	0.3%	1.4%	1.9%
CD34	0.1%	1.1%	0.2%	1.2%	0.9%
CD11b	0.0%	0.3%	0.1%	1.1%	1.0%

Table 3-4: Immunophenotypic data for differently-sourced hMSCs.

A Isotype controls

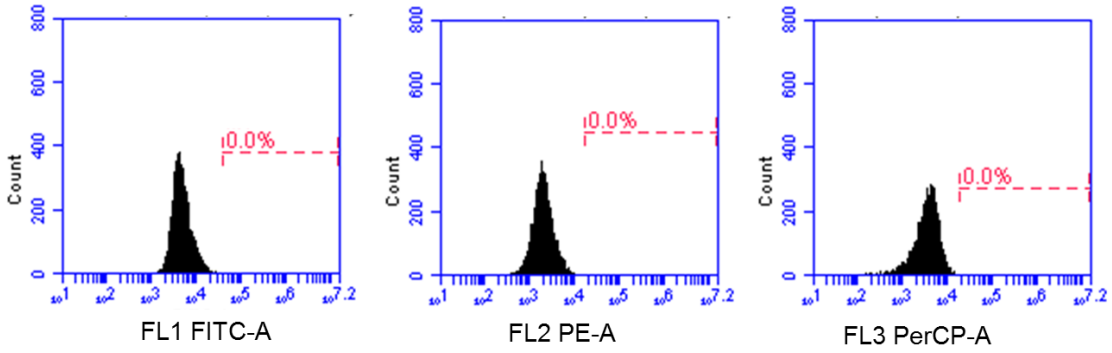

B P6 (PDL 8) Individual donor hBM-MSCs

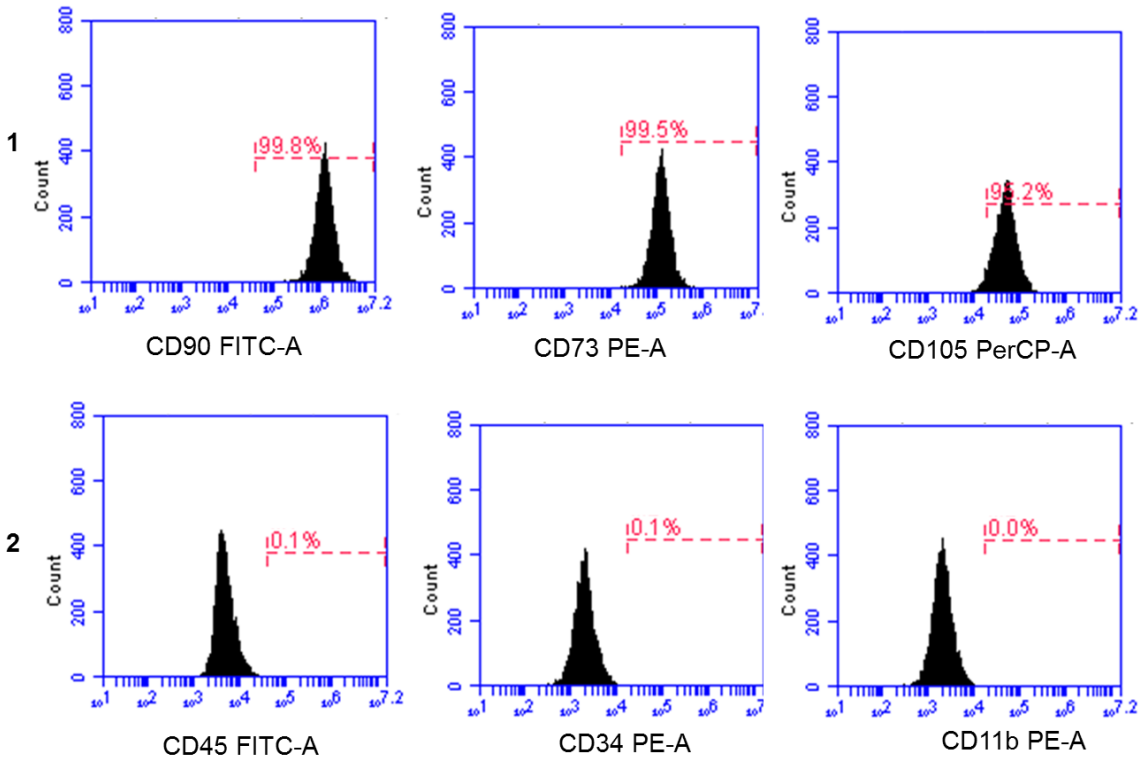

Figure 3-3: Immunophenotype by flow cytometry analysis of individual donor P6 (PDL 8) hBM-MSCs expanded in complete medium. (A) isotype controls were run in parallel to the experimental samples. (B, 1) results reported positive expression of hMSC markers (CD90, CD73, and CD105); (B, 2) less than 1% of hMSCs expressed negative markers (CD45, CD34, and CD11b). The red horizontal line on each histogram represents the percentage of positive cells for each surface protein.

C Isotype controls

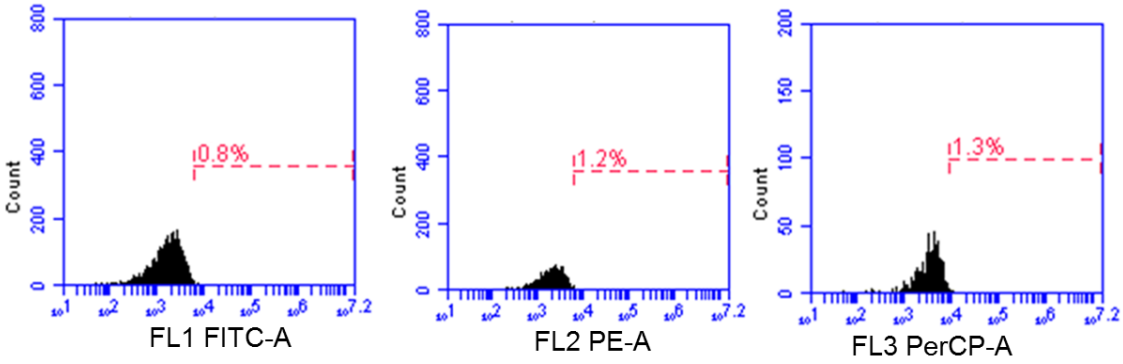

D PDL 14 low-serum commercial hBM-MSCs

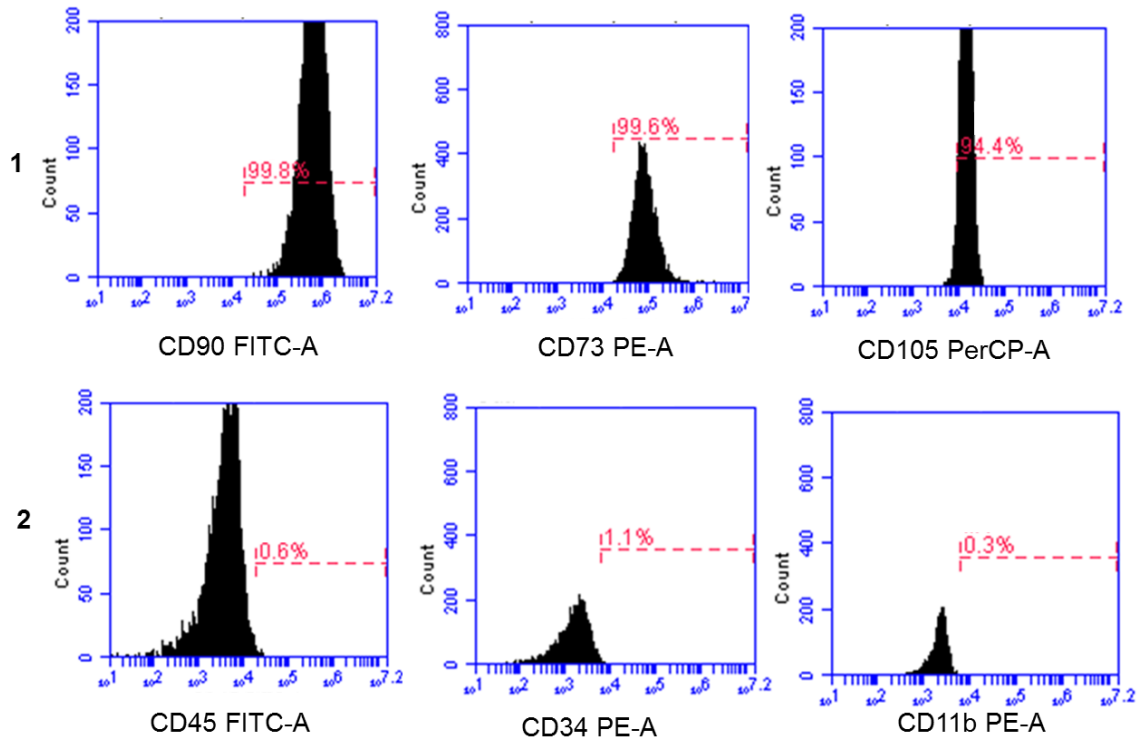

Figure 3-4: Immunophenotype by flow cytometry analysis of low-serum PDL 14 hBM-MSCs. (C) isotype controls were run in parallel to the experimental samples. (D, 1) results reported positive expression of hMSC markers (CD90, CD73, and CD105); (D, 2) less than 1% of hMSCs expressed negative markers (CD45, CD34, and CD11b). The red horizontal line on each histogram represents the percentage of positive cells for each surface protein.

E Isotype controls

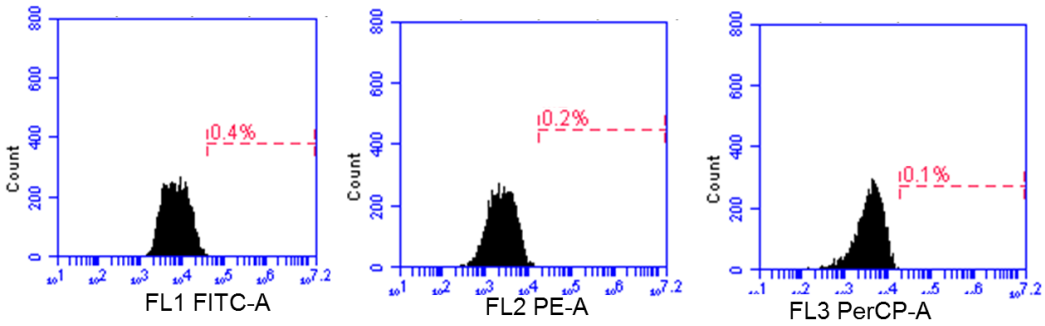

F PDL 17 low-serum commercial hBM-MSCs

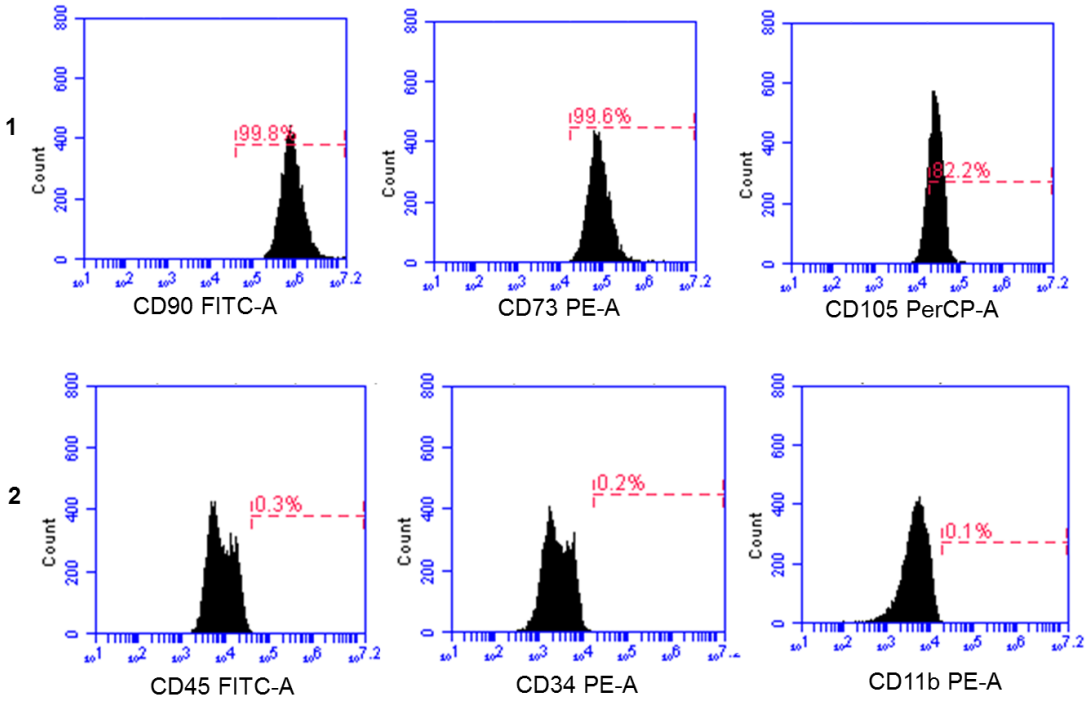

Figure 3-5: Immunophenotype by flow cytometry analysis of low-serum PDL 17 hBM-MSCs. (E) isotype controls were run in parallel to the experimental samples. (F, 1) results reported positive expression of hMSC markers (CD90, CD73, and CD105); (F, 2) less than 1% of hMSCs expressed negative markers (CD45, CD34, and CD11b). The red horizontal line on each histogram represents the percentage of positive cells for each surface protein.

G Isotype controls

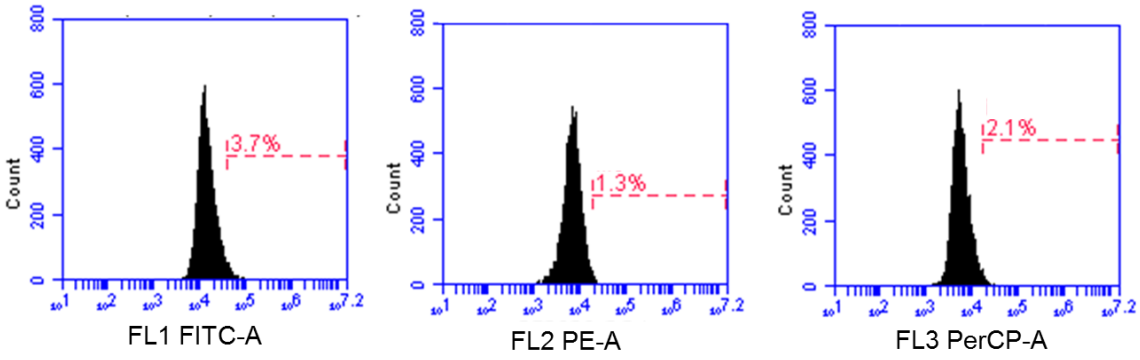

H P11 hUC-MSCs

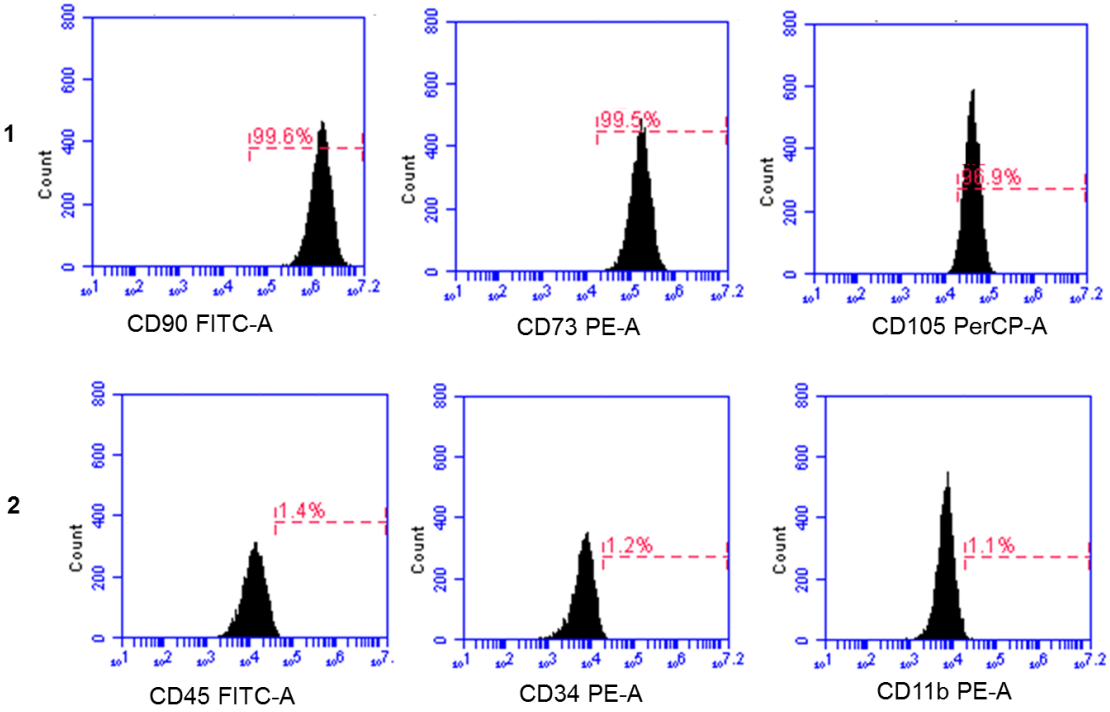

Figure 3-6: Immunophenotype by flow cytometry analysis of low-serum P11 hUC-MSCs. (G) isotype controls were run in parallel to the experimental samples. (H, 1) results reported positive expression of hMSC surface markers (CD90, CD73, and CD105); (H, 2) less than 1% of hMSCs expressed negative markers (CD45, CD34, and CD11b). The red horizontal line on each histogram represents the percentage of positive cells for each surface protein.

I Isotype controls

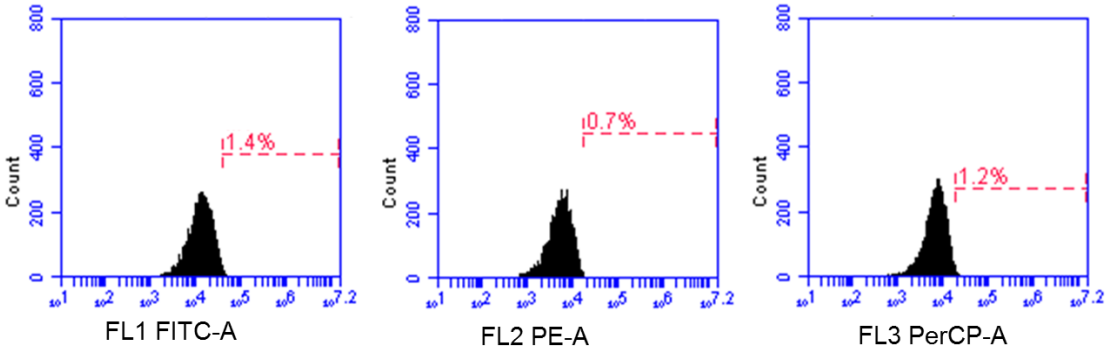

J P13 hUC-MSCs

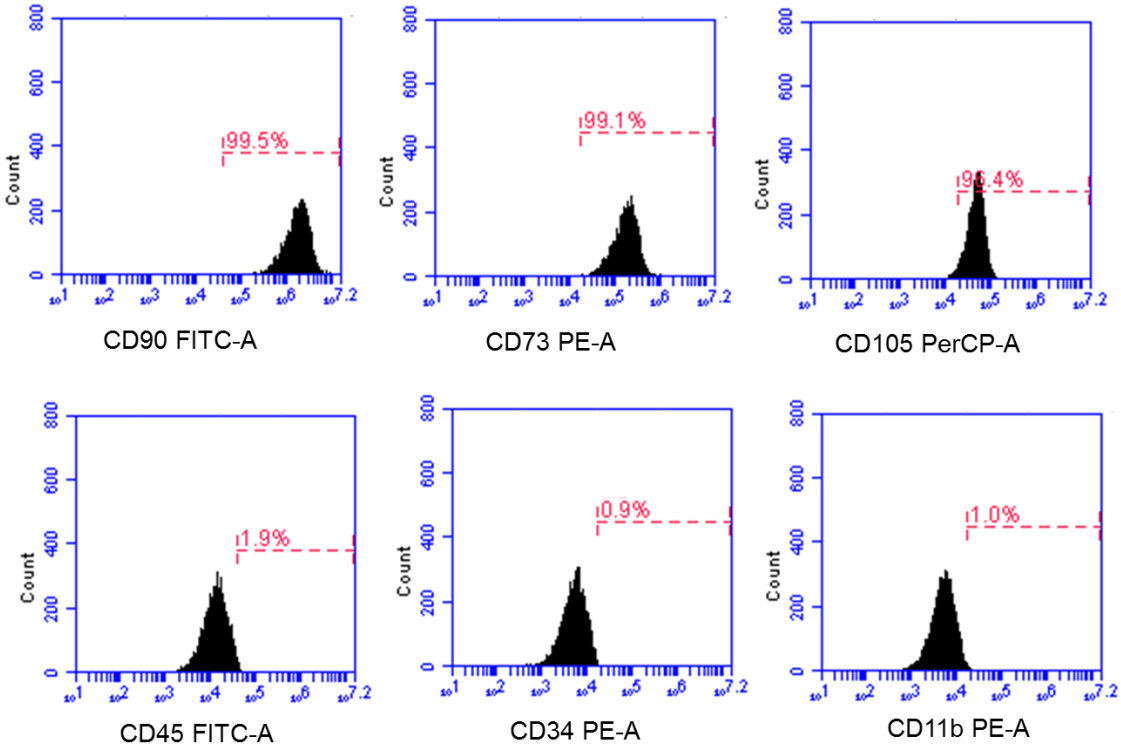

Figure 3-7: Immunophenotype by flow cytometry analysis of low-serum P13 hUC-MSCs. (I) isotype controls were run in parallel to the experimental samples. (J, 1) results reported positive expression of hMSC surface markers (CD90, CD73, and CD105); (J, 2) less than 1% of hMSCs expressed negative markers (CD45, CD34, and CD11b). The red horizontal line on each histogram represents the percentage of positive cells for each surface protein.

3.4.2: Attachment Assays

3.4.2.1: Cell attachment quantification

Attachment assays were carried out after the hMSCs reached 80-90% confluency. Three differently-sourced hMSCs were tested at the following passage numbers or PDL: P4 (PDL 5) individual donor gx11 hBM-MSCs, P6 (PDL 8) individual donor gx11 hBM-MSCs, PDL 15 commercial low-serum hBM-MSCs, P11 hUC-MSCs and P13 hUC-MSCs. In order to measure the effect of priming hMSCs with Notch ligands wells were imaged using an inverted light microscope at X4 magnification (five random fields of view per well). Following this, the number of cells that attached to the fibronectin surfaces was quantified automatically by using the ImageJ "analyse particles" tool. An example of triplicate wells of adhered P11 hUC-MSCs is shown in Figure 3-8, which suggests that the number of adherent cells for the sJag-1-primed cells was higher than that of the UT and the sDll4 samples. This observation was confirmed in the quantification data in Figure 3-11 A.

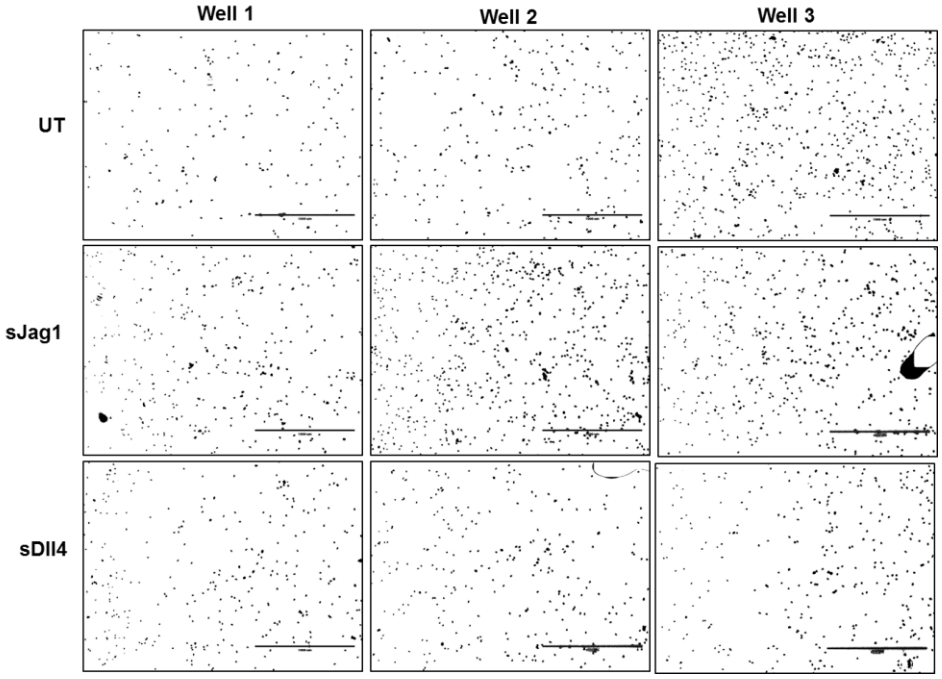

Figure 3-8: Sample phase contrast images of P11 hUC-MSCs after 20 min of adhesion on FN coated wells. Cells were quantified using the ImageJ cell plugin software. Scale bars = 1000 µm.

3.4.2.2: Attachment of differently-sourced hMSCs

The data for the individual donor gx11 hBM-MSCs showed that there were no marked differences between adhesion at 20 min and 45 min, this trend was observed for both P4 (PDL 5) and P6 (PDL 8) hBM-MSCs (Figure 3-9). The data also revealed that there were no evident differences in adhesion observed as a result of cell pre-stimulation by sJag1 and sDll4 over the untreated cells. However, as shown in Figure 3-9 A, there was a constant trend for both P4 (PDL 5) and P6 (PDL 8) hMSCs at both 20 min and 45 min where cells preconditioned with sJag1 exhibited a modestly higher cell adhesion when compared to the UT groups. This trend was more evident in the P6 (PDL 8) hBM-MSC groups at 45 min (Figure 3-9 A). In addition, the error bars for the P4 (PDL 5) gx11 hBM-MSCs were tighter than those observed for the P6 (PDL 8) cells.

A

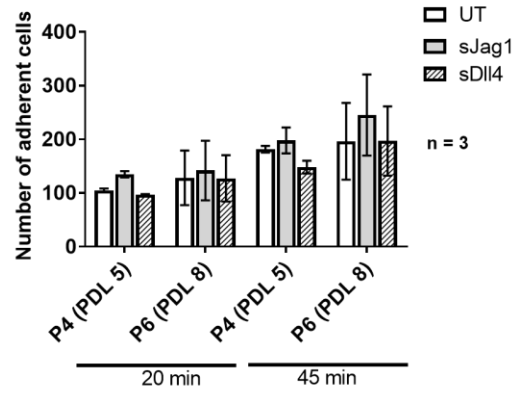

B

Time	Passage/PDL	UT			sJag1			sDll4		
20 min	P4 (PDL 5)	99	111	105	125	145	135	99	95	97
45 min	P6 (PDL 8)	95	228	62	107	251	68	150	188	44
20 min	P4 (PDL 5)	171	192	182	156	240	198	128	169	148
45 min	P6 (PDL 8)	184	326	79	207	391	138	261	262	68

Figure 3-9: (A) Quantification of cell count adhesion of P4 (PDL 5) gx11 hBM-MSCs and P6 (PDL 8) gx11 hBM-MSCs on FN coated surfaces at 20 min and 45 min. The data indicated the mean ± SEM of triplicate samples from 3 independent experiments. (B) Raw data from (A) of the three independently repeated experiments.

Similarly to the gx11 cells (Figure 3-9), no noticeable difference in cell attachment was observed between the commercial hBM-MSCs that were primed with sJag1 and sDll4 over the UT cells (see 20 min and 45 min; Figure 3-10).

A

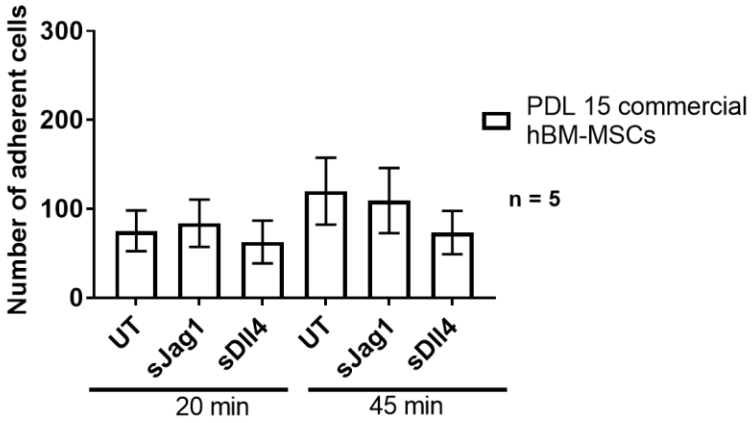

B

Time	Condition	PDL 15 commercial low-serum hBM-MSCs				
20 min	UT	128	134	28	44	43
20 min	sJag1	158	121	16	32	93
20 min	sDll4	125	118	19	26	26
45 min	UT	197	217	100	24	62
45 min	sJag1	155	233	47	54	59
45 min	sDll4	136	130	34	31	36

Figure 3-10: (A) Quantification of cell count adhesion of PDL 15 commercial hBM-MSCs on FN coated surfaces at 20 min and 45 min. The data indicated the mean ± SEM of triplicate samples from 5 independent experiments. (B) Raw data from (A) of the four independently repeated experiments.

Comparative adhesion studies were also carried out for P11 hUC-MSCs and P13 hUC-MSCs at 20 min and 45 min. The results showed that the adhesion of P11 hUC-MSCs primed with sJag1 at 20 min and 45 min and 20% O_2 and 2% O_2 respectively was approximately two-fold higher than that observed for the UT cells (Figure 3-11 A). However, this trend was not observed for the P13 hUC-MSCs where pre-stimulation by sJag1 appeared to have no marked effect on attachment (see Figure 3-11 B, 20 min and 45 min at 20% and 2%). On the other hand, sDll4 priming did not appear to benefit cell adhesion and this trend was evident in both slightly-older and slightly-younger cells (Figure 3-11 A and B).

Furthermore, the data revealed no marked differences between adhesion at 20% O_2 and 2% O_2, this trend was observed for both P11 and P13 hUC-MSCs for all conditions (see Figure 3-11 A and B, 20 min and 45 min, 20% O_2 and 2% O_2 for UT, sJag1 and sDll4). Next, the comparative data in Figure 3-11 C revealed that the P11 hUC-MSCs showed at least a two-fold increase in adhesion to fibronectin than the P13 hUC-MSCs at 20 min for 20% O_2 and 2% O_2 respectively, these differences were more obvious in the sJag1 groups. At 45 min the differences in cell adhesion between the P11 and the P13 hUC-MSCs for the UT and the sDll4 groups were not as obvious as those observed at 20 min. However, for the sJag1 groups at 20 min and 45 min, it was evident that the P11 hUC-MSCs performed noticeably better than the P13 cells with at least a two-fold increase in adhesion to fibronectin. Overall these results indicated that increase in cell age may decrease the adhesion properties of hUC-MSCs (Figure 3-11 C). However, further work will need to be carried out with more hUC-MSC donors.

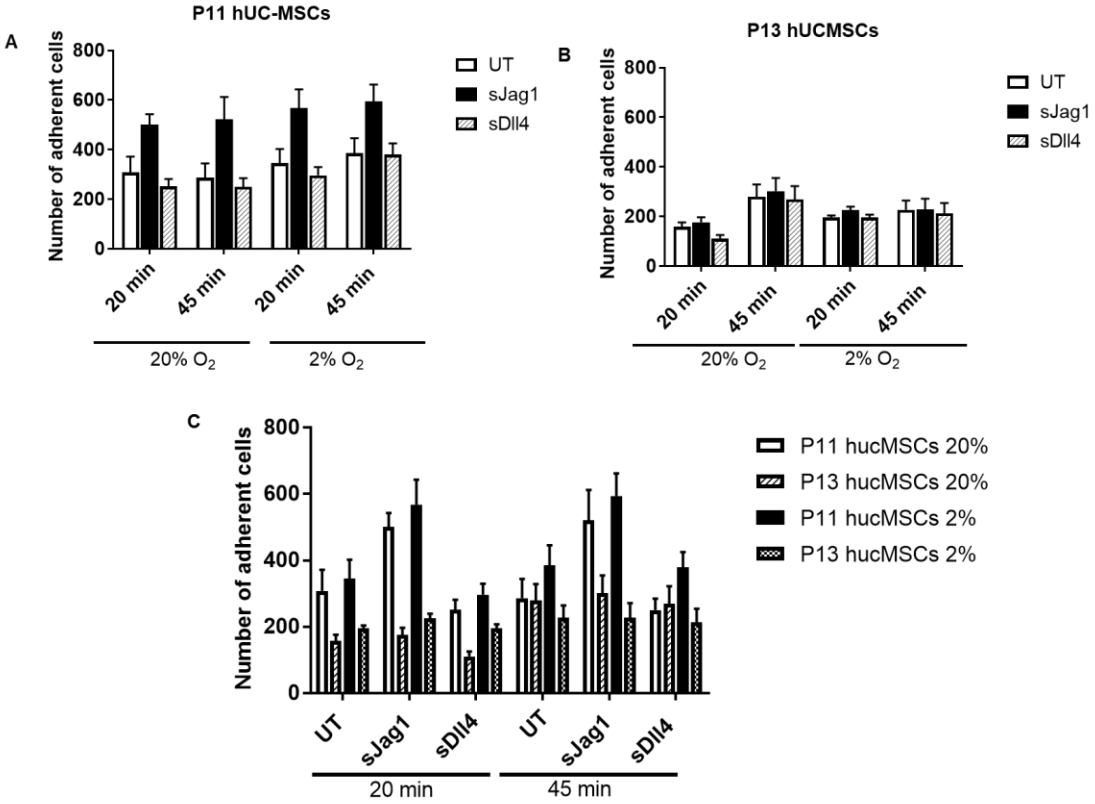

Figure 3-11: Comparison of cell adhesion using P11 (A) and P13 (B) hUC-MSCs at 20% and 2% oxygen tensions for 20 min and 45 min time points. (C) Comparison of P11 and P13 hUC-MSCs at different conditions. The results in (A), (B) and (C) indicated the mean ± SEM of triplicate samples from n = 4 independent experiments.

3.4.2.3: Comparing the effect of different sJag1 and sDll4 concentrations on the adhesion of commercial hBM-MSCs

In the present study commercial hBM-MSCs were treated with various concentrations of Notch ligands (sJag1 or sDll4 priming at 200 ng/ml, 500 ng/ml and 800 ng/ml) and two different concentrations of FN (5 µg/ml and 20 µg/ml) were also investigated.

The data revealed that there were no noticeable differences in cell adhesion at 20 min between the different concentrations of FN and of Notch ligands (Figure 3-12 A). In addition, no evident trends were observed between the sJag1, sDll4, and UT groups at 20 min (Figure 3-12 A). Next, the hMSCs primed with 800 ng/ml sJag1 consistently showed the lowest adhesion to FN (Figure 3-12 A and B), and this difference in adhesion became more evident with increase in incubation time. In fact, at 45 min the values for the 200 ng/ml sJag1 were almost double that of the cells primed with 800 ng/ml sJag1 (Figure 3-12 A and B).

Furthermore, it was also observed that the sDll4 cells exhibited a concentration-dependent trend. In fact, with the increase in sDll4 concentration, the adhesion of the cells to FN decreased. However, the cells primed with 800 ng/ml sDll4 did not follow this trend (Figure 3-12 A and B).

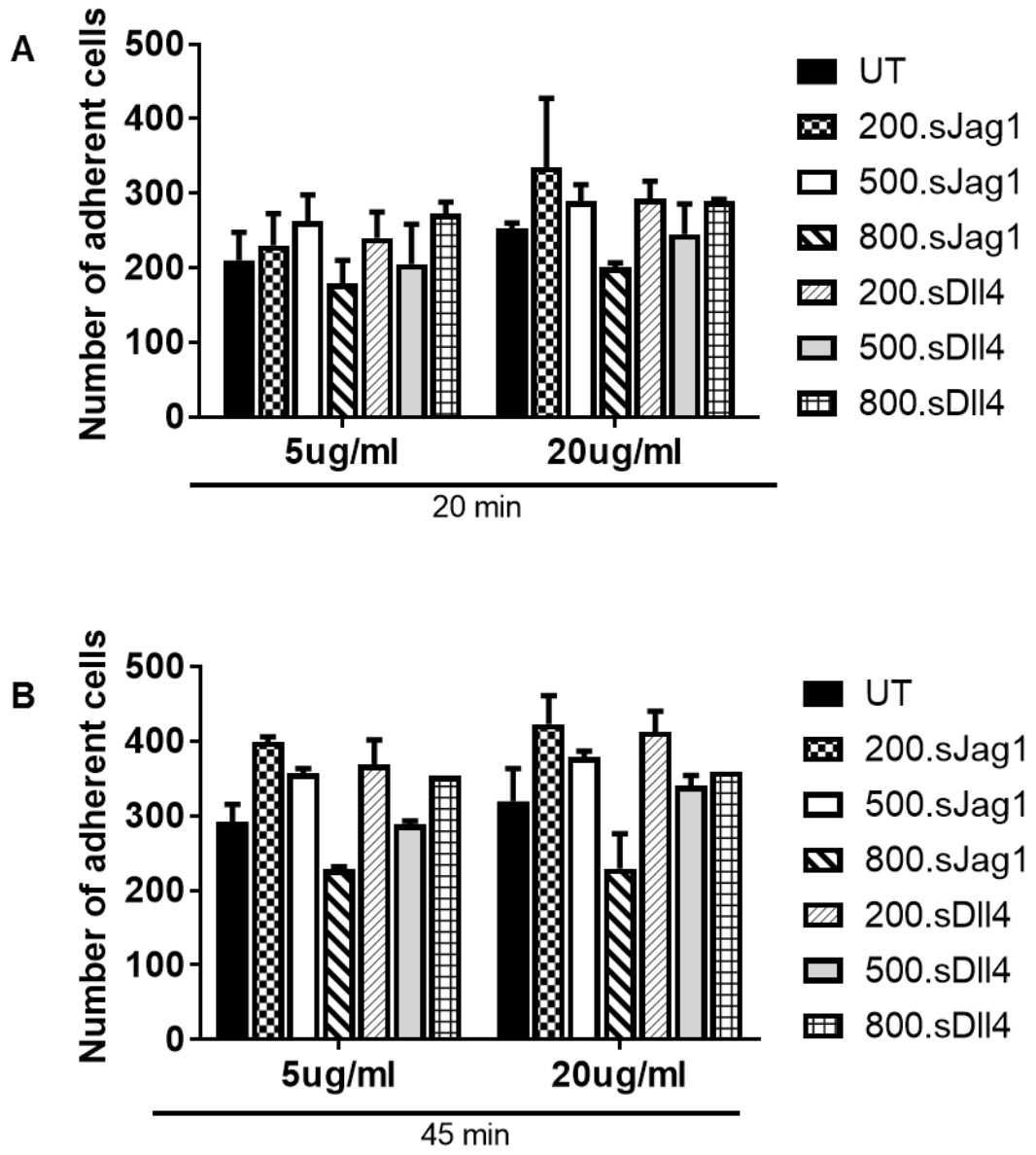

Figure 3-12: Effect of different sJag1 and sDll4 concentrations on the adhesion of PDL 15 commercial hBM-MSCs. Cells were seeded on FN coated plates at 5 µg/ml and 20 µg/ml respectively. The data in (A) indicates the mean ± SEM of triplicate samples from 3 independent experiments. The data in (B) indicates the mean ± SD of triplicate samples from 2 independent experiments.

3.4.2.4: Beta integrin staining for commercial hBM-MSCs

Cell adhesion is mainly mediated by integrin protein heterodimers formed by non-covalently assembled α and β subunits (Veevers-Lowe et al., 2011). This study investigated the expression of the active and inactive form of integrin β-1 in sJag1-primed hMSCs upon seeding to FN surfaces. PDL15 commercial hBM-MSCs were cultured on FN surfaces for 45 min, washed and stained with antibodies against total integrin β-1 (recognizes both active and inactive form of integrin β-1) and active integrin β-1 (also known as CD29). Total and active integrin β-1 were used to determine whether any differences in attachment were apparent between the UT groups and the groups of cells primed with the different concentrations of sJag1 (Figure 3-13). An intensity analysis was carried out to investigate differences in integrin β-1 activation between sJag1-primed cells and untreated samples.

The immunofluorescence results indicated that in the UT groups fewer cells expressed the active integrin β-1 in comparison to the cells that were primed with sJag1 (Figure 3-13 A). On the other hand, the total integrin β-1 levels seemed to be equal in all of the conditions (Figure 3-13 A). Furthermore, the normalized mean intensity was quantified by developing an ImageJ script that automatically measured values for integrated density (sum of the intensity of pixels), area (number of pixels) and mean intensity (integrated density/area). Images were scaled in μm by obtaining the value in pixels of the scale bar on the image.

The data indicated that the overall active integrin β-1 / total integrin β-1 mean intensity (ratio of sum of intensity of pixels that are positive in the red channel / area, and then sum of the intensity of pixels that are positive in the green channel / area) was higher in sJag1 treated cells over the control groups (Figure 3-13 D). In particular, cells primed with 500 ng/ml sJag1 showed nearly double the values of mean intensity than that of the untreated samples, however it was not possible to carry out statistical analysis as only one independent experiment was carried out (Figure 3-13 D).

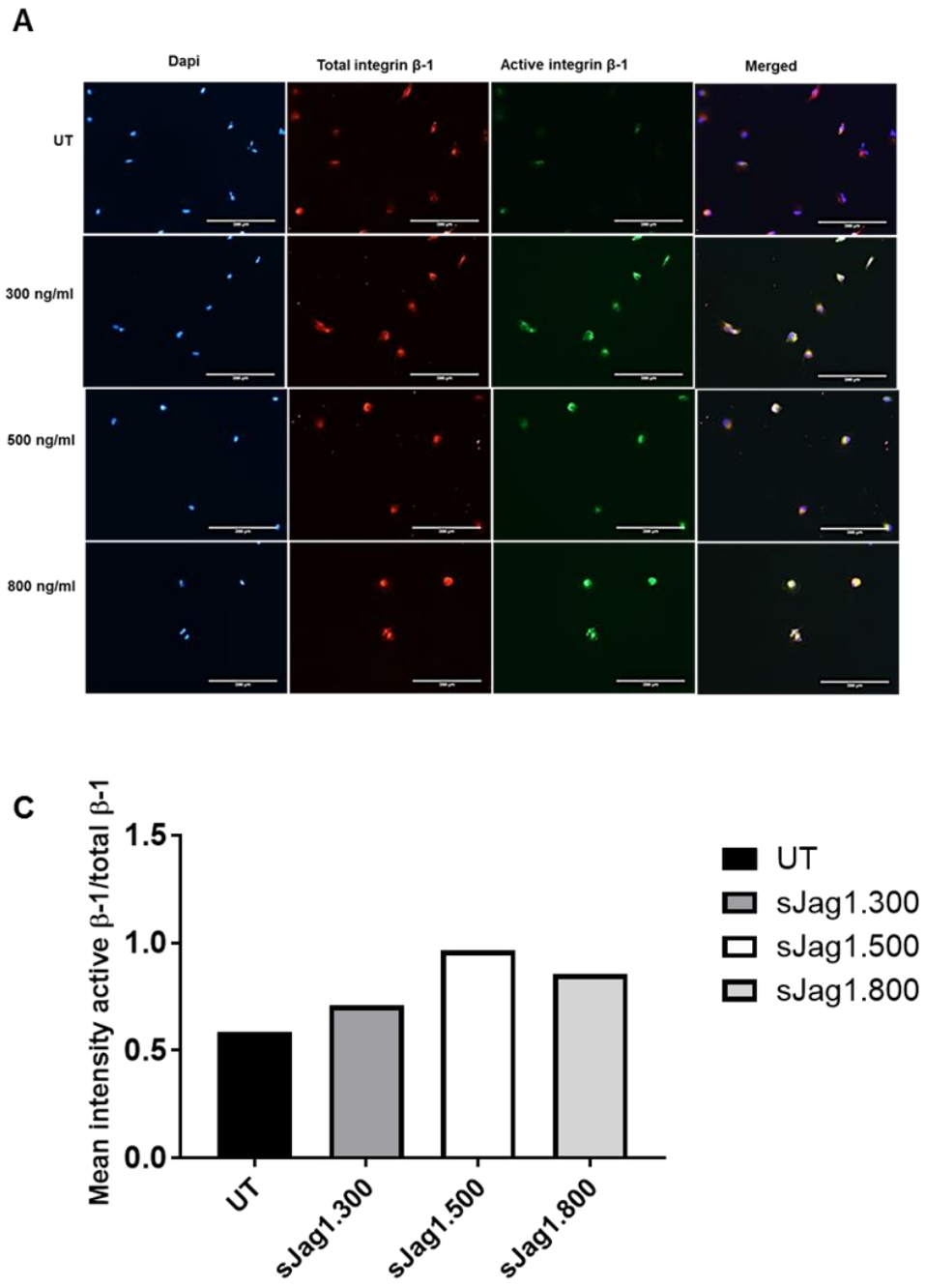

Figure 3-13: (A) Positive staining for total (stained red) and active integrin β-1 (stained green) using commercial low-serum PDL15 hBM-MSCs primed with different concentrations of sJag1 after 45 min adhesion at 20% O_2. DAPI stain (in blue) was performed to visualize the nuclei of the cells. Scale bars = 200 µm. (B) Quantification of cell fluorescence using ImageJ, where mean intensity represented integrated density/area occupied by integrin β-1. The data indicated the mean ±SD of five pictures of a well for sJag1 at 300 ng/ml, 500 ng/ml and 800 ng/ml respectively, and triplicate values for UT with each value representing five pictures per well.

3.4.3: Effect of low oxygen on the migration abilities of commercial low-serum hBM-MSCs

The phase contrast images for the normoxic hBM-MSC experiments showed that there was stronger migration across FN when PDG-BB was present (Figure 3-14 A). This was expected, as PDGF-BB is an important chemoattractant for mesenchymal cells as previously reported in other studies (Veevers-Lowe et al., 2011). The results also showed that there were no obvious differences in migration between UT (+PDGF-BB), sJag1 (+PDGF-BB) and sDll4 (+PDGF-BB) groups.

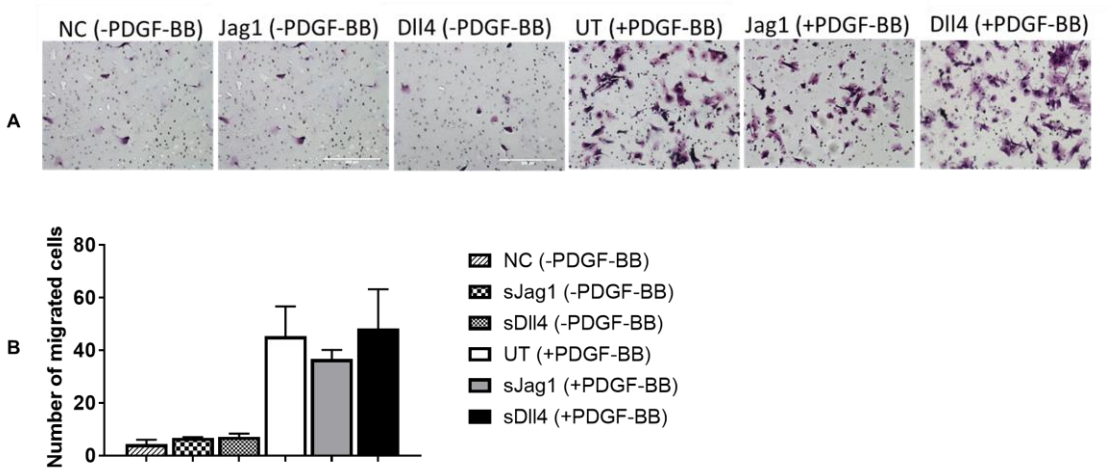

Figure 3-14: (A) Representative transwell migration phase contrast images of normoxic PDL 15 commercial hBM-MSCs. Assays were performed in ambient oxygen conditions. Scale bars = 200 µm. (B) Quantification of the number of migrated cells across fibronectin. The data in indicated the mean ± SEM of triplicate samples from 3 independent experiments.

The phase contrast images for the normoxic hBM-MSC experiments showed that there was high variability between the independently repeated experiments that were mainly introduced by the values in experiment 3 (Figure 3-15 A and C). The data showed there were no obvious differences in migration between the sJag1 pre-conditioned groups and untreated groups + or - PDGF-BB (Figure 3-15 B). However, the values for the sDll4 groups showed approximately a two-fold decrease in migration compared to the untreated groups and also against the cells treated with sJag1 (Figure 3-15 B). Based on the mean data of experiment 2, the values for sJag1 and sDll4 might have been considered as outliers since there was less variability between experiment 1 and experiment 3 (Figure 3-15 B and C). However, as experiment 2 performed best and it followed the expected

trend of higher migration across fibronectin in the presence of a chemoattractant (PDGF-BB), there is a need to carry out further experiments to draw conclusions.

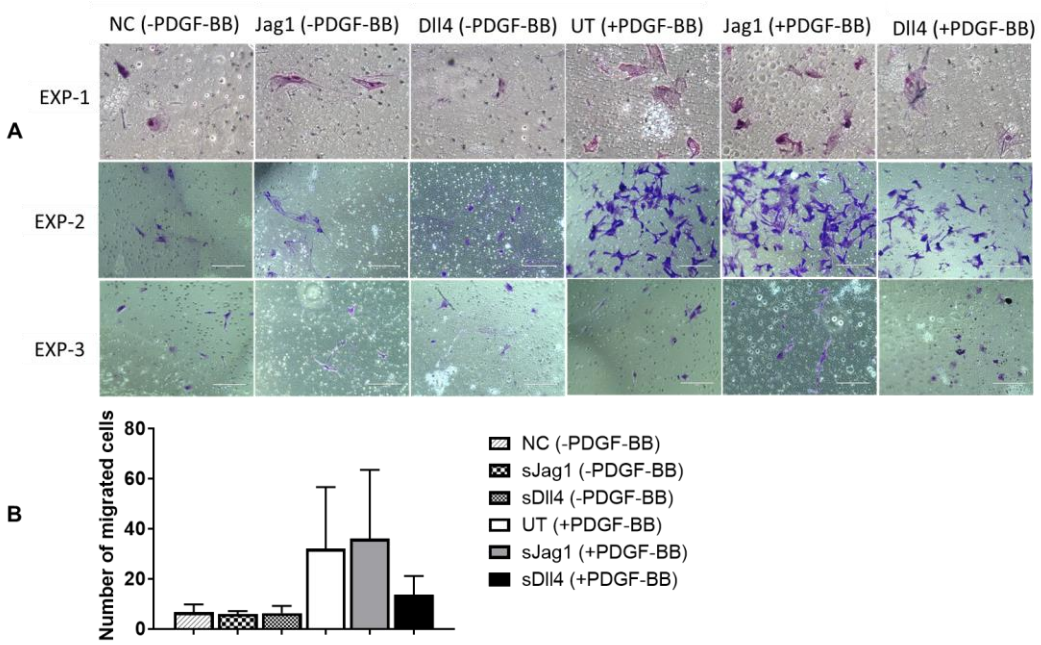

C

Conditions	Experiment1	Experiment 2	Experiment 3
NC (-PDGF-BB)	12	7	1
sJag1 (-PDGF-BB)	6	4	8
sDll4 (-PDGF-BB)	11	7	1
UT (+PDGF-BB)	13	**81**	2
sJag1 (+PDGF-BB)	11	**91**	6
sDll4 (+PDGF-BB)	13	27	1

Figure 3-15: (A) Representative transwell migration phase contrast images of hypoxic PDL 15 commercial hBM-MSCs for each independently Assays were carried out in ambient oxygen conditions. Scale bars = 200 µm. (B) Quantification of the number of migrated cells across fibronectin. The data in indicated the mean ± SEM of triplicate samples from 3 independent experiments. (C) Raw data from (B) of the three independently repeated experiments.

The results also indicated that there were no obvious differences in the number of migrated cells between the normoxic and the hypoxic hBM-MSCs for the sJag1 groups (Figure 3-16). On the other hand, the number of migrated cells for the normoxic hMSCs primed with sDll4 were at least two-fold higher than those observed for the hypoxic hMSCs (see sDll4 groups; Figure 3-16). This result suggested that hypoxic pre-conditioning may not be beneficial for cell migration on cells primed with sDll4. Next, there was a higher number of migrated cells in the UT groups when using the normoxic hMSCs in comparison to the hypoxic groups however, differences were not as marked as it was observed in the sDll4 groups. It is notable that there was a much tighter distribution for normoxic hMSC groups in comparison to that observed for the hypoxic hMSC groups. Therefore, more experiments will need to be performed to validate these trends.

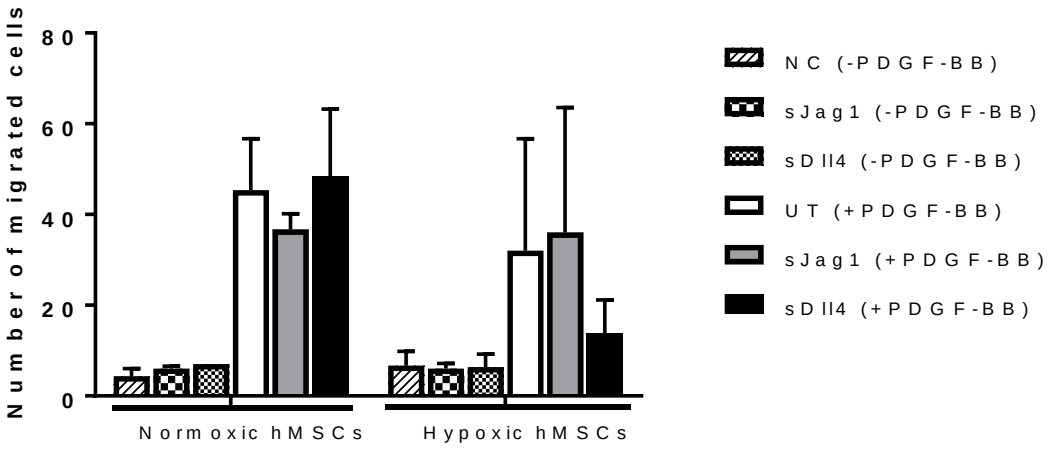

Figure 3-16: Quantification of number of migrated cells using either normoxic hMSCs or hypoxic hMSCs. Experiments were carried out at ambient oxygen conditions. The data indicated the mean ± SEM of triplicate samples from 3 independent experiments.

3.5: Discussion

Previous literature showed that hMSCs from different sources exhibit different proliferation and growth abilities (Chen et al., 2014). In fact, even though hUC-MSCs have been shown to have similarities to hBM-MSCs (Hass et al., 2011), evidence suggests that they exhibit greater proliferation capacity and faster growth *in vitro* than bone marrow-derived MSCs (Jin et al., 2013; Chen et al., 2014). For example, hUC-MSCs have been shown to have doubling times of 2-3 days from P0 to P3 in comparison to ~5 days (P1-2) and ~11-12 days (P2-3) observed for BM-MSCs (Mennan et al., 2013).

In this work, first tri-lineage differentiation studies were performed to confirm that UC-MSCs underwent differentiation in response to chemical stimuli similar to BM-MSCs. Next, the second aim was to assess whether there were any differences in cell attachment between UC-MSCs and those isolated from bone marrow. Since cell age has also been shown be another factor impacting on the potency of MSCs (Ullah et al., 2015), comparative studies were carried out between slightly earlier and slightly later passage hMSCs. All of the cells used in this study displayed a spindle-like morphology typical of hMSCs (Figure 3-1). However, with the increase in cell age, the MSCs became less spatially organized and they appeared to increase in size (Figure 3-1). As observed in other studies, the morphological changes observed in older MSCs (e.g. increase in size) due to cell age may not be necessarily associated with a decrease in positive MSC surface marker expression (Dominici et al., 2006; Lo Surdo and Bauer, 2012; Whitfield et al., 2013). For example, in one study hBM-MSCs from two different donors and three different passage numbers (P3, P5, and P6) were compared in terms of marker expression and cell morphology. The study showed that the cells from the two different donors and three different passage numbers maintained over 95% expression of all the positive markers described in the ISCT paper (Dominici et al., 2006). The results from the characterization studies were also in line with the work of Chen et al. where it was shown that old hUC-MSCs (passag15) were still able to meet the surface expression standards set by the ISCT (Chen et al., 2014).

The immunophenotype analysis indicated that positive marker expression of the slightly earlier and slightly older passage hMSCs was in line with the guidelines set by the ISCT (>95% positive expression; Caplan, 2007). However, the expression of CD105 for the PDL17 hBM-MSCs was lower (82.2%) compared to that of the PDL 14 hBM-MSCs (94.4%) and gx11 P6 (PDL 8) hBM-MSCs (96.2%) (Figure 3-3 B1; Figure 3-4 D1; and Figure 3-5 F1). The evident decrease in CD105 expression for commercial PDL17 hBM-MSCs indicated a loss of differentiation potential. Contrasting results have been reported in the literature in relation to the expression of CD105 by UC-MSCs. In fact, whilst some studies reported the expression of CD105 even at later passages (> passage 16; Shi et al., 2015), other studies showed that either CD105 is not expressed by these cells or that it is expressed only in early passage UC-MSCs (Kadam et al., 2009; Bakshi et al., 2008). Overall, the data from the phase contrast images together with the immunophenotype results showed that the PDL 17 hBM-MSCs were able to proliferate in culture and to express high levels of the positive markers (>95%) as well as negligible levels of the negative markers (<2%) (Figure 3-2; Figure 3-5 F1).

Next, all of the differently-sourced MSCs were able to undergo tri-lineage differentiation with positive osteogenic, adipogenic and chondrogenic staining (Figure 3-2). The results from this study were line with previous work that showed that UC-MSCs are able to undergo tri-lineage differentiation (Mennan et al., 2013). Differently from previous studies, there were no marked differences in terms of osteogenic and adipogenic differentiation between UC-MSCs and BM-MSCs. In fact, both umbilical-derived and bone-marrow derived cells were able to form mature adipocytes and the size of the vacuoles in these cells appeared to be the same. Furthermore, in agreement with previous work, the microscopy images also showed no obvious differences in chondrogenic differentiation between the differently-sourced cells (Figure 3-2; Mennan et al., 2013).

The current work demonstrated that all of the hMSCs used in this study (slightly earlier and slightly later passage) were able to attach to the FN-coated surfaces. However, only P11 hUC-MSCs showed a significant adhesion response to sJag1 priming, with the adhesion values for the sJag1 groups being approximately two-fold higher than those of the UT groups. Furthermore, no evident difference in

adhesion was observed when cells were pre-stimulated with sDll4 in comparison to the untreated samples. Following this, P11 hUC-MSCs appeared to perform better than the gx11 hBM-MSCs (Figure 3-9) and the older P13 hUC-MSCs (Figure 3-11 B); this trend was observed for all of the conditions (UT, sJag1, and sDll4). This data is in line with previous *in vivo* work which showed that UC-MSCs have higher engraftment abilities in comparison to bone marrow cells hence resulting in the lower numbers of UC cells required (Broxmeyer et al., 2013). However, as this study only used one donor for either UC-MSCs or BM-MSCs, the positive results observed for the UC-MSCs, can only be attributed to the specific cell populations used. Therefore, further work will need to be carried out using a bigger number of donors to confirm these results. However, previous work also showed that UC-MSCs have less inter-donor variability compared to other MSCs sources (Wegmeyer et al., 2013), hence suggesting that the positive outcomes in this study could be observed in other UC-MSC cell populations.

Next, no evident differences were observed for the individual donor gx11 hBM-MSCs (earlier and late passage/PDL) and in the P13 hUC-MSCs. However, all of the UC-MSC and gx11 B-MSCs showed a constant trend where sJag1 primed cells displayed higher adhesion to FN-coated wells. It is odd that there were no apparent differences with sJag1-priming or between younger and older individual donor hBM-MSCs because other research showed that they did. For example, contrarily to the results from this study (Figure 3-9), it was shown that slightly later passage (P5) bone marrow MSCs adhered to FN surfaces at a significantly faster rate than slightly earlier passage (P3) cells. Previous work also demonstrated that at 40 min adhesion sJag1-primed hBM-MSCs showed a significant higher adhesion to FN surfaces than untreated cells and these differences were not observed/obvious in this work (Figure 3-9). On the other hand, the data for the 20 min adhesion (Figure 3-9) was in line with the work of Detela (2014) which showed that the adhesion of sJag1-primed cells to fibronectin was not considerably higher than that of the untreated cells.

The work of Detela (2014) also demonstrated that hBM-MSCs exhibit donor-dependent variability which could have resulted in different outcomes in this study

(Bain et al., 2014; Detela et al., 2018). Future work, could focus on comparing the adhesion abilities of hBM-MSCs from different donors to investigate inter-donor variability and to further confirm the data obtained in this study.

The higher heterogeneity observed in the gx11 hBM-MSCs may have played a role in the increased variability observed in the P6 (PDL 8) experiments in comparison to the P4 (PDL 5) experiments. Therefore, from a manufacturing perspective using the later passage hBM-MSCs would decrease process consistency. The increased cell heterogeneity of hBM-MSCs expanded in culture for longer times (>5 passages) has also been reported in the literature (Whitfield et al., 2013). Cell age also seemed to affect the hUC-MSCs, as the later passage cells displayed less adherence post pre-stimulation and did not show the significant adhesion in response to sJag1 observed in the younger cells (Figure 3-11 A, B and C).

This study also showed that when P13 hUC-MSCs were primed with sDll4 and incubated at ambient oxygen, there was a two-fold decrease in the number of cells adhering to fibronectin at 20 min in comparison to the 45 min adhesion (Figure 3-11 B). This result suggested that effective cell adhesion was not achievable at lower time points when pre-stimulating P13 hUC-MSCs with sDll4 and that therefore it may not be beneficial to use hUC-MSCs older than P11 for clinical application. However, the variability encountered within experiments (Figure 3-11 A and B) which can be associated with the use of biological reagents such as the serum and other components from animal origin, as well as the manual errors that can come from the intensive manipulation of cells to achieve specific concentrations affects the reliability of the system.

Another major challenge is the tracking of cells by the passage number. This is not a reliable way of quantifying cell age, as it only represents how many times the physical act of harvesting and re-plating takes place. The seeding density, time in between splits, and harvest density would then affect the true age or PDL of the harvested cells. In addition, performing the experiments at different times

brings in its own right different outcomes and therefore comparing across different cells processed at different times can be a huge challenge. Therefore, in order to improve the reliability of these assays, there is a need to eliminate/reduce serum where possible, track cell age by PDL instead of passage number, minimise operator error and variability when culturing cells and setting up experiments by including automated processing systems. These would be a less-time consuming option and it would increase data robustness.

A recent study showed that low oxygen environment enhanced the proliferation and differentiation of MSCs to cardiomyocyte-like cells when these were cultivated at 3% O_2 but this was not observed at 1% and 5% O_2 (Zhang et al., 2015). It has also been reported that bone marrow MSCs subject to 5% O_2 displayed higher adhesion and increased levels of extracellular matrix molecules (Basciano 2011). However, Bain and colleagues showed that when bone marrow MSCs were subject to 2% oxygen tension for 20 min there was a decrease in adhesion abilities (Bain et al., 2014). Differences in cell source, low oxygen conditions and pre-conditioning time make it difficult to make reliable conclusions. Therefore, there is a need for different research groups to carry out comparative studies on the effect of oxygen concentration for the specific cells used in those studies and then make comparisons where possible.

The current work showed that there were no evident differences in adhesion between low and ambient oxygen conditions in both the early and late passage hUC-MSCs (Figure 3-11 A and B). This result was not in line with previous work by Bain and colleagues that showed a decreased attachment to fibronectin after only 20 min of priming the MSCs in low oxygen. This outcome may be associated with the use of .differently-sourced MSCs (i.e. hBM-MSCs were used in the studies of Bain and colleagues).

Additionally to this, most studies showing the enhanced proliferation, differentiation and the elevated expression of energy metabolism-associated genes with hypoxic pre-conditioning (<5%) used much younger hUC-MSCs (P<5)

than those used in this study (Lavrentieva et al., 2010; Zhang et al., 2015). However, in the later passage hUC-MSCs there was an evident increase in adhesion in the sDll4 groups between the 20 min and the 45 min time points at ambient oxygen (see 20% O_2, sDll4 at 20 min and 45 min; Figure 3-11 B). On the other hand, no differences in cell adhesion were observed between sDll4 groups at 20 min and 45 min at low oxygen (see 2% $O_{2;}$ sDll4 at 20 min and 45 min; Figure 3-11 B). This result is in line with previous work which showed that low oxygen conditions increase the adhesion abilities of MSCs expressing Dll4 (Ciria et al., 2017).

Next, it was decided to carry out a titration study investigating the impact of different concentrations of sJag1 and sDll4 on the commercial hBM-MSCs. This was done because no clear trend in cell adhesion could be determined using these cells (Figure 3-10). The results from these experiments showed that hBM-MSCs primed with 800 ng/ml of sJag1 consistently showed the lowest adhesion to FN and this difference in adhesion became evident with the increase in incubation time to 45 min (Figure 3-12). This data suggested that a plateau might have been reached before 800 ng/ml where any further increase in sJag1 concentration might have led to a decrease in adhesion efficiency, whilst the sDll4-primed cells performed similarly at all concentrations. In contrast to the results from the migration studies, the β-integrin staining experiments suggested that the presence of sJag1 at the different concentrations of sJag1 is beneficial for attachment to FN. However, it was not possible to obtain conclusive answers from the staining work as not enough experiments were carried out to test statistical significance.

Increasing the number of hMSCs adhering to the infarcted heart has been a major goal for clinical applications. Previous work reported that the number of hMSCs retained in the heart after 24 hours amounted to less than 1% (Cheng et al., 2008). For this reason, the current work focused on increasing the retention properties of hMSCs in the heart as it is necessary to use cells that can firmly and rapidly attach. Furthermore, a study investigating the effect of cell adhesion using hMSC sheets reported effective cell adhesion to a porcine heart tissue after 30

min whilst adhesion at 15 min was not effective (Chang et al., 2015). Following this, the current work investigated the time required for adequate adhesion to FN coats. This study revealed that there was no apparent difference in adhesion between the 20 min and 45 min experiments for P4 (PDL 5) gx11 hBM-MSCs, P6 (PDL 8) gx11 hBM-MSCs, P11 hUC-MSCs, commercial PDL15 hBM-MSCs and P13 hUC-MSCs for the UT and sJag1 groups only. As a result it was possible to conclude that efficient attachment took place within 20 minutes of seeding and that cells did not migrate with increase in incubation time. This was a positive outcome as it has been previously reported that waiting long for effective cell adhesion leads to higher post-surgical complications (Chang et al., 2015).

Previous literature showed that hypoxia pre-conditioning increased the migration abilities of MSCs by increasing the protein levels of Jagged 1-2 and Delta-like (Dll)1, Dll3, and Dll4 (Ciria et al., 2017) after cultivating the cells in 1% O_2 for 4 hours. For this reason, this study investigated the effect of preconditioning the hMSCs in hypoxic conditions for longer times to see whether there were changes in the migration MSCs or not. However, no evident differences were observed between preconditioned hypoxic and normoxic hMSCs, except in the sDll4 groups where using the normoxic hMSCs led to at least a two-fold increase in migration (Figure 3-16). Carrying out the migration experiments in ambient oxygen conditions might have switched off genes activated by the low oxygen priming. Therefore, it may be worth to carry out gene expression analysis on hypoxic hMSCs moved to ambient oxygen conditions for a few hours.

Overall, this study confirmed that hUC-may be were superior in adhesion when compared to the gx11 hBM-MSCs especially since they were used at higher passages. However, as only one donor was used for each, there is a need to perform more experiments testing a bigger range of donors to confirm these results.This study, also indicated that 20 min may be a sufficient time to achieve effective cell adhesion to FN-coated wells and that sJag1 can be stimulatory to earlier passage hUC-MSCs.

Chapter 4: Optimization of endothelial cell *in vitro* vascular assays as platforms to examine the supportive role of hMSCs in ischemic injury

4.1: Introduction

In the following section I will summarize the relevant literature which I have discussed in Chapter 1.

Ischemic heart disease is one of the leading causes of mortality in the world (Finegold et al., 2013). Multiple clinical trials have explored the use of MSCs for therapeutic angiogenesis for the treatment of ischemic cardiac injury (Cashman et al., 2013; Eckert et al., 2013; Huang et al., 2015). For example, in one study it was shown that when mesenchymal cells were injected into patients with MI, there was increase in angiogenesis and perfusion at the site of injury which led to a decrease in contractile dysfunction of the myocardium (Shake at el., 2001).

Angiogenesis and vasculogenesis are key processes involved in the *de novo* synthesis of new blood vessels or the formation of blood vessels from existing blood vessels e.g. spouting and branching (Jain, 2003). These processes are necessary for the supply of oxygen and nutrients for the body's tissues and therefore for the regeneration of the ischemic myocardium. Vascularization is a complex process and in order to understand the role of endothelial cells and MSCs in promoting angiogenesis, there is a need to create adequate assays that can validate their functions. However, there is a lack of biomarkers and potency assays that can give a predictive readout of the mode of action of cell products in the clinical setting (Galipeau and Krampera, 2015; Ketterl et al., 2015).

For this reason, *in vitro* cell-based potency assays have been proposed as a potential tool to measure the intended therapeutic response of cell therapy products (CTPs), other than simple surface marker expression (Galipeau and Krampera, 2015; Samsonraj et al., 2015; Thej et al., 2017). Furthermore, there is a need to first measure and understand key functions of endothelial cells in

tubules assays and then use them as robust platforms to study the mode of action of MSCs.

Human umbilical vein endothelial cells (HUVECs) are the most widely used for *in vitro* studies and they are a useful *in vitro* models that have unveiled major insights in angiogenesis and the regulation of endothelial cell function (Smith and Staton et al., 2007; Cao et al., 2017). HUVECs are primary cells and therefore they are more likely to be chosen over immortalised cell lines as they better resemble ECs *in vivo* (Cao et al., 2017). Furthermore, they can be easily isolated in the lab (Smith and Staton, 2007). In addition, they are also commercially available (Cao et al., 2017).

HUVECs have been shown to respond to a variety of physiological stimuli such as shear stress, high glucose and hypoxic pre-conditioning (Zhang et al., 2012; Cao et al., 2017). Furthermore, they can be used to understand the effect of different substances and factors (e.g. cell age) on the endothelium through tube formation assays (Smith and Staton et al., 2007; Cao et al., 2017). In these assays, cells are seeded onto a basement-membrane-like substrate on which the cells are able to form capillary-like networks in a short amount of time (Arnoutova et al., 2010). In this way, it is possible to study the effect of different factors that have a role in angiogenesis.

In vitro vascular assays have many limitations including the undefined chemical composition of the reagents e.g. Matrigel (Arnaoutova and Kleinman, 2010) and the heterogeneity observed between endothelial cells (Arnaoutova et al., 2009). Specific issues associated with tubule formation assays are related to the use of Matrigel. This solubilized basement membrane preparation is extracted from the Engelbreth-Holm-Swarm (EHS) sarcoma, a type of cancer, and is composed of a mixture of extracellular basement membrane proteins such as collagen IV and laminin. Matrigel, is the preferred matrix for vascular tubule assays (Khoo et al., 2011) as it allows for the formation of capillary-like networks in a short time scale (4-12 hours), whilst other matrices such as collagen take up to five days to show vessel

formation (Smith and Staton, 2007). However, the composition of Matrigel is poorly characterised as it contains extracellular matrix proteins, growth factors, collagenases and many undefined components. The heterogeneity of Matrigel and its uncharacterized components creates a key disadvantage for tubule formation assays, as it reduces the reproducibility of these assays (Arnaoutova and Kleinman, 2010). Therefore, this chapter also focused on measuring key functions of HUVEC tubule formation. In the current work a range of matrices were assayed- Cell Start, (GFR) Matrigel, and GFR Geltrex. The latter, is also derived from mouse EHS tumour and in comparison to Matrigel it offers a 2-fold decrease in several growth factors and a consistent manufacturing process. The latter ensures a protein concentration with very little variation between batches.

This study also investigated whether lower matrix volumes of Matrigel could be used to minimize assay costs. Previous literature indicated that using HUVECs older than P10 would reduce tubule network formation (O' Donnell et al., 2000; Staton et al., 2007). Therefore, the current work investigated the impact of passage number on tubule formation capacity, to determine whether an increased number of assays is possible from one single batch of cells. In addition, manual quantification was compared to an automated counting technique to measure attributes of the branching network. Using the latter would be advantageous as it avoids the bias introduced when performing the manual counts as well as the difficulty of accurately measuring the length of the branches.

Ultimately the data from this study will give valuable insights into key functions of endothelial tubule formation and strategies to reduce assay-costs and increase their robustness.

4.2: Aims and hypotheses

4.2.1: Aims

- To use a methodological approach to determine key functions of HUVEC tubule formation.

- To evaluate the ability of old (> P10) HUVECs to efficiently form tubule networks.

- To investigate if automated counting methods can be used as a replacement to manual counting methods.

4.2.2: Hypotheses

- As cell age impacts on efficient tubule network formation, it is hypothesized that cells older than P10 will not be able to form tubule networks efficiently.

- It is hypothesized that the automated counting method will follow the same trend as the manual counting trend.

4.3: Materials and methods

All the general materials and methods that are not specific to this chapter are described in Chapter 2.

4.4: Results

4.4.1: Cell morphology and immunostaining

The morphological characteristics of HUVECs were observed using an inverted light microscope. HUVECs grew as a homogeneously distributed monolayer of polygonal cells (Figure 4-1). In addition, they maintained their cobblestone morphology even after they reached 80% confluency (Figure 4-1, day 4).

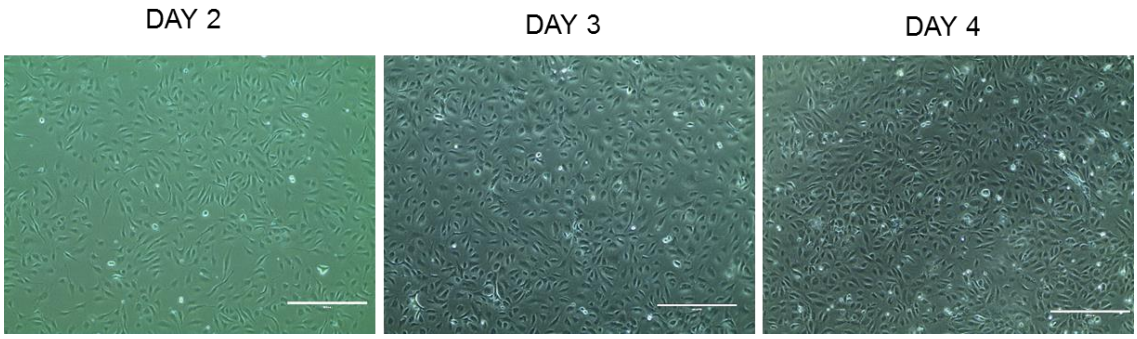

Figure 4-1: Morphology of P9 HUVECs. Representative phase-contrast images of P9 HUVECs displaying a cobblestone morphology. Scale bars = 1000 µm.

The identity of the P7 and P13 HUVECs was confirmed by immunofluorescence labelling using antibodies targeting the endothelial cell markers Von Willebrand Factor (vWF) and CD31 (Figure 4-2 and Figure 4-3) after one to three days. vWF is a glycoprotein which is only produced by endothelial cells (ECs) and it is generally used to identify ECs (Zanetta et al., 2000). CD31 is a cell surface glycoprotein highly expressed in ECs and it is involved in cell adhesion and signalling (Lalor et al., 2006). Negative controls using only the secondary antibodies were run in parallel to the stained cells (Figure 4-1 B and D; Figure 4-2 B and D). Cells stained with the vWF and CD31 confirmed the positive expression of the two markers in the older (Figure 4-1 A and C) and the younger (Figure 4-2 A and C) cells. On the other hand no staining was observed for the negative controls, indicating no cross-reaction from the secondary antibodies (Figure 4-1 B and D; Figure 4-2 B and D).

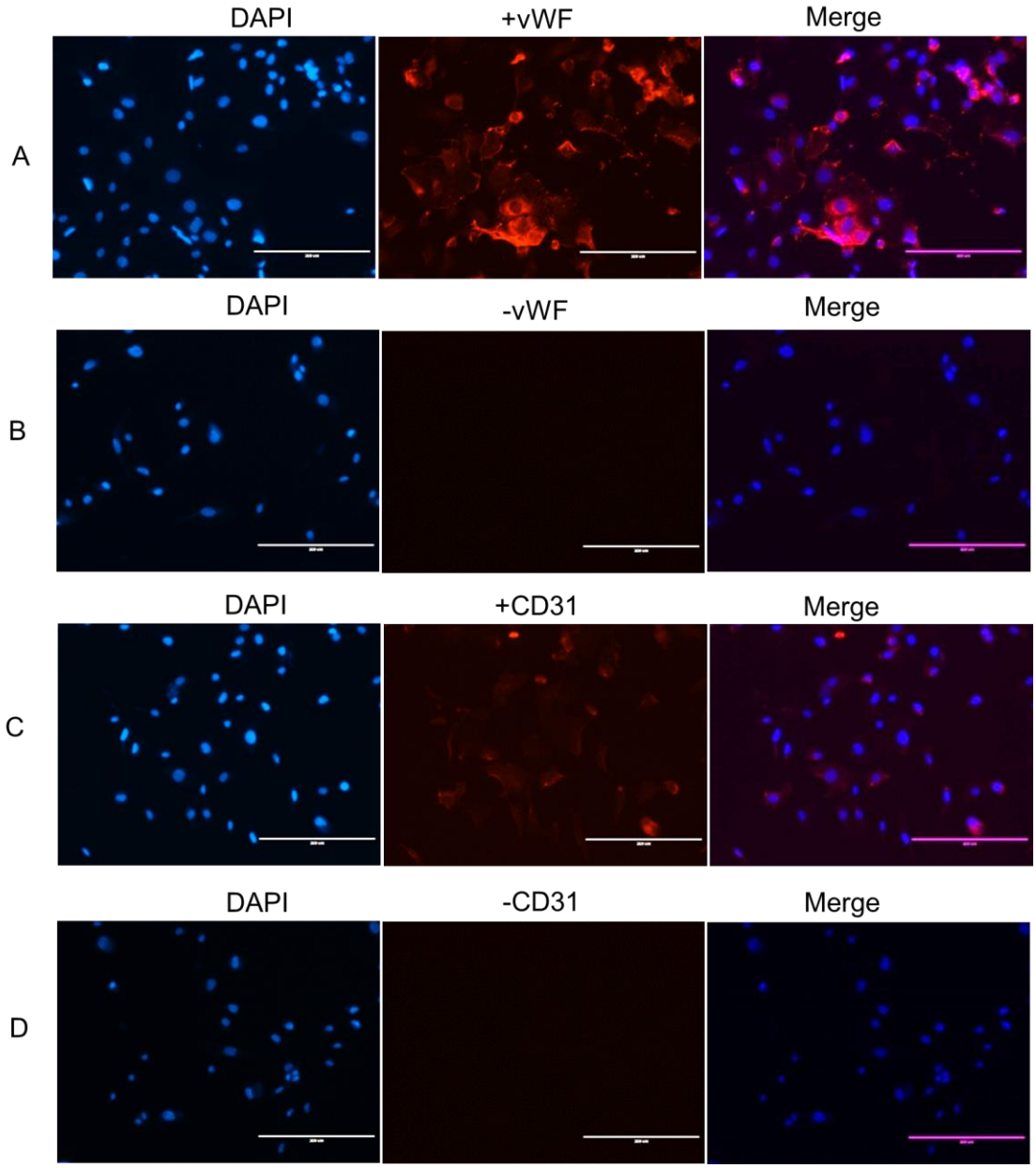

Figure 4-2: Immunostaining. Characterization of P7 HUVECs. Cells were stained for the expression of the endothelial markers: vWF and CD31. After three days in culture, HUVECs showed the expression of vWF and CD31 respectively (A and C). Controls for both markers were negative for the expression of vWF and CD31 (B and D). Nuclei were stained with 4', 6-Diamidino-2-phenylindole (DAPI). Scale bars = 200 µm.

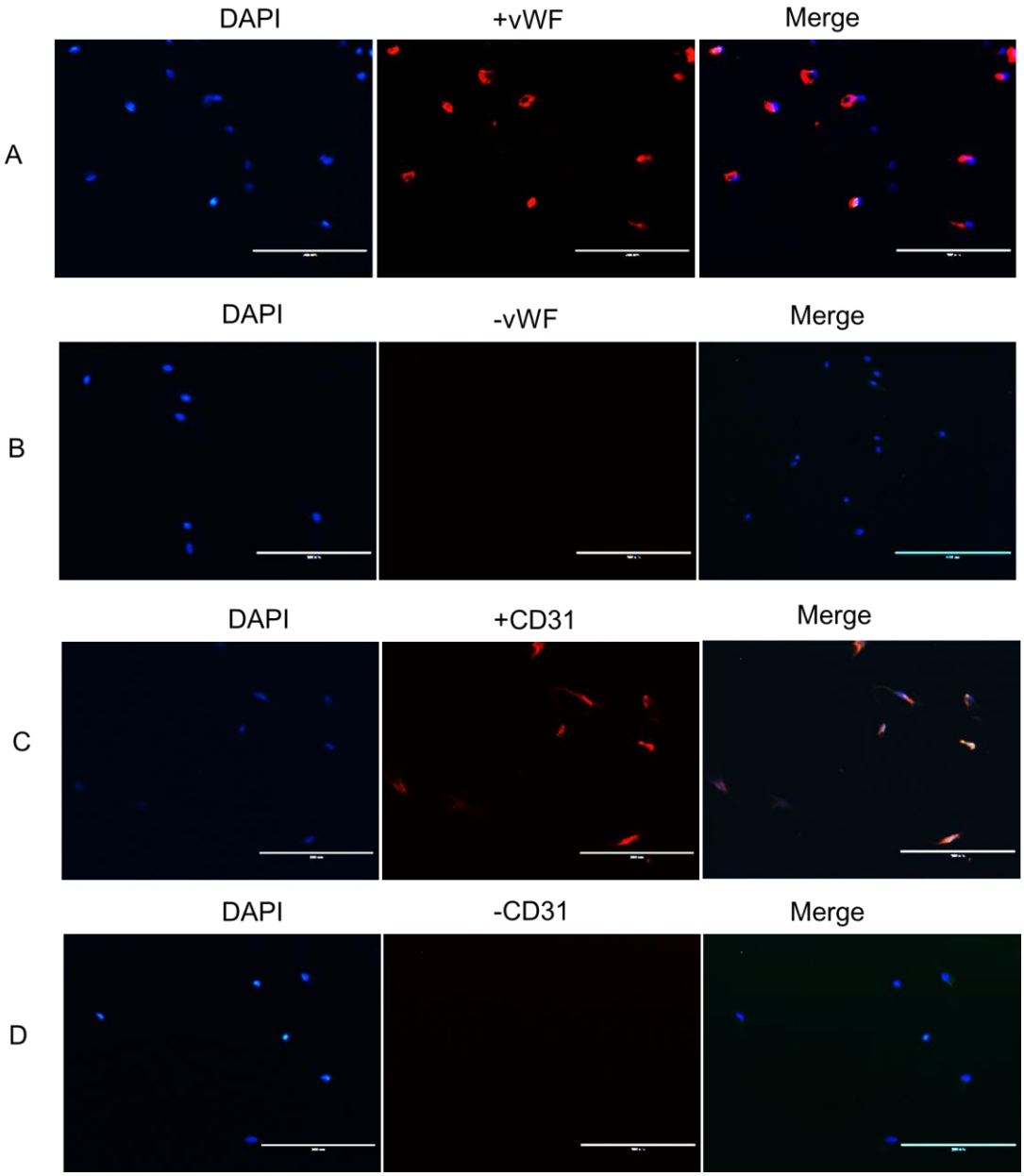

Figure 4-3: Immunostaining. Characterization of green fluorescent protein (GFP) stained P13 HUVECs. Cells were stained for the expression of the endothelial markers: vWF and CD31. After one day in culture, HUVECs showed the expression of vWF and CD31 respectively (A and C). Controls for both markers were negative for the expression of vWF and CD31 (B and D). Nuclei were stained with DAPI. Scale bars = 200 µm.

4.4.2: Hypoxic chamber oxygen measurements

A modular in house manufactured chamber (Mondragon-Teran et al., 2009) was used to achieve hypoxic conditions for the assays (Figure 2-2-1). The sealed chambers were purged with a gas mixture of 2% O_2/5% CO_2/ 93% N_2 balanced for the *in vitro* angiogenesis assays to mimic the low oxygen environment found in the ischemic cardiac tissue (Bain et al., 2014). In order to validate the effectiveness of the chamber in achieving relevant physiological oxygen levels, studies were conducted to monitor the gas-phase at the top of the chamber, the bottom of the chamber and within the liquid in the water dish. The chamber was purged for 5 minutes, prior to commencing the experiments. Measurements were taken every minute, for 24 hours. Figure 4-4 shows a representative trace of the oxygen monitoring that was performed and indicates that the oxygen at the top and the bottom of the chamber remained constant at 2% oxygen tension. On the other hand, the percentage of dissolved oxygen in the water dish although initially high (~18%) remained stable at ~3.8 % after one hour. This result was unexpected as it was previously reported that it takes > 3 hours for oxygen content in the medium present in the plates (no cells present) to achieve equilibrium (Allen et al., 2001). This is because oxygen has low solubility in aqueous solutions and therefore, the quick drop in oxygen in the medium might have been associated with issues relating to the calibration of the 96-well oxygen sensor plates. In addition, different oxygen sensors were used to measure the oxygen inside the water dish and that at the wall of the chamber. Therefore, another explanation for these results could be that the sensors in the 96-well plates were too old and therefore not as efficient in measuring dissolved oxygen.

For the purpose of the current work, it was decided to refer to the oxygen tension achieved in the chambers purged with 2% oxygen as “low oxygen” or “reduced oxygen”, relative to the “ambient oxygen” tension (~ 20% O_2).

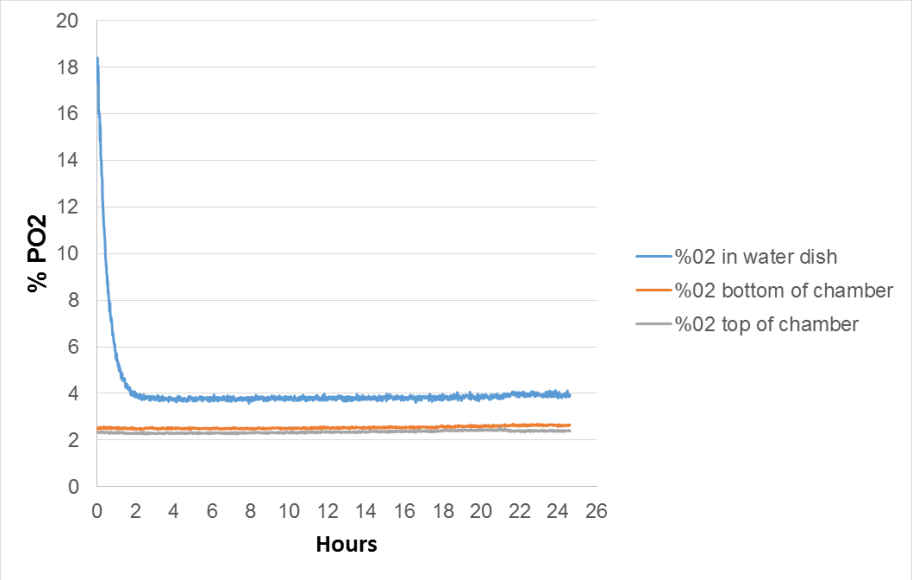

Figure 4-4: Hypoxic chamber oxygen measurements. Oxygen tension was measured every minute by Oxy-4 using fibre optic transmission. The oxygen measurement was done over 24 hours.

4.4.3: Branch network formation on gel coated wells

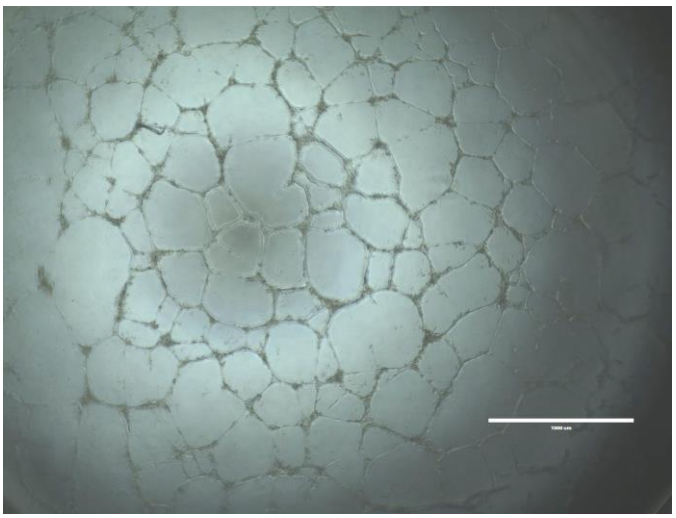

Figure 4-5: Branch network formation on gel coated wells. (A) Representative image showing network formation after 18 hours under an inverted light microscope. Scale bars = 1000 µm.

4.4.4: Time lapse experiment for vascular tubule formation

HUVECs were expanded for four days in EGM-2 medium which is composed of a basal medium (EBM-2) supplemented with VEGF, human epidermal growth factor (hEGF), recombinant 3-insulin-like growth factor-1 (R3-IGF-1) and hFGF-beta, which are growth factors known to stimulate angiogenesis (Folkman and D

'amore, 1996). Cells were used for experiments after reaching 80-90% confluence. Following trypsinization, cells were seeded on top of GFR Matrigel and GFR Geltrex coated wells and left to form tubules after 18 hours of incubation at low (2% O_2) and ambient (20% O_2) oxygen tensions (Figure 4-5). Initial optimization tests were carried out to examine the kinetics of network formation and to identify the best time point at which solid networks formed. P9 HUVECs were cultured for four days with medium change after every two days. On day five, HUVECs were seeded on 96-well plates with both GFR Matrigel and GFR Geltrex respectively at 55 µl and 35 µl. The morphological changes of the HUVECs were captured using a phase-contrast inverted microscope. Cells aggregated and elongated into tubule-like structures within 3 hours (Figure 4-6, A-D). After 6 hours, they started forming enclosed areas of vessel-like networks which became sparse and wide during the 12 hour period. No obvious morphological differences were observed between Matrigel and Geltrex for HUVEC tubule formation. Branch networks at 3 hours and 6 hours were difficult to quantify as some cells still didn't make contact and tubule networks appeared to be less robust than those formed at 9 and 12 hours (Figure 4-6). Hence from the data it was concluded that tubule quantification was not possible until after 6 hours. The data in Figure 4-6 showed that when cells were seeded on top of the basement membranes they would migrate towards each other align and form tubes. In the first 3 hours, it was observed that the networks closer to the edges of the wells would form faster than those in the middle, perhaps due to the higher concentration of cells pooling towards the middle of the 96 wells than at the edges (Figure 4-6).

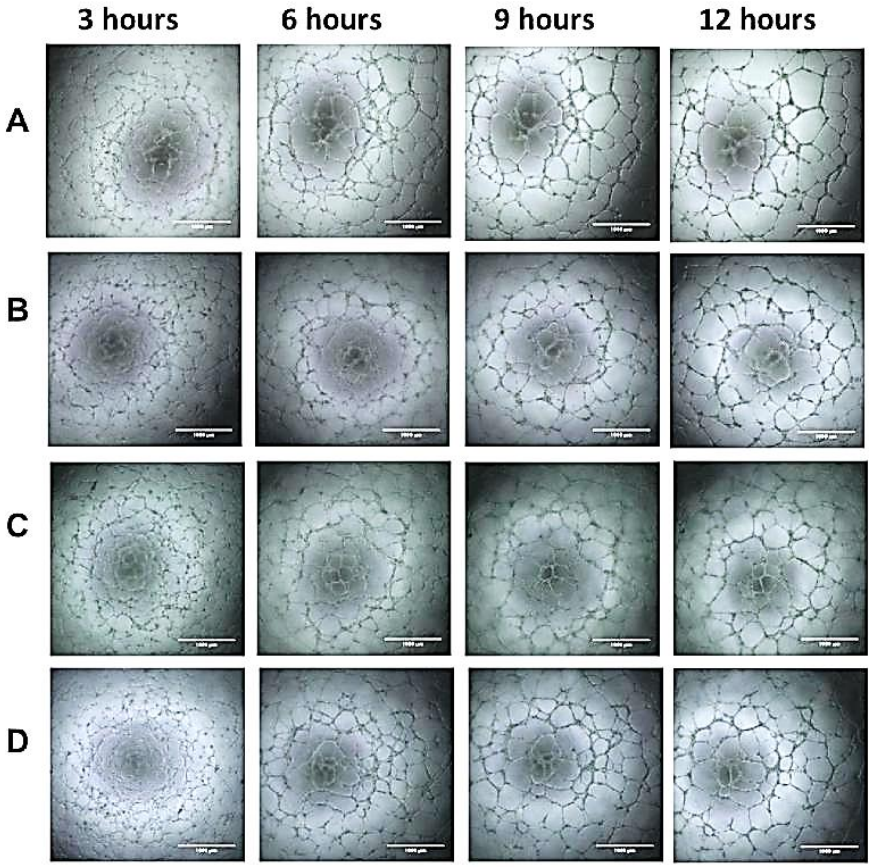

Figure 4-6: Time course dynamics of P9 HUVECs after plating on Matrigel at 35 µl (A) and 55 µl (B) and Geltrex at 35 µl (C) and 55 µl (D). Images were taken every 3 hours. Scale bars = 1000 µm.

4.4.5: Effect of cell seeding density, passage number and oxygen tension on vascular efficiency

All initial optimization studies were carried out using a range of seeding densities: 0.67 x 10^5 cells/ml, 1x10^5 cells/ml and 1.3 x10^5 cells/ml respectively, to determine the optimal cell seeding density. After being maintained in EGM-2 for three to four days, HUVECs (P7 and P10) were trypsinized and seeded on GFR Geltrex, GFR Matrigel and xeno-free Substrate Cell Start. The results showed that Cell Start allowed cell attachment and proliferation but it did not induce any tubule formation (Figure 4-7 A).

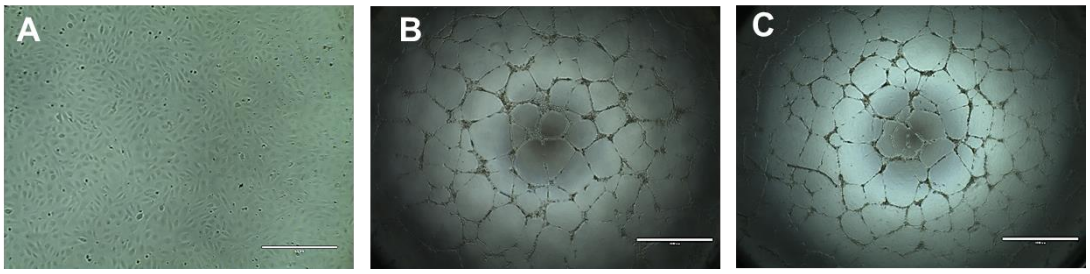

Figure 4-7: (A-C) Phase contrast representative images showing tubule network formation of P9 HUVECs on (A) Cell Start, (B) GFR Matrigel, and (C) GFR Geltrex. Tubule network formation was not observed on Cell Start (A). Pictures were taken at 10X (A) and 4X (B and C). Scale bars = 400 µm (A), 1000 µm (A and B).

The data also indicated that HUVECs were able to form tubule networks at all seeding densities. However, it was observed that there were more connected networks at higher seeding densities (Figure 4-8 and Figure 4-9). Branches also appeared to be more robust when using 1 x 10^5 cells/ml and 1.3 x 10^5 cells/ml instead of 0.67 x 10^5 cells/ml (Figure 4-9).

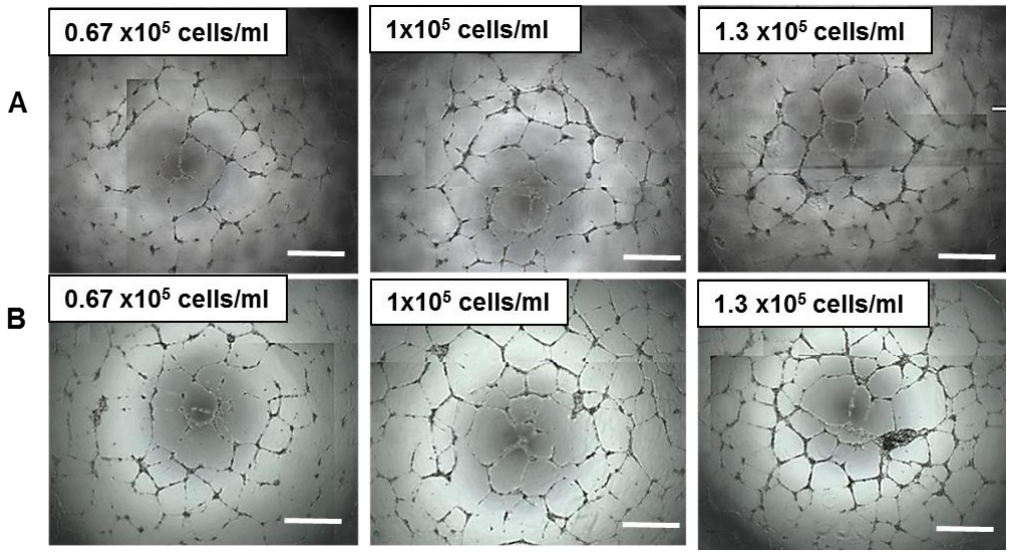

Figure 4-8: Phase contrast representative images of tubule networks formed using P10 HUVECs in GFR Matrigel (A) and GFR Geltrex (B). Three different seeding densities were used: 0.67 x 10^5 cells/ml, 1 x 10^5 cells/ml and 1.3 x 10^5 cells/ml Tubules were imaged after 18 hours (ambient oxygen 20%). Scale bars = 1000 µm.

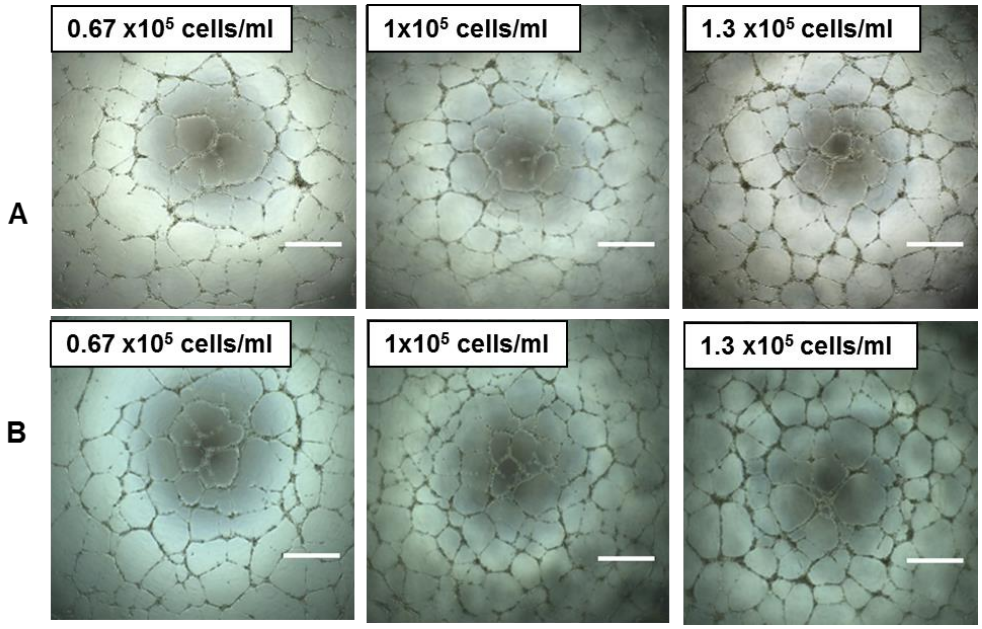

Figure 4-9: Phase contrast representative images of tubule networks formed using P10 HUVECs in GFR Matrigel (A) and GFR Geltrex (B). Three different seeding densities were used: 0.67 x 10^5 cells/ml, 1 x 10^5 cells/ml and 1.3 x 10^5 cells/ml. Tubules were imaged after 18 hours (ambient oxygen 2%). Scale bars = 1000 µm.

4.4.6: Cost comparison of Matrigel and Geltrex at 55 µl and 35 µl

Assay development involves finding cost effective solutions where there is a compromise between good data quality and quantity of reagents required. Matrigel and Geltrex were the most costly reagents in the assays (Table 4.1). This is why matrix volume was chosen as a key variable for process optimization. A basic cost of goods (CoG) analysis was carried out to compare the costs of using GFR Geltrex and GFR Matrigel at the lower volumes. The reagent CoG for using either Matrigel or Geltrex at 55 µl was found to be £1118 and at 35 µl it totalled to £848 (Table 4.1) for 50 tests. Using 35 µl Geltrex reduced the costs of the assays by 25%.

Reagents	Cost	Date of purchase		Cost per assay (55 µl of GFR Matrigel) (£)	% of the cost	Cost per assay (35 µl of GFR Matrigel) (£)	% of the cost	Cost per assay (55 µl of GFR Geltrex) (£)	% of the cost	Cost per assay (35 µl of GFR Geltrex) (£)	% of the cost
Matrix	0.03	2017	£/µl	14.9	66	9.45	56	14.9	66	9.45	56
96 well plate	1.5	2017	£/plate	1.5	7	1.5	9	1.5	7	1.5	9
EGM-2 Medium (EBM-2 Medium + BulletKit)	0.3	2017	£/ml	6.0	27	6.0	35	6.0	27	6.0	35
Total per assay	-	-	-	22.35	100	16.95	100	22.35	100	16.95	100
Total for 50 assays	-	-	-	1118	-	848	-	1118	-	848	-

Table 4.1: Cost comparison for GFR Matrigel and GFR Geltrex using 55 µl and 35 µl matrix volumes. The CoG analysis indicated a 25% reduction in costs when using the lower matrix volumes (35 µl).

In terms of branch point efficiency, there were no statistically significant differences between the three seeding densities for three independently carried out experiments per condition. The quantification data in Figure 4-10 A and B, indicated that there was also no significant difference in network efficiency when using ambient versus low oxygen concentrations for both P7 and P10 HUVECs. Following this, higher variability was observed in the 20% O_2 P7 HUVECs results, whilst the distribution appeared to be tighter at the lower oxygen tensions.

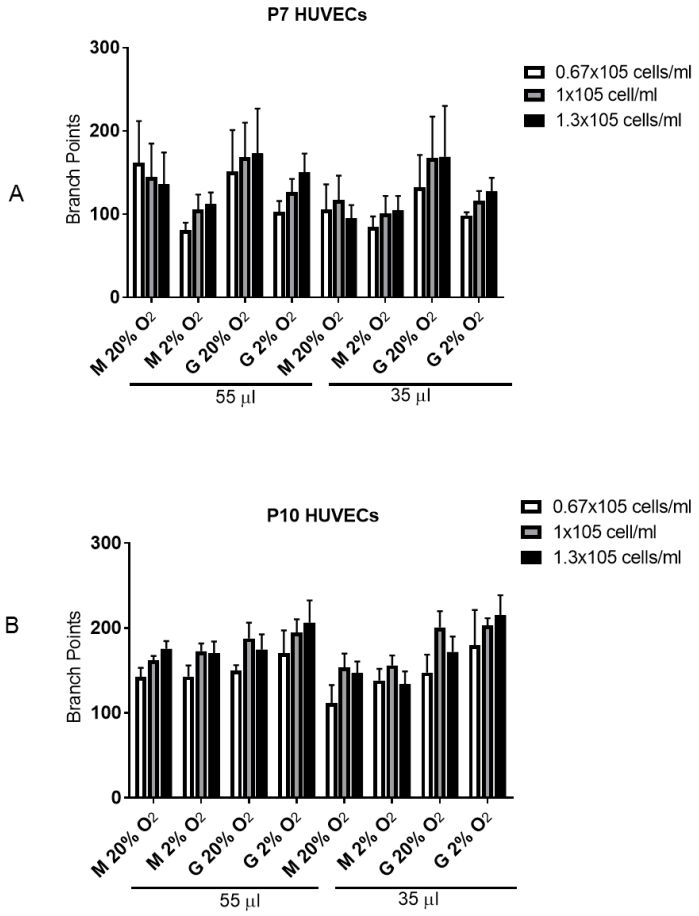

Figure 4-10: Branch point quantification for different seeding densities. Effect of cell seeding density and oxygen tension on vascular network efficiency using HUVECs at P7 and P10 at low oxygen (2% O_2) and ambient oxygen (20% O_2). The error bars indicate the mean ± SEM of n = 3 experiments for each condition performed on different HUVEC donors with triplicate wells for each experiment. There were no statistically significant differences between seeding densities, 20% O_2 versus 2% O_2, Matrigel versus Geltrex groups, and 55 µl versus 35 µl group means as determined by two-way ANOVA ($p > 0.05$).

4.4.7: Cell morphology and vascular network formation in younger and older HUVECs

Comparative studies were carried out between HUVECs at passage 7, passage 10, passage 13 and passage 15 to study the effect of cell age on branch network formation. HUVECs were grown for 3 to 4 days, trypsinized and seeded on GFR Geltrex and GFR Matrigel respectively at two different matrix volumes, 55 µl and 35 µl. The phase contrast images indicated that ECs were still able to proliferate at the higher passage numbers (Figure 4-11 A) as well as consistently forming branch networks when seeded at the lower matrix volumes (Figure 4-11 B).

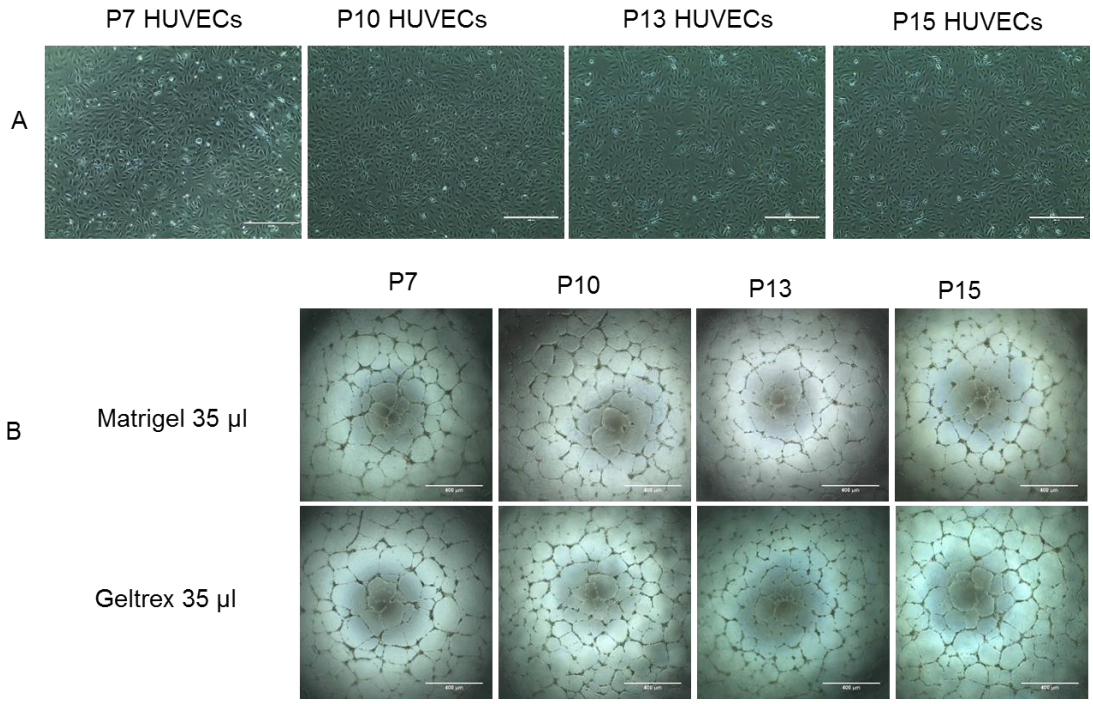

Figure 4-11: A) Phase contrast representative images of P7, P10, P13 and P15 HUVECs after four days of culture. Scale bars = 400 µm. (B) Effect of passage number on vascular efficiency for GFR Matrigel and GFR Geltrex respectively at low (2%) oxygen. Scale bars = 1000 µm. The data shows that the endothelial cells are able to still proliferate in culture and form robust branches at the higher passage numbers (> P10).

4.4.8: Manual versus automated counting techniques

In order to reduce the time involved in analysing the data, it was decided to carry out a comparative study between automated and manual methods. Initially whole well images were taken at x2 magnification however, it was difficult for the ImageJ program to easily recognize the tubule networks. For this reason, in the next couple of experiments, it was decided to perform the counts over a series of images taken at x4 magnification using an inverted microscope and merged (x9 images per whole well; PanoramaStudio2Pro software, Sulzfeld EU). Counts were then performed manually and using the automated counting technique. Manual counts were performed by quantifying the number of branch points per image. On the other hand, automated counts were performed using the angiogenesis analyser (ImageJ) to compute the number of branch points and also the number of junctions and meshes (Figure 4-12) in a visually user-friendly fashion. Comparisons between manual and automated counting techniques were performed based on the number of branch points (Figure 4-13).

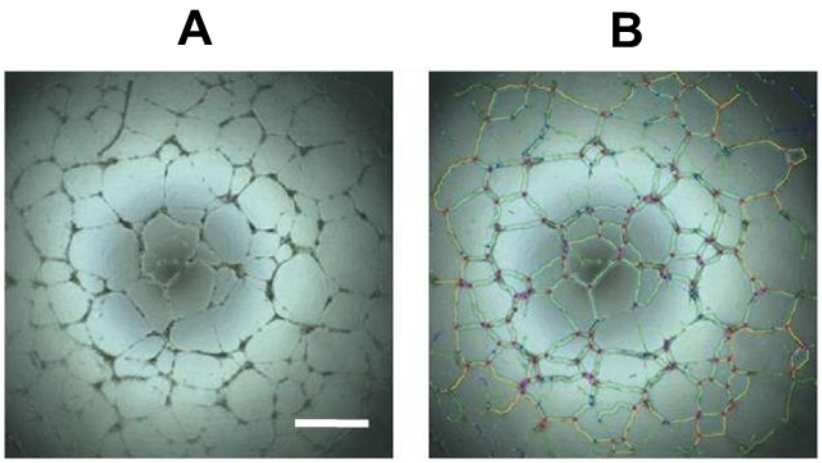

Figure 4-12: Image before (A) and after (B) being processed using the angiogenesis imageJ analyser. Branches are shown in yellow. Branch points are shown in pink. Meshes represent the enclosed areas between the branches. Images were taken at x4 magnification. Scale bar = 1000 µm.

The data indicated that both manual and automated counts followed the same trend and no statistical differences were observed between the two methods (Figure 4-13). This trend was maintained for all of the passage numbers investigated in this study (Figure 4-13 A to D).

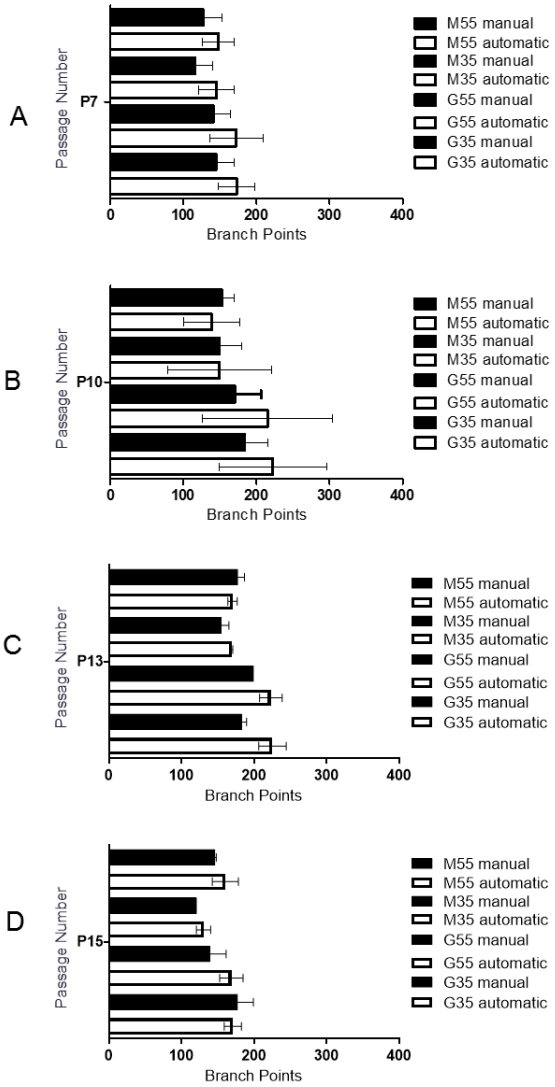

Figure 4-13: Data comparison between manual and automated counting techniques for A) P10 HUVECs B) P13 HUVECs C) P7 HUVECs and D) P15 HUVECs . All conditions were carried out using a seeding density 1 x 10^5 cells/ml. The error bars indicate the mean ± SEM of n = 3 experiments for each condition performed on different HUVEC donors with triplicate wells for each experiment. One Way ANOVA for each group- Bonferroni post-hoc analysis revealed $p > 0.05$.

4.4.9: Multivariate analysis of the effect of passage number, type of matrix and matrix volume in tubule angiogenesis assays

Branch point efficiency between P7 and P13 HUVECs for Geltrex at 55 µl ($p = 0.0006$) and 35 µl ($p = 0.0009$), indicated that Geltrex performed better at higher passage numbers. Differences were also observed between P7 and P13 HUVECs where Matrigel at P13 and 35 µl showed a significantly higher number of branch points compared to Matrigel at P7 and 35 µl ($p = 0.0486$). Also, branch point efficiency between P13 and P15 HUVECs for Geltrex at 55 µl ($p = 0.0469$) and 35 µl (0.0452), indicated that Geltrex performed better at P13. Next, the one-way ANOVA revealed that for the P13 HUVEC groups, Geltrex 35 µl was more efficient against the Matrigel 55 µl control group ($p = 0.0469$).

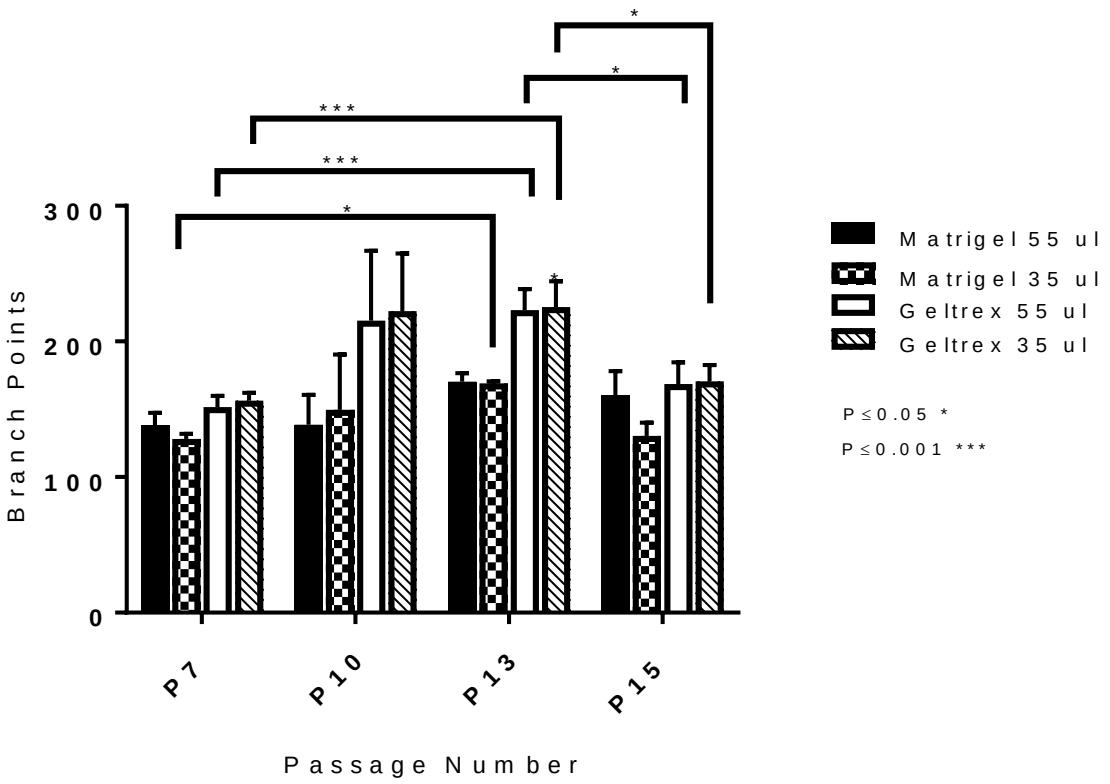

Figure 4-14: Branch point quantification for P7, P10, P13 and P15 HUVECs at high (55 µl) and low (35 µl) matrix volumes. The error bars indicate the mean ± SEM of n = 3 experiments for each condition performed on different HUVEC donors with triplicate wells for each experiment. There were statistically significant differences between group means for passage number as determined by two-way ANOVA, Bonferroni post-hoc analysis. One-way ANOVA, Bonferroni post-hoc analysis revealed significant differences between Matrigel 55 µl and Geltrex 35 µl for the P13 HUVECs ($p \leq 0.05$). Matrigel 55 µl was used as a control group for comparison. Refer to text for a detailed description of the results.

Vascular efficiency was also observed by measuring the number of meshes (enclosed areas between branches). The results suggested that there were no significant differences between the numbers of meshes formed at the different passage numbers (Figure 4-15). However, the trend indicated that there was a higher number of meshes formed on Geltrex at both 35 µl and 55 µl when compared to network formation on Matrigel.

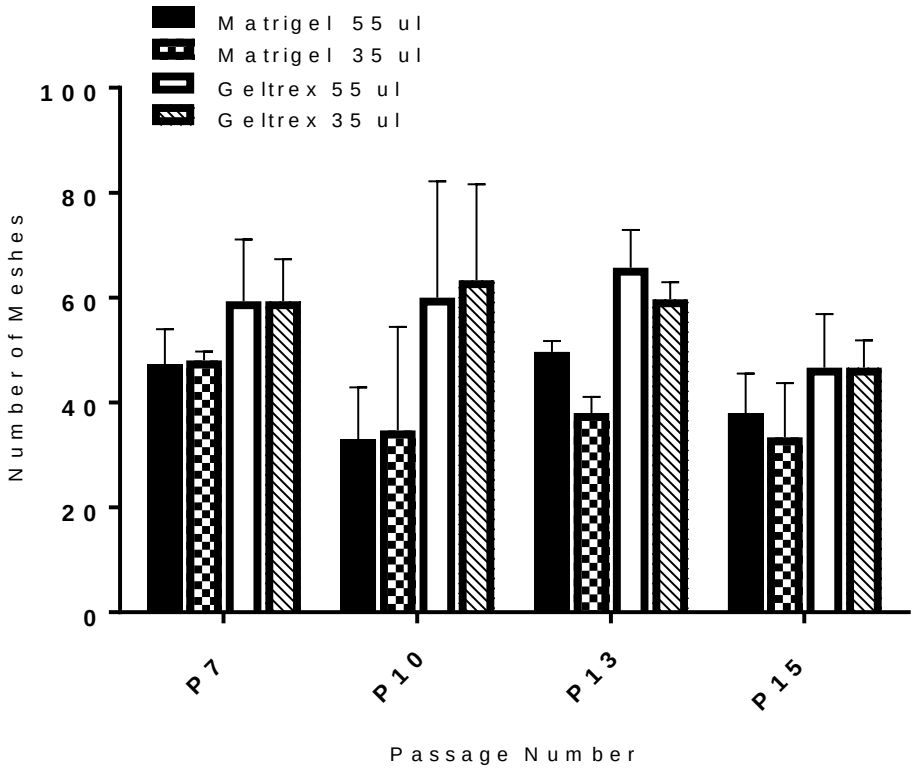

Figure 4-15: Number of meshes quantification for P7, P10, P13 and P15 HUVECs at high (55 µl) and low (35 µl) matrix volumes. There were no statistically significant differences between group means for passage number as determined by two-way ANOVA, post-hoc analysis ($p = 0.9647$). Values are mean ± SEM of $n = 4$ (P7 HUVECs) and $n = 3$ (P10 to P15 HUVECs) experiments performed on different HUVEC donors with triplicate wells for each experiment.

4.5: Discussion

The current study investigated the effect of key input variables on tubule network efficiency, to optimize vascular assays for the assessment of angiogenesis. Current vascular assays present many challenges, specifically the inherent biological variability of the reagents used (Auerbach *et al.*, 2000; Smith and Staton, 2007) and the high costs associated with carrying out the assays (Smith and Staton, 2007). For this reason, a multivariate screening approach was used to systematically optimize key parameters that affect the tubule-formation capacity of ECs, with an aim of making the assays more standardized, reducing costs and increasing the number of assays that can be performed.

Initial time-lapse experiments were carried out to observe the dynamics of tubule formation. The time lapse experiment showed that ECs were able to form quantifiable capillary networks even at 6 hours which further confirmed the ease and the rapidity at which tubules are formed on Matrigel and Geltrex. The results in Figure 4-5 agreed with previous work which showed that tubule formation on Matrigel can vary from 4 to 24 hours (Staton et al., 2004). However, the formation of tubules after only 3 hours also revealed the difficulty of Matrigel assays to mimic the *in vivo* situation. In fact, these assays do not measure as many steps in angiogenesis as tubule formation on other matrices such as collagen (Arnaoutova and Kleinman, 2010). It has been reported that seeding cells on different types of collagen affects the rate of tubule formation. For example, it was shown that seeding cells on interstitial collagen (collagen I and collagen III) increased cell proliferation but severely reduced tubule formation. On the other hand, when endothelial cells were plated on collagen from the basement membrane (collagen IV and collagen V), there was not much proliferation occurring but the rate of tubule formation was high (Calderon et al., 2017; Gambino et al., 2017). Collagen assays are more time consuming than Matrigel assays as it takes several days for capillary-like structures to form. Branch quantification in these gels is difficult because the tubule organization in collagen is in 3-D and requires the sectioning of the gel or photography at multiple focal planes (Goodwin, 2007). In addition, not all of the cells form tubules which adds to the difficulty in quantifying network formation (Arnaoutova and Kleinman, 2010). For this reason, Matrigel 2-D assays, which are

easy to quantify seem to be the best option whilst looking for more powerful image analysis programs to quantify the angiogenesis potential of collagen.

The optimized assays from this study showed that lower matrix volumes of 35 µl could be used for efficient tubule formation. As reported in the literature, using volumes lower than 34 µl per well of a 96 well plate (1.2 µl/mm^2) creates a well effect which leads to having more cells at the centre of the well than at the edge hence making tubule formation difficult (Smith and Staton, 2007). Whilst it was reported that using extremely low levels of Matrigel may also avoid the pooling effect, there is a risk that the manual spreading required to distribute Matrigel around the well could lead to uneven distribution (Staton et al., 2004). The current work also investigated the ability of Cell Start and Geltrex to form capillary-like networks. The data indicated that Geltrex was able to successfully form branches. However, Cell Start still failed to form tubules (Figure 4-7 A); for this reason no further work was carried out using this matrix.

When carrying out *in vitro* assays it is necessary to use process conditions that mimic the physiologic site to which the product will be delivered as closely and as reasonably possible. This is done so that the assay measurement reflects the anticipated mode of action in the injury site that the cells will be delivered to in *vivo.* The *in vivo* site is often an extreme environment due to ischemia-reperfusion injury and high levels of oxidative stress. Differently from the typical cell culture environment that is made of ~20% O_2, most tissues in the body experience oxygen levels of around 1% to 5%, whilst blood vessels experience 5% to 7% O_2 (Kusuma et al., 2014). Several studies have also reported that ischemia, which can result from lack of nutrients and oxygen, stimulates blood vessel recruitment (Kusuma et al., 2014). In the present work, comparative studies were run between vascular assays subject to ambient (20%) and low (2%) oxygen tension, to observe any differences between the two conditions. However, the initial findings showed that hypoxic conditions did not affect the rate of tubule formation in the assays (Figure 4-10). Future studies could investigate the effect of both oxygen conditions for prolonged times (>7 days) instead of imaging the tubules after 18 hours. In this way it would be easier to recognize the beneficial effects of low oxygen on the stability of the vessels formed. The current study also investigated the effect of cell seeding density on vascular efficiency. The findings from the study revealed

that an increase in seeding density corresponded with robust branches. These findings agreed with previous work where it was reported that high cell seeding densities on the basement membranes can lead to large areas of clustered, undifferentiated cells, whilst seeding at too low density hinders tubule formation as cells do not make contact (Staton et al., 2007). Future work could investigate a wider range of seeding densities to find the optimum range for network formation.

This study adopted a multivariate approach for studying the interactions between passage number, type of matrix and matrix volume on vascular efficiency. This approach was undertaken to achieve a more robust and cost-effective assay. This study showed that Geltrex can work as well or better than Matrigel. Using Geltrex as a replacement to Matrigel would account for less assay variability as it is more consistent in formulation, making the former a viable option for an optimized tubule assay. The CoG analysis showed that the highest costs in the assays came from the matrices and that using 35 µl instead of 55 µl would reduce the costs by 25% for 50 assays. The possibility of using lower matrix volumes would increase the number of assays achievable from a single batch of substrate product and it would also reduce assays costs. Future work could assess using much lower matrix volumes to further reduce the costs incurred in matrix usage.

The current work investigated whether HUVECs older than passage 10 could still be used to achieve efficient network formation. The findings from this study showed an increase in network formation until P13 HUVECs and a decline in vascular efficiency at P15 HUVECs. However, P15 HUVECs performed as well as P7 HUVECs. Previous studies analysing the effect of cell age in HUVECs showed that younger HUVECs were consistently superior in forming vascular vessels than those at the later passage numbers (Schechner et al., 2000). However, some studies observed that this was not always the case. For example, in one study they showed that the vascular efficiency of endothelial cells was best between the second and the sixth passage number and that the assay would not work well if endothelial cells were used before the second or after the tenth passage (DeCicco-Skinner et al., 2014). Similarly, to this study, the findings of the current work showed that the assays would work best after P10 and before P15 at which a decline in the branching was observed (Figure 4-14 and Figure 4-15). The possibility of using older cells means that more experiments could be carried out

using the same batch of cells, hence eliminating the issues of donor-to-donor variability and reducing costs related to purchasing new cell lines. However, increase in cell age may also increase intra-donor variability, as EC monolayers will become more heterogeneous with an increase in cell age. This trend was not observed in the current work. For example, the error bars for the P15 HUVECs appeared to be tighter than those observed for the P10 HUVECs. Furthermore, since it was only possible to perform experiments on n = 3 HUVEC donors which represents a small sample size, there is a need to perform experiments on a greater number of primary cell isolations to confirm these results. In addition, since only HUVECs were tested in this study, future work will need to include the testing of ECs from different sources and the impact of cell age on each one of them. In fact, the difference between HUVECs and other types of endothelial cells has been widely reported in the literature and it is one of the main factors hindering data comparison between *in vitro* assays (Cao et al., 2017). For example, whilst human microvascular endothelial cells can be activated by palmitic acid *in vitro*, the same is not observed in HUVECs (Cao et al., 2017).

The present work also investigated whether the automated software was powerful enough to quantify the phase contrast images accurately or not. To avoid the variability in counts from the meniscus effect in the 96 well plates, it was decided to consistently select the large middle region of the well. This study showed that automated techniques can be used as a less time-consuming method to the manual counts (Zudaire et al., 2011). In addition, the measurements performed using this method are more standardised than the manual counts and they avoid the variability that is added when different users count the same image. Moreover, reducing the time involved in performing the counts by switching to an automated method would also bring down the CoG associated with operator time. Overall, this study allowed for the understanding of key characteristics of endothelial cells. Further work could be done to investigate a wider range for each variable studied. In addition, the reliability of the data from the *in vitro* assays could be confirmed using *in vivo* tests, as the former may not always be representative of the complex mechanisms in a living organism (Staton et al., 2004; Xie et al., 2016).

Chapter 5: Effect of vasculogenic enhancement potential of hMSCs from different sources

5.1: Introduction

The following section will summarize the relevant literature discussed in Chapter 1.

The mechanism of action (MOA) of hMSCs after transplantation into the heart is still not well known (Singh et al., 2016). For example, some studies indicated that MSCs may rescue the myocardium by differentiating into cardiomyocytes (CMs) (Li et al., 2006). However, this would not explain their beneficial effects on the myocardium, as it was reported that only <2% of the transplanted MSCs transdifferentiate into cardiomyocytes (Arnous et al., 2012). More recently some studies reported that MSCs may act through paracrine effects (Zhang et al., 2012) whilst other studies showed that these cells trigger angiogenesis by assuming a “perivascular-like” phenotype in the basement membranes of newly forming blood vessels. In this way they were shown to favour and contribute to the stabilization of newly formed capillaries (Kean et al., 2013).

In order to improve cellular therapies it is fundamental to understand the mode of action of MSCs and to then develop methods to improve their function at the site of injury (Bain et al., 2014). To make this possible, it is important to develop *in vitro* assays whose parameters more closely reflect the physiologic environment, rather than ambient conditions that do not enable prediction of how the cells will work upon transplantation *in vivo*. For example, by performing assays in lower oxygen levels more reflective of the physiologic oxygen tension and by measuring cell responses on extracellular matrix rather than directly on tissue culture plastic.

Recently one study reported that when BM-MSCs were subject to hypoxic conditions (1%) for 24 hrs, the cells were able to engraft in an animal model of idiopathic pulmonary fibrosis four times better than the untreated cells (Lan et

al., 2015). The benefits of hypoxic preconditioning for myocardial repair were also reported in the first-in-man intracoronary administration of hypoxic bone marrow mononuclear cells, which led to improved heart function (Hu et al., 2015).

Another strategy to improve the function of MSCs in cardiac repair has been associated with priming MSCs with Notch ligands (Lu et al., 2016). The Notch pathway can be triggered via the Notch receptors binding to one of their ligands which include Jagged 1 and Delta-like 4 (Gridley, 2010). This pathway was shown to cover a fundamental role in regulating the function of endothelial cells (ECs) during sprouting and angiogenesis, by aiding communication between adjacent cells (Benedito et al., 2009; Lu et al., 2016). The overexpression of Jagged 1 was shown to enhance angiogenesis, whereas the opposite was observed in mutants lacking Jagged 1 (Benedito et al., 2009).

Given that MSCs have been shown to improve angiogenesis (Zhang et al., 2012) and that MSCs from different sources may possess different proliferation capacities and angiogenesis potential (Hsieh et al., 2013; Chen et al., 2014; Singh et al., 2016), it may be beneficial to investigate the angiogenesis modulatory effects of hMSCs from different sources.

5.2: Aim and hypotheses

5.2.1: Aim

- To test the vascular support abilities of hMSCs primed with Notch ligands in co-culture vascular assays, and to determine the effect of other variables such as type of matrix and oxygen tension on vascular network formation.

5.2.2: Hypotheses

- Differently-sourced MSCs will exert differences in angiogenic abilities.

- The vascular support ability of hMSCs can be enhanced by Notch ligand pre-conditioning.

5.1 Materials and methods

All the general materials and methods are described in Chapter 2.

5.2.3: Cell staining to distinguish hMSCs from HUVECs

hMSCs were cultured in ambient (20% O_2) and low (2% O_2) oxygen tensions until they reached 80-90% confluency. Live cell staining was performed on hMSCs and HUVECs to observe the interaction between the two cell types. HUVECs were stained with CellTracker Green CMFDA (1:1000, green fluorescence, Invitrogen, Paisley UK) and hMSCs were stained with Vybrant DiI Cell-Labeling solution (1:200, red fluorescence, Life Technologies, Paisley UK); cells were incubated with the dyes for 1 hour at 37 ^{o}C. Following this, both HUVECs and hMSCs were washed once in their own pre-growth medium and incubated for a minimum of 30 minutes at 37 ^{o}C to allow the cells to incorporate the dye molecules in the plasma membranes. Positive staining was confirmed under a fluorescence microscope.

5.2.4: Co-culture vascular assay

Following the staining with the red fluorescent dye, the hMSCs were detached from the flasks as described in sections 2.1.1 and 2.1.2. Pellets were then resuspended in 3 ml of pre-warmed EGM-2 medium and counted using the Trypan Blue exclusion method described in section 2.1.3. Following this, cells were diluted to 1.8 x 10^5 total cells/ml in EGM-2 medium contained in 15 ml Falcon tubes and preconditioned with soluble Notch ligands as described in section 2.5. Meanwhile, HUVECs were detached as per usual when passaging and resuspended in EGM-2 medium at 0.67 x 10^5 cells/ml. For the control groups, 150 µl of cell suspension was seeded in triplicate on top of the wells coated with 35 µl of either GFR Matrigel or GFR Geltrex.

Following preconditioning with soluble Notch ligands, hMSCs were diluted at 0.67 x 10^5 cells/ml in EGM-2 medium and mixed gently. The HUVEC suspension was then added at the desired ratio to each hMSCs-containing tube followed by gentle mixing.150 µl of each mix was then seeded on top of the Matrigel-coated and the Geltrex-coated wells respectively. Following this, the 96-well plates were placed

in a hypoxic chamber purged with 2% O_2, and then placed in a humidified incubator at 37 ^oC for 18-19 hrs. Images were visualised using an inverted light microscope and then put together using the PanoramaStudio2 software. The differences in vascular efficiency between the different conditions (normoxic-hMSCs/HUVECs vs. hypoxic-hMSCs/HUVECs on either GFR Matrigel or GFR Geltrex with hMSCs primed with either sJag1, sDll4 or left untreated) were measured by manually counting the number of branch points over the entire well. Measurements were carried out by considering one branch point as the meeting point between three branches, 2 branch points as the meeting point between 4 branches and 3 branch points as the junction of 5 branches. Tubule length was analysed manually by drawing a line along each tubule and measuring the length of the line in µm.

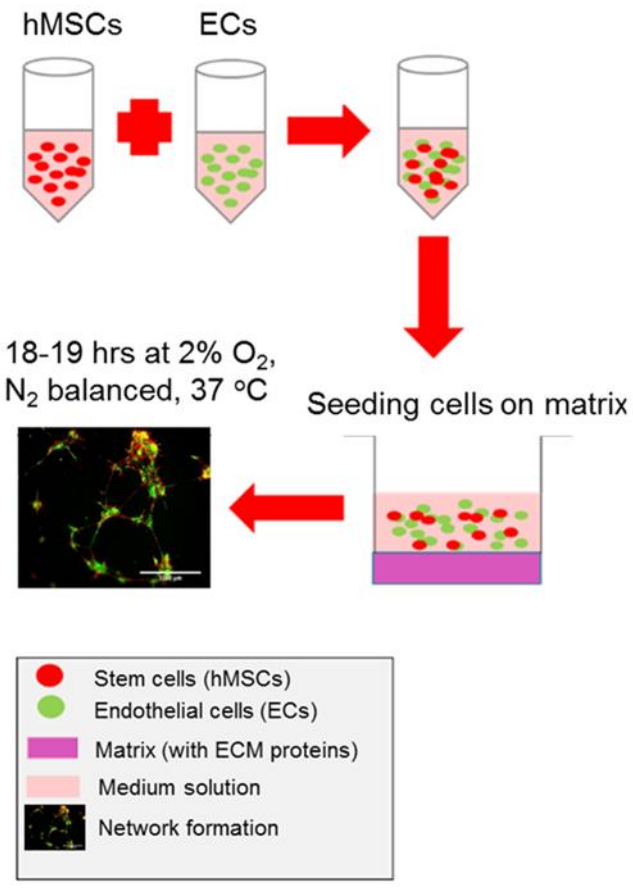

Figure 5-1: Diagram summarizing experimental setup for co-culture assay.

5.2.5: Vascular support assay

Following staining with viable dyes, hMSCs were treated with Notch ligands as described in section 2.5 and diluted at a concentration of 0.67 x 10^5 cells/ml. 150 µl of hMSC suspension was seeded into the 96-well plates in triplicate for each experimental condition and incubated at 37 ºC for 24 hours. Following this, hMSCs were then washed once with EGM-2 medium and 55 µl of either GFR Matrigel or GFR Geltrex was carefully pipetted on top of the hMSCs.

Plates were then placed in a humidified incubator at 37 ºC for 1 hour. After gelation, 150 µl of a HUVEC suspension was added at a concentration of 0.67 x 10^5 cells/ml to each well containing the hMSCs/Matrigel or Geltrex stacks. For the control groups, 150 µl of HUVEC suspension was seeded on top of the gel-coated wells in triplicate. Following this, the plates were positioned in a hypoxic chamber purged with 2% O_2 which was then placed in a humidified incubator at 37 ºC for 18-19 hrs.

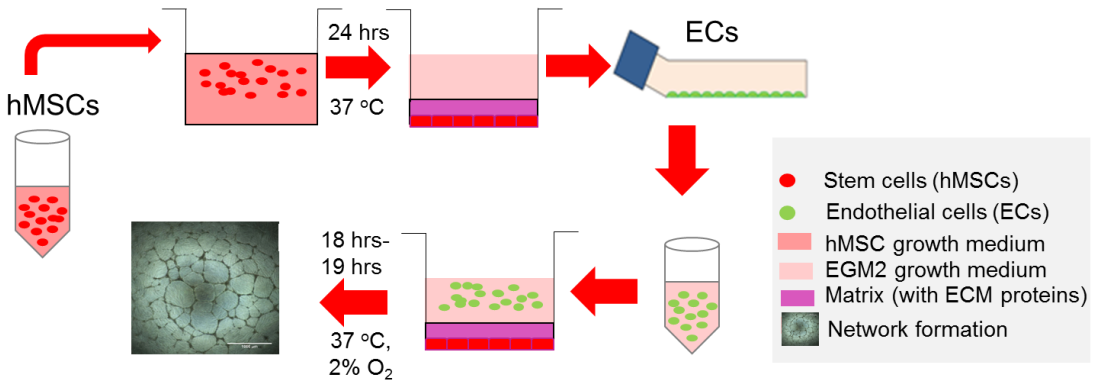

Figure 5-2: Diagram summarizing experimental setup for support assay.

5.3: Results

5.3.1: Cell morphology

Cells were imaged after being cultured in either 20% O_2 or 2% O_2 (for 5 days) to verify morphological differences between the differently-sourced hMSCs. The phase contrast images (Figure 5-3 A-F) indicated that the cells tested in this study exhibited adherence to tissue culture plastic, active proliferation and a homogeneously distributed monolayer of elongated spindle-shaped cells similar to those described by Pittenger et al., 1999; this was observed at both 20% O_2 and 2% O_2 (Figure 5-3 A-F). The data also showed that the individual donor hBM-MSCs (Figure 3-1A and B) and the P11 hUC-MSCs (Figure 5-3 E and F) appeared to be more confluent than the commercial hBM-MSCs (Figure 5-3 C and D). However, as growth rate studies of the cells were not carried out it was not possible to quantify these differences.

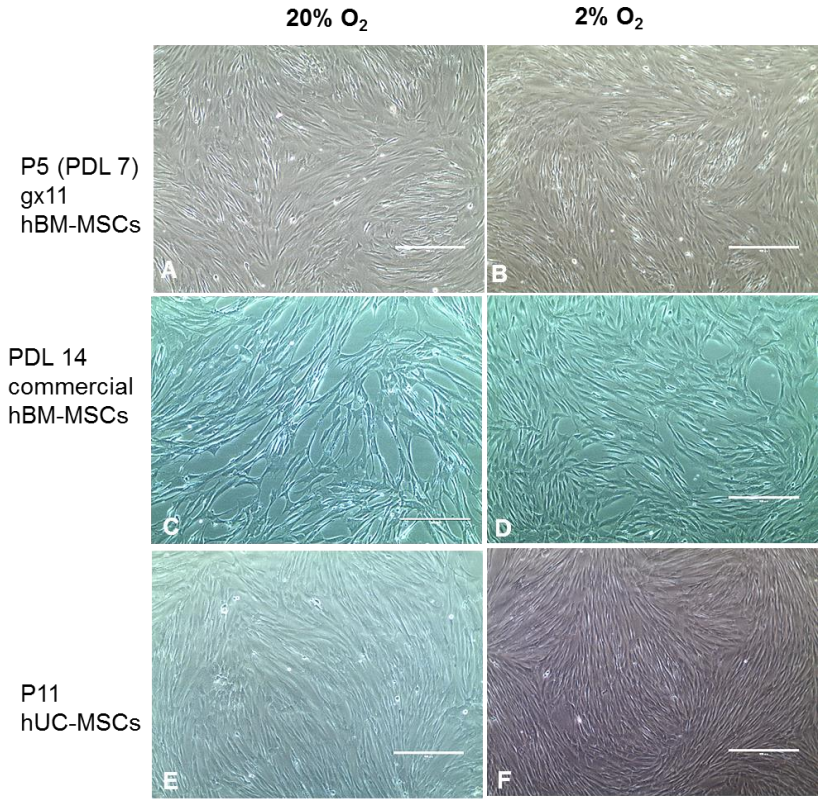

Figure 5-3: Cell morphology of hMSCs after 5 days in culture. Individual donor gx11 P5 (PDL 7) hBM-MSCs at 20% O_2 (A) and 2% O_2 (B) were expanded in complete medium; PDL 14 commercial hBM-MSCs at 20% O_2 (C) and 2% O_2 (D) were expanded in their own High Performance Medium; P11 hUC-MSCs at 20% O_2 (E) and 2% O_2 (F) were expanded in complete medium. Scale bars = 400 µm.

5.3.2: qPCR

Preliminary experiments of quantitative real-time PCR (qPCR) were carried out on hMSCs preconditioned in either low oxygen (2% O_2) or in ambient oxygen (20% O_2) tensions followed by priming with sJag1 or sDll4 or left untreated and let attach to fibronectin surfaces for 45 min. qPCR was carried out as explained in section 2.6. The activation of the Notch pathway was investigated by analysing the expression of JAG1, DLL4, HES1 and HEY1 in cells that have been cultured in 2% O_2 or 20% O_2. On the other hand, the effect of cell preconditioning in low oxygen compared to the untreated cells was assessed by analysis of HIF1 and HIF3. It is notable that in some experiments HIF3 (Figure 5-4 and Figure 5-5) and DLL4 (Figure 5-4 and Figure 5-5) were not measured. The single experiment for the individual donor hBM-MSCs showed that the expression of HIF1, JAG1, HES1 and HEY1 was consistently higher in cells preconditioned with sJag1 (see grey and black bars, Figure 5-4 A, B, C, and D). This was more evident for the expression of HES1 in sJag1 samples pre-treated in hypoxia (Figure 5-4 C). In fact, the results showed that HES1 expression for the hypoxic-hBM-MSCS pre-treated with sJag1 was almost double than the one observed for the control groups (Figure 5-4 C). On the other hand, the expression of HIF1, JAG1, HES1 and HEY1 for the hMSCs pre-treated with sDll4 cultured in 20% O_2 was consistently lower than that of the control groups (Figure 5-4 A, B, C, and D). The data also suggested that all of the samples pre-treated with sDll4 appeared to show higher values of the JAG1, HES1 and HEY1 genes when using the hypoxic hMSCs compared to the cells treated in ambient oxygen conditions (Figure 5-4 A, B, C, and D). This result indicated that low oxygen may be beneficial for the expression of genes involved in Notch through sDll4 pre-treatment.

The SD error bars indicated that there was very little variation between the technical replicates hence confirming low pipetting errors and validating the methods' measurements. However, in order to get more accurate results there is the need to repeat the experiment at least twice more.

Overall these preliminary results indicated that for the P5 hBM-MSCs the untreated cells performed similarly at either 20% O_2 or 2% O_2 (Figure 5-4 A, B, C, and D). On the other hand, low oxygen conditions appeared to increase the expression of HIF1, JAG1, HES1 and HEY1 in the sDll4-treated cells in comparison to those expanded in ambient oxygen conditions (see sDll4 grey bars versus black bars, Figure 5-4 A, B, C, and D). Next, the cells pre-treated with sJag1 showed consistently higher expression of HIF1, JAG, HES1 and HEY1 compared to the control groups; in particular for the HES1 gene in Figure 5-4 C. These trends suggested that the expression of HES1 may be up-regulated by sJag1 priming (at 20% O_2 and 2% O_2) and down-regulated by sDll4 priming (only at 20% O_2). In addition, the data also showed that culturing sDll4-treated cells in hypoxia could upregulate the expression of Notch ligand genes.

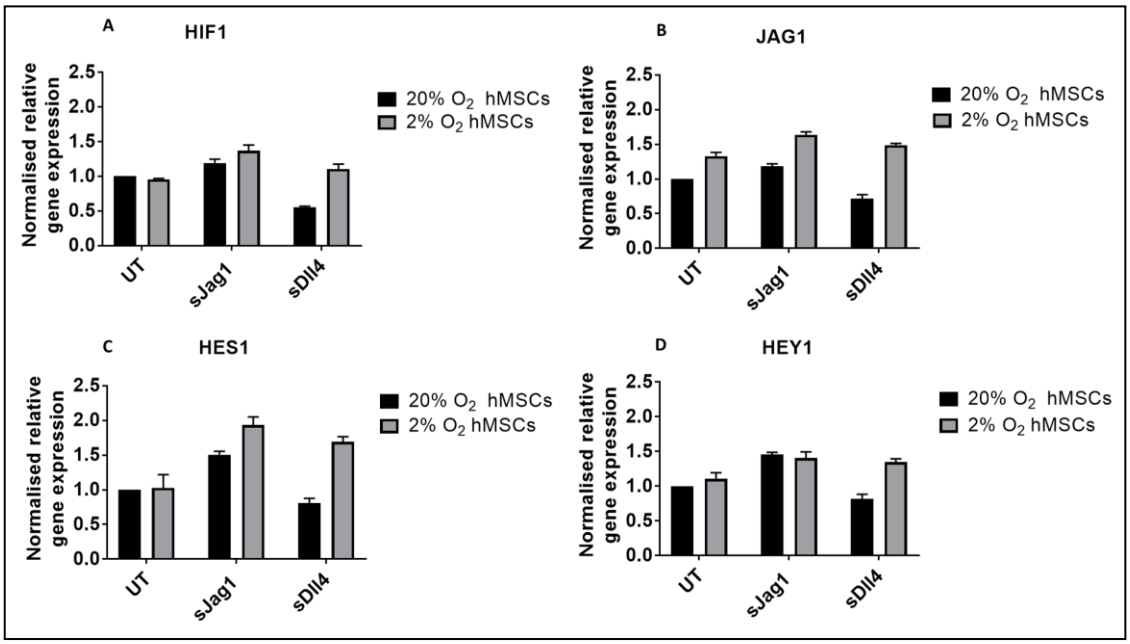

Figure 5-4: The normalised relative expression of HIF1, JAG1, HES1 and HEY1, was analysed for normoxic or hypoxic individual donor P5 (PDL 7) hBM-MSCs after they were preconditioned with either sJag1 or sDll4 or left untreated and seeded on FN-coated wells for 45 min. Data for A, B, C and D are shown as one independent experiment with duplicate observations for each sample (UT, sJag1, and sDll4) as mean ± SD.

qPCR was also carried on commercial PDL 14 hBM-MSCs for the expression of HIF1, HIF3, JAG1, HES1, and HEY1. The data showed that treating the cells in hypoxia did not activate the HIF1 gene, this was observed in both experiment 1 and experiment 2 (Figure 5-5 A). On the other hand, even though there was variation between the two experiments, looking at HIF3 expression, the trend was that HIF3 was overexpressed in the cells conditioned to low oxygen (see grey

bars for UT, sJag1 and sDll4 Figure 5-5 B) in comparison to the control groups (see black bar UT, Figure 5-5 B). The expression of HIF3 in sDll4 and sJag1 samples was at least 5-fold higher than that of the control groups (Figure 5-5 B). However, the big variations between the two experimental repeats for HIF3 suggested that experiments need to be carried out at least two more times to see whether this trend is maintained or not.

Following this, the study investigated whether low oxygen had an effect on the expression of Notch target genes or not. The data indicated that preconditioning the cells with sJag1 had no effect on JAG1 expression (Figure 5-5 C). On the other hand, the Notch target gene HES1 was almost two-fold higher for the sDll4 and sJag1-treated cells at 20% O_2 in comparison to the control groups (see black bars 20% O_2; Figure 5-5 D). In addition, the HES1 gene appeared to be expressed at least five-folds more at low oxygen (see grey bars 2% O_2; Figure 5-5 C). In particular, the hBM-MSCs treated with sDll4 and low oxygen exhibited a 15 fold expression of HES1 in comparison to the UT groups (Figure 5-5 C).

Next, the results showed that in experiment 1 (Figure 5-5 E), HEY1 was upregulated in cells expanded at ambient oxygen conditions and exposed to either sJag1 or sDll4. However, in the second experiment, it appeared that Notch priming had no effect on HEY1 expression. For this reason, it was not possible to make any conclusion from this data (Figure 5-4 E). Overall these results should be treated carefully and they could be used to support other observations but on their own, they cannot be used to draw any conclusion as more repeats will need to be carried out.

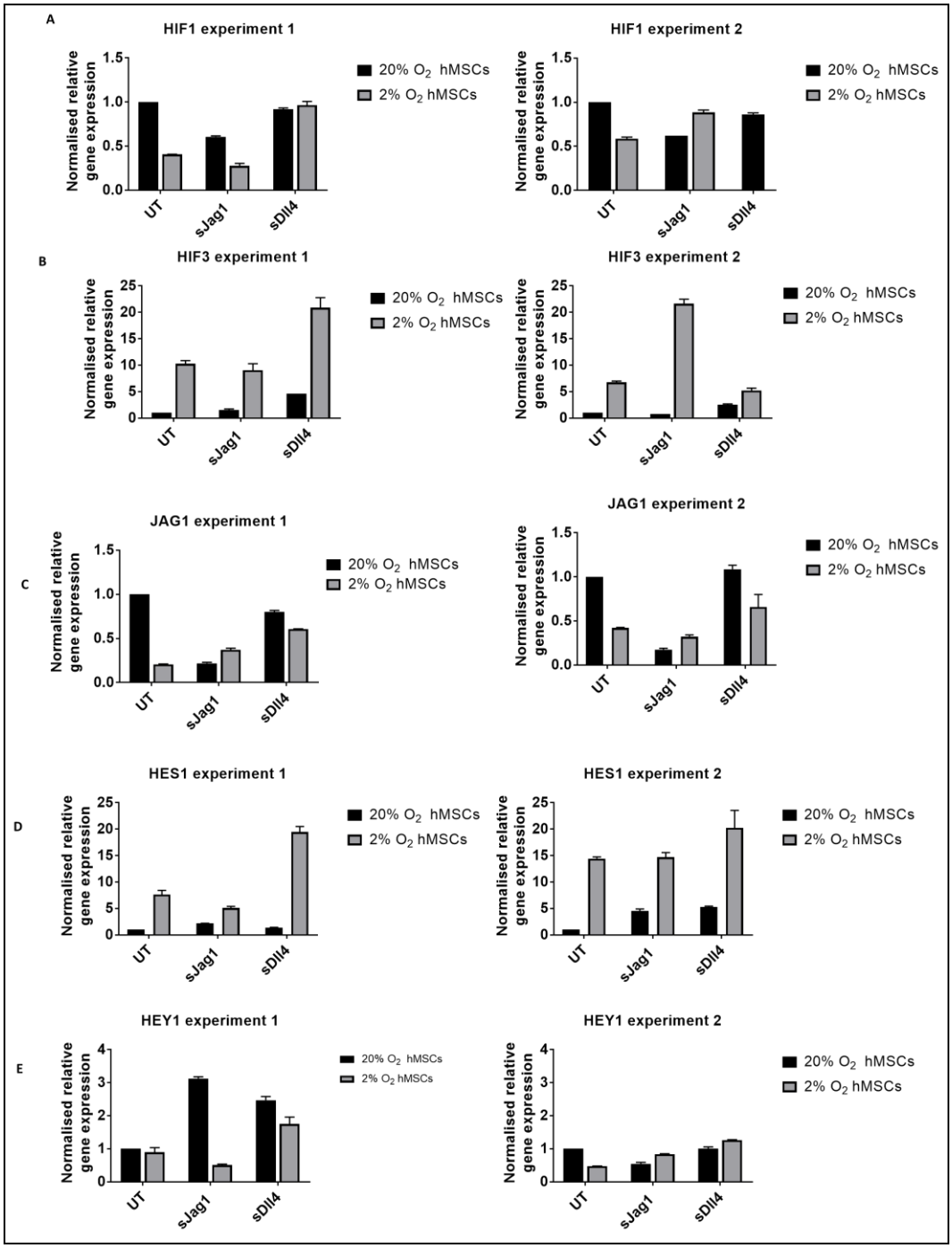

Figure 5-5: The normalised relative expression of (A) HIF1 (B) HIF3, (C) JAG1, (D) HES1 and (E) HEY1 was analysed for normoxic or hypoxic commercial PDL 14 hBM-MSCs after they were preconditioned with either sJag1 or sDll4 or left untreated and seeded on FN-coated wells for 45 min. Gene expression was normalised to 18S and control group. Data are shown for single representative experiments carried out with separately prepared cell suspensions on 2 different days with duplicate observations for each bar as mean ± SD.

The qPCR data for the P11 hUC-MSCs showed that there was approximately a two-fold increase in HIF1 expression in comparison to the control groups for the normoxic cells exposed to either sDll4 or sJag1 (see black bars; Figure 5-6 A). Next, it was not possible to make a conclusion regarding the effect of HIF1 expression for the hypoxic cells exposed to sJag1 (see grey bars for sJag1; Figure 5-6 A). In fact, experiment 1 showed that sJag1 priming had no effect on HIF1 expression, whilst experiment 2 showed that sJag1 priming downregulated HIF1 expression. On the other hand, the data for the hypoxic sDll4-treated cells showed that there was an increase in HIF1 expression in comparison to the UT groups. However, in experiment 2, the sDll4 cells exhibited strong upregulation (see grey bars for sDll4; Figure 5-6 A) and in experiment 1 there was only a modest increase in comparison to the UT groups. Therefore, more experiments will need to be carried out to perform statistical analysis and obtain conclusive answers.

Following this, exposing the hypoxic hMSCs to sJag1 appeared to downregulate JAG1 activation (Figure 5-6 B). On the other hand, when either normoxic or hypoxic hMSCs were exposed to sDll4 there was no effect on JAG1 activation (see grey and black bars; Figure 5-6 B).

Next, when the hypoxic hMSCs were primed with sJag1 there was a downregulation of HES1 expression (see grey bars for sJag1 in experiment 1 and 2; Figure 5-6 D). On the other hand, the normoxic sJag1-treated cells showed an increase in HES1 expression. However, this was more evident in experiment 1 with a 3 fold increase in expression over the UT cells. Next, the sDll4-treated normoxic and hypoxic cells only showed a modest increase in HES1 expression (Figure 5-6 D). Following this, the sDll4-treated hypoxic hMSCs only showed a modest increase in HEY1 expression. As only an n = 1 was carried out for the hypoxic hMSCs with 2 measurements, it was not possible to make any conclusion for the 2% O_2 sDll4-treated cells (HES1 and HEY1, Figure 5-6 D and E).

The results also showed that the expression of the HEY1 gene in sJag1-treated hypoxic cells was low in comparison to the UT cells, this was observed in both experiment 1 and 2 (Figure 5-6 E). On the other hand, there was at least a three-fold increase in expression of HEY1 in the sJag1-treated normoxic cells (see

black bars 20% O_2, Figure 5-6 E). Similarly, HEY1 also appeared to be overexpressed in sDll4-treated normoxic cells but the variation between the two experiments was not enough to say whether these differences were significant or not (see black bars for sDll4 20%, Figure 5-6 E).

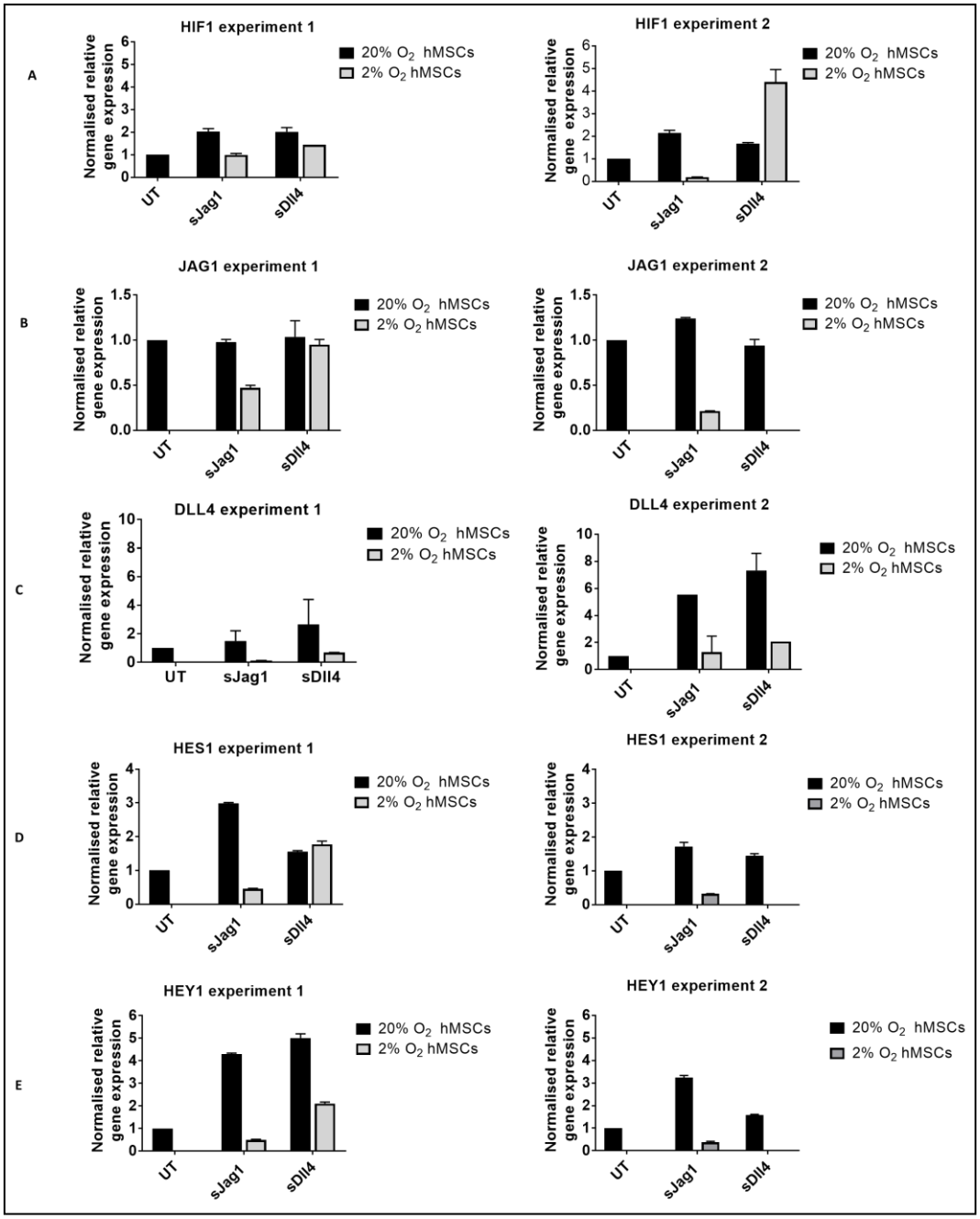

Figure 5-6: The normalised relative expression of (A) HIF1 (B) JAG1, (C) DLL4, (D) HES1 and (D) HEY1 was analysed for normoxic or hypoxic P11 hUC-MSCs after they were preconditioned with either sJag1 or sDll4 or left untreated and seeded on FN-coated wells for 45 min. Data are shown for single representative experiments carried out with separately prepared cell suspensions on 2 different days with duplicate observations for each bar as mean ± SD.

5.3.3: Co-culture assays

5.3.3.1: Staining of cell monolayer with viable cell fluorescent dyes

hMSCs (see phase contrast; Figure 5-7) and HUVECs (see phase contrast; Figure 5-7) were visualised under an inverted light microscope to confirm that they were still actively proliferating and to estimate if they reached 80-90% confluency by ensuring that most of the area in the flask was covered. hMSCs and HUVECs were stained separately (see red and green staining; Figure 5-7) and successful staining was observed by the red fluorescence of the hBM-MSCs and the green fluorescence of the HUVECs which would allow for the cells to be distinguished in the *in vitro* co-culture assays (Figure 5-7).

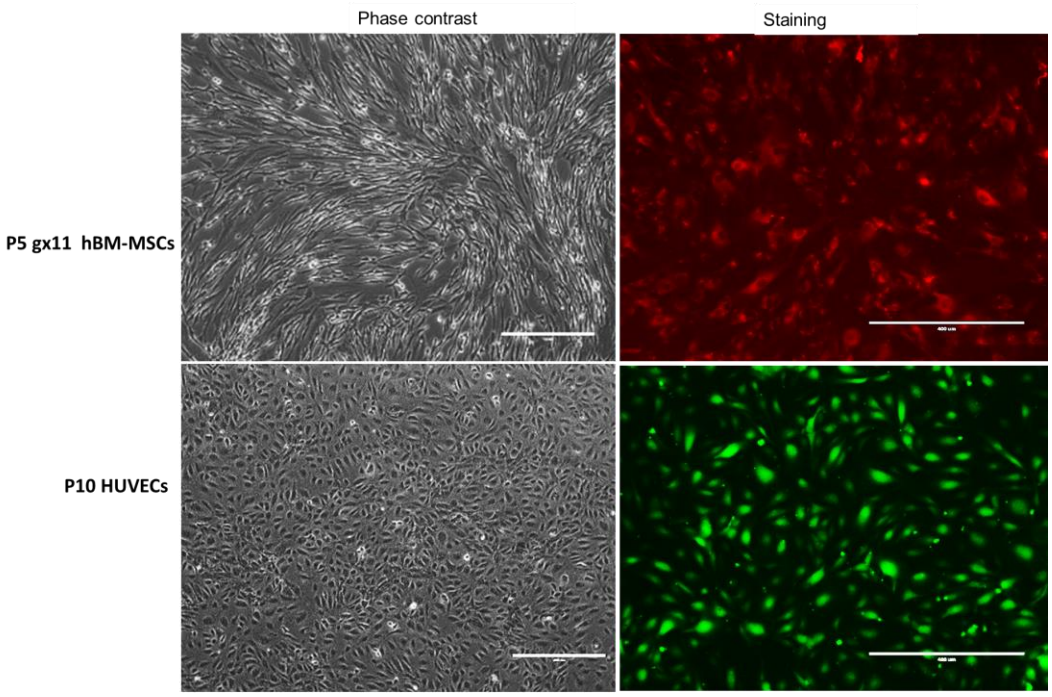

Figure 5-7: Representative phase contrast and staining images of P5 (PDL 7) gx11 hBM-MSCs and P10 HUVECs with viable fluorescent cell dyes for *in vitro* vascular assays. Successful staining was confirmed by observing the uptake of the dye using a fluorescence microscope where hMSCs were stained in red and HUVECs were stained in green. Scale bars = 400 µm.

5.3.3.2: Interaction of hMSCs with HUVECs in co-culture assays

Following successful staining cells were diluted at 0.67 x 10^5 cells/ml in complete EGM-2 medium, mixed at a 1:1 ratio and seeded on either Matrigel-coated or Geltrex-coated wells. HUVECs cultured separately on top of the gel-coated wells were used as positive controls. The phase contrast images for the control groups indicated the formation of well-connected vascular networks on Matrigel and Geltrex respectively at both 20% O_2 and 2% O_2 (Figure 5-8 A). Furthermore, no apparent differences in network formation were observed for the different conditions (Figure 5-8 A). Following this, the fluorescence images data (Figure 5-8 B) confirmed that all of the HUVECs stained with the green fluorescent dye and that the stain did not fade off after 18 hours of incubation.

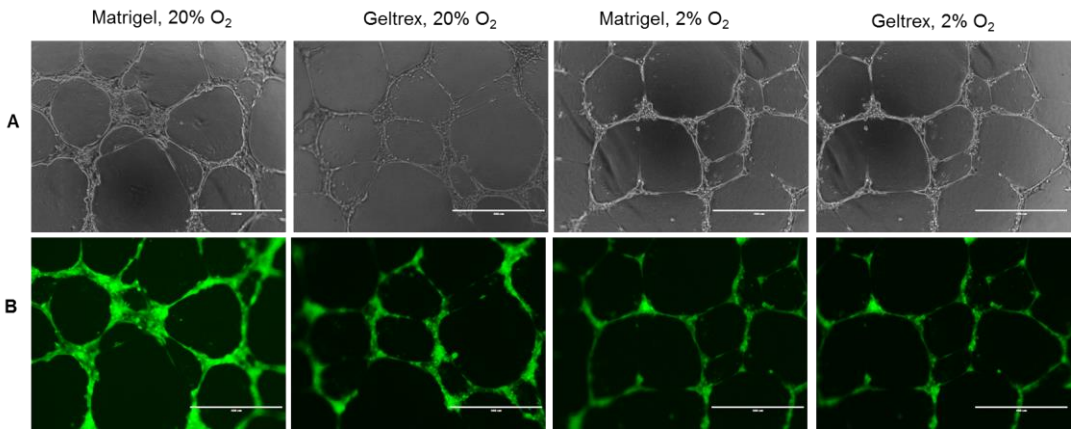

Figure 5-8: Representative staining images of P10 HUVECs (control groups) in (A) phase contrast and (B) stained with CellTracker Green CMFDA using Matrigel and Geltrex. Experiments were carried out at 20% O_2 and 2% O_2. Scale bars = 400 µm.

Co-culture assays were carried out to assess the interactions between HUVECs and individual donor hBM-MSCs on the gel-coated wells. The staining images showed that the normoxic and hypoxic hBM-MSCs exerted a pericyte-like behaviour by aligning at the periphery of the tubules or bridging between them, this was observed for both Matrigel and Geltrex (see UT, sJag1, sDll4 at 20% O_2 or 2% O_2; Figure 5-9 1-6 and Figure 5-10 7-12).

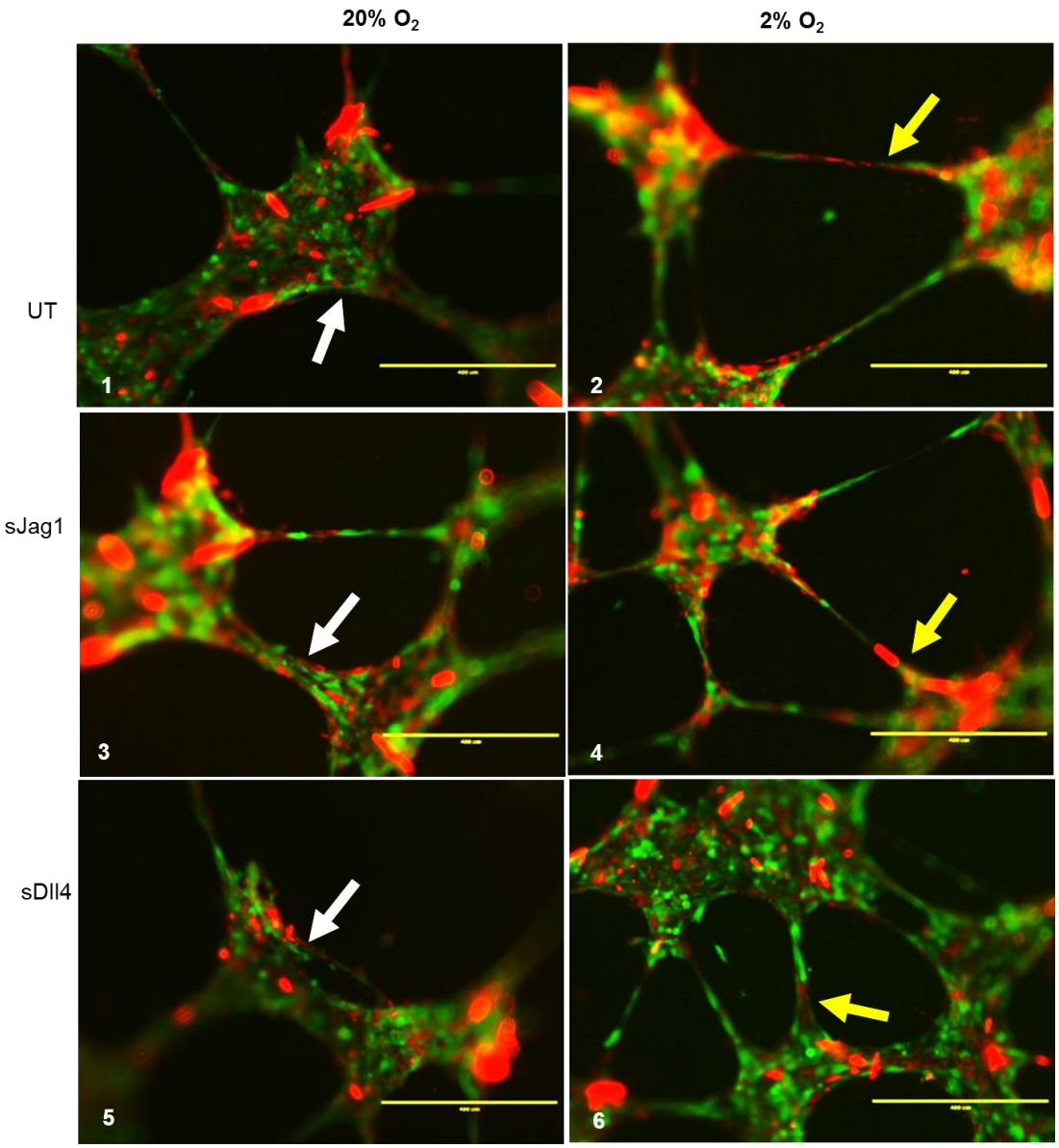

Figure 5-9: Co-culture vessel formation after 18 hours of P5 (PDL 7) gx11 hBM-MSCs (in red) and P10 HUVECs (in green) seeded at a 1:1 ratio. Experiments were carried out on GFR Matrigel. Images were visualised using a fluorescence microscope. Yellow arrows represent the hBM-MSCs bridging between HUVECs. White arrows represent the hBM-MSCs surrounding the network structures. Scale bars = 400 µm.

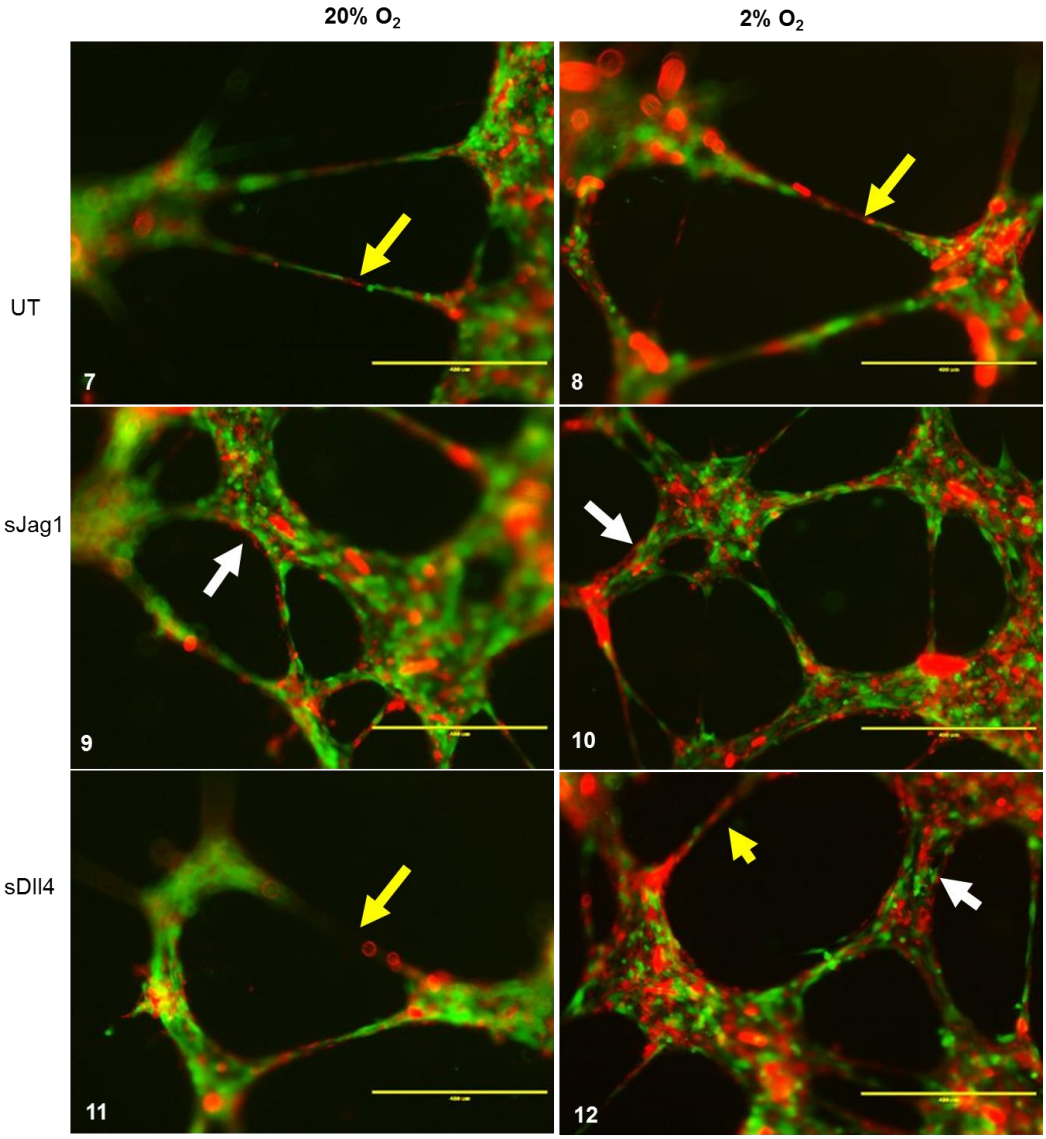

Figure 5-10: Co-culture vessel formation after 18 hours of P5 (PDL 7) gx11 hBM-MSCs (in red) and P10 HUVECs (in green) seeded at a 1:1 ratio. Experiments were carried out on GFR Geltrex. Images were visualised using a fluorescence microscope. Yellow arrows represent the hBM-MSCs bridging between HUVECs. White arrows represent the hBM-MSCs surrounding the network structures. Scale bars = 400 µm.

Next, it was observed that the PDL 14 commercial hBM-MSCs co-localised with the HUVEC structures. This behaviour suggested that the hMSCs (in red) were exerting a pericyte-like behaviour by and aligning around the endothelial cells (in green, Figure 5-11, 13-18; Figure 5-12, 19-24).

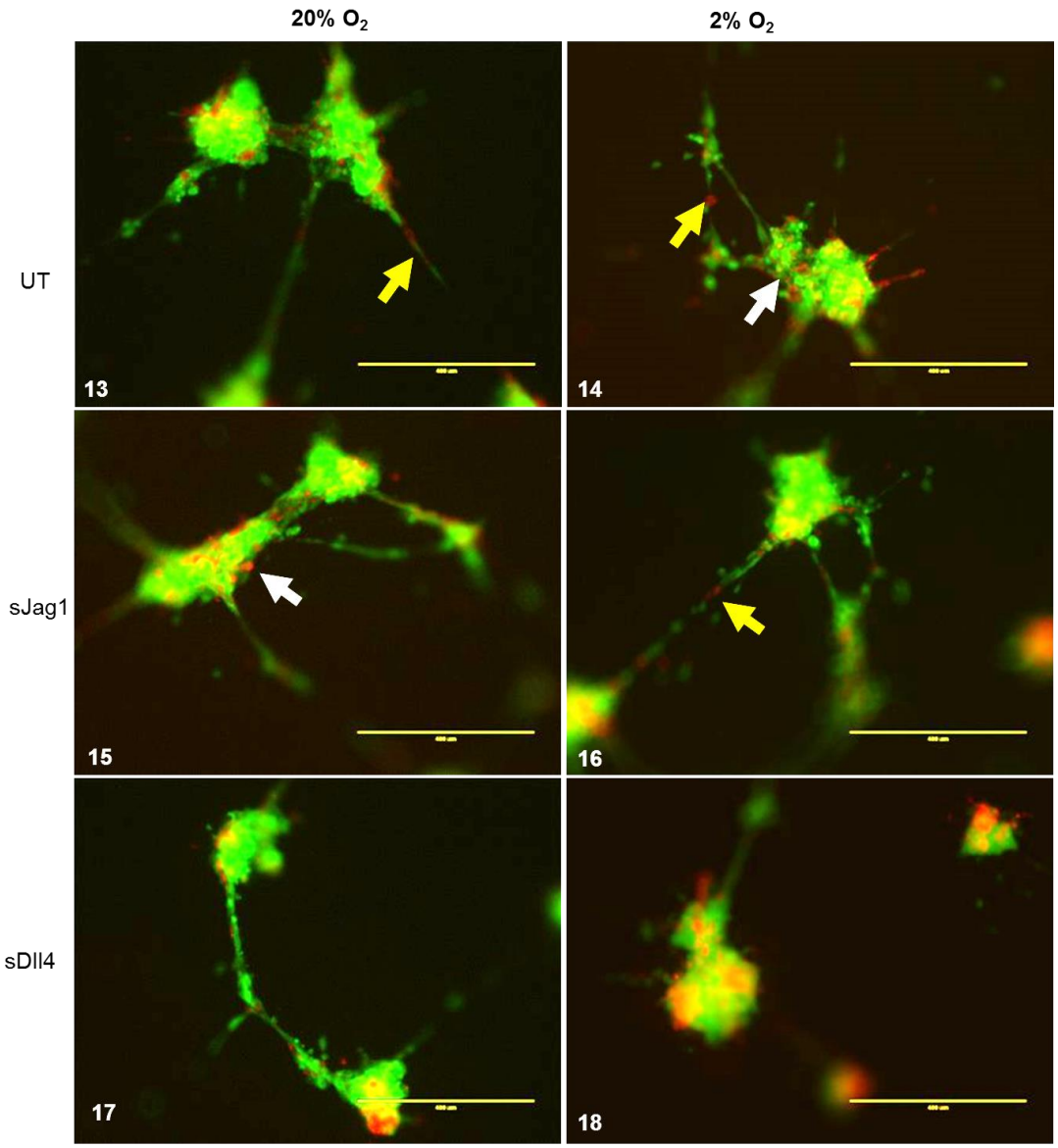

Figure 5-11: Co-culture vessel formation after 18 hours of commercial PDL14 hBM-MSCs (in red) and P10 HUVECs (in green) seeded at a 1:1 ratio. Experiments were carried out on GFR Matrigel. Images were visualised using a fluorescence microscope. Yellow arrows represent the hBM-MSCs bridging between HUVECs. White arrows represent the hBM-MSCs surrounding the network structures. Scale bars = 400 µm.

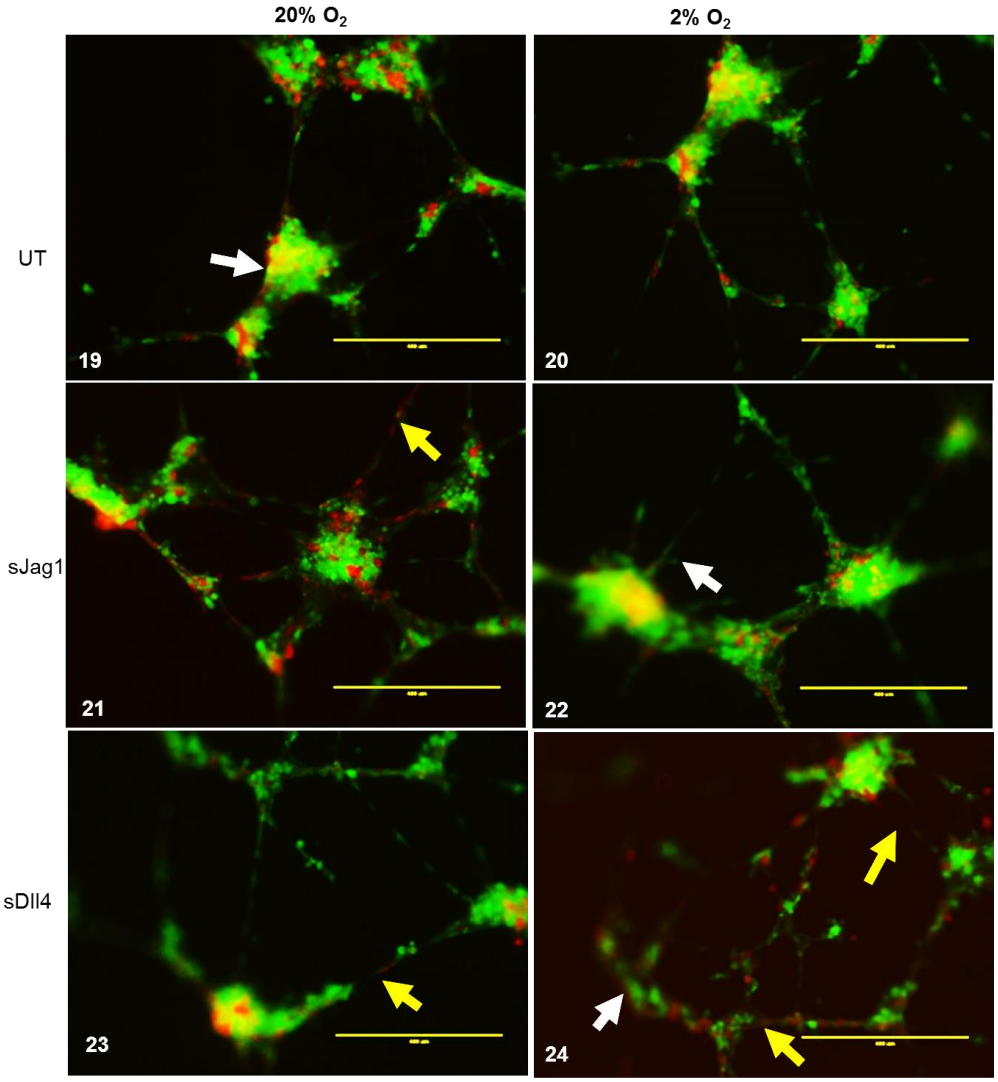

Figure 5-12: Co-culture vessel formation after 18 hours of commercial PDL14 hBM-MSCs (in red) and P10 HUVECs (in green) seeded at a 1:1 ratio. Experiments were carried out on GFR Geltrex. Images were visualised using a fluorescence microscope. Yellow arrows represent the hBM-MSCs bridging between HUVECs. White arrows represent the hBM-MSCs surrounding the network structures. Scale bars = 400 µm.

The fluorescence images of the P11 hUC-MSCs seeded with P10 HUVECs at a 1:1 ratio (Figure 5-13) indicated no formation of vessel structures. However, the images suggested the hUC-MSCs were still co-localizing with the HUVECs in the clump structures (Figure 5-13 25-30). These images also suggested that hMSCs may have a modulatory role in the formation of vessel-like structures by HUVECs as when the hUC-MSCs were co-cultured with the HUVECs there was no tubule formation, whilst the endothelial cells alone were able to form vessel-like structures (Figure 5-8). As shown in Figure 5-13, the hUC-MSCs appeared to engulf around the HUVECs which might have hindered the ECs from migrating and forming networks. On the other hand, when hBM-MSCs were co-cultured on the same day and with the same HUVECs used for the hUC-MSCs they also co-

localised with the HUVECs but cells were able to form vessel-like structures (Figure 5-9 and Figure 5-10). This observation further suggests that hMSCs may modulate network formation and that differently-sourced hMSCs may behave differently.

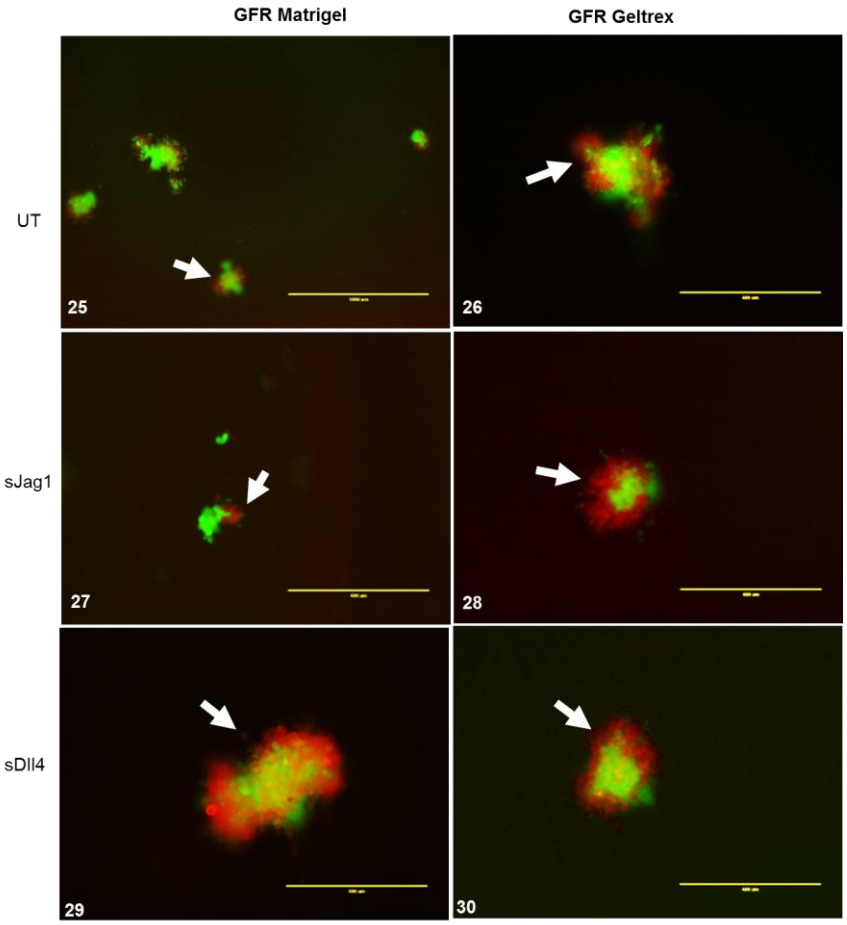

Figure 5-13: Co-culture vessel formation after 18 hours of P11 hUC-MSCs (in red; hUC-MSCs were previously cultured in either 20% O_2 or 2% O_2) and P10 HUVECs (in green; previously cultured in ambient oxygen conditions). Experiments were carried out using either GFR Matrigel or GFR Geltrex. Images were visualised using a fluorescence microscope. White arrows represent the hUC-MSCs surrounding the HUVEC structures. Scale bars = 400 µm.

5.3.3.3: Branch point quantification of co-culture assays using P10 HUVECs and individual donor P5 (PDL 7) hBM-MSCs

Co-culture assays were performed using P10 HUVECs and P5 (PDL 7) individual donor hBM-MSCs to assess differences in tubule network morphology and efficiency. The phase contrast images showed that the formation of tubule-like structures was different in HUVECs-only and co-culture assays. In fact, the tubules formed in the co-culture assays (see UT, sJag1, and sDll4; Figure 5-14 B and C) appeared to be more heterogeneous than the control groups (Figure 5-14 A) consisting of more elongated interconnecting tubules that more closely resembled capillaries *in vivo* than the HUVECs-only assays. Vascular networks formed in the co-cultures (Figure 5-14 B and C) also demonstrated a diminished ability to form endothelial networks on gel-coated wells (Figure 5-14 A).

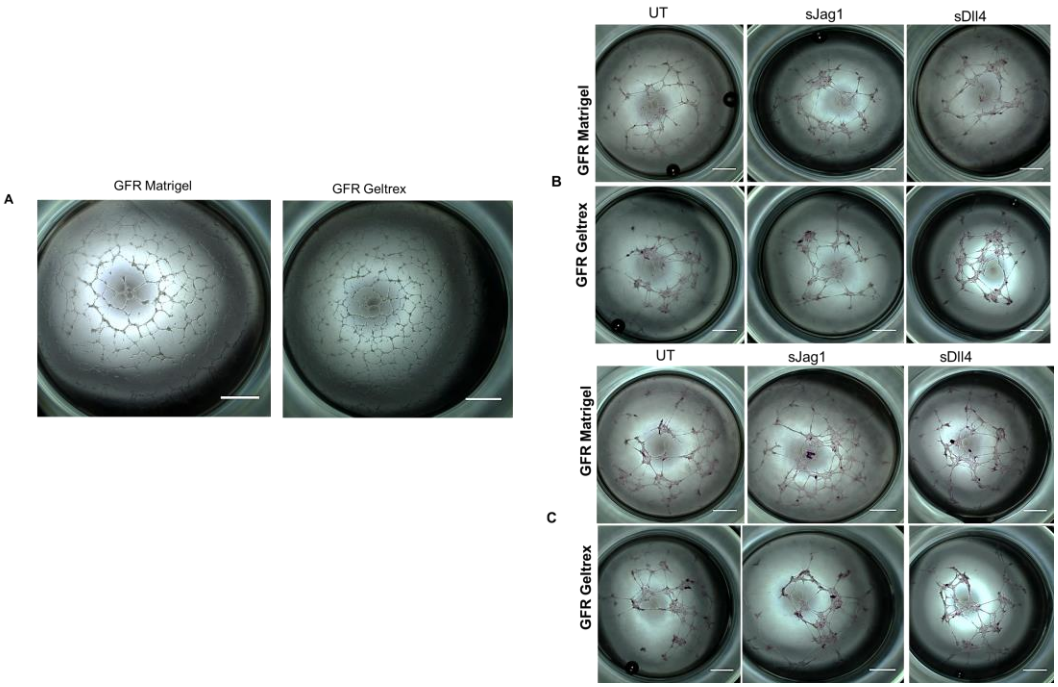

Figure 5-14: (A) Positive controls were run for the co-culture assays by seeding P10 HUVECs on either GFR Matrigel or GFR Geltrex. Co-cultures were carried by seeding P10 HUVECs with either (B) normoxic P5 (PDL 7) gx11 hBM-MSCs or (C) hypoxic P5 (PDL 7) gx11 hBM-MSCs mixed at a ratio of 1:1 and seeded on either 35 µl of GFR Matrigel or 35 µl of GFR Geltrex. Experiments were carried out at 2% O_2. Scale bars = 1000 µm.

The branch point quantification data indicated 2-3 folds increase in the number of branch points formed using the HUVECs-only positive control groups (coated on either GFR Matrigel or GFR Geltrex) in comparison to the co-cultures (see

normoxic hBM-MSCs and hypoxic hBM-MSCs, Figure 5-15 A and B). This might be due to the fact that the co-cultures only had half the number of vascular endothelial cells in the system which was going to in itself reduce the number of branch points. Next, the normoxic hBM-MSCs and the hypoxic hBM-MSCs seemed to work similarly on both Matrigel and Geltrex coated wells, this was observed for both individual experiments (Figure 5-15 A and B).

Following this, the data for the gx11 hBM-MSCs showed that Matrigel performed better than Geltrex in forming branch networks in co-culture (Figure 5-15 A). However, since only one experiment was performed using this donor it was not possible to establish whether these differences were significant or not, hence these findings were deemed to be inconclusive. Both Matrigel and Geltrex are derived from mouse sarcoma explaining why they might have worked similarly well. Furthermore, the results for the gx10 hBM-MSCs indicated that Matrigel and Geltrex worked similarly well in co-culture assays (see experiment 2, Figure 5-15 B). The values of Matrigel in both experiments were similar whilst the values of Geltrex were higher in experiment 2 (Figure 5-15 B) with the number of branch points using the normoxic hMSCs being almost double in experiment 2 compared to experiment 1 (Figure 5-15 A and B). The overall conclusion from this data is that when HUVECs alone are seeded on either Matrigel or Geltrex, they form a higher number of branch points compared to co-cultures. Moreover, priming the hBM-MSCs with Notch ligands did not seem to impact on the tubule formation efficiency.

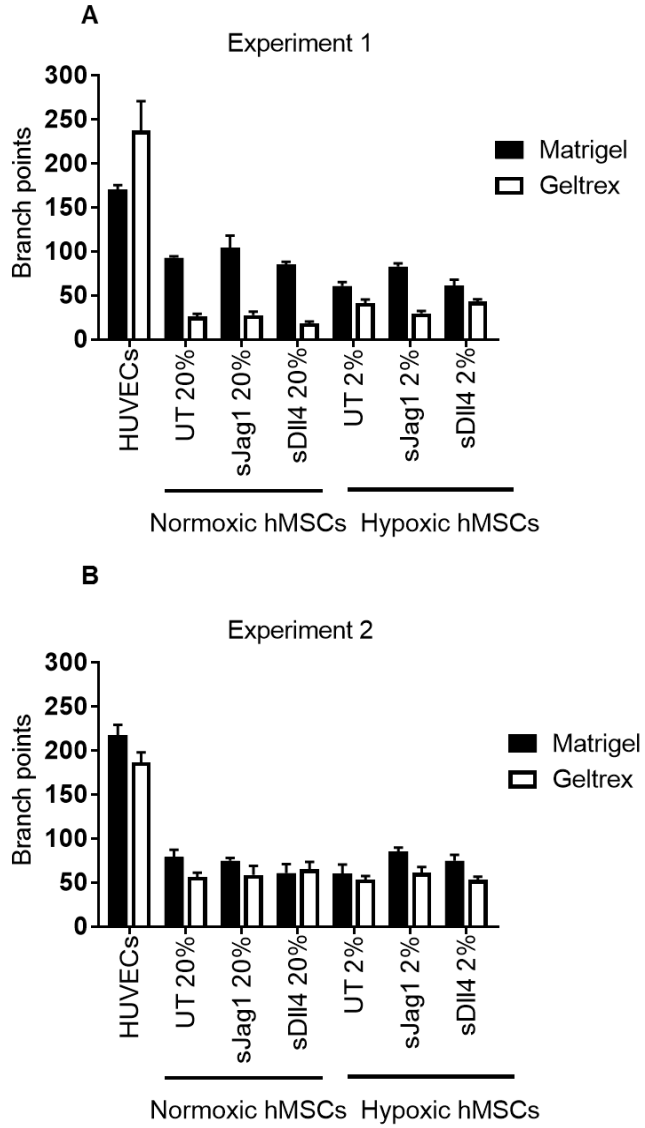

Figure 5-15: Branch point quantification of P10 HUVECs seeded with either (A) gx11 P5 (PDL 7) hBM-MSCs or (B) gx10 P5 (PDL 7) hBM-MSCs previously cultured under normoxic (20% O_2) and hypoxic (2% O_2) conditions respectively for 5 days. Error bars represent observations of three technical replicates for each biological repeat as mean ± SD. Experiments were carried out twice using hMSC batches isolated and expanded from two different donors; A (gx11) and B (gx10).

5.3.3.4: Average tubule length quantification of co-culture assays using P10 HUVECs and individual donor P5 (PDL 7) hBM-MSCs

The average tubule length of the co-culture assays in both the GFR Matrigel and GFR Geltrex assays was at least double that of the HUVECs-only control groups (see HUVECs against UT, sJag1, and sDll4; Figure 5-16 A and B). The results showed that the pre-stimulation of the hMSCs by Notch ligands did not impact on the length of the vessels. However, it is notable that for the gx11 hBM-MSCs the

normoxic sJag1-treated cells seeded on Geltrex appeared to be longer than those formed in the UT and the sDll4 groups (Figure 5-16 A). Overall Matrigel and Geltrex worked similarly well at all of the conditions.

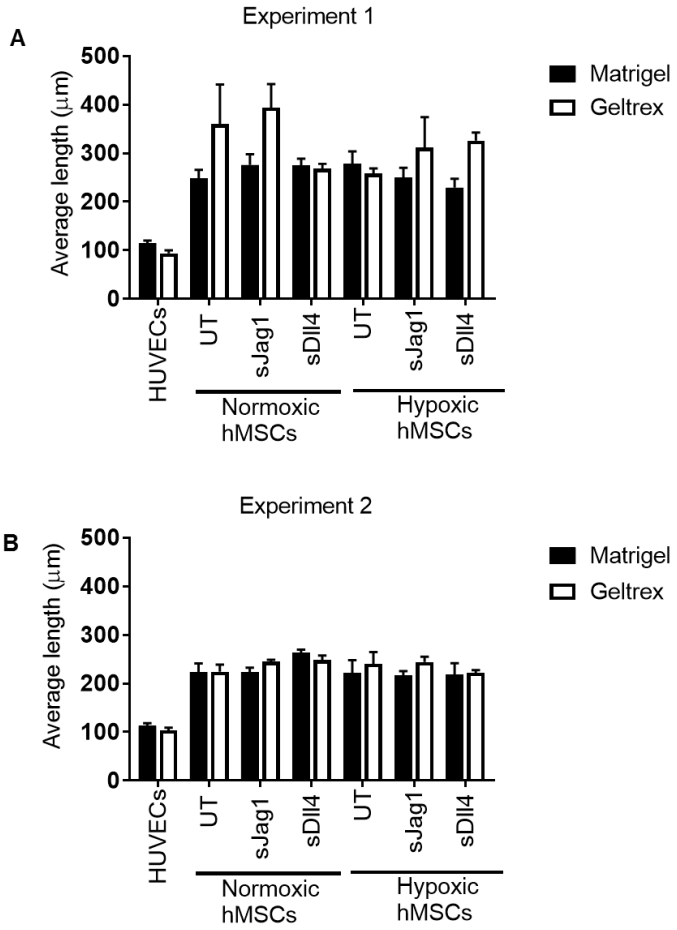

Figure 5-16: Average tubule length quantification of P10 HUVECs seeded with either (A) gx11 P5 (PDL 7) hBM-MSCs or (B) gx10 P5 (PDL 7) hBM-MSCs previously expanded in normoxic (20% O_2) or hypoxic (2% O_2) conditions. Error bars represent observations of three technical replicates for each biological repeat as mean ± SD. Experiments were carried out twice using hBM-MSC batches isolated and expanded from two individual donors; A (gx11) and B (gx10).

5.3.3.5: Cumulative tubule length quantification of co-culture assays using P10 HUVECs and individual donor P5 (PDL 7) hBM-MSCs

The HUVECs-only control groups showed higher cumulative tubule length values than the co-cultures (see HUVECs against UT, sJag1, and sDll4; Figure 5-17 A and B). In particular, on Geltrex the normoxic sJag1-treated and UT gx11 hBM-MSCs showed almost 2 fold decrease in cumulative tubule length values in comparison to the HUVECs-only groups (Figure 5-17 A). Next, the data for experiment 1 showed that the sDll4-treated normoxic hMSC groups seeded on Geltrex, appeared to show higher cumulative length values than the UT and the

sJag1 groups, but this was trend was not observed in experiment 2 and that could be related to using a different MSC donor (see experiment 1; Figure 5-17 A). On the other hand, for the hypoxic hBM-MSCs, there was a trend where the sJag1 groups appeared to show higher values than the UT and the sDll4-treated cells and this was observed using both Matrigel and Geltrex (see hypoxic hMSCs; Figure 5-17 A and B). This observation indicated that preconditioning hMSCs in low oxygen may enhance the effects of sJag1 in co-culture assays. Following this, there was no obvious trend for the normoxic gx11 hMSCs seeded on Matrigel and the normoxic gx10 hMSCs seeded on either Matrigel or Geltrex (see UT against sJag1 and sDll4; Figure 5-17 A and B). More experiments will need to be performed to confirm whether these differences are significant or not. It is notable that the HUVECs-only groups had double the number of endothelial cells than the co-cultures where the other half was replaced by hBM-MSCs. This might have contributed to the higher cumulative tubule length values observed for the HUVEC-only groups.

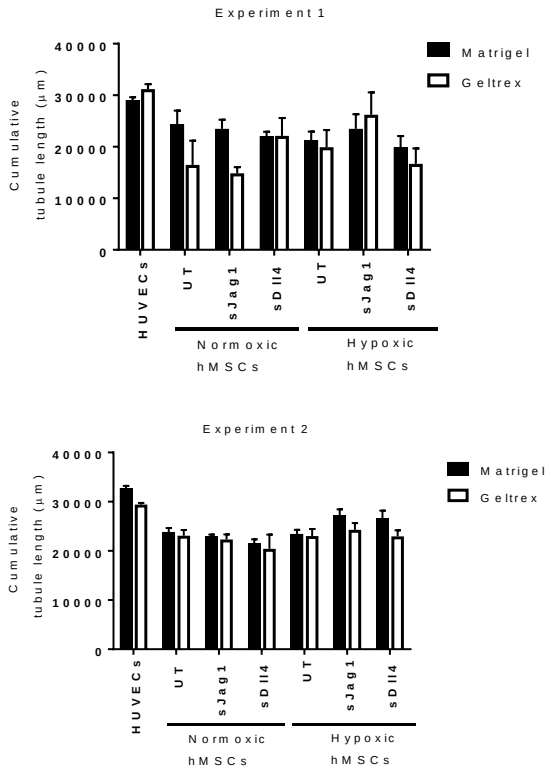

Figure 5-17: Cumulative tubule length quantification of P10 HUVECs seeded with either (A) gx11 P5 (PDL 7) hBM-MSCs or (B) gx10 P5 (PDL 7) hBM-MSCs previously cultured under normoxic (20% O_2) or hypoxic (2% O_2) conditions. Error bars represent observations of three technical replicates for each biological repeat as mean ± SD. Experiments were carried out twice using hBM-MSC batches isolated and expanded from two individual donors; A (gx11) and B (gx10).

5.3.3.6: Quantification of vessel-like networks in the presence of commercial hBM-MSC/HUVEC co-cultures

The phase contrast images showed that the HUVECs that were co-cultured with the MSCs demonstrated a diminished ability to form vascular-like networks (Figure 5-18 B and C). On the other hand, when HUVECs were seeded separately on either Matrigel or Geltrex, they acquired an increased ability to form vascular tubules (Figure 5-18 A). This indicated that the physical interaction of the hBM-MSCs with the HUVECs was inhibitory to the angiogenic potential of endothelial cells to form networks. In addition, branches formed in the co-culture assays looked more elongated (Figure 5-18 B and C) than those observed for the control groups (Figure 5-18 A). Next, it was observed that when the ECs were seeded with the hypoxic hBM-MSCs (Figure 5-18 C), more vascular networks were formed than when using the normoxic hBM-MSCs (Figure 5-18 B). Vascular efficiency was measured by manually counting the number of branch points formed (Figure 5-19).

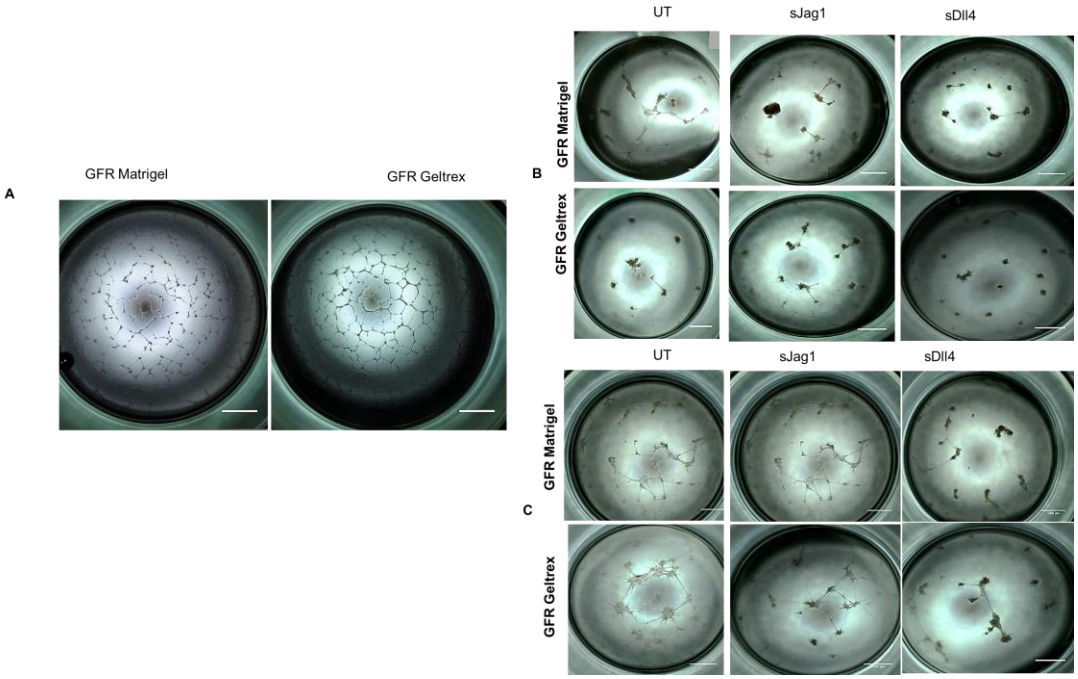

Figure 5-18: (A) Positive controls were run for the co-culture assays by seeding P10 HUVECs on either GFR Matrigel or GFR Geltrex. Co-culture assays were carried out by seeding P10 HUVECs with either (B) normoxic commercial PDL14 hBM-MSCs or (C) hypoxic commercial PDL14 hBM-MSCs mixed at a ratio of 1:1 and seeded on either 35 µl of GFR Matrigel or 35 µl of GFR Geltrex. Experiments were carried out at 2% O_2. Scale bars = 1000 µm.

The cumulative quantification data for the PDL14 commercial hBM-MSCs showed that the positive controls (with endothelial cells alone) formed a significantly

higher number of branch points than the co-cultures (see HUVECs, Figure 5-19 E). The very low number of branch points for the co-culture assays suggested that the presence of hMSCs might have been inhibitory to efficient network formation. In fact, the physical interaction between hMSCs and HUVECs might have also changed the release of a soluble factor(s) that affects the angiogenic capacity of endothelial cells (Menge et al., 2012). In addition, the ratio chosen for the hMSCs and HUVECs might not have been optimal for network formation. Each experimental repeat indicated large error bars between technical replicates (Figure 5-19 A-C). Sources of variability might have been associated with the methodology of the assays (e.g. extensive serial dilutions of samples to obtain wanted concentrations), mixing of the samples or decrease in cell viability during the experiments, suggesting the need for assay optimization. Next, the trend between the first two experiments was similar and the number of networks formed when using the untreated hypoxic hMSCs seeded on Geltrex was at least 10 folds higher than when the normoxic hBM-MSCs were used (see UT, Figure 5-19 A and B). Similarly, when the hypoxic sJag1-treated hBM-MSCs were used, the number of branch points formed was at least 4 times higher than that obtained when using the sJag1-treated normoxic hBM-MSC groups, this trend was maintained in both experiment 1 and experiment 2 (see sJag1; Figure 5-19 A and B). Next, experiment 3 showed that the number of branch points formed when using the hypoxic hBM-MSCs was considerably higher in comparison to the normoxic hBM-MSCs, and this trend was observed for each UT, sJag1 and sDll4 groups. In particular, the networks formed on Geltrex using the hypoxic hBM-MSCs were at least 60 folds higher than those formed using the normoxic hBM-MSCs (see UT, sJag1, and sDll4 groups; Figure 5-19 C).

The variability dependent on the different batches of hMSCs was shown in the cumulative data (Figure 5-19 D). However, there was a trend where the number of branch points formed using the hypoxic hMSCs was higher than those observed in the normoxic hMSC group. In particular, this trend was more evident on Geltrex, with at least double the number of branch points formed in the normoxic UT and sJag1 groups in comparison to those obtained when the cells were seeded on Matrigel (Figure 5-19 D). These results suggest that hypoxic preconditioning may have a positive effect on the angiogenic abilities of MSCs. Furthermore, differences between UT and sJag1 were more apparent in the

Matrigel groups, especially using the hypoxic hMSCs where the number of branch points formed using the sjag1-primed hMSCs was almost two-fold higher than that of the UT group (see black bars, UT 2% against sJag1 2%, Figure 5-19 C).

Based on the mean data (Figure 5-19 A, B and C), experiment 3 (Figure 5-19 C) might have been considered as an outlier as shown in the raw data in Figure 5-18 E as there was less variance between the other two experiments (Figure 5-19 C). However, as it performed best especially at low oxygen and considering that there was a high degree of variability within the experiments themselves, it was not possible to draw any clear conclusion from this study.

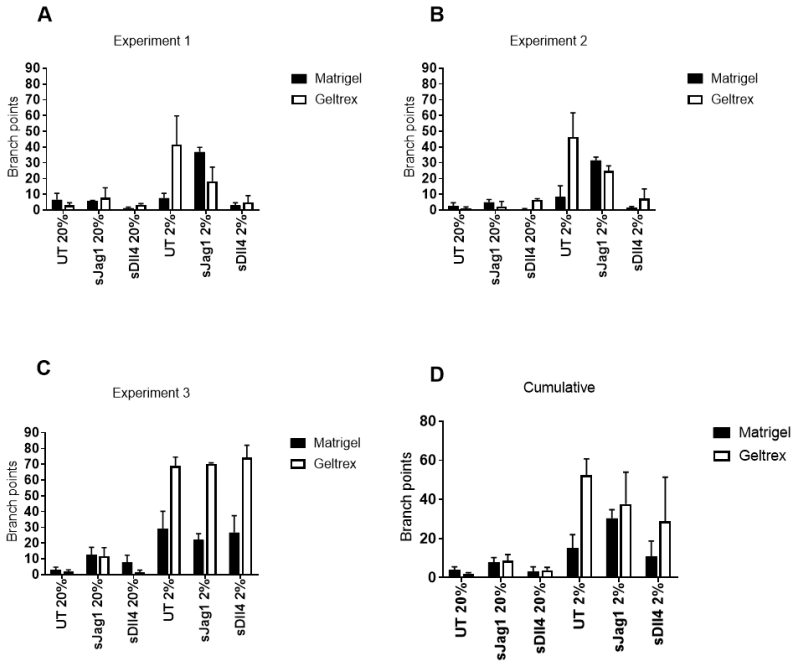

E

	Matrigel			Geltrex		
HUVECs	170	218	190	237	187	213
UT 20% hBM-MSCs	7	3	3	3	1	2
sJag1 20% hBM-MSCs	6	5	13	12	2	12
sDll4 20% hBM-MSCs	1	0	8	4	7	1
UT 2% hBM-MSCs	8	8	29	42	46	69
sJag1 2% hBM-MSCs	37	32	22	18	25	70
sDll4 2% hBM-MSCs	4	2	27	5	7	74

Figure 5-19: Branch point quantification for P10 HUVECs seeded at a 1:1 ratio with commercial PDL14 hBM-MSCs expanded in normoxic (20% O_2) and hypoxic (2% O_2) conditions. The results in (A), (B) and (C) are shown as three independent experimental repeats using different hMSC batches derived from the same donor. Error bars represent observations of three technical replicates for each experimental repeat as mean ± SD. Cumulative data is shown in (D) and error bars represent the mean ± SEM of the three independent experimental repeats. Raw data of the three repeated experiments are shown in (E).

5.3.3.7: Average tubule length quantification of co-culture assays using P10 HUVECs and commercial low serum hBM-MSCs

The average tubule length quantification data for the commercial PDL 14 hBM-MSCs indicated that when hBM-MSCs were present, there was at least a two-fold increase in branch length compared to the HUVECs-only groups (Figure 5-20). Therefore, the vascular networks observed in the co-culture assays were more representative of the capillaries *in vivo* than those formed when endothelial cells alone were present. Also, no obvious differences were observed in relation to oxygen environment or type of matrix (Figure 5-20). However, in the hypoxic hMSCs group there was a modest trend where cells primed with sJag1 showed higher average tubule length in both the Matrigel and Geltrex groups. Overall networks formed using HUVECs alone showed lower average length values than that observed for the co-cultures.

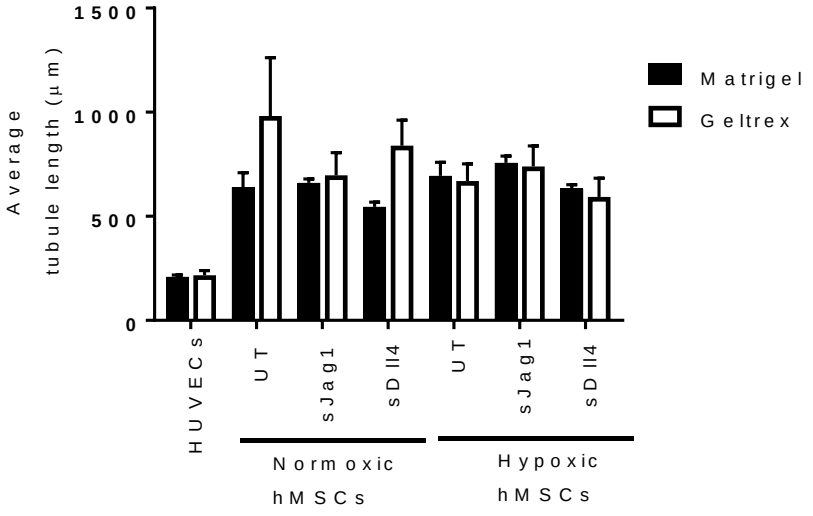

Figure 5-20: Average tubule length quantification for P10 HUVECs seeded with commercial PDL 14 hBM-MSCs which were previously cultured under normoxic (20% O_2) and hypoxic (2% O_2) conditions respectively. Error bars represent the mean ± SEM of three independent experimental repeats carried out using different hMSC batches derived from the same donor. Refer to text for a detailed description of results.

5.3.3.8: Cumulative tubule length quantification of co-culture assays using P10 HUVECs and commercial low serum hBM-MSCs

The results showed that the cumulative tubule length values for the normoxic and hypoxic co-cultures on either Matrigel or Geltrex were at least two-fold lower than

those of the HUVECs-only groups, except for the hypoxic UT and the sJag1 groups which showed similar values to the assays performed using only endothelial cells (Figure 5-21). Next, for the assays performed on Matrigel and using the hypoxic hMSCs, it was evident that sJag1 priming appeared to have a positive effect on cumulative tubule length with almost a two-fold increase in comparison to the UT samples.

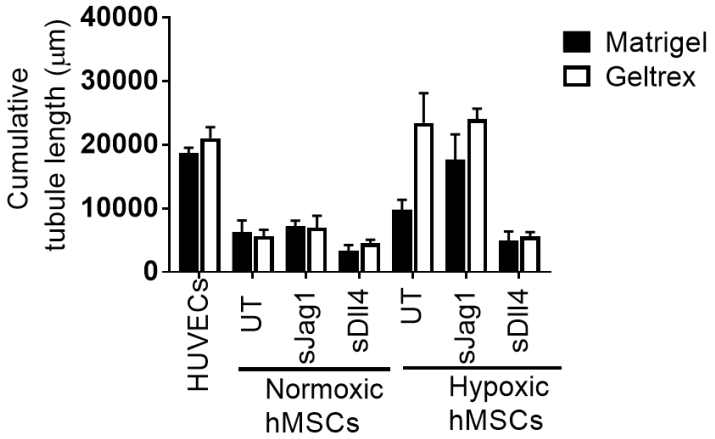

Figure 5-21: Cumulative tubule length quantification for P10 HUVECs seeded with commercial PDL 14 hBM-MSCs which were previously cultured under normoxic (20% O_2) and hypoxic (2% O_2) conditions respectively. Error bars represent the mean ± SEM of three independent experimental repeats carried out using different hMSC batches derived from the same donor. Refer to text for a detailed description of results.

5.3.3.9: Quantification of P11 hUC-MSCs/HUVECs vascular structures

The phase contrast images showed that when the P11 hUC-MSCs were co-cultured with the HUVECs, the experiments failed as there was no formation of vessel structures (Figure 5-22 B and C). This observation was further confirmed by the HUVECs-only positive controls which were able to successfully form vessel-like structures in all of the 8 independently carried out experiments (Figure 5-22 B and C). One reason explaining these results could be that the seeding ratio of hMSCs to HUVECs was not optimal for vascular network formation. Also, it was previously demonstrated in Chapter 3 that P11 hUC-MSCs had enhanced adhesion capabilities especially when the cells were primed with sJag1. Furthermore, their strong adhesion might have been another factor in reducing their spreading and hindering the formation of vessel-like networks.

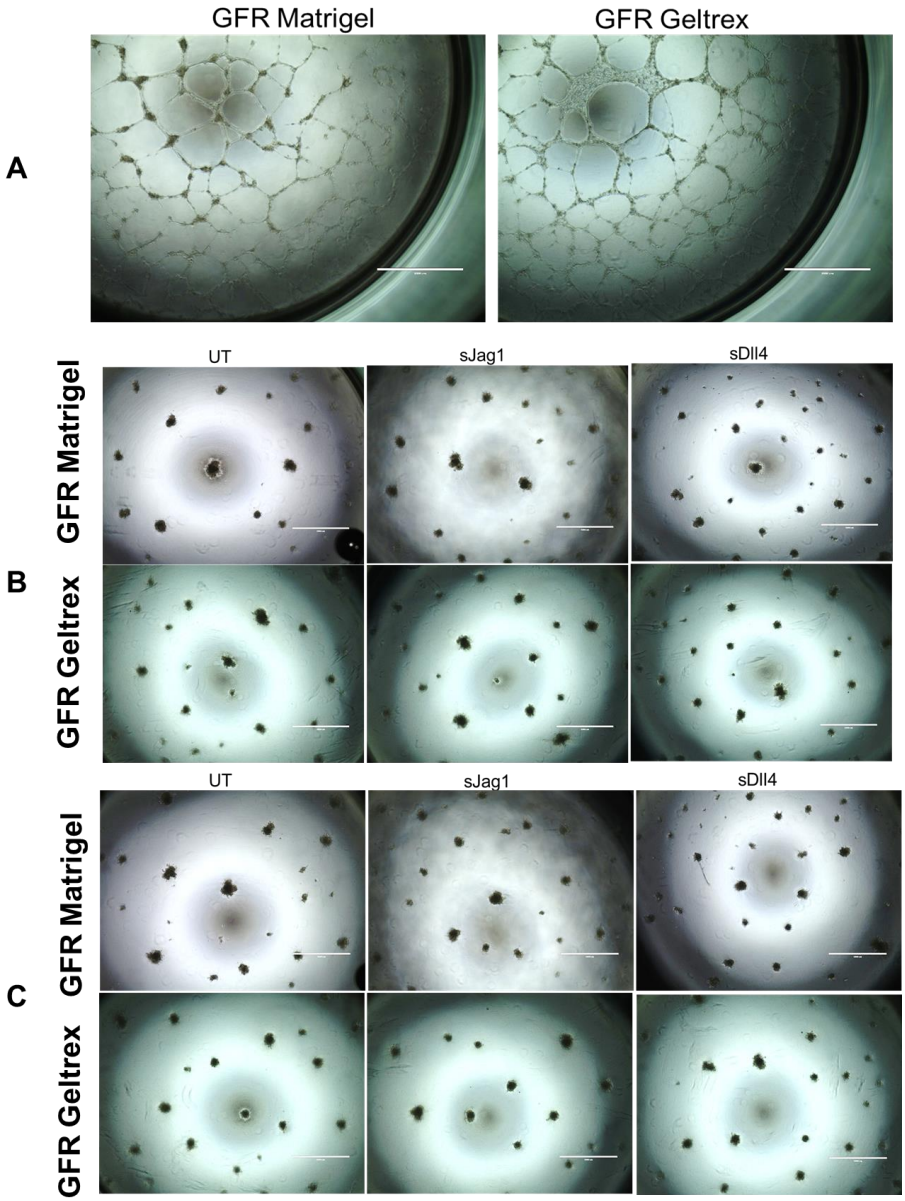

Figure 5-22: (A) Positive controls were run for the co-culture assays by seeding P10 HUVECs on either GFR Matrigel or GFR Geltrex. Co-cultures were carried out with either (B) normoxic P11 hUC-MSCs or (C) hypoxic P11 hUC-MSCs mixed at a ratio of 1:1 with P10 HUVECs using either 35 µl of GFR Matrigel or 35 µl of GFR Geltrex. Experiments were carried out at 2% O_2. No tubule formation was observed after 18 hours incubation. n = 8 independent experimental repeats were carried out using different hMSC batches derived from the same donor. Scale bars = 1000 µm.

5.3.4: Testing the functionality of commercial hBM-MSCs in support assays

Studies were carried out to investigate the supportive role of hBM-MSCs primed with Notch ligands when these were seeded below the HUVECs (Figure 5-23). The fluorescence images indicated that there the hMSCs formed a supportive layer beneath the HUVECs. However, no physical interaction was observed between the two cell types. Next, the fluorescence images showed that there were fewer MSCs for sJag1 and sDll4 whilst it appeared that there was a strong labelling for UT hBM-MSCs.

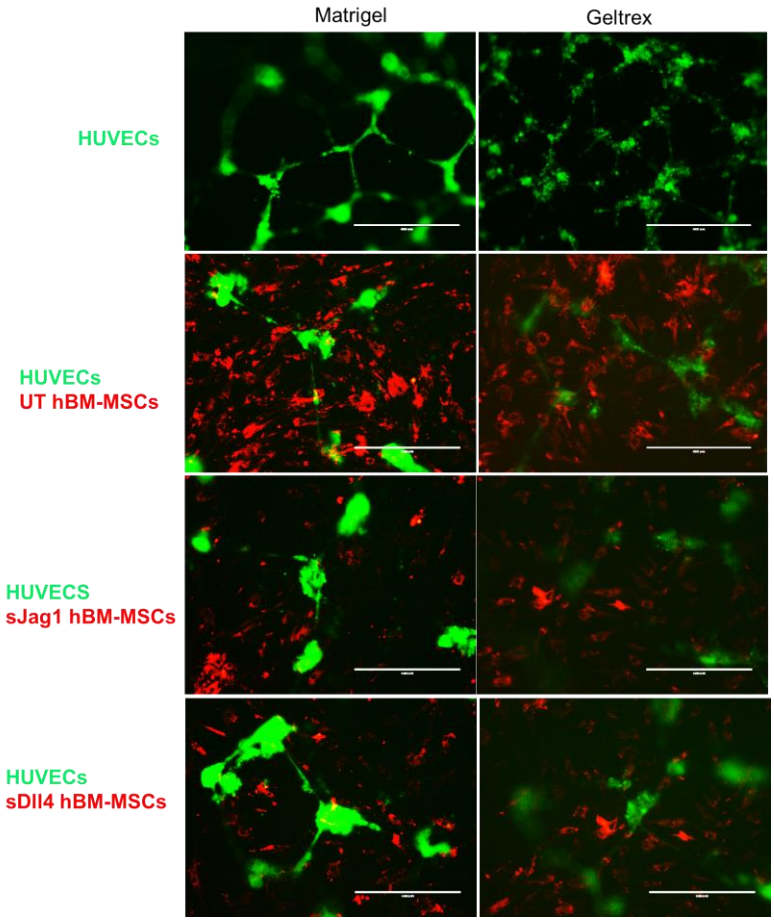

Figure 5-23: Vessel formation in support assays after 18 hours of seeding P10 HUVECs (green cells) on top of the commercial PDL14 hBM-MSCs (red cells) stacked with either Matrigel or Geltrex and previously left untreated or primed with either sJag1 or sDll4. HUVECs-only positive controls were run in parallel. Scale bars = 400 µm.

The phase contrast images in Figure 5-24 showed that network formation and vessel length in the support assays (see UT, sJag1, and sDll4; Figure 5-24 B and C) was similar to that of the control groups (see HUVECs; Figure 5-24 A).

Branches appeared to be more robust when using the normoxic hBM-MSCs (Figure 5-24 B)

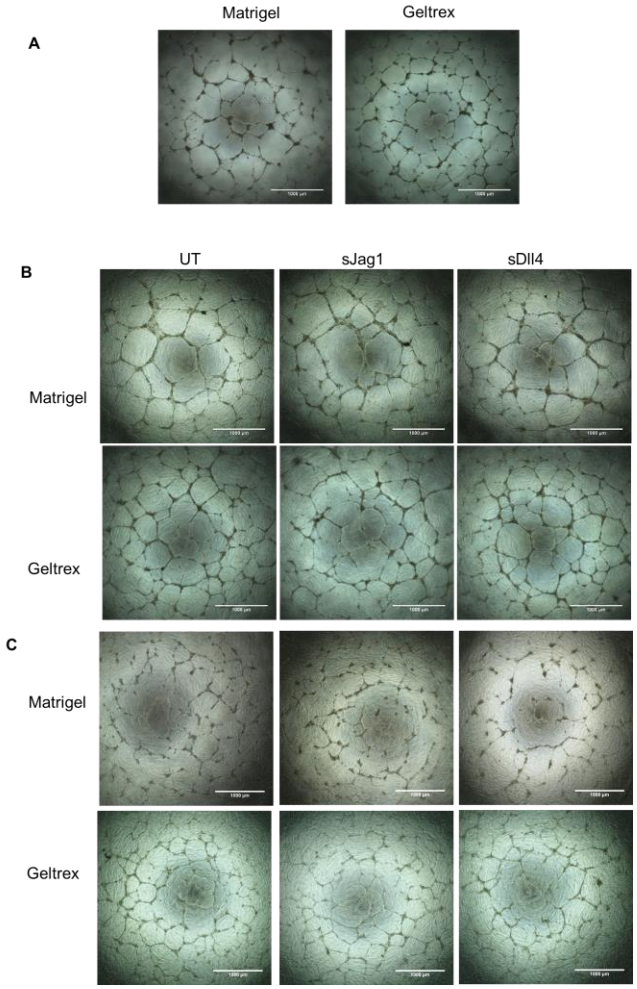

Figure 5-24: Phase contrast representative images of (A) HUVECs-only control groups (B) support assays using normoxic hBM-MSCs and (C) support assays using hypoxic hBM-MSCs. Scale bars = 1000 µm.

One aim of the support assays was to assess if priming the hBM-MSCs with sJag1 or sDll4 was going to enhance the secretion of paracrine factors that could further promote enhanced angiogenesis in the overlying endothelial cells. Another aim of this work was to compare the performance of Geltrex over Matrigel to promote efficient tubule formation which was quantified in terms of the number of branch points. The study also compared the effect of expanding hBM-MSCs in low oxygen (2% O_2) on their ability to support angiogenesis. The results indicated that there appeared to be no obvious differences between the experiments that were carried out using either normoxic hMSCs or hypoxic hMSCs (see black bars versus white bars, Figure 5-25). Furthermore, the differences between the normoxic and the hypoxic hBM-MSCs might have been decreased by running the

support assays at 2% O_2 for 18 hours hence by this point the normoxic hBM-MSCs could have been affected by the low oxygen conditions. However, there was a trend where more branch points formed on Geltrex over Matrigel when using hypoxic hBM-MSCs (see black bars versus white bars, Figure 5-25). GFR Geltrex comes at a consistent protein concentration of 15 mg/ml (Life Technologies, Paisley UK) whilst the protein concentration for GFR Matrigel ranges from 8-12 mg/ml (BD Biosciences, Maryland USA) and it is batch specific. For this reason, the slightly lower concentration of Matrigel could have led to differences between the two matrices.

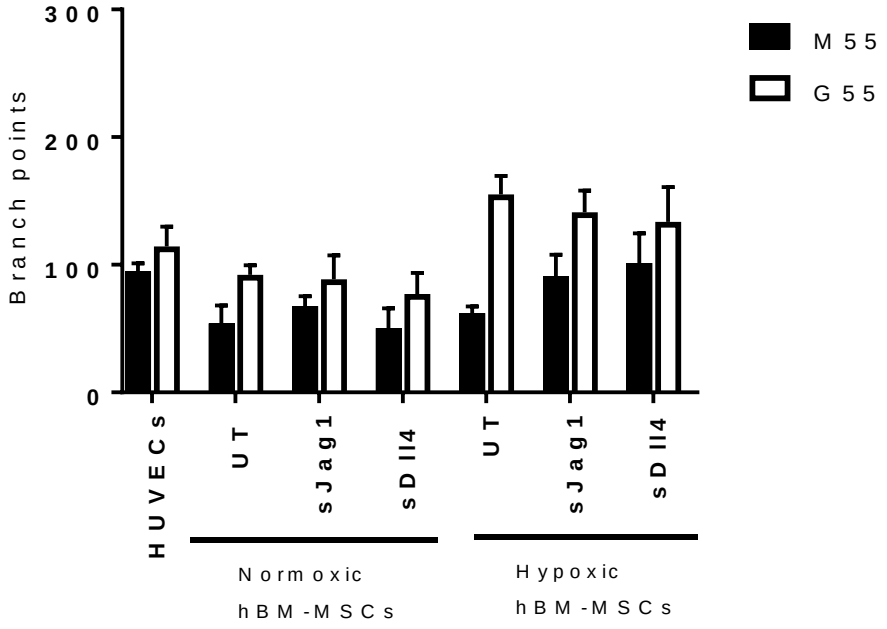

Figure 5-25: Branch point quantification of vascular support by commercial PDL14 hBM-MSCs previously cultured under hypoxic (2% O_2) or normoxic (20% O_2) conditions followed by priming with either sJag1, sDll4 or left untreated (UT). Error bars represent the mean ± SEM of n = 3 independent experimental repeats carried out using different hBM-MSC batches derived from the same donor.

5.4: Discussion

In the current work, qPCR was carried to compare differences in expression of Notch ligand genes between hypoxic and normoxic hMSCs (Figure 5-4, Figure 5-5 and Figure 5-6). The findings from this study showed an increase in the level of Notch signalling and its downstream gene HES1 by hypoxia, in individual donor hBM-MSCs primed with either sDll4 or sJag1 (Figure 5-4 C and D). This was in line with previous work which showed that culturing MSCs in low oxygen was linked with an increase in the expression of its downstream gene HES1 (Moriyama et al., 2014) or its ligands which included JAG1 and DLL4 (Gonzalez-King et al., 2017). These findings were also in line with previous work on hBM-MSCs (Detela, 2014) which indicated that the soluble forms of Dll4 and Jag1 stimulate Notch signalling better at 2% O_2 than at 20% O_2. The upregulation of HES1 was also evident in hypoxic commercial hBM-MSCs (Figure 5-5 C). However, this trend was not observed for the hUC-MSCs where low oxygen appeared to have no effect or downregulate the expression of JAG1, DLL4, HES1 and HEY1 (Figure 5-6 B-E). More experiments will need to be carried out to make strong conclusions on the upregulation of Notch signalling by hypoxia.

Several studies looked into the effect of hypoxia on hBM-MSCs however, not as much work has been carried out on hUC-MSCs (Lavrentieva et al., 2010; Griffon et al., 2016). The current work indicated that the effect of hypoxia and priming with Notch ligands on hMSCs may be source-specific. In support of this finding, some studies showed that umbilical cord hMSCs displayed metabolic differences in response to hypoxia when compared to hBM-MSCs. For example, even though hUC-MSCs were previously shown to increase metabolism and hence lactate production from glucose in response to hypoxia, these were reported to be significantly lower than those observed in hBM-MSCs and adipose-derived MSCs (Lavrentieva et al., 2010). Although it may be true that the effect of hypoxia on MSCs may be source-specific, previous studies reported an increase in mRNA expression levels of HIF1 in hUC-MSCs which is known to regulate the expression of the Notch signalling pathway (Lavrentieva et al., 2010; Ejtehadifar et al., 2015). However, this trend was not observed in this study and no clear trend was observed for the effect of hypoxia on HIF1 expression (Figure 5-6 A). Furthermore, in terms of process optimization, cells

could be expanded in low oxygen for more than two passages since the effects of hypoxia on hMSCs have been shown to be also time-dependent (Bain et al., 2014; Ding et al., 2014).

The variability in the qPCR experiments made it difficult to make clear conclusions. Variability in the experiments may be linked to variations in the master mix preparation and differences in the volume of cDNA added as volumes in PCR are small. For this reason, future work could include more qPCR experiments to confirm the qPCR results. In addition, other methods such as western blot could be investigated to make a comparative analysis.

Previous studies have reported that hMSCs may have a pericyte-like role (Crisan et al., 2008). For example, in one study pericytes were recovered from different organs such as the placenta or adipose tissue and they were shown to exhibit osteogenic, chondrogenic and adipogenic potential, they expressed MSC markers and they were myogenic in culture (Crisan et al., 2008). These findings indicated that pericytes might be giving origin to MSCs or that MSCs may in fact be pericytes (Crisan et al., 2008).

The current work was in line with the findings of Crisan et al., 2008 as hMSCs appeared to co-localize with the endothelial cells at the periphery of the vessels, bridging between and around the capillary-like structures (Figure 5-10-Figure 5-13). Moreover, this study suggested that similarly to pericytes, hMSCs might have a role in modulating vascular network formation through direct physical contact and paracrine signalling. hMSCs are known to release several growth factors including platelet-derived growth factor (PDGF), transforming growth factor (TGF-β) and vascular endothelial growth factor (VEGF) which are known to promote angiogenesis (Shi et al., 2012; Tao et al., 2016).

Both individual donor and commercial hBM-MSCs appeared to have a role in modulating vessel formation in the co-culture assays (fluorescence staining images Figure 5-9, Figure 5-10, Figure 5-11 and Figure 5-12; phase contrast images Figure 5-14 and Figure 5-18). The results for the hBM-MSCs were in line with previous work which showed that when HUVECs were co-cultured with the hBM-MSCs there was still the formation of vascular networks (Menge et al.,

2012). The data in Figure 5-15 and Figure 5-19 showed that the number of vessels formed in the co-culture assays was 2-3 fold lower than those formed in the HUVEC-only groups. Some studies hypothesized that the reduction in branch point formation in MSC:EC co-cultures may be due to the MSCs inhibiting endothelial cell proliferation and angiogenesis via physical contact (Menge et al., 2012). However, the significant reduction in branch points in the co-cultures can be attributed to the presence of only half of the HUVECs in the co-cultures with the other half being replaced by hMSCs. Previous gene expression studies indicated that MSCs cultured in direct contact with HUVECs differentiated towards a pericyte-like phenotype *in vitro* with the upregulation of the pericytes markers CD146, NG2, and αSMA (Loibl et al., 2014) therefore branch point quantification is not the only metric of vascular efficiency (Donovan et al., 2001).

Even though there were significantly fewer branch networks formed in co-culture assays compared to the HUVECs-only groups, the phase contrast images in Figure 5-14 and Figure 5-18 and the quantification data of average length for the individual donor hBM-MSCs (Figure 5-16), showed that the branches formed in the co-culture assays were more elongated than those formed when ECs alone were seeded on the gel-coated wells. This indicated that the branches formed in the co-culture assays more closely mimicked the capillaries in the *in vivo* environment. Next, the cumulative tubule length values in the co-culture assays for the individual donor hBM-MSCs (Figure 5-17 A and B) were similar to those of the HUVECs. This may be associated with the fact that the co-culture groups included only half of the HUVECs and the other half was the hBM-MSCs, hence the HUVECs-only groups were expected to form more branches than that of the co-cultures and this will have increased the values for the cumulative length.

The higher values of cumulative tubule length due to the addition of only half of the HUVECs in the co-cultures was more evident when using the commercial hBM-MSCs (Figure 5-21), this may be because they formed fewer branches than the individual donor hBM-MSCs.

The addition of hMSCs can be seen as one more factor to make the process of tubule formation *in vitro* more complex and closer to what it would be expected

in a physiological environment (Donovan et al., 2001). In terms of bioprocessing and optimized quality control testing, using co-culture *in vitro* tests as surrogate potency tests or in pre-clinical studies would be more beneficial because it would allow the screening of the molecules in an environment that more closely reflects the complexity of the *in vivo* milieu.

Next, both phase contrast and staining results for the P11 hUC-MSCs co-culture assays (Figure 5-13 and Figure 5-22) indicated that the stem cells appeared to hinder vessel formation rather than promoting the ECs to form vessel structures. The lack of vessel formation was observed in 8 experiments using two different hUC-MSC donors. This result was not expected as recent work showed that UC-MSCs have higher angiogenic abilities than hBM-MSCs (Shen et al., 2015). In addition, it has been shown that UC-MSC conditioned medium increases the lengths of the tubes formed in UC-MSC and HUVEC angiogenesis assays in comparison to BM-MSCs (Shen et al., 2015). Therefore, the lack of tubule formation in the UC-MSC co-cultures may be related to the ratio of MSC:HUVEC used in this study. More experiments will need to be carried out on a bigger number of donors, as outcomes in branching may be different between different populations of MSCs derived from the same source.

Next, commercial and individual donor hBM-MSCs displayed similar functionalities in co-culture assays. However, as only one or two donors were used in these experiments, there is also a need to test more donors to confirm these results.

In vitro co-culture and support assays include a lot variability because of the use of biological materials such as the media used, the cells and the matrices. For this reason, it was decided to test Geltrex and Matrigel side to side and see whether the former could also be used to replace Matrigel. The main components of Matrigel and Geltrex are laminin and collagen IV which are known to promote endothelial cell proliferation and differentiation (Stamati et al., 2014). However, Matrigel needs to be bought in bulk when carrying out experiments because there is a great deal of batch to batch variability and the relative concentration of different components can vary considerably, whilst Geltrex has been put on the market as an alternative due to more consistent

protein concentration lot-to-lot, which would reduce assay variability (Life Technologies, Paisley UK).

The current work showed that Geltrex worked as well as Matrigel for the co-culture assays (Figure 5-15, Figure 5-16, Figure 5-19 and Figure 5-20), whilst for the support assays there was a consistent trend of Geltrex forming more networks than Matrigel especially using the hypoxic hBM-MSCs, with the branch point values of Geltrex being almost two-fold higher than that of Matrigel. Furthermore, this study confirmed that Geltrex could be used in co-culture and vascular support assays as an alternative to Matrigel as part of assay optimization. In addition, Geltrex can be used at a 1 in100 dilution (Life Technologies, Paisley UK; Ulrich and Negraes, 2016), whereas Matrigel is typically used at a 1 in 30 dilution (BD Biosciences, Maryland USA; Gage et al., 2013). For this reason, more comparative support assays could be carried out to investigate the use of diluted GFR Matrigel and GFR Geltrex to reduce the interphase between the MSCs and the endothelial cells giving further insights into the vasculogenic potential of the stem cells and also to make the assays cheaper for future cell-therapy routine screening.

Capillaries *in vivo* are reported to consist of a single layer of ECs with occasional pericytes present in the basement membrane (Truskey, 2010). For this reason, reducing the interphase between MSCs and ECs could give more insights into the pericyte-like behaviour of hMSCs. In addition, the effect of the MSCs in the co-culture and the support assays could be further investigated by checking vessel-forming efficiency after 24 hours, one week and three weeks. In this way, it would be easier to see whether the presence of MSCs in the vascular assays has a beneficial effect in supporting angiogenesis. In the current work, hMSCs were expanded in 20% O_2 and 2% O_2 and the assays were performed in hypoxic conditions. The data for the individual-donor hBM-MSCs (Figure 5-15) is not in agreement with previous results which showed that hypoxia drives angiogenesis and the formation of capillary-like structures in MSCs (Annabi et al., 2003). The lack of differences between hypoxic and normoxic hMSCs might indicate that the cells previously cultured in ambient oxygen might have adapted to hypoxia during the 18 hours of incubation in the assays. In fact, based on previous studies from which this work was pursued, it

was observed that low oxygen may increase the vascular efficiency of MSC:HUVEC networks after 18 hours of incubation (Detela, 2014; Bain, 2014). On the other hand, the hypoxic preconditioning of commercial hBM-MSCs appeared to show positive outcomes especially on Geltrex (Figure 5-19 A, B, C and D). However, the large error bars in the results, suggest that more experiments will need to be performed to validate the results. In addition, as only one or two donors were used in these experiments, future work will need to include the use of a bigger number of hBM-MSC donors.

Future work could also look into culturing the hMSCs in a continuous normoxic or hypoxic environment to detect any differences. However, as part of assay development it would be beneficial to expand the hMSCs in a hypoxic environment to better mimic the physiological environment in which MSCs naturally reside in.

Following this, the current work also showed that Notch ligand pre-stimulation did not/modestly impacted on vascular efficiency compared to the untreated cells, even at low oxygen (Figure 5-15, Figure 5-16, Figure 5-19, Figure 5-20 and Figure 5-25). These results are contradictory to previous work, which indicated that when sJag1-treated individual donor hBM-MSCs were used in co-culture, these formed significantly higher branch networks than the untreated cells especially in hypoxia (Detela, 2014). The different trends observed between this study and previous studies (Detela, 2014), indicate that these assays may not be robust and that there is a need to further optimize them to obtain similar results between different users, as well as including SOPs that are more detailed where possible and introduce automation to avoid errors related to the user. As part of assay development, vascular assays could be performed in microfluidic devices that would enable 3D angiogenesis models and more accurately mimic the physiological environment. For example, by subjecting cells to shear stresses similar to those found *in vivo* (Zhang and Austin, 2012; Reichen et al., 2013) and this would significantly reduce the number of reagents used in the assays.

Chapter 6: Discussion and future work

6.1: Key findings, process development and limitations

The driving force behind developing *in vitro* potency assays that could closely reflect the physiologic environment was the current limitation associated with release assays such as ELISA and gene expression microarrays. In fact, such tests may not be able to address the complexity of the cell therapy product, they are time-consuming and they include a lot of variability due to the very low volumes, the dilutions involved and the long steps involved in obtaining the data (Leng et al., 2008). This work focused on the validation and optimization of *in vitro* tests that could give an indication of functional characteristics of hMSCs and endothelial tubule formation that may be useful in the clinical setting.

Comparative studies were carried out between MSCs derived from the bone marrow and the umbilical cord, as well as commercial hBM-MSCs cultured in their own High Performance Medium (<5% serum). Initially, the differently-sourced MSCs were characterized according to the ISCT guidelines which revealed that they were all able to undergo trilineage differentiation and that they expressed the positive MSC surface markers (>95%) and lacked the negative markers (<2%).

Next, *in vitro* static (adhesion assays) were carried out on fibronectin-coated surfaces in low/hypoxic (2% O_2) and ambient/normoxic (20% O_2) oxygen conditions. Due to limitations in the stocks of individual donor hBM-MSCs and hUC-MSCs, it was decided to carry out the dynamic (migration assays) only using the commercial hBM-MSCs. Comparative studies were carried out with commercial low serum hBM-MSCs expanded under hypoxic and normoxic conditions. Similarly to previous *in vitro* work that used individual donor hBM-MSCs (Detela, 2014) there was a trend where the cells primed with sJag1 showed higher adhesion than the UT and the sDll4 groups but differences were modest. These results unveil a major issue in assay development where the outcomes from different research groups can be majorly attributed to the different users performing the experiments. Therefore, there is a need for more detailed SOPs and automated methods that can standardize and make the processes

more robust by excluding user error. In addition, different results could also be attributed to inter-donor variability issues between BM-MSCs.

Contrarily to the initial hypothesis that changing the source of MSCs was not going to impact on cell adhesion, the results from chapter 3 showed that Jag-1 priming considerably enhanced the adhesion capabilities of the slightly-younger hUC-MSCs. In addition, the umbilical cord MSCs showed higher adhesion than those derived from an adult source. The higher engraftment capabilities of hUC-MSCs over bone marrow-derived MSCs were previously reported by other research groups (Acosta et al., 2013; Broxmeyer et al., 2003). However, since the adhesion assays for the differently-sourced MSCs were performed at different times this in itself might have contributed to different outcomes. In addition, one of the limitations of this study was that the umbilical cord MSC stocks arrived at higher passages than the hBM-MSCs, which meant that the outcomes from the experiments might have also resulted from different cell age. It is notable that the characterization studies reported no differences between the differently-sourced MSCs at the different passages, and therefore it may be beneficial to perform the experiments again in parallel using cells of similar age. Also, since only one or two donors were used, there is a need to perform further experiments using a bigger number of donors to confirm the results from these studies and to establish whether differences in adhesion and angiogenesis are attributed to inter-donor variability between MSC populations or the use of different cell source.

Next, a higher degree of variability was observed in the adhesion assays performed with the P6 individual donor hBM-MSCs compared to the slightly-younger cells. Moreover, from a manufacturing and process development perspective, the increase in cell heterogeneity observed in the older cells might have affected the consistency of the experimental data. Whilst, for the hUC-MSCs the slightly-older cells displayed less adherence to fibronectin when compared to the younger UC-MSCs. In support to the theory that sJag1 priming may be beneficial to MSC adhesion, the β-integrin staining experiments performed on commercial hBM-MSCs showed that the integrin β-1 / total integrin β-1 mean intensity was higher in sJag1 treated cells over the control groups.

Chapter 4 focused on using a methodological approach to identify key functions of endothelial tubule formation that could be used as the basis of the co-culture assays. The first aim was to test a series of variables that could impact on the abilities of endothelial cells to form tubules to then make the assays more cost-effective. The second aim was to find the best way to measure successful vascular formation and assess the effectiveness of automated counting techniques over manual measurements. The first aim was achieved by using Geltrex, a similar matrix to Matrigel that has the advantage of less variation lot-to-lot. In addition, lower matrix volumes were investigated to see whether they could induce efficient tubule formation or not and also reduce costs associated with performing the assays. The second aim was achieved by looking at different magnifications for branch counting. For example, the x2 magnification was able to show the whole well however, it was more difficult quantify the vessels and therefore it involved more inaccuracies especially for automated counting. For this reason, it was decided to take x4 magnification images instead and put them together through Panorama Pro. In order to avoid quantification issues due to the meniscus, the edges of the wells were excluded and a large area of the well was selected for quantification, this also made it easier to carry out the automated batch measurements.

The manual and automated comparative studies showed that although the latter would always give the same output and it followed the same trend as the manual counts, it was not efficient in separating debris from vessels and this might have accounted for a less consistent analysis. Ultimately, the automated counting method is advantageous for quantification as it is less time-consuming and there is no variation between repeated counts on the same image. However, there is a need to refine the system for it to recognize debris from tubules.

Next, the *in vitro* studies in chapter 5 demonstrated that the individual donor and commercial BM-MSCs displayed a pericyte-like behaviour in co-cultures, whilst this was not observed when using hUC-MSCs. It is possible that the functional differences observed between the hBM-MSCs and hUC-MSCs may be attributed to different populations of MSCs as only two donors were used for each or to the

different tissues of origin and cell age. In fact, the age of the hUC-MSCs (P11) may have contributed to a decrease in their angiogenic potential. It is notable, that the MSC/HUVEC ratio may not have been optimal for the umbilical cord MSCs. For example, the data in Appendix C showed that although the commercial hBM-MSCs formed branches at the MSC:HUVEC 1:1 ratio, increasing the ratio of the HUVECs to 1:4 showed a significant increase in networks. Similarly, the hUC-MSCs might have shown network formation by increasing the ratio of HUVECs in the co-cultures. One of the limitations in co-culture assays was the cell manipulation involved in achieving specific concentrations and the inherent biological variability of the reagents used such as Matrigel. This was particularly observed in the co-culture assays when using the commercial hBM-MSCs (Figure 5-18). In fact, these assays showed high variability between both technical and biological repeats even though the cells were derived from the same donor.

Since both umbilical cord and bone marrow-derived MSCs are found in low oxygen concentrations *in vivo*, it was decided to carry out comparative studies assessing differences in angiogenic potential between cells expanded in hypoxia and normoxia. The results in chapter 5, showed that hypoxic individual donor hBM-MSCs performed similarly to those expanded in normoxia. On the other hand, the co-culture and support assays for the commercial hBM-MSCs showed that cells expanded in low oxygen were generally performing better than those expanded under normoxic conditions. This suggests that hypoxia/HIF signalling pathway may be a key therapeutic target for vascular diseases. This data confirms that *in vitro* potency assays can give better insights into the mechanism of action of cell products. Overall, the findings from this study are fundamental bioprocess development data in the cell therapy industry and for the use of MSCs in clinics.

6.2: Future work

- Construct metabolic gene knockout mutants involving the deletion of one or more genes to assess the importance of signalling pathways. This work could also investigate the impact of different orders of gene deletion on the proliferation of MSCs and their angiogenesis, adhesion and migration abilities. Therefore, future work may involve constructing MSC strains with industrial relevance.
- This study showed that the expansion of MSCs in low oxygen after one passage did not have significant effects on the efficiency of the co-cultures and support assays. Further work could be carried out to assess the effect of long-term cell culture in low oxygen on the angiogenesis, migration, proliferation and surface marker expression of MSCs, since the effects of hypoxia on mesenchymal cells have been shown to be time dependent (Bain et al., 2014; Ding et al., 2014). Future work could also look into assessing the effect of a range of low oxygen conditions (e.g. 1% O_2, 2% O_2, 5% O_2, and 20% O_2) on the functional abilities of MSCs. In fact, different research groups have shown contrasting results due to differences in oxygen tension ranging from 0.1 to 5%, and different culture times ranging from a few minutes to 2 months (Bain et al., 2014; Basciano et al., 2011). In addition, the effect of hypoxia may also be source-specific (Lavrentieva et al., 2010). Therefore, comparative studies could be carried out to assess the effect of various oxygen conditions on the functionalities and characteristics of differently-sourced MSCs. A DOE approach could be used to investigate the interaction between key input variables and minimise the number of reagents used.
- The experiments performed in this study involved the use of hMSCs from one or two donors. Furthermore, future studies need to be performed on a bigger number of donors to confirm the differences observed in this study.
- The lack of tubule formation in the hUC-MSC:HUVEC co-cultures (chapter 5) suggests that although umbilical cord MSCs are very similar to those obtained from the bone marrow (Dalous et al., 2012) they may have different functional characteristics (Lavrentieva et al., 2010). For this reason, it is necessary to carry out further optimization work such as testing different MSC:HUVEC ratios for the differently-sourced MSCs. In

this way it would be possible to gain further understanding on the effect of MSCs cultured in direct contact with endothelial cells, the functional differences between MSCs from various sources and the optimal MSC:HUVEC ratio for tubule formation.

- More titration experiments will need to be performed to identify the optimum concentration range of sJag1 and sDll4 respectively for differently-sourced MSCs. hMSCs could also be pre-stimulated with sJag1 and sDll4 at the same time to see whether the combination of the two will affect the functional properties of these cells.
- Carry out comparative chemotaxis studies between differently-sourced MSCs and also assess the effect of other substrates other than fibronectin on cell migration.
- Investigate the impact of cryopreservation, cell age (much older and much younger MSCs) and seeding density on the functionality of differently-sourced MSCs.
- Carry out comparative studies between different users who will follow the same SOP to assess the impact of user error on the experiments and to identify the effect of biological reagents on the consistency of the results.
- Perform further optimization work using DOE by investigating lower matrix volumes to reduce assay costs or by diluting the matrices further. In addition, there is a need to optimize cell-seeding density in the co-culture assays to make sure that there are enough cells to contribute to adequate vessel formation at lower ratios.
- The tubule formation assays were performed using HUVECs with n = 3 donors. Future work could investigate a bigger number of donors and also test the functional differences between differently-sourced HUVECs.
- The studies performed with the commercial low serum hBM-MSCs have raised questions about the effectiveness of serum free media for cell expansion, migration and angiogenesis potential. In addition, one bottle of High Performance Medium costs £1379 with a shipping charge of £400 compared to DMEM medium, which costs £8 per bottle. Therefore, even though it is fundamental to reduce or eliminate serum for the reasons highlighted in section 1.4.2.1 the costs for the low serum RoosterBio Inc High Performance Medium need to be reduced, especially since the use of

medium for large scale applications may be high. Although the low serum medium has <5% FBS it is still boosted with various growth factors which can mask the effects of priming by candidate molecules. Chemically defined media can be used as a replacement to animal-derived media thus enabling for the complete removal of serum from small and large-scale processes (A. K.-L. Chen et al., 2013; Tekkatte et al., 2011). The components in serum-free media are usually basal media (e.g. DMEM) onto which is added albumin, transferrin, growth factors, attachment and spreading factors, hormones, lipoproteins and trace elements. Other alternatives to serum and serum-free media include human platelet lysate (hPL), autologous or allogeneic human blood-derived materials and umbilical cord blood serum (UCB). Human sourced media supplements seem to be viable alternatives to serum. However, they also present drawbacks for the successful expansion and therapeutic use of hMSCs. For example, the issues relating to batch-to-batch variation due to the inherent variability that is associated with using biological materials and the risk of contamination linked to the presence of human pathogenic agents in blood-derived alternatives. Future work could look into comparing the effects of different types of media.

- The automated method is more robust than the manual counting technique however, further work is required to refine it. For example, develop automated counting methods that can recognise cells from debris.
- Current *in vitro* migration and vascular assays do not precisely reflect the local environment *in vivo.* Moreover, they are not easy to control and they are time-consuming in terms of data analysis. Microfluidics may represent a more robust system to mimic the *in vivo* environment for example, by investigating the effect of static/flow conditions in MSC:HUVEC co-cultures in the microfluidic channels or by monitoring cell migration (Tanimura et al., 2013). Microfluidic platforms would enable the high throughput screening of several variables.
- *In vivo and ex vivo procedures* such as Langendorff could be used to assess the reliability of *the in vitro* assays and to assess the percentage of primed MSCs that have engrafted on the heart of murine or rats that have undergone a coronary ligation occlusion.

Chapter 7: References

Acosta, S.A., Franzese, N., Staples, M., Weinbren, N.L., Babilonia, M., Patel, J., Merchant, N., Simancas, A.J., Slakter, A., Caputo, M., Patel, M., Franyuti, G., Franzblau, M.H., Suarez, L., Gonzales-Portillo, C., Diamandis, T., Shinozuka, K., Tajiri, N., Sanberg, P.R., Kaneko, Y., Miller, L.W., Borlongan, C. V, 2013. Human umbilical cord blood for transplantation therapy in myocardial infarction. *Journal of Stem Cell Research and Therapy*, (Suppl. 4): S4-005.

Acquistapace, A., Bru, T., Lesault, P.F., Figeac, F., Coudert, A.E., Le Coz, O., Christov, C., Baudin, X., Auber, F., Ylou, R., Dubois-Randé, J.L., Anne-Marie, R., 2011. Human mesenchymal stem cells reprogram adult cardiomyocytes toward a progenitor-like state through partial cell fusion and mitochondria transfer. *Stem Cells*, 29 (5): 812-824.

Ades, E.W., C, F.J., Candal, F.J., Swerlick, R.A., George, V.G., Summers, S., Bosse, D.C., Lawley, T.J., 1992. HMEC-1: establishment of an immortalized human microvascular endothelial cell line. *Journal of Investigative Dermatology*, 99 (6): 683-690.

Allen, C.B., Schneider, B.K., White, C.W., 2001. Limitations to oxygen diffusion and equilibration in *in vitro* cell exposure systems in hyperoxia and hypoxia. *American Journal of Physiology Lung Cellular and Molecular Physiology*, 281 (4): L1021-L1027.

Alves, H., van Ginkel, J., Groen, N., Hulsman, M., Mentink, A., Reinders, M., van Blitterswijk, C., de Boer, J., 2012. A mesenchymal stromal cell gene signature for donor age. *PLoS One*, 7(8): e42908.

Amorin, B., Alegretti, A.P., Valim, V., Pezzi, A., Laureano, A.M., da Silva, M.A.L., Wieck, A., Silla, L., 2014. Mesenchymal stem cell therapy and acute graft-versus-host disease: a review. *Human Cell*, 27 (4): 137-150.

Armulik, A., Genové, G., Betsholtz, C., 2011. Pericytes: developmental, physiological, and pathological perspectives, problems, and promises. *Developmental Cell*, 21(2): 193-215.

Arnaoutova, I., George, J., Kleinman, H.K., Benton, G., 2009. The endothelial cell tube formation assay on basement membrane turns 20: state of the science and the art. *Angiogenesis*, 12(3): 267-274.

Arnaoutova, I., Kleinman, H.K., 2010. *In vitro* angiogenesis: endothelial cell tube formation on gelled basement membrane extract. *Nature Protocols*, 5(4): 628-635.

Arutyunyan, I., Elchaninov, A., Makarov, A., Fatkhudinov, T., 2016. Umbilical Cord as prospective source for mesenchymal stem cell-based therapy. *Stem Cells International*, 2016: 6901286.

Au, P., Tam, J., Fukumura, D., Jain, R.K., 2008. Bone marrow derived mesenchymal stem cells facilitate engineering of long-lasting functional vasculature. *Blood*, 111(9): 4551-4558.

Auerbach, R., Lewis, R., Shinners, B., Kubai, L., Akhtar, N., 2003. Angiogenesis assays: a critical overview. *Clinical Chemistry*, 49(1): 32-40.

Aziz, N., Nishanian, P., Mitsuyasu, R., Detels, R., Fahey, J.L., 1999. Variables that affect assays for plasma cytokines and soluble activation markers. *Clinical and Diagnostic Laboratory Immunology*, 6(1): 89-95.

Bain, O., Detela, G., Kim, H.-W., Mason, C., Mathur, A., Wall, I.B., 2014. Altered hMSC functional characteristics in short-term culture and when placed in low oxygen environments: implications for cell retention at physiologic sites. *Regenerative Medicine*, 9(2): 153-165.

Bain O. (2014). *In vitro* enhancement of retention and vascular support capacity of bone marrow derived stem cells for cardiac repair. (PhD thesis), University College London.

Bakhshi, T., Zabriskie, R.C., Bodie, S., Kidd, S., Ramin, S., Paganessi, L.A., Gregory, S.A., Fung, H.C., Christopherson, K.W., 2008. Mesenchymal stem cells from the Wharton's jelly of umbilical cord segments provide stromal support for the maintenance of cord blood hematopoietic stem cells during long-term *ex vivo* culture. *Transfusion*, 48(12): 2638-2644.

Ball, S.G., Bayley, C., Shuttleworth, C.A., Kielty, C.M., 2010. Neuropilin-1 regulates platelet-derived growth factor receptor signalling in mesenchymal stem cells. *Biochemical Journal*, 427(1): 29-40.

Balsam, L.B., Wagers, A.J., Christensen, J.L., Kofidis, T., Weissman, I.L., Robbins, R.C., 2004. Haematopoietic stem cells adopt mature haematopoietic fates in ischaemic myocardium. *Nature*, 428(6983): 668-673.

Bartunek, J., Behfar, A., Dolatabadi, D., Vanderheyden, M., Ostojic, M., Dens, J., El Nakadi, B., Banovic, M., Beleslin, B., Vrolix, M., Legrand, V., Vrints, C., Vanoverschelde, J.L., Crespo-Diaz, R., Homsy, C., Tendera, M., Waldman, S., Wijns, W., Terzic, A., 2013. Cardiopoietic stem cell therapy in heart failure: the C-CURE (cardiopoietic stem cell therapy in heart failURE) multicenter randomized trial with lineage-specified biologics. *Journal of the American College of Cardiology*, 61(23): 2329-2338.

Basciano, L., Nemos, C., Foliguet, B., de Isla, N., de Carvalho, M., Tran, N., Dalloul, A., 2011. Long term culture of mesenchymal stem cells in hypoxia promotes a genetic program maintaining their undifferentiated and multipotent status. *BMC Cell Biology*, 12(1): 1-12.

Bartolucci J., Verdugo F.J., González P.L., Larrea R.E., Abarzua E., Goset C., Rojo P., Palma I., Lamich R., Pedreros P.A., Valdivia G., Lopez V.M., Nazzal C., Alcayaga-Miranda F., Cuenca J., Brobeck M.J., Patel A.N., Figueroa F.E., Khoury M., 2017. Safety and efficacy of the intravenous infusion of umbilical cord mesenchymal stem cells in patients with heart failure: a phase 1/2 randomized controlled trial (RIMECARD Trial [Randomized Clinical Trial of Intravenous Infusion Umbilical Cord Mesenchymal Stem Cells on Cardiopathy]). *Circulation Research*, 121(10): 1192-1204.

Beane, O.S., Fonseca, V.C., Cooper, L.L., Koren, G., Darling, E.M., 2014. Impact of aging on the regenerative properties of bone marrow-, muscle-, and adipose-derived mesenchymal stem/stromal cells. *PLoS One*, 9(12): e115963.

Becker, A. De, Riet, I. Van, 2016. Homing and migration of mesenchymal stromal cells: how to improve the efficacy of cell therapy? *World Journal of Stem Cells*, 8(3): 73-87.

Benedito, R., Roca, C., Sörensen, I., Adams, S., Gossler, A., Fruttiger, M., Adams, R.H., 2009. The Notch ligands Dll4 and Jagged1 have opposing effects on angiogenesis. *Cell*, 137(6): 1124-1135.

Berger, M., Bergers, G., Arnold, B., Hämmerling, G.J., Ganss, R., 2005. Regulator of G-protein signaling-5 induction in pericytes coincides with active vessel remodeling during neovascularization. *Blood*, 105(3): 1094-1101.

Bishop, E.T., Bell, G.T., Bloor, S., Broom, I.J., Hendry, N.F., Wheatley, D.N., 1999. An i*n vitro* model of angiogenesis: basic features. *Angiogenesis*, 3(4): 335-344.

Blocki, A., Wang, Y., Koch, M., Peh, P., Beyer, S., Law, P., Hui, J., Raghunath, M., 2013. Not all MSCs can act as pericytes: functional *in vitro* assays to distinguish pericytes from other mesenchymal stem cells in angiogenesis. *Stem Cells and Development*, 2(17): 2347-2355.

Bravery, C.A., Carmen, J., Fong, T., Oprea, W., Hoogendoorn, K.H., Woda, J., Burger, S.R., Rowley, J.A., Bonyhadi, M.L., Van'T Hof, W., 2013. Potency assay development for cellular therapy products: An ISCT* review of the requirements and experiences in the industry. *Cytotherapy*, 5(1): 9-19.

Broxmeyer, H.E., Srour, E.F., Hangoc, G., Cooper, S., Anderson, S.A., Bodine, D.M., 2003. High-efficiency recovery of functional hematopoietic progenitor and stem cells from human cord blood cryopreserved for 15 years. *Proceedings of the National Academy of Sciences of the United States of America*, 100(2): 645-650.

Bruna, F., Contador, D., Conget, P., Erranz, B., Sossa, C.L., Arango-Rodríguez, M.L., 2016. Regenerative potential of mesenchymal stromal cells: age-related changes. *Stem Cells International*, 2016: 1461648.

Bryder, D., Rossi, D.J., Weissman, I.L., 2006. Hematopoietic stem cells: the paradigmatic tissue-specific stem cell. The American Journal of Pathology, 169(2): 338-346.

Burchfield, J.S., Xie, M., Hill, J.A., 2013. Pathological ventricular remodeling: mechanisms: part 1 of 2*. Circulation*, 128(4): 388-400.

Calderon, G.A., Thai, P., Hsu, C.W., Grigoryan, B., Gibson, S.M., Dickinson, M.E., Miller, J.S., 2017. Tubulogenesis of co-cultured human iPS-derived endothelial cells and human mesenchymal stem cells in fibrin and gelatin methacrylate gels. *Biomaterial Science*, 5(8): 1652-1660.

Cao, Y., Gong, Y., Liu, L., Zhou, Y., Fang, X., Zhang, C., Li, Y., Li, J., 2017. The use of human umbilical vein endothelial cells (HUVECs) as an in vitro model to assess the toxicity of nanoparticles to endothelium: a review. *Journal of Applied Toxicology*, 37(12): 1359-1369.

Cao, Z., Zhang, G., Wang, F., Liu, H., Liu, L., Han, Y., Zhang, J., Yuan, J., 2013. Protective effects of mesenchymal stem cells with CXCR4 up-regulation in a rat renal transplantation model. *PLoS One*, 8(12): e82949.

Caplan, A.I., 2007. Adult mesenchymal stem cells for tissue engineering versus regenerative medicine. *Journal of Cellular Physiology*, 213(2): 341-347.
Caplan, A.I., Correa, D., 2011. The MSC: an injury drugstore. *Cell Stem Cell*, 9(1): 11-5.

Carmeliet, P., Jain, R.K., 2011. Molecular mechanisms and clinical applications of angiogenesis. *Nature*, 473(7347): 298-307.

Carmen, J., Burger, S.R., McCaman, M., Rowley, J. a, 2012. Developing assays to address identity, potency, purity and safety: cell characterization in cell therapy process development. *Regenerative Medicine*, 7(1): 85-100.

Cashman, T.J., Gouon-Evans, V., Costa, K.D., 2013. Mesenchymal stem cells for cardiac therapy: practical challenges and potential mechanisms. *Stem Cell Rev*, 9(3): 254-265.

Chang, D., Shimizu, T., Haraguchi, Y., Gao, S., Sakaguchi, K., Umezu, M., Yamato, M., Liu, Z., Okano, T., 2015. Time course of cell sheet adhesion to porcine heart tissue after transplantation. *PLoS One*, 10(10): e0137494.

Chen, A.K.-L., Reuveny, S., Oh, S.K.W., 2013. Application of human mesenchymal and pluripotent stem cell microcarrier cultures in cellular therapy: achievements and future direction. *Biotechnology Advances*, 31(7): 1032-1046.

Chen, G., Yue, A., Ruan, Z., Yin, Y., Wang, R., Ren, Y., Zhu, L., 2014. Human umbilical cord-derived mesenchymal stem cells do not undergo malignant transformation during long-term culturing in serum-free medium. *PLoS One*, 9(6): e98565.

Chen, M.-Y., Lie, P.-C., Li, Z.-L., Wei, X., 2009. Endothelial differentiation of Wharton's jelly–derived mesenchymal stem cells in comparison with bone marrow–derived mesenchymal stem cells. *Experimental Hematology*, 37(5): 629-640.

Chen, S., Fang, W., Ye, F., Liu, Y.-H., Qian, J., Shan, S., Zhang, J., Chunhua, R.Z., Liao, L., Lin, S., Sun, J., 2004. Effect on left ventricular function of intracoronary transplantation of autologous bone marrow mesenchymal stem cell in patients with acute myocardial infarction. *American Journal of Cardiology*, 94(1): 92-95.

Chen, Z., Wen, Z., Bai, X., 2013. In vivo Chick Chorioallantoic Membrane (CAM) angiogenesis assays. *Bio-Protocol*, 3(18): 1-5.

Chimenti, I., Smith, R.R., Li, T.S., Gerstenblith, G., Messina, E., Giacomello, A., Marbán, E., 2010. Relative roles of direct regeneration versus paracrine effects of human cardiosphere-derived cells transplanted into infarcted mice. *Circulation Research*, 106(5): 971-980.

Chin, B.B., Nakamoto, Y., Bulte, J.W.M., Pittenger, M.F., Wahl, R., Kraitchman, D.L., 2003. 111In oxine labelled mesenchymal stem cell SPECT after intravenous administration in myocardial infarction. *Nuclear Medicine Communications*, 24(11): 1149-1154.

Choi, J.S., Lee, B.J., Park, H.Y., Song, J.S., Shin, S.C., Lee, J.C., Wang, S.G., Jung, J.S., 2015. Effects of donor age, long-term passage culture, and cryopreservation on tonsil-derived mesenchymal stem cells. *Cellular Physiology and Biochemistry*, 36(1): 85-99.

Ciria, M., García, N.A., Ontoria-Oviedo, I., González-King, H., Carrero, R., De La Pompa, J.L., Montero, J.A., Sepúlveda, P., 2017. Mesenchymal stem cell migration and proliferation are mediated by hypoxia-inducible factor-1α upstream of Notch and SUMO Pathways. *Stem Cells and Development*, 26(13): 973-985.

Crisan, M., Corselli, M., Chen, W.C.W., Pe, B., 2012. Perivascular cells for regenerative medicine. *Journal of Cellular and Molecular Medicine*, 16 (12): 2851-2860.

Crisan, M., Yap, S., Casteilla, L., Chen, C.W., Corselli, M., Park, T.S., Andriolo, G., Sun, B., Zheng, B., Zhang, L., Norotte, C., Teng, P.N., Traas, J., Schugar, R., Deasy, B.M., Badylak, S., Buhring, H.J., Giacobino, J.P., Lazzari, L., Huard, J., Péault, B., 2008. A perivascular origin for mesenchymal stem cells in multiple human organs. *Cell Stem Cell*, 3(3): 301-313.

De Becker, A., Riet, I. Van, 2016. Homing and migration of mesenchymal stromal cells: How to improve the efficacy of cell therapy? *World Journal of Stem Cells*, 8(3): 73-87.

de Witte, S.F.H., Lambert, E.E., Merino, A., Strini, T., Douben, H.J.C.W., O'Flynn, L., Elliman, S.J., de Klein, A.J.E.M.M., Newsome, P.N., Baan, C.C., Hoogduijn, M.J., 2017. Aging of bone marrow– and umbilical cord–derived mesenchymal stromal cells during expansion. *Cytotherapy*, 19(7): 798-807.

DeCicco-Skinner, K.L., Henry, G.H., Cataisson, C., Tabib, T., Gwilliam, J.C., Watson, N.J., Bullwinkle, E.M., Falkenburg, L., O'Neill, R.C., Morin, A., Wiest, J.S., 2014. Endothelial cell tube formation assay for the *in vitro* study of angiogenesis. *Journal of Visualized Experiments*, (91): e51312.

Detela G. (2014). Enhancing functional responses of MSCs for ischemic injury using *ex vivo* pre-conditioning strategies. (PhD thesis), University College London.

Detela, G., Bain, O.W., Kim, H.W., Williams, D.J., Mason, C., Mathur, A., Wall, I.B., 2018. Donor variability in growth kinetics of healthy hMSCs using manual processing: Considerations for manufacture of cell therapies. *Biotechnology Journal*, 13(2): 1700085.

Dettmer, K., Aronov, P.A., Hammock, B.D., 2007. Mass spectrometry-based metabolomics. *Mass Spectrometry Reviews*, 26(1): 51-78.

Deveza, L., Choi, J., Yang, F., 2012. Therapeutic angiogenesis for treating cardiovascular diseases. *Theranostics*, 2(8): 801-814.

Dobaczewski, M., Gonzalez-Quesada, C., Frangogiannis, N.G., 2010. The extracellular matrix as a modulator of the inflammatory and reparative response following myocardial infarction. *Journal of Molecular and Cellular Cardiology*, 48(3): 504-511.

Dominici, M., Le Blanc, K., Mueller, I., Slaper-Cortenbach, I., Marini, F., Krause, D., Deans, R., Keating, a, Prockop, D., Horwitz, E., 2006. Minimal criteria for defining multipotent mesenchymal stromal cells. The International Society for Cellular Therapy position statement. *Cytotherapy*, 8(4): 315-317.

Donnelly, R., Manning, G., 2007. Angiotensin-converting enzyme inhibitors and coronary heart disease prevention. *Journal of the Renin-Angiotensin-Aldosterone System*, 8(1): 13-22.

Donovan, D., Brown, N.J., Bishop, E.T., Lewis, C.E., 2001. Comparison of three *in vitro* human 'angiogenesis' assays with capillaries formed *in vivo*. *Angiogenesis*, 4(2): 113-121.

Dowell, J.D., Rubart, M., Pasumarthi, K.B.S., Soonpaa, M.H., Field, L.J., 2003. Myocyte and myogenic stem cell transplantation in the heart. *Cardiovascular Research*, 58(2): 336-350.

Eckert, M. a, Vu, Q., Xie, K., Yu, J., Liao, W., Cramer, S.C., Zhao, W., 2013. Evidence for high translational potential of mesenchymal stromal cell therapy to improve recovery from ischemic stroke. J*ournal of Cerebral Blood Flow and Metabolism*, 33(9): 1322-1334.

Elnakish, M.T., Hassan, F., Dakhlallah, D., Marsh, C.B., Alhaider, I.A., Khan, M., 2012. Mesenchymal stem cells for cardiac regeneration: translation to bedside reality. *Stem Cells International*, 2012: 646038.

Erickson, G.A., Bolin, S.R., Landgraf, J.G., 1991. Viral contamination of fetal bovine serum used for tissue culture: risks and concerns. *Developments in Biological Standardization*, 75: 173-175.

Escobedo-Lucea, C., Bellver, C., Gandia, C., Sanz-Garcia, A., Esteban, F.J., Mirabet, V., Forte, G., Moreno, I., Lezameta, M., Ayuso-Sacido, A., Garcia-Verdugo, J.M., 2013. A Xenogeneic-free protocol for isolation and expansion of human adipose stem cells for clinical uses. *PLoS One*, 8(7): e67870.

European Medicines Agency, 2016. Guideline on potency testing of cell based immunotherapy medicinal products for the treatment of cancer. *European Medicine Agency*, 44:1-8.

Ezquer, F.E., Ezquer, M.E., Vicencio, J.M., Calligaris, S.D., 2017. Two complementary strategies to improve cell engraftment in mesenchymal stem cell-based therapy: increasing transplanted cell resistance and increasing tissue receptivity. *Cell Adhesion and Migration*, 11(1): 110-119.

Faulkner, A., Purcell, R., Hibbert, A., Latham, S., Thomson, S., Hall, W.L., Wheeler-Jones, C., Bishop-Bailey, D., 2014. A thin layer angiogenesis assay: a modified basement matrix assay for assessment of endothelial cell differentiation. *BMC Cell Biology*, 15(41): 1-9.

Food and Drug Administration CDER, Guidance for Industry Q8 (R2) Pharmaceutical Development, Rockville, 2009.

Food and Drug Administration. Final report on pharmaceutical cGMPs for the 21st century – A risk based approach, Rockville, 2004.

Food and Drug Administration. Guidance for industry. PAT – A framework for innovative pharmaceutical manufacturing and quality assurance. Pharmaceutical cGMPs. Rockville, 2004.

Fortier, L.A., Travis, A.J., 2011. Stem cells in veterinary medicine. *Stem Cell Research and Therapy*, 2(9): 1-6.

Fraisl, P., Mazzone, M., Schmidt, T., Carmeliet, P., 2009. Regulation of angiogenesis by oxygen and metabolism. *Developmental Cell*, 16(2): 167-179.

Furtado, M.B., Nim, H.T., Boyd, S.E., Rosenthal, N.A., 2016. View from the heart: cardiac fibroblasts in development, scarring and regeneration. *Development*, 143(3): 387-397.

Gallery, E.D.M., Rowe, J., Schrieber, L., Jackson, C.J., 1991. Isolation and purification of microvascular endothelium from human decidual tissue in the late phase of pregancy. *American Journal of Obstetrics and Gynecology*, 165(1): 191-196.

Gambino, T.J., Williams, S.P., Caesar, C., Resnick, D., Nowell, C.J., Farnsworth, R.H., Achen, M.G., Stacker, S.A., Karnezis, T., 2017. A three-dimensional lymphatic endothelial cell tube formation assay to identify novel kinases involved in lymphatic vessel remodeling. *Assay Drug Development Technologies*, 15(1): 30-43.

Gan, S.D., Patel, K.R., 2013. Enzyme immunoassay and enzyme-linked immunosorbent assay. *Journal of Investigative Dermatology*, 133(9): e12.

Gao, L.R., Chen, Y., Zhang, N.K., Yang, X.L., Liu, H.L., Wang, Z.G., Yan, X.Y., Wang, Y., Zhu, Z.M., Li, T.C., Wang, L.H., Chen, H.Y., Chen, Y.D., Huang, C.L., Qu, P., Yao, C., Wang, B., Chen, G.H., Wang, Z.M., Xu, Z.Y., Bai, J., Lu, D., Shen, Y.H., Guo, F., Liu, M.Y., Yang, Y., Ding, Y.C., Yang, Y., Tian, H.T., Ding, Q.A., Li, L.N., Yang, X.C., Hu, X., 2015. Intracoronary infusion of Wharton's jelly-derived mesenchymal stem cells in acute myocardial infarction: double-blind, randomized controlled trial. *BMC Medicine*, 13: 162.

Gnecchi, M., Danieli, P., Cervio, E., 2012. Mesenchymal stem cell therapy for heart disease. *Vascular Pharmacology*, 57(1): 48-55.

Govindasamy, V., Ronald, V.S., Abdullah, A.N.B., Ganesan Nathan, K.R., Aziz, Z.A.C.A., Abdullah, M., Zain, R.B., Kasim, N.H.A., Musa, S., Bhonde, R.R., 2011. Human platelet lysate permits scale-up of dental pulp stromal cells for clinical applications. *Cytotherapy*, 13(10): 1221-1233.

Gridley, T., 2010. Notch signaling in the vasculature. *Current Topics in Developmental Biology*, 92: 277-309.

Guedez, L., Rivera, A.M., Salloum, R., Miller, M.L., Diegmueller, J.J., Bungay, P.M., Stetler-Stevenson, W.G., 2003. Quantitative assessment of angiogenic responses by the directed *in vivo* angiogenesis assay. *The American Journal of* Pathology, 162(5): 1431-1439.

Hare, J.M., Fishman, J.E., Gerstenblith, G., DiFede Velazquez, D.L., Zambrano, J.P., Suncion, V.Y., Tracy, M., Ghersin, E., Johnston, P. V., Brinker, J.A., Breton, E., Davis-Sproul, J., Schulman, I.H., Byrnes, J., Mendizabal, A.M., Lowery, M.H., Rouy, D., Altman, P., Wong Po Foo, C., Ruiz, P., Amador, A., Da Silva, J., McNiece, I.K., Heldman, A.W., 2012. Comparison of allogeneic vs autologous bone marrow-derived mesenchymal stem cells delivered by transendocardial injection in patients with ischemic cardiomyopathy: The POSEIDON randomized trial. *The Journal of American Medical Association*, 308(22): 2369-2379.

Hass, R., Kasper, C., Böhm, S., Jacobs, R., 2011. Different populations and sources of human mesenchymal stem cells (MSC): A comparison of adult and neonatal tissue-derived MSC. *Cell Communication and Signaling*, 9(12): 1-14.

Hassan, S., Simaria, A.S., Varadaraju, H., Siddharth, G., Warren, K., Farid, S.S., Gupta, S., Warren, K., Farid, S.S., 2015. Allogeneic cell therapy bioprocess economics and optimization: downstream processing decisions. *Regenerative Medicine*, 10(5): 591-609.

Haudek, S.B., Xia, Y., Huebener, P., Lee, J.M., Carlson, S., Crawford, J.R., Pilling, D., Gomer, R.H., Trial, J., Frangogiannis, N.G., Entman, M.L., 2006. Bone marrow-derived fibroblast precursors mediate ischemic cardiomyopathy in mice. *Proceedings of the National Academy of Sciences of the United States of America*, 103(48): 18284-18289.

Herrmann, M., Bara, J.J., Sprecher, C.M., Menzel, U., Jalowiec, J.M., Osinga, R., Scherberich, A., Alini, M., Verrier, S., 2016. Pericyte plasticity – comparative investigation of the angiogenic and multilineage potential of pericytes from different human tissues. *European Cells and Materials*, 31: 236-249.

Holzwarth, C., Vaegler, M., Gieseke, F., Pfister, S.M., Handgretinger, R., Kerst, G., Müller, I., 2010. Low physiologic oxygen tensions reduce proliferation and differentiation of human multipotent mesenchymal stromal cells. *BMC Cell Biology*, 11: 11.

Horwitz, E.M., Gordon, P.L., Koo, W.K., Marx, J.C., Neel, M.D., McNall, R.Y., Muul, L., Hofmann, T., 2002. Isolated allogeneic bone marrow-derived mesenchymal cells engraft and stimulate growth in children with osteogenesis imperfecta: Implications for cell therapy of bone. *Proceedings of the National Academy of Sciences of the United States of America*, 99(13): 8932-8937.

Hourd, P., Ginty, P., Chandra, A., Williams, D.J., 2014. Manufacturing models permitting roll out/scale out of clinically led autologous cell therapies: regulatory and scientific challenges for comparability. *Cytotherapy*, 16(8): 1033-1047.

Houtgraaf, J.H., Den Dekker, W.K., Van Dalen, B.M., Springeling, T., De Jong, R., Van Geuns, R.J., Geleijnse, M.L., Fernandez-Aviles, F., Zijlsta, F., Serruys, P.W., Duckers, H.J., 2012. First experience in humans using adipose tissue-derived regenerative cells in the treatment of patients with ST-segment elevation myocardial infarction. *Journal of the American College of Cardiology*, 59(5): 539-540.

Huang, L., Niu, C., Willard, B., Zhao, W., Liu, L., He, W., Wu, T., Yang, S., Feng, S., Mu, Y., Zheng, L., Li, K., 2015. Proteomic analysis of porcine mesenchymal stem cells derived from bone marrow and umbilical cord: implication of the proteins involved in the higher migration capability of bone marrow mesenchymal stem cells. *Stem Cell Research & Therapy*, 6: 77.

Huang, S., Leung, V., Peng, S., Li, L., Lu, F.J., Wang, T., Lu, W., Cheung, K.M.C., Zhou, G., 2011. Developmental definition of MSCs: new insights into

pending questions. *Cellular Reprogramming*, 13(6): 465-472.

Hu, X., Huang, X., Yang, Q., Wang, L., Sun, J., Zhan, H., Lin, J., Pu, Z., Jiang, J., Sun, Y., Xiang, M., Liu, X., Xie, X., Yu, X., Chen, Z., Tse, H.F., Zhang, J., Wang, J., 2015. Safety and efficacy of intracoronary hypoxia-preconditioned bone marrow mononuclear cell administration for acute myocardial infarction patients: The CHINA-AMI randomized controlled trial. *International Journal of Cardiology*, 184: 446-451.

Ingber, D.E., 2002. Mechanical signaling and the cellular response to extracellular matrix in angiogenesis and cardiovascular physiology. *Circulation Research*, 91(10): 877-887.

Ishikawa, F., Shimazu, H., Shultz, L.D., Fukata, M., Nakamura, R., Lyons, B., Shimoda, K., Shimoda, S., Kanemaru, T., Nakamura, K.-I., Ito, H., Kaji, Y., Perry, A.C.F., Harada, M., 2006. Purified human hematopoietic stem cells contribute to the generation of cardiomyocytes through cell fusion. *The FASEB Journal*, 20(7): 950-952.

Jackson, C.J., Nguyen, M., 1997. Human microvascular endothelial cells differ from macrovascular endothelial cells in their expression of matrix metalloproteinases. *The International Journal of Biochemistry & Cell Biology*, 29(10): 1167-1177.

Jackson, K.A., Majka, S.M., Wang, H., Pocius, J., Hartley, C.J., Majesky, M.W., Entman, M.L., Michael, L.H., Hirschi, K.K., Goodell, M.A., 2001. Regeneration of ischemic cardiac muscle and vascular endothelium by adult stem cells. *Journal of Clinical Investigation*, 107(11): 1395-1402.

Jain, R.K., 2003. Molecular regulation of vessel maturation. Nat. Med., 9(6):685-93.

Janssens, S., Dubois, C., Bogaert, J., Theunissen, K., Deroose, C., Desmet, W., Kalantzi, M., Herbots, L., Sinnaeve, P., Dens, J., Maertens, J., Rademakers, F., Dymarkowski, S., Gheysens, O., Van Cleemput, J., Bormans, G., Nuyts, J., Belmans, A., Mortelmans, L., Boogaerts, M., Van De Werf, F., 2006. Autologous bone marrow-derived stem-cell transfer in patients with ST-segment elevation myocardial infarction: double-blind, randomised controlled trial. *The Lancet*, 367(9505): 113-121.

Jawad, H., Ali, N.N., Lyon, A.R., Chen, Q.Z., Harding, S.E., Boccaccini, A.R., 2007. Myocardial tissue engineering: a review. *Journal of Tissue Engineering and Regenerative Medicine*, 1(5): 327-342.

Jin, H.J., Bae, Y.K., Kim, M., Kwon, S.-J., Jeon, H.B., Choi, S.J., Kim, S.W., Yang, Y.S., Oh, W., Chang, J.W., 2013. Comparative analysis of human mesenchymal stem cells from bone marrow, adipose tissue, and umbilical cord blood as sources of cell therapy. *International Journal of Molecular Sciences*, 14(9): 17986-18001.

Jochems, C.E.A., Van der Valk, J.B.F., Stafleu, F.R., Baumans, V., 2002. The use of fetal bovine serum: ethical or scientific problem? *ATLA Alternatives to Laboratory Animals*, 30(2): 219-227.

Johnston, D.A., Dong, B., Hughes, C.C.W., 2009. TNF induction of jagged-1 in endothelial cells is NF-κB-dependent. *Gene*, 435(1-2): 36-44.

Kadam, S.S., Tiwari, S., Bhonde, R.R., 2009. Simultaneous isolation of vascular endothelial cells and mesenchymal stem cells from the human umbilical cord. *In Vitro Cellular & Developmental Biology - Animal*, 45 (1-2): 23-27.

Kamei, N., Atesok, K., Ochi, M., 2017. The use of endothelial progenitor cells for the regeneration of musculoskeletal and neural tissues. *Stem Cells International*, 2017: 1960804.

Kamihata, H., Matsubara, H., Nishiue, T., Fujiyama, S., Tsutsumi, Y., Ozono, R., Masaki, H., Mori, Y., Iba, O., Tateishi, E., Kosaki, A., Shintani, S., Murohara, T., Imaizumi, T., Iwasaka, T., 2001. Implantation of bone marrow mononuclear cells into ischemic myocardium enhances collateral perfusion and regional function via side supply of angioblasts, angiogenic ligands, and cytokines. *Circulation*, 104(9): 1046-1052.

Katz, A., 2011. Physiology of the heart, 25: 45-52. Philadelphia, USA: Lippincott Williams and Wilkins.

Katz, T.C., Singh, M.K., Degenhardt, K., Rivera-Feliciano, J., Johnson, R.L., Epstein, J.A., Tabin, C.J., 2012. Distinct compartments of the proepicardial organ give rise to coronary vascular endothelial cells. *Developmental Cell*, 22(3): 639-650.

Kawamoto, A., Tkebuchava, T., Yamaguchi, J.-I., Nishimura, H., Yoon, Y.-S., Milliken, C., Uchida, S., Masuo, O., Iwaguro, H., Ma, H., Hanley, A., Silver, M., Kearney, M., Losordo, D.W., Isner, J.M., Asahara, T., 2003. Intramyocardial transplantation of autologous endothelial progenitor cells for therapeutic neovascularization of myocardial ischemia. *Circulation*, 107(3): 461-468.

Kean, T.J., Lin, P., Caplan, A.I., Dennis, J.E., 2013. MSCs: delivery routes and engraftment, cell-targeting strategies, and immune modulation. *Stem Cells International*, 2013: 732742.

Kern, S., Eichler, H., Stoeve, J., Klüter, H., Bieback, K., 2006. Comparative analysis of mesenchymal stem cells from bone marrow, umbilical cord blood, or adipose tissue. *Stem Cells*, 24(5): 1294-1301.

Kirklin, J.K., Naftel, D.C., Kormos, R.L., Stevenson, L.W., Pagani, F.D., Miller, M.A., Baldwin, J.T., Timothy Baldwin, J., Young, J.B., 2013. Fifth INTERMACS annual report: risk factor analysis from more than 6,000 mechanical circulatory support patients. *The Journal of Heart and Lung Transplantation*, 32(2): 141-156.

Knepper, P.A., Mayanil, C.S., Goossens, W., McLone, D.C., Hayes, E., 1998. The presence of transcription factors in fetal bovine sera. *In Vitro Cellular & Developmental Biology – Animal*, 34(2): 170-173.

Koninckx, R., Hensen, K., Daniëls, A., Moreels, M., Lambrichts, I., Jongen, H., Clijsters, C., Mees, U., Steels, P., Hendrikx, M., Rummens, J.-L., 2009. Human bone marrow stem cells co-cultured with neonatal rat cardiomyocytes display limited cardiomyogenic plasticity. *Cytotherapy*, 11(6): 778-792.

Konstam, M. a, Rousseau, M.F., Kronenberg, M.W., Udelson, J.E., Melin, J., Stewart, D., Dolan, N., Edens, T.R., Ahn, S., Kinan, D., 1992. Effects of the angiotensin converting enzyme inhibitor enalapril on the long-term progression of left ventricular dysfunction in patients with heart failure. SOLVD Investigators. *Circulation*, 86(2): 431-438.

Korf-Klingebiel, M., Kempf, T., Sauer, T., Brinkmann, E., Fischer, P., Meyer, G.P., Ganser, A., Drexler, H., Wollert, K.C., 2008. Bone marrow cells are a rich source of growth factors and cytokines: implications for cell therapy trials after myocardial infarction. *European Heart Journal*, 29(23): 2851-2858.

Kouris, N.A., Schaefer, J.A., Hatta, M., Freeman, B.T., Kamp, T.J., Kawaoka, Y., Ogle, B.M., 2012. Directed fusion of mesenchymal stem cells with cardiomyocytes via VSV-G facilitates stem cell programming. *Stem Cells International*, 2012: 414038.

Kowsari, A., Jafarian, Z., Tabatabaei, R. Q., Sheikholeslami, A., Kalhor, N., Fazaeli, H., Sheykhhasan, M., 2017. *Stem Cell Research and Therapeutics*, 3(2): 00094.

Krock, B.L., Skuli, N., Simon, M.C., 2011. Hypoxia-induced angiogenesis: good and evil. *Genes Cancer*, 2(12): 1117-1133.

Kubo, H., Jaleel, N., Kumarapeli, A., Berretta, R.M., Bratinov, G., Shan, X., Wang, H., Houser, S.R., Margulies, K.B., 2008. Increased cardiac myocyte progenitors in failing human hearts. *Circulation*, 118(6): 649-657.

Kurtz, A., 2008. Mesenchymal stem cell delivery routes and fate. *International Journal of Stem Cells*, 1(1): 1-7.

Kusuma, S., Peijnenburg, E., Patel, P., Gerecht, S., 2014. Low oxygen tension enhances endothelial fate of human pluripotent stem cells. *Arteriosclerosis, Thrombosis, and Vascular Biology*, 34(4): 913-920.

Lalor, P.F., Lai, W.K., Curbishley, S.M., Shetty, S., Adams, D.H., 2006. Human hepatic sinusoidal endothelial cells can be distinguished by expression of phenotypic markers related to their specialised functions *in vivo*. *World Journal of Gastroenterology*, 12 (34): 5429–5439.

Lan, Y.-W., Choo, K.-B., Chen, C.-M., Hung, T.-H., Chen, Y.-B., Hsieh, C.-H., Kuo, H.-P., Chong, K.-Y., 2015. Hypoxia-preconditioned mesenchymal stem cells attenuate bleomycin-induced pulmonary fibrosis. *Stem Cell Research and Therapy*, 6(1): 97.

Lavrentieva, A., Majore, I., Kasper, C., Hass, R., 2010. Effects of hypoxic culture conditions on umbilical cord-derived human mesenchymal stem cells. *Cell Communication and Signaling*. 8 (18), 1-17.

Le Blanc, K., Tammik, L., Sundberg, B., Haynesworth, S.E., Ringdén, O., 2003. Mesenchymal stem cells inhibit and stimulate mixed lymphocyte cultures and mitogenic responses independently of the major histocompatibility complex. *Scandinavian Journal of Immunology*, 57(1): 11-20.

Lee, S., Choi, E., Cha, M.J., Hwang, K.C., 2015. Cell adhesion and long-term survival of transplanted mesenchymal stem cells: a prerequisite for cell therapy. *Oxidative Medicine and Cellular Longevity*, 2015: 632902.

Lemcke, H., Gaebel, R., Skorska, A., Voronina, N., Lux, C.A., Petters, J., Sasse, S., Zarniko, N., Steinhoff, G., David, R., 2017. Mechanisms of stem cell based cardiac repair-gap junctional signaling promotes the cardiac lineage specification of mesenchymal stem cells. *Scientific Reports*, 7(1): 9755.

Leng, S.X., McElhaney, J.E., Walston, J.D., Xie, D., Fedarko, N.S., Kuchel, G.A., 2008. ELISA and multiplex technologies for cytokine measurement in inflammation and aging research. *The journals of gerontology. Series A, Biological sciences and medical sciences*, 63(8): 879-884.

Li, H., Yu, B., Zhang, Y., Pan, Z., Xu, W., Li, H., 2006. Jagged1 protein enhances the differentiation of mesenchymal stem cells into cardiomyocytes. *Biochemical and Biophysical Research Communications*, 341(2): 320-325.

Li, N., Wang, C., Jia, L., Du, J., 2014. Heart regeneration, stem cells, and cytokines. *Regenerative Medicine*, 2(1): 1-6.

Li, Y., Hiroi, Y., Liao, J.K., 2010. Notch signaling as an important mediator of cardiac repair and regeneration after myocardial infarction. *Trends in Cardiovascular Medicine*, 20(7): 228-231.

Liao, S., Luo, C., Cao, B., Hu, H., Wang, S., Yue, H., Chen, L., Zhou, Z., 2017. Endothelial progenitor cells for ischemic stroke: update on basic research and application. *Stem Cells International*, 2017: 2193432.

Liu, L., Marti, G.P., Wei, X., Zhang, X., Zhang, H., Liu, Y. V., Nastai, M., Semenza, G.L., Harmon, J.W., 2008. Age-dependent impairment of HIF-1alpha expression in diabetic mice: correction with electroporation-facilitated gene therapy increases wound healing, angiogenesis, and circulating angiogenic cells. *Journal of Cellular Physiology*, 217(2): 319-327.

Losordo, D.W., Vale, P.R., Hendel, R.C., Milliken, C.E., Fortuin, F.D., Cummings, N., Schatz, R.A., Asahara, T., Isner, J.M., Kuntz, R.E., 2002. Phase 1/2 placebo-controlled, double-blind, dose-escalating trial of myocardial vascular endothelial growth factor 2 gene transfer by catheter delivery in patients with chronic myocardial ischemia. *Circulation*, 105(17): 2012-2018.

Losordo, D.W., Vale, P.R., Symes, J.F., Dunnington, C.H., Esakof, D.D., Maysky, M., Ashare, A.B., Lathi, K., Isner, J.M., 1998. Gene therapy for myocardial

angiogenesis : initial clinical results with direct myocardial injection of phVEGF165 as sole therapy for myocardial ischemia. *Circulation*, 98(25): 2800-2804.

Lu, L., Liu, Y., Yang, S., Zhao, Q., Wang, X., Gong, W., Han, Z., Xu, Z., Lu, Y., Liu, D., Chen, Z., 2006. Isolation and characterization of human umbilical cord mesenchymal stem cells with hematopoiesis-supportive function and other potentials. *Haematologica*, 91(8): 1017-1026.

Lu, Z., Chen, W., Li, Y., Li, L., Zhang, H., Pang, Y., Xiao, Z., Xiao, H., Xiao, Y., 2016. TNF-α enhances vascular cell adhesion molecule-1 expression in human bone marrow mesenchymal stem cells via the NF-κB, ERK and JNK signaling pathways. *Molecular Medicine Reports*, 14(1): 643-648.

Lunde, K., Solheim, S., Aakhus, S., Arnesen, H., Abdelnoor, M., Egeland, T., Endresen, K., Ilebekk, A., Mangschau, A., Fjeld, J.G., Smith, H.J., Taraldsrud, E., Grøgaard, H.K., Bjørnerheim, R., Brekke, M., Müller, C., Hopp, E., Ragnarsson, A., Brinchmann, J.E., Forfang, K., 2006. Intracoronary injection of mononuclear bone marrow cells in acute myocardial infarction. *The New England Journal of Medicine*, 355 (12): 1199-1209.

Ma, J., Yang, F., Both, S.K., Prins, H.-J., Helder, M.N., Pan, J., Cui, F.-Z., Jansen, J. a, van den Beucken, J.J.J.P., 2014. *In vitro* and i*n vivo* angiogenic capacity of BM-MSCs/HUVECs and AT-MSCs/HUVECs cocultures. *Biofabrication*, 6(1): 015005.

Mackensen, a, Dräger, R., Schlesier, M., Mertelsmann, R., Lindemann, a, 2000. Presence of IgE antibodies to bovine serum albumin in a patient developing anaphylaxis after vaccination with human peptide-pulsed dendritic cells. *Cancer Immunology, Immunotherapy*, 49(3): 152-156.

Makkar, R.R., Smith, R.R., Cheng, K., Malliaras, K., Thomson, L.E.J., Berman, D., Czer, L.S.C., Marbán, L., Mendizabal, A., Johnston, P. V., Russell, S.D., Schuleri, K.H., Lardo, A.C., Gerstenblith, G., Marbán, E., 2012. Intracoronary cardiosphere-derived cells for heart regeneration after myocardial infarction (CADUCEUS): a prospective, randomised phase 1 trial. *Lancet*, 379(9819): 895-904.

Malgieri, A., Kantzari, E., Patrizi, M.P., Gambardella, S., 2010. Bone marrow and umbilical cord blood human mesenchymal stem cells: state of the art. *International Journal of. Clinical and Experimental Medicine*, 3(4): 248-269.

Malik, N.N., 2012. Allogeneic versus autologous stem-cell therapy: a comparison of manufacturing costs and commercialization challenges. *BioPharm International*, 25(7): 36-40.

Mao, A.S., Mooney, D.J., 2015. Regenerative medicine: current therapies and future directions. *Proceedings of the National Academy of Sciences of the United States of America*, 112(47): 14452-14459.

Marenzi, G., Bartorelli, A.L., 2007. Improved clinical outcome after intracoronary administration of bone marrow-derived progenitor cells in acute myocardial infarction: Final 1-year results of the REPAIR-AMI trial [2]. *European Heart Journal*, 27(23): 2775-2783.

Mason, C., Dunnill, P., 2008. A brief definition of regenerative medicine. *Regenerative Medicine*, 3(1): 1-5.

Mathur, A., Arnold, R., Assmus, B., Bartunek, J., Belmans, A., Bönig, H., Crea, F., Dimmeler, S., Dowlut, S., Fernández-Avilés, F., Galiñanes, M., Garcia-Dorado, D., Hartikainen, J., Hill, J., Hogardt-Noll, A., Homsy, C., Janssens, S., Kala, P., Kastrup, J., Martin, J., Menasche, P., Miklik, R., Mozid, A., San Román, J.A., Sanz-Ruiz, R., Tendera, M., Wojakowski, W., Ylä-Herttuala, S., Zeiher, A., 2017. The effect of intracoronary infusion of bone marrow-derived mononuclear cells on all-cause mortality in acute myocardial infarction: rationale and design of the BAMI trial. *European Journal of Heart Failure*, 19(11): 1545-1550.

Mayourian J, Savizky RM, Sobie EA, Costa KD, 2016. Modeling electrophysiological coupling and fusion between human mesenchymal stem cells and cardiomyocytes. *PLOS Computational Biology*, 12(7): e1005014.

Melero-Martin, J.M., De Obaldia, M.E., Kang, S.Y., Khan, Z.A., Yuan, L., Oettgen, P., Bischoff, J., 2008. Engineering robust and functional vascular networks i*n vivo* with human adult and cord blood-derived progenitor cells. *Circulation Research*, 103(2): 194-202.

Menasché, P., 2008a. Current status and future prospects for cell transplantation to prevent congestive heart failure. Semininars in Thoracic and Cardiovascular Surgery, 20(2): 131-137.

Menasché, P., 2008b. Skeletal myoblasts and cardiac repair. *Journal of Molecular and Cellular Cardiology*, 45(4): 545-553.

Menasché, P., Hagège, A.A., Vilquin, J.T., Desnos, M., Abergel, E., Pouzet, B., Bel, A., Sarateanu, S., Scorsin, M., Schwartz, K., Bruneval, P., Benbunan, M., Marolleau, J.P., Duboc, D., 2003. Autologous skeletal myoblast transplantation for severe postinfarction left ventricular dysfunction. *Journal of the American College of Cardiology*, 41(7): 1078-1083.

Menasché, P., Vanneaux, V., Fabreguettes, J.-R., Bel, A., Tosca, L., Garcia, S., Bellamy, V., Farouz, Y., Pouly, J., Damour, O., Périer, M.-C., Desnos, M., Hagège, A., Agbulut, O., Bruneval, P., Tachdjian, G., Trouvin, J.-H., Larghero, J., 2015. Towards a clinical use of human embryonic stem cell-derived cardiac progenitors: a translational experience. *European Heart Journal*, 36(12): 743-750.

Mennan, C., Wright, K., Bhattacharjee, A., Balain, B., Richardson, J., Roberts, S., 2013. Isolation and characterisation of mesenchymal stem cells from different regions of the human umbilical cord. *Biomedical Research*, 2013: 916136.

Min, J.-Y., Yang, Y., Converso, K.L., Liu, L., Huang, Q., Morgan, J.P., Xiao, Y.-F., 2002. Transplantation of embryonic stem cells improves cardiac function in postinfarcted rats. *Journal of Applied Physiology*, 92(1): 288-296.

Montesano, R., Pepper, M.S., Orci, L., 1993. Paracrine induction of angiogenesis in vitro by Swiss 3T3 fibroblasts. *Journal of Cell Science*, 105: 1013-1024.

Moriyama, H., Moriyama, M., Isshi, H., Ishihara, S., Okura, H., Ichinose, A., Ozawa, T., Matsuyama, A., Hayakawa, T., 2014. Role of notch signaling in the maintenance of human mesenchymal stem cells under hypoxic conditions. *Stem Cells and Development*, 23(18): 2211-2224.

Nair, V., Madan, H., Sofat, S., Ganguli, P., Jacob, M.J., Datta, R., Bharadwaj, P., Sarkar, R.S., Pandit, A.J., Nityanand, S., Goel, P.K., Garg, N., Gambhir, S., George, P.V., Chandy, S., Mathews, V., George, O.K., Talwar, K.K., Bahl, A., Marwah, N., Bhatacharya, A., Bhargava, B., Airan, B., Mohanty, S., Patel, C.D., Sharma, A., Bhatnagar, S., Mondal, A., Jose, J., Srivastava, A.; 2015. Efficacy of stem cell in improvement of left ventricular function in acute myocardial infarction - MI3 trial. *Indian Journal of Medical Research*, 142(2):165-74.

Nauta, A.J., Westerhuis, G., Kruisselbrink, A.B., Lurvink, E.G.A., Willemze, R., Fibbe, W.E., 2006. Donor-derived mesenchymal stem cells are immunogenic in an allogeneic host and stimulate donor graft rejection in a nonmyeloablative setting. *Blood*, 108(6): 2114-2120.

Nguyen, P.K., Rhee, J.-W., Wu, J.C., 2016. Adult stem cell therapy and heart failure, 2000 to 2016: a systematic review. *JAMA Cardiology*, 1(7): 831-841

Nisato, R.E., Harrison, J.A., Buser, R., Orci, L., Rinsch, C., Montesano, R., Dupraz, P., Pepper, M.S., 2004. Generation and characterization of telomerase-transfected human lymphatic endothelial cells with an extended life span. *The American Journal of Pathology*, 165(1): 11-24.

Norrby, K., 2006. *In vivo* models of angiogenesis. *Journal of Cellular and Molecular Medicine*, 10(3): 588-612.

O'Rourke, S.T., 2007. Antianginal actions of beta-adrenoceptor antagonists. *American Journal of Pharmaceutical Education*, 71(5):95, 1-6.

Oikawa, T., Sasaki, M., Inose, M., Shimamura, M., Kuboki, H., Hirano, S.I., Kumagai, H., Ishizuka, M., Takeuchi, T., 1997. Effects of cytogenin, a novel microbial product, on embryonic and tumor cell-induced angiogenic responses *in vivo*. *Anticancer Research*, 17(3C): 1881-1886.

O'Donnell, J., Mille-Baker, B., Laffan, M., 2000. Human umbilical vein endothelial cells differ from other endothelial cells in failing to express ABO blood group antigens. *Journal of Vascular Research*, 37(6): 540-547.

Osafune, K., Caron, L., Borowiak, M., Martinez, R.J., Fitz-Gerald, C.S., Sato, Y., Cowan, C.A., Chien, K.R., Melton, D.A., 2008. Marked differences in differentiation propensity among human embryonic stem cell lines. *Nature Biotechnology*, 26(3): 313-315.

Piepoli, M.F., Vallisa, D., Arbasi, M., Cavanna, L., Cerri, L., Mori, M., Passerini, F., Tommasi, L., Rossi, A., Capucci, A., 2010. Bone marrow cell transplantation improves cardiac, autonomic, and functional indexes in acute anterior myocardial infarction patients (Cardiac Study). *European Journal of Heart Failure*, 12(2): 172-180.

Pitchford, S.C., Furze, R.C., Jones, C.P., Wengner, A.M., Rankin, S.M., 2009. Differential mobilization of subsets of progenitor cells from the bone marrow. *Cell Stem Cell*, 4(1): 62-72.

Porat, Y., Abraham, E., Karnieli, O., Nahum, S., Woda, J., Zylberberg, C., 2015. Critical elements in the development of cell therapy potency assays for ischemic conditions. *Cytotherapy*, 17(7): 817-831.

Prasajak, P., Leeanansaksiri, W., 2014. Mesenchymal stem cells: current clinical applications and therapeutic potential in liver diseases. *Journal of Bone Marrow Research*, 2: 137.

Raheja, L.F., Genetos, D.C., Yellowley, C.E., 2010. The effect of oxygen tension on the long-term osteogenic differentiation and MMP/TIMP expression of human mesenchymal stem cells. *Cells Tissues Organs*, 191(3): 175-184.

Ratcliffe, E., Thomas, R.J., Williams, D.J., 2011. Current understanding and challenges in bioprocessing of stem cell-based therapies for regenerative medicine. *British Medical Bulletin*, 100: 137-155.

Renault, M.A., Losordo, D.W., 2007. Therapeutic myocardial angiogenesis. *Microvascular Research*, 74(2-3): 159-171.

Rezvani, H.R., Ali, N., Nissen, L.J., Harfouche, G., de Verneuil, H., Taïeb, A., Mazurier, F., 2011. HIF-1α in epidermis: oxygen sensing, cutaneous angiogenesis, cancer, and non-cancer disorders. *Journal of Investigative Dermatology*, 131(9): 1793-1805.

Richardson, W.J., Clarke, S.A., Alexander Quinn, T., Holmes, J.W., 2015. Physiological implications of myocardial scar structure. *Comprehensive Physiology*, 5(4): 1877-1909.

Rizzo, P., Mele, D., Caliceti, C., Pannella, M., Fortini, C., Clementz, A.G., Morelli, M.B., Aquila, G., Ameri, P., Ferrari, R., 2014. The role of notch in the cardiovascular system: potential adverse effects of investigational notch inhibitors. *Frontiers in Oncology*, 4:384.

Rosenstrauch, D., Poglajen, G., Zidar, N., Gregoric, I.D., 2005. Stem cell therapy for ischemic heart failure. *Texas Heart Institute Journal*, 32(3): 339-347.

Sanganalmath, S.K., Bolli, R., 2013. Cell therapy for heart failure: a comprehensive overview of experimental and clinical studies, current challenges, and future directions. *Circulation Research*, 113(6): 810-834.

Sassoli, C., Pini, A., Mazzanti, B., Quercioli, F., Nistri, S., Saccardi, R., Orlandini, S.Z., Bani, D., Formigli, L., 2011. Mesenchymal stromal cells affect cardiomyocyte growth through juxtacrine Notch-1/Jagged-1 signaling and paracrine mechanisms: Clues for cardiac regeneration. *Journal of Molecular and Cellular Cardiology*, 51(3): 399-408.

Schächinger, V., Assmus, B., Britten, M.B., Honold, J., Lehmann, R., Teupe, C., Abolmaali, N.D., Vogl, T.J., Hofmann, W.K., Martin, H., Dimmeler, S., Zeiher, A.M., 2004. Transplantation of progenitor cells and regeneration enhancement in acute myocardial infarction: Final one-year results of the TOPCARE-AMI trial. Journal of the *American College of Cardiology*, 44(8): 1690-1699.

Schumacher, B., Pecher, P., von Specht, B.U., Stegmann, T., 1998. Induction of neoangiogenesis in ischemic myocardium by human growth factors: first clinical results of a new treatment of coronary heart disease. *Circulation*, 97(7): 645-650.

Scruggs, B.A., Semon, J.A., Zhang, X., Zhang, S., Bowles, A.C., Pandey, A.C., Imhof, K.M., Kalueff, A. V, Gimble, J.M., Bunnell, B.A., 2013. Age of the donor reduces the ability of human adipose-derived stem cells to alleviate symptoms in the experimental autoimmune encephalomyelitis mouse model. *Stem Cells Translational Medicine*, 2(10): 797-807.

Semenza, G.L., 1999. Regulation of mammalian O_2 homeostasis by hypoxia-inducible factor 1. *Annual Review of Cell and Developmental Biology*, 15: 551-578.

Semon, J.A., Nagy, L.H., Llamas, C.B., Tucker, H.A., Lee, R.H., Prockop, D.J., 2010. Integrin expression and integrin-mediated adhesion *in vitro* of human multipotent stromal cells (MSCs) to endothelial cells from various blood vessels. *Cell and Tissue Research*, 341(1): 147-58.

Shake, J.G., Gruber, P.J., Baumgartner, W.A., Senechal, G., Meyers, J., Redmond, J.M., Pittenger, M.F., Martin, B.J., 2002. Mesenchymal stem cell implantation in a swine myocardial infarct model: engraftment and functional effects. *The Annals of Thoracic Surgery*, 73(6): 1919-1926.

Shen, C., Lie, P., Miao, T., Yu, M., Lu, Q., Feng, T., Li, J., Zu, T., Liu, X., Li, H., 2015. Conditioned medium from umbilical cord mesenchymal stem cells induces migration and angiogenesis. *Molecular Medicine Reports*, 12(1): 20-30.

Shin, E.Y., Kim, S.Y., Kim, E.G., 2001. c-Jun N-terminal kinase is involved in motility of endothelial cell. *Experimental and Molecular Medicine*, 33(4): 276-283.

Shi, Z., Zhao, L., Qiu, G., He, R., Detamore, M.S., 2015. The effect of extended passaging on the phenotype and osteogenic potential of human umbilical cord mesenchymal stem cells. *Molecular and Cellular Biochemistry*, 401(1-2): 155-164.

Simaria, A.S., Hassan, S., Varadaraju, H., Rowley, J., Warren, K., Vanek, P., Farid, S.S., 2014. Allogeneic cell therapy bioprocess economics and optimization: single-use cell expansion technologies. *Biotechnology and Bioengineering*, 111: 69-83.

Smith, E.J., Staton, C.A., 2007. Tubule formation assays, in: angiogenesis assays: a critical appraisal of current techniques, 65-87. Chichester, UK: John Wiley & Sons, Ltd.

Song, H., Chang, W., Lim, S., Seo, H.-S., Shim, C.Y., Park, S., Yoo, K.-J., Kim, B.-S., Min, B.-H., Lee, H., Jang, Y., Chung, N., Hwang, K.-C., 2007. Tissue transglutaminase is essential for integrin-mediated survival of bone marrow-derived mesenchymal stem cells. *Stem Cells*, 25(6): 1431-1438.

Squillaro, T., Peluso, G., Galderisi, U., 2016. Clinical trials with mesenchymal stem cells: an update. *Cell Transplant*, 25 (5), 829-848.

Stamati, K., Priestley, J. V., Mudera, V., Cheema, U., 2014. Laminin promotes vascular network formation in 3D *in vitro* collagen scaffolds by regulating VEGF uptake. *Experimental Cell Research*, 327(1): 68-77.

Staton, C.A., Lewis, C., Bicknell, R., 2007. Angiogenesis assays: a critical appraisal of current techniques, 1-390. Chichester, UK: John Wiley & Sons, Ltd.

Staton, C.A., Reed, M.W.R., Brown, N.J., 2009. A critical analysis of current methods *in vitro* and i*n vivo* angiogenesis assays. *International Journal of Clinical and Experimental Pathology*, 90(3): 195-221.

Staton, C.A., Stribbling, S.M., Tazzyman, S., Hughes, R., Brown, N.J., Lewis, C.E., 2004. Current methods for assaying angiogenesis *in vitro* and i*n vivo*. *International Journal of Experimental Pathology*, 85(5): 233-248.

Steinwender, C., Hofmann, R., Kammler, J., Kypta, A., Pichler, R., Maschek, W., Schuster, G., Gabriel, C., Leisch, F., 2006. Effects of peripheral blood stem cell mobilization with granulocyte-colony stimulating factor and their transcoronary transplantation after primary stent implantation for acute myocardial infarction. *American Heart Journal*, 151(6): 1296.e7-13.

Stroncek, D.F., Jin, P., Wang, E., Jett, B., 2007. Potency analysis of cellular therapies: the emerging role of molecular assays. *Journal of Translational* Medicine, 5: 24.

Suh, S.H., Choi, S., Kim, J.A., Kim, K.C., 2015. Isolation and *in vitro* culture of vascular endothelial cells from mice. *The Korean Journal of Physiology and Pharmacology*, 19(1): 35-42.

Tahergorabi, Z., Khazaei, M., 2012. A review on angiogenesis and its assays. *Iranian Journal of Basic Medical Sciences*, 15(6): 1110-1126.

Tao, H., Han, Z., Han, Z.C., Li, Z., 2016. Proangiogenic features of mesenchymal stem cells and their therapeutic applications. *Stem Cells International*, 2016: 1314709.

Taylor AM, Zon LI, 2009. Zebrafish tumor assays: the state of transplantation. *Zebrafish*, 6(4): 339-346.

Taylor, D. a, Atkins, B.Z., Hungspreugs, P., Jones, T.R., Reedy, M.C., Hutcheson, K. a, Glower, D.D., Kraus, W.E., 1998. Regenerating functional myocardium: improved performance after skeletal myoblast transplantation. *Nature Medicine*, 4(8): 929-933.

Tekkatte, C., Gunasingh, G.P., Cherian, K.M., Sankaranarayanan, K., 2011. 'Humanized' stem cell culture techniques: the animal serum controversy. *Stem Cells International*, 2011: 504723.

Thej, C., Ramadasse, B., Walvekar, A., Majumdar, A.S., Balasubramanian, S., 2017. Development of a surrogate potency assay to determine the angiogenic activity of Stempeucel®, a pooled, *ex-vivo* expanded, allogeneic human bone marrow mesenchymal stromal cell product. *Stem Cell Research and Therapy*, 8(47): 1-14.

Thomas, R.J., Hourd, P.C., Williams, D.J., 2008. Application of process quality engineering techniques to improve the understanding of the *in vitro* processing of stem cells for therapeutic use. *Journal of Biotechnology*, 136(3-4): 148-155.

Till, J.E., McCulloch, E.A., 1961. A Direct measurement of the radiation sensitivity of normal mouse bone marrow cells. *Radiation Research*, 14(2): 213-222.

Tsuji, H., Miyoshi, S., Ikegami, Y., Hida, N., Asada, H., Togashi, I., Suzuki, J., Satake, M., Nakamizo, H., Tanaka, M., Mori, T., Segawa, K., Nishiyama, N., Inoue, J., Makino, H., Miyado, K., Ogawa, S., Yoshimura, Y., Umezawa, A., 2010. Xenografted human amniotic membrane-derived mesenchymal stem cells are immunologically tolerated and transdifferentiated into cardiomyocytes. *Circulation Research*, 106(10): 1613-1623.

Ullah, I., Baregundi Subbarao, R., Rho, G.-J., 2015. Human mesenchymal stem cells - current trends and future prospective. *Bioscience Reports*, 35(2).

Unger, E.F., Banai, S., Shou, M., Lazarous, D.F., Jaklitsch, M.T., Scheinowitz, M., Correa, R., Klingbeil, C., Epstein, S.E., 1994. Basic fibroblast growth factor enhances myocardial collateral flow in a canine model. *American Journal of Physiology*, 266(4 Pt 2): H1588-95.

Wang, S., Lu, H., Cheng, L., 2018. [Angiogenic ability of 3 different tissues-derived mesenchymal stem cells on endothelial progenitor cells]. 43(2):184-191.

Wegmeyer, H., Bröske, A.-M., Leddin, M., Kuentzer, K., Nisslbeck, A.K., Hupfeld, J., Wiechmann, K., Kuhlen, J., von Schwerin, C., Stein, C., Knothe, S., Funk, J., Huss, R., Neubauer, M., 2013. Mesenchymal stromal cell characteristics vary depending on their origin. *Stem Cells and Development*, 22(19): 2606–2618.

van der Strate, B.W.A., Popa, E.R., Schipper, M., Brouwer, L.A., Hendriks, M., Harmsen, M.C., van Luyn, M.J.A., 2007. Circulating human CD34(+) progenitor cells modulate neovascularization and inflammation in a nude mouse model. *Journal of Molecular and Cellular Cardiology*, 42(6): 1086-1097.

Van Dijk, A., Niessen, H.W.M., Ursem, W., Twisk, J.W.R., Visser, F.C., Van Milligen, F.J., 2008. Accumulation of fibronectin in the heart after myocardial infarction: a putative stimulator of adhesion and proliferation of adipose-derived stem cells. *Cell and Tissue Research*, 332: 289-298.

Veevers-Lowe, J., Ball, S.G., Shuttleworth, A., Kielty, C.M., 2011. Mesenchymal stem cell migration is regulated by fibronectin through α5β1-integrin-mediated activation of PDGFR-β and potentiation of growth factor signals. *Journal of Cell Science*, 124 (Pt 8): 1288-1300.

Velazquez, O.C., 2007. Angiogenesis and vasculogenesis: Inducing the growth of new blood vessels and wound healing by stimulation of bone marrow-derived progenitor cell mobilization and homing. *Journal of Vascular Surgery*, 45 (Suppl. A): 39-47.

Wang, L., Tran, I., Seshareddy, K., Weiss, M.L., Detamore, M.S., 2009. A comparison of human bone marrow-derived mesenchymal stem cells and human umbilical cord-derived mesenchymal stromal cells for cartilage tissue engineering. *Tissue Engineering*, 15(8): 2259-2266.

Wanjare, M., Kusuma, S., Gerecht, S., 2013. Perivascular cells in blood vessel regeneration. *Biotechnology Journal*, 8(4): 434-447.

Wen, Y., Meng, L., Xie, J., Ouyang, J., 2011. Direct autologous bone marrow-derived stem cell transplantation for ischemic heart disease: a meta-analysis. *Expert Opinion on Biological Therapy*, 11(5): 559-567.

Williams, A.R., Hare, J.M., 2011. Mesenchymal stem cells: biology, pathophysiology, translational findings, and therapeutic implications for cardiac disease. *Circulation Research*, 109(8): 923-940.

Williams, D.J., Thomas, R.J., Hourd, P.C., Chandra, a., Ratcliffe, E., Liu, Y., Rayment, E. a., Archer, J.R., 2012. Precision manufacturing for clinical-quality regenerative medicines. *Philosophical Transactions of the Royal Society A*, 370(1973): 3924-3949.

Wilson, S.R., Mudge, G.H., Stewart, G.C., Givertz, M.M., 2009. Evaluation for a ventricular assist device: selecting the appropriate candidate. *Circulation*, 119(16): 2225-2232.

Wollert, K.C., Meyer, G.P., Lotz, J., Ringes-Lichtenberg, S., Lippolt, P., Breidenbach, C., Fichtner, S., Korte, T., Hornig, B., Messinger, D., Arseniev, L., Hertenstein, B., Ganser, A., Drexler, H., 2004. Intracoronary autologous bone-marrow cell transfer after myocardial infarction: The BOOST randomised controlled clinical trial. *Lancet*, 364(9429): 141-148.

Wu, S.M., Fujiwara, Y., Cibulsky, S.M., Clapham, D.E., Lien, C. ling, Schultheiss, T.M., Orkin, S.H., 2006. Developmental origin of a bipotential myocardial and smooth muscle cell precursor in the mammalian heart. *Cell*, 127(6): 1137-1150.

Xie, D., Ju, D., Speyer, C., Gorski, D., Kosir, M.A., 2016. Strategic endothelial cell tube formation assay: comparing extracellular matrix and growth factor reduced extracellular matrix. *Journal of Visualized Experiments*, 114: 1-6.

Xie, J., Wang, W., Si, J.-W., Miao, X.-Y., Li, J.-C., Wang, Y.-C., Wang, Z.-R., Ma, J., Zhao, X.-C., Li, Z., Yi, H., Han, H., 2013. Notch signaling regulates CXCR4 expression and the migration of mesenchymal stem cells. *Immunology and Cell Biology*, 281(1): 68-75.

Xin, M., Olson, E.N., Bassel-Duby, R., 2013. Mending broken hearts: cardiac development as a basis for adult heart regeneration and repair. *Nature Reviews Molecular Cell Biology*, 14(8): 529-541.

Yang, Z., Zhang, F., Ma, W., Chen, B., Zhou, F., Xu, Z., Zhang, Y., Zhang, D., Zhu, T., Wang, L., Wang, H., Ding, Z., Zhang, Y., 2010. A novel approach to transplanting bone marrow stem cells to repair human myocardial infarction: Delivery via a noninfarct-relative artery. *Cardiovascular Therapeutics*, 28(6): 380-385.

Yoon, J., Shim, W.J., Ro, Y.M, Lim, D-S, 2005. Transdifferentiation of mesenchymal stem cells into cardiomyocytes by direct cell-to-cell contact with neonatal cardiomyocyte but not adult cardiomyocytes. *Annals of Hematology*, 84(11): 715-721.

Yousef, M., Schannwell, C.M., Köstering, M., Zeus, T., Brehm, M., Strauer, B.E., 2009. The BALANCE Study: Clinical Benefit and long-term outcome after intracoronary autologous bone marrow cell transplantation in patients with acute myocardial Infarction. *Journal of the American College of Cardiology*, 53(24): 2262-2269.

Yu, X., Cohen, D.M., Chen, C.S., 2012. miR-125b is an adhesion-regulated microRNA that protects mesenchymal stem cells from anoikis. *Stem Cells*, 30(5): 956-964.

Zammaretti, P., Jaconi, M., 2004. Cardiac tissue engineering: regeneration of the wounded heart. *Current Opinion in Biotechnology*, 15(5): 430-434.

Zanetta, L., Marcus, S.G., Vasile, J., Dobryansky, M., Cohen, H., Eng, K., Shamamian, P., Mignatti, P., 2000. Expression of von Willebrand factor, an endothelial cell marker, is up-regulated by angiogenesis factors: a potential method for objective assessment of tumor angiogenesis. *International Journal of Cancer*, 85 (2): 281-288.

Zhang, B., Yang, S., Zhang, Y., Sun, Z., Xu, W., Ye, S., 2012. Co-culture of mesenchymal stem cells with umbilical vein endothelial cells under hypoxic condition. *Journal of Huazhong University of Science and Technology Medical Sciences*, 32(2): 173-180.

Zhang, L., Yang, J., Tian, Y.-M., Guo, H., Zhang, Y., 2015. Beneficial effects of hypoxic preconditioning on human umbilical cord mesenchymal stem cells. *Chinese Journal of Physiology*, 58(5): 343-353.

Zhang, X., Liu, L., Wei, X., Tan, Y.S., Tong, L., Chang, R., Ghanamah, M.S., Reinblatt, M., Marti, G.P., Harmon, J.W., Semenza, G.L., 2010. Impaired angiogenesis and mobilization of circulating angiogenic cells in HIF-1α heterozygous-null mice after burn wounding. *Wound Repair Regeneration*, 18(2): 193-201.

Zudaire, E., Gambardella, L., Kurcz, C., Vermeren, S., 2011. A computational tool for quantitative analysis of vascular networks. *PLoS One*, 6 (11): e27385.

Chapter 8: Appendices

8.1: Appendix A Analysis of the effect of passage number, type of matrix and matrix volume on number of branch points

Comparative studies were carried out between HUVECs at passage 7, passage 10, passage 13 and passage 15 to study the effect of cell age on branch network formation. HUVECs were cultured for 3 to 4 days, trypsinized and seeded on GFR Geltrex and GFR Matrigel respectively at two different volumes, 55 µl and 35 µl for each substrate. A screening model was then designed using the Design Expert software to identify the key parameters involved in branch network formation. The interaction plot in Figure 8-1 indicated an increase in vascular efficiency up to passage 13 with the peak decreasing at passage 15.

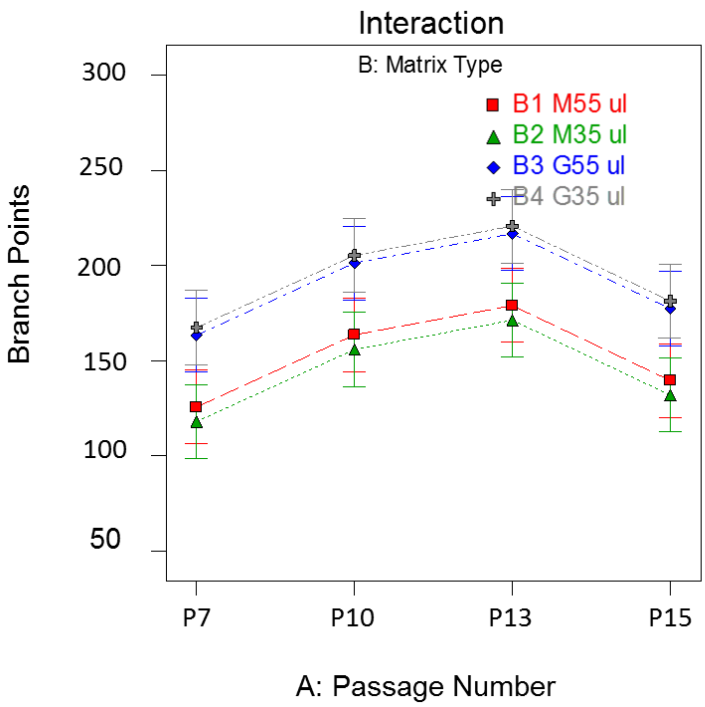

Figure 8-1: Interaction plot comparing the effect of passage number for GFR Matrigel and GFR Geltrex at higher (55 µl) and lower (35 µl) volumes.

A 3-D plot was then generated to better visualize the interactions between the different input variables in the model (Figure 8-1 and Figure 8 2). The 3-D plot indicated that GFR Geltrex was more efficient than GFR Matrigel in forming branch networks. Firstly the plane for GFR Matrigel was lower than the plane for

the GFR Geltrex and secondly, the z plane of the graphs showed that GFR Geltrex was able to form more branch points. In addition, the flat planes observed in both the GFR Matrigel and GFR Geltrex 3-D plots confirmed that using the lower substrate volumes and higher passage numbers did not impact on branch efficiency hence suggesting that lower substrate volumes and higher passage numbers could be used to obtain more cost-effective high throughput assays.

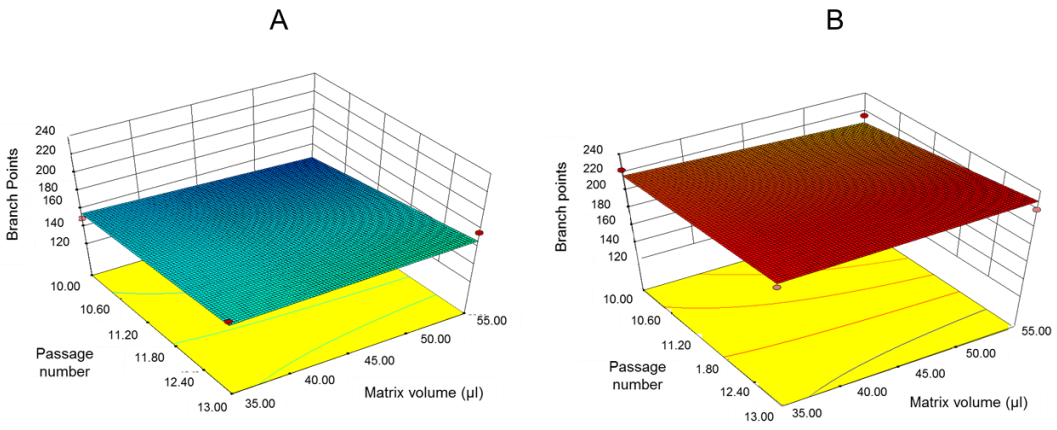

Figure 8-2: Interaction plot comparing the effect of passage number for (A) GFR Matrigel and (B) GFR Geltrex at higher (55 µl) and lower (35 µl) volumes.

8.2: Appendix B Effect of matrix volume and type of matrix on vascular network formation in co-cultures

The gx11 individual donor hBM-MSCs were stained with Vybrant DiI Cell-Labelling Solution (in red) whilst the HUVECs were stained with Green Cell Tracker (in green). The wells were imaged after 18 hours. As shown in the results, the hBM-MSCs co-localized with and bridged between the HUVECs (Figure 8-3).

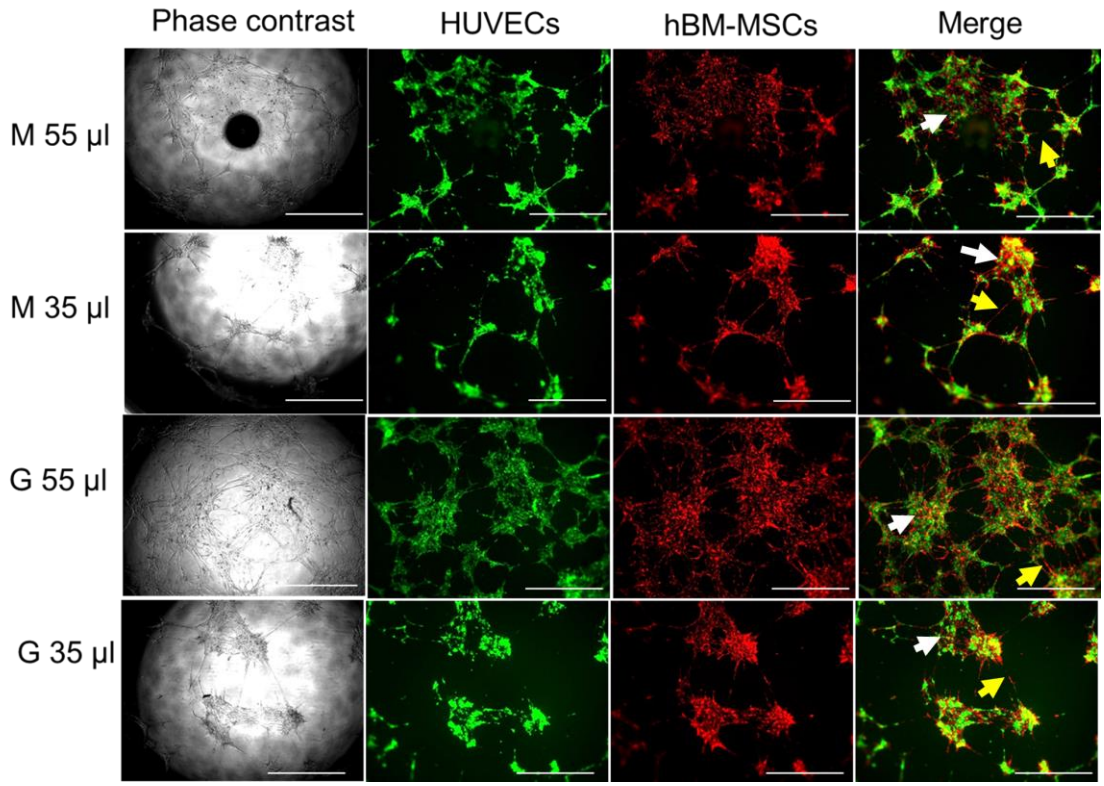

Figure 8-3: Co-culture vessel formation after 18 hours of individual donor gx11 P5 (PDL 7) hBM-MSCs (in red) and P10 HUVECs (in green; previously cultured in ambient oxygen conditions) seeded at a 1:1 ratio. Experiments were carried out on GFR Matrigel (M) and GFR Geltrex (G) at 35 µl and 55 µl respectively. Images were visualised using a fluorescence microscope. Yellow arrows represent the hBM-MSCs bridging between HUVECs. White arrows represent the hBM-MSCs co-localizing with the HUVECs. Scale bars = 1000 µm.

As part of the current optimization studies, different variables were assessed to obtain the best condition for tubule formation, and one of them was matrix volume. This was done to understand if reducing matrix volume would still allow for efficient network formation and could therefore be used to decrease costs associated with performing the assays. Next, different seeding densities of 1:1 hBM-MSCs:HUVECs were tested to see if fewer cells could be used to achieve

similar performance to the higher seeding densities. The phase contrast images (Figure 8-4) showed that more networks formed at 0.5 x 10^5 cells/ml and 0.67 x 10^5 cells/ml than at 0.3 x 10^5 cells/ml. The images also showed that tubule formation on Geltrex was less efficient than that observed for Matrigel, and this was more evident when using the lower seeding densities of 0.3 x 10^5 cells/ml and 0.5 x 10^5 cells/ml (see J, K, N, O; Figure 8-4).

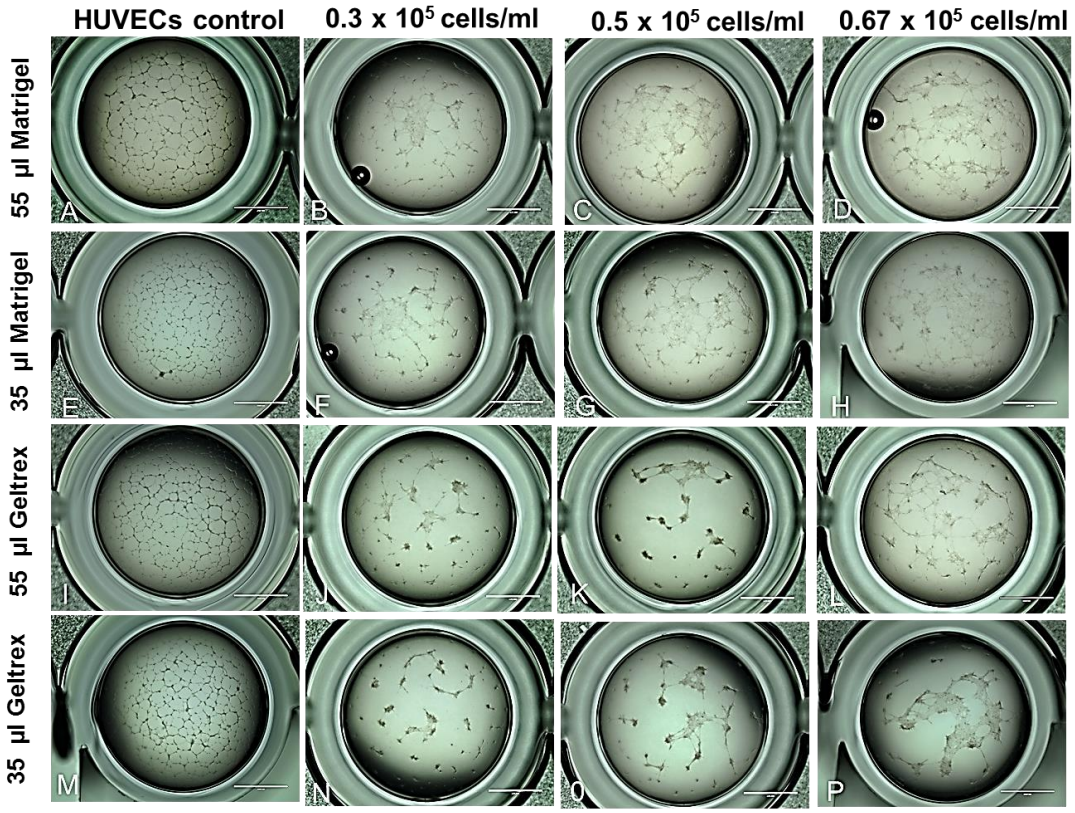

Figure 8-4: Representative phase contrast images of gx11 P5 (PDL 7) hBM-MSCs: P10 HUVECs co-cultures seeded at a 1:1 ratio for a total cell concentration of either 0.3 x 10^5 cell/ml, 0.5 x 10^5 cell/ml or 0.67 x 10^5 cell/ml respectively using either 35 µl or 55 µl of GFR Matrigel and GFR Geltrex respectively. Scale bars = 2000 µm.

As shown in Figure 8-5, the values for Geltrex at either 55 µl or 35 µl appeared to be lower than those observed in Matrigel especially at the higher cell concentrations where the values of Matrigel were almost two-fold higher than those of Geltrex (see M 55 µl and M 35 µl versus G 55 µl and G 35 µl; Figure 8-5). In addition, the differences in branch point efficiency between the higher and the lower cell concentrations were more evident in the Matrigel groups. In particular, when using M 55 µl there was a concentration-dependent trend where the branch point values obtained using 0.67 x10^5 cells/ml were at least two-fold higher than those obtained using 0.3 x10^5 cells/ml (Figure 8-5).

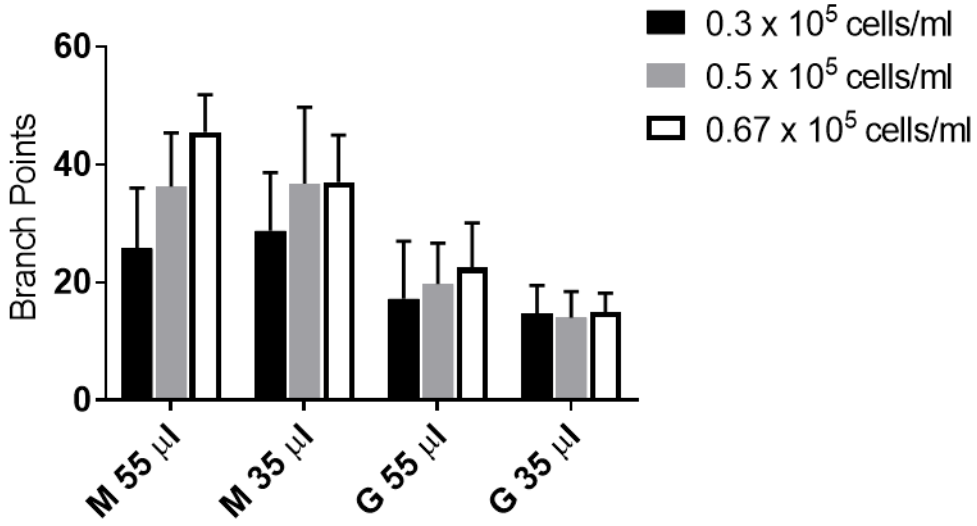

Figure 8-5: Branch point quantification of gx11 P5 (PDL 7) hBM-MSCs: P10 HUVECs co-cultures seeded at a 1:1 ratio for a total cell concentration of either 0.3 x 10^5 cell/ml, 0.5 x 10^5 cell/ml or 0.67 x 10^5 cell/ml respectively. Experiments were carried out at 2% O_2. The data indicated the mean ± SEM of triplicate samples from 3 independent experiments using different hBM-MSC batches derived from the same donor (gx11 donor).

8.3: Appendix C Co-culture optimization study

Co-culture assays were carried out after the hMSCs reached 80-90% confluency. Three different MSC:HUVEC ratios were investigated 1:1 ratio, 1:4 ratio and 4:1 ratio using either GFR Geltrex (G) or GFR Matrigel (M). In order to investigate the effect of priming hMSCs with Notch ligands, 0.67 x 10^5 cells/well was seeded on the substrates. In order to count the number of branch points, wells were imaged using an inverted light microscope at X4 magnification. An example of triplicate wells of co-cultures seeded on Geltrex using normoxic hBM-MSCs is shown in Figure 8-6. As shown in Figure 8-6, the number of networks formed using the 1:4

ratio appears to be superior to the 1:1 and 4:1 ratio. This observation was confirmed in the quantification data in Figure 8-7.

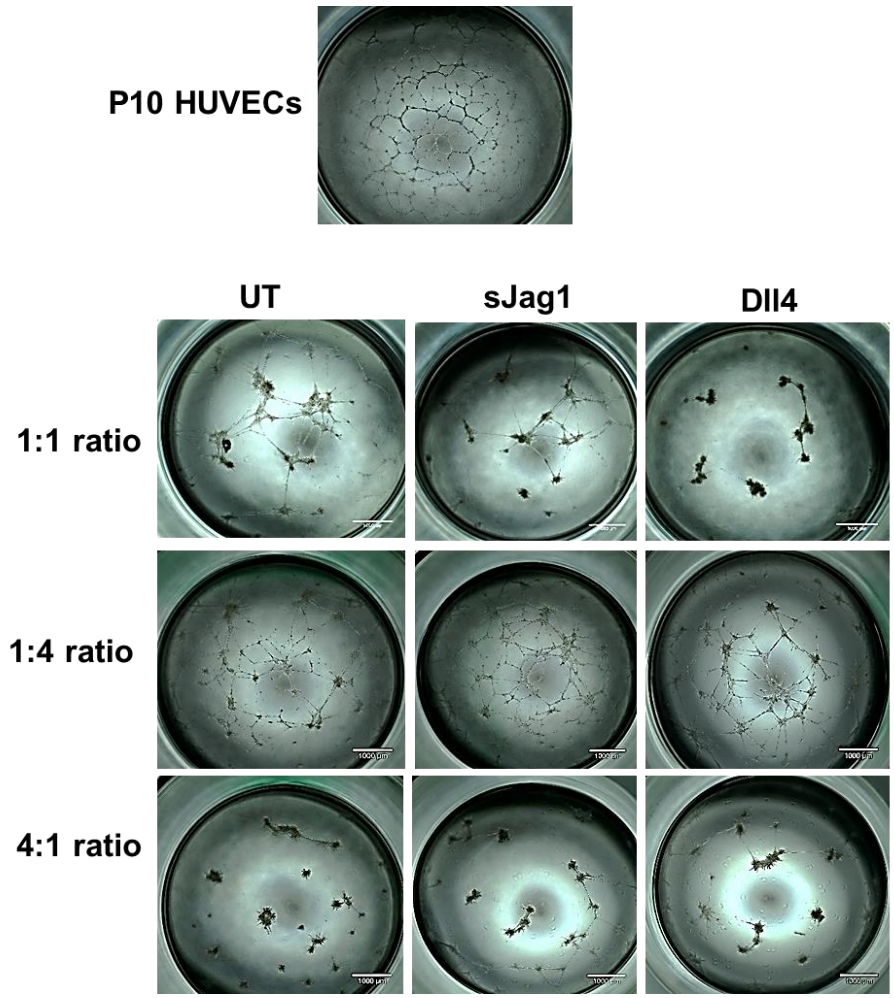

Figure 8-6: Sample phase contrast representative images of tubule networks formed in commercial PDL 14 hBM-MSCs:P10 HUVECs co-cultures seeded at 1:1, 1:4 and 4:1 ratios on 35 µl Gelltrex. Experiments were carried out at 2% O_2. Scale bars = 1000 µm

8.3.1: Effect of commercial low-serum hMSCs:HUVECs ratio and type of matrix on vascular efficiency

The results showed that the number of branch points formed on Geltrex at the 1:4 ratio using the sJag1-treated hBM-MSCs was higher than that of the UT and the sDll4-treated groups (see G 1:4; Figure 8-7). However, more experiments will need to be performed to confirm whether these differences are statistically significant or not. Next, the data for Geltrex showed that higher branch point numbers (at least four-fold increase) were observed for the UT, sJag1 and sDll4 groups at the 1:4 ratio in comparison to the branch point values obtained at the

1:1 and 4:1 ratios.(Figure 8-7). These results could be associated with the higher number of HUVECs in the 1:4 ratio.

Next for sJag1, the M 1:4 group showed at least a five-fold decrease in vascular efficiency in comparison to the G 1:4 group. A similar trend was also observed for the UT (~2-fold increase for G 1:4 vs M 1:4) and the sDll4 groups (~4-fold increase for G 1:4 vs M 1:4). Overall, the 1:4 ratio led to the formation of evidently higher number of branch points compared to the 1:1 ratio and the 4:1 ratio which worked similarly. The data also suggested that sJag1 priming enhances angiogenesis when using Geltrex at the higher HUVEC ratio of 1:4. Furthermore, the trend for all of the experiments performed on Geltrex was that the groups with sJag1-treated hBM-MSCs showed higher adhesion than the UT groups even though the results for the G 1:1 and G 4:1 were modest (see G 1:1, G 1:4 and G 4:1; Figure 8-7).

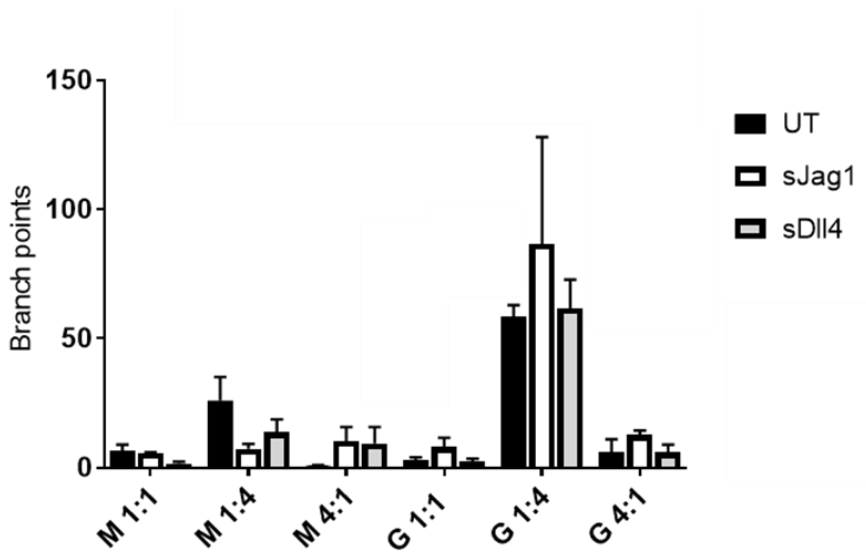

Figure 8-7: Branch point quantification of normoxic commercial PDL 14 hBM-MSCs:P10 HUVECs co-cultures seeded at 1:1, 1:4 and 4:1 ratios. Experiments were carried out at 2% O_2. The data indicated the mean ± SEM of triplicate samples from 3 independent experiments using different hBM-MSC batches derived from the same donor. Refer to text for a detailed description of the results.

Next comparative studies were carried out between MSC:HUVEC 1:1 ratio and 4:1 ratio by using hBM-MSCs previously expanded in hypoxic conditions at 2% O_2. The data indicated that for M 1:1 the sJag1 group showed at least a three-fold increase in branch points in comparison to the UT group (M 1:1, UT versus

sJag1; Figure 8-8). On the other hand for G 1:1 the UT group demonstrated at least a two-fold increase in branch points in comparisons to the sJag1 group and at least a three-fold increase in branch points in comparison to the sDll4 group (Figure 8-8). Next, Geltrex showed at least a three-fold increase in branch points in comparison to Matrigel for the UT 1:1 groups (see M1:1 versus G 1:1, UT; Figure 8-8). On the other hand, Matrigel showed at least a two-fold increase in branch points in comparison to Geltrex for the sJag1 1:1 groups (see M 1:1 versus G 1:1, sJag1; Figure 8-8). However, there were no evident differences in vascular efficiency between the M 4:1 group and the G 4:1 groups. The very low values of branch points for the 4:1 groups in comparison to the 1:1 groups, indicated inefficient branch formation. Furthermore, the results suggested that seeding the co-cultures at a 1:1 ratio promotes a higher number of branch points than using the 4:1 ratio. This result was expected as the 4:1 ratio involves using a higher number of hBM-MSCs than HUVECs. Also, there was a trend where the sDll4 groups showed a lower number of branch points in comparison to the UT and the sJag1 groups and this trend was maintained for all of the conditions (see M 1:1, M 4:1, G 1:1 and G 4:1; Figure 8-8). Therefore, sDll4 priming of hBM-MSCs appeared to hinder angiogenesis.

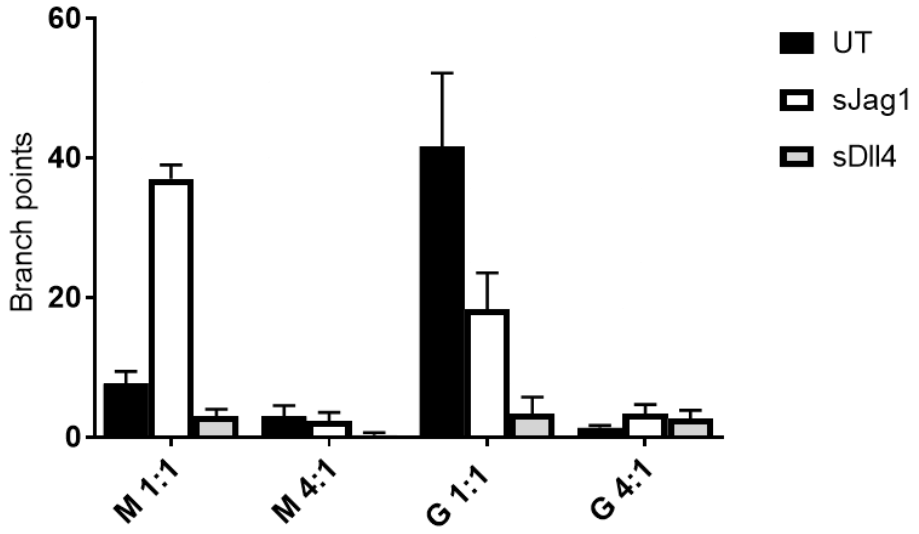

Figure 8-8: Branch point quantification for hypoxic commercial PDL 14 hBM-MSCs:P10 HUVECs co-cultures seeded at 1:1, 1:4 and 4:1 ratios. Experiments were carried out at 2% O_2. The data indicated the mean ± SEM of triplicate samples from 3 independent experiments using different hBM-MSC batches derived from the same donor. Refer to text for a detailed description of the results.

8.3.2: Effect of low oxygen and type of matrix on vascular efficiency

The data showed that there were mostly no evident differences in branch points between the co-cultures that were performed using the normoxic and the hypoxic hBM-MSCs. However, the M 1:1 sJag1 group showed at least a three-fold increase in branch points when using the hypoxic hBM-MSCs compared to the experiments performed using the normoxic hBM-MSCs (see M 1:1 normoxic versus M 1:1 hypoxic; Figure 8-9). Similarly, the G 1:1 UT condition showed at least a four-fold increase in branch points using the hypoxic hBM-MSCs in comparison to the normoxic group (see G 1:1 normoxic versus G 1:1 hypoxic; Figure 8-9).

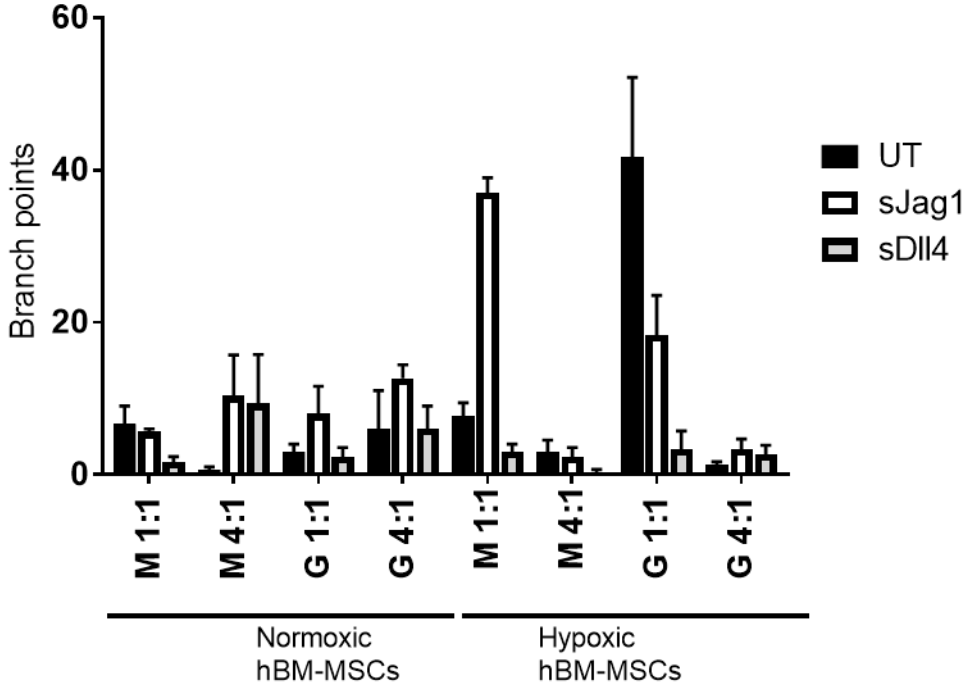

Figure 8-9: Comparative study between co-cultures carried out using normoxic (20% O_2) and hypoxic (2% O_2) commercial PDL 14 hBM-MSCs at 1:1 and 4:1 MSC:HUVEC ratios using either GFR Matrigel (M) or Geltrex (G). Experiments were performed under 2% O_2. The data indicated the mean ± SEM of triplicate samples from 3 independent experiments using different hBM-MSC batches derived from the same donor. Refer to text for a detailed description of the results.